Examining the Ecosystem Evolution of Nikanotee Fen Watershed: An Ecohydrological Perspective

by

Nataša Popović

A thesis
presented to the University of Waterloo
in fulfilment of the
thesis requirement for the degree of
Doctor of Philosophy
in
Geography

Waterloo, Ontario, Canada, 2024
© Nataša Popović 2024

Examining Committee Membership

The following served on the Examining Committee for this thesis. The decision of the Examining Committee is by majority vote.

External Examiner	Dr. Dale Vitt Professor, Department of Plant Biology, Southern Illinois University
Supervisor	Dr. Richard Petrone Professor, Geography and Environmental Management, University of Waterloo
Internal Examiner	Dr. Jonathan Price, Professor, Geography and Environmental Management, University of Waterloo
Internal-External Member	Dr. Brian Branfireun Professor, Department of Biology, University of Western Ontario
Other Member	Dr. Felix Nwaishi Associate Professor, Department of Earth and Environmental Science, Mount Royal University

Author's Declaration

This thesis consists of material all of which I authored or co-authored: see Statement of Contributions included in the thesis. This is a true copy of the thesis, including any required final revisions, as accepted by my examiners.

I understand that my thesis may be made electronically available to the public

Statement of Contributions

This thesis has been structured in accordance with the manuscript option. Chapter two and three have been published and Chapter four and five have been submitted and are currently under peer-review. Consequently, should these manuscripts also be accepted for publication they may differ from what is presented in this thesis due to comments and feedback following peer-review.

The Nikanotee Fen Watershed project is a large multi-year project spanning multiple labs and contributors. This is reflected in the authorship of publications. Nataša Popović conducted the data analysis and visualization presented herein, as well as writing the first draft of all manuscripts. Nataša Popović conducted all field work from the start of her time on the project (2017) onwards. Field measurements prior to 2017 were collected by Adam Green and several summer field assistants and prior grad students. Dr. Rich Petrone is the thesis advisor, Dr. Jonathan Price and Dr. Maria Strack are co-PI's (with Dr. Petrone) on the Nikanotee Fen Watershed project. As such, input and guidance from all three was instrumental in the planning and execution of all research presented in the following chapters. Adam Green and Dr. Myroslava Khomik are additional co-authors on Chapter 2 and 3 due to their expertise and help in eddy covariance data collection, management, post-processing and analysis.

Chapter two is published as:

Popović, N., Petrone, R. M., Green, A., Khomik, M., Price, J. S. (2022). A temporal snapshot of ecosystem functionality during the initial stages of reclamation of an upland-fen complex. *Journal of Hydrology: Regional Studies*, *41*, 101078.

Nataša Popović conceptualized the manuscript theme and objectives, compiled data, completed data analysis and visualization and wrote the first draft of the manuscript. Dr. Richard Petrone and Dr. Jonathan Price provided valuable feedback on results interpretation and editorial manuscript revisions. Adam Green and Dr. Myrosalva Khomik were instrumental in eddy covariance data management and post-processing.

Chapter three is published as:

Popović, N., Petrone, R. M., Green, A., Khomik, M., Price, J. S. (2023) Evolution of ecosystem-scale surface energy fluxes of a newly constructed, boreal upland-fen watershed. *Ecological Engineering*, *194,* 107059.

Similar to the first manuscript, Nataša Popović conceptualized the manuscript theme and

objectives, compiled data, completed data analysis and visualization and wrote the first draft of the manuscript. Dr. Richard Petrone and Dr. Jonathan Price provided valuable feedback on results interpretation and manuscript revisions and edits. Adam Green and Dr. Myrosalva Khomik were instrumental in eddy covariance data management and post-processing. Dr. Myrosalva Khomik also provided valuable insight and edits following peer-review comments.

Chapter four is submitted as:

Popović, N., Petrone, R. M., Strack, M. An assessment of carbon dioxide following vascular plant establishment in a constructed boreal watershed. *Science of The Total Environment.* STOTEN-D-24-09785

Nataša Popović completed all the fieldwork, data collection, analysis and visualization, formed the study design of upland tree flux measurements and wrote the first draft of this manuscript. Dr. Richard Petrone and Dr. Maria Strack conceptualized the study following initial site construction and provided valuable feedback on results interpretation and writing revisions.

Chapter five is submitted as:

Popović, N., Petrone, R. M., and Price, J.S Evapotranspiration dynamics during the initial seven years following construction of a boreal upland-fen watershed. *Ecohydrology.* ECO-24-0076

Nataša Popović conceptualized the manuscript theme and objectives, compiled data, completed data analysis and visualization and wrote the first draft of the manuscript. Dr. Richard Petrone and Dr. Jonathan Price provided valuable feedback on results interpretation and writing revisions.

By signing below, I indicate that I agree with the evaluation of the roles and contributions of the various authors expressed above.

R. Petrone J. Price M. Strack A. Green M. Khomik

Abstract

Recognition of the environmental ramifications of long-term natural resource development in the Athabasca Oil Sands Region (AOSR) has prompted the implementation of sustainable land use practices. This includes obligatory regulations that require impacted landscapes to be returned to their pre-disturbance functionality. Ecosystem function (e.g., carbon sequestration) is driven by soil-plant-atmosphere exchanges of energy, carbon and water resources. Given the magnitude of disturbance during surface mining (i.e., removal of vegetation and the subsurface) the reestablishment of ecosystem function requires extensive reclamation. This involves the complete reconstruction of surface and subsurface ecosystem components including the establishment of a hydrological regime. Thus, reclamation ultimately creates 'new' landscapes, often beginning with a bare ground phase followed by planting campaigns, and the eventual development of widespread plant communities. An understanding of ecohydrological processes throughout the different post-construction evolutionary phases is necessary to evaluate i) ecosystem function and trajectory and ii) reclamation design and success. As the natural, undisturbed landscape of the AOSR consists of hydrologically connected upland forests and fen peatlands, two pilot-scale watersheds incorporating these landscapes have been constructed to examine the viability and design of multi-landscape reclamation endeavours in the region.

This thesis captures the evolving ecohydrological regime during the first seven years (2013 - 2019) post-construction at one of the novel, constructed watersheds in the region, Nikanotee Fen Watershed (NFW). Ecosystem function and evolution of both the fen and

upland were quantified based on key ecohydrological indicators (net ecosystem exchange (NEE), evapotranspiration (ET) and water-use efficiency (WUE)) using a multi-scale (ecosystem and plant community), multi-method (remote sensing, eddy covariance, instantaneous chamber measurements) approach.

Over the course of the study period, both landscapes exhibited significant biophysical evolution, from bare ground to fully vegetated ecosystems, resulting in physical (e.g., altered albedo, surface roughness and producing plant-mediated shading) and functional (e.g., transpiration and carbon sequestration) transformations.

Initially, during bare ground conditions, surface-atmosphere exchanges were driven by abiotic factors (atmospheric and edaphic conditions) and controlled by soil water availability. In the fen, due to near-surface water table, high soil moisture content, surface ponding and the low albedo of wet, bare peat, most available energy was partitioned to latent heat and a high degree of decoupling between the surface-atmosphere was observed. During this time, surface evaporation rates were consistently high and comparable to open-water values in the region. Due to the lack of plant community, the fen was a source of CO_2 and WUE was low and driven by high evaporative losses. In the upland, the exposed dry sand-loam cover soil resulted in higher albedo and equal partitioning between latent and sensible heat. The drier edaphic conditions resulted in limited evaporation, with only small increases in response to precipitation events. Moreover, these conditions resulted in net carbon losses and similar to the fen, limited WUE.

Once plant community became established, edaphic controls decreased, and surface-atmosphere exchanges were driven by plant-mediated responses to atmospheric conditions. In the fen, as water availability remained high, latent heat continued to be the dominant energy flux, but a larger proportion of available energy was partitioned to sensible heat, particularly during drier periods. Widespread plant coverage and the establishment of a thick litter layer supressed surface evaporative losses and increased transpiration, resulting in lower ET rates compared to bare ground conditions and greater surface-atmosphere coupling. Coinciding with plant growth, the fen quickly evolved from a CO_2 source to a sink by year three post-construction. Moreover, once fully vegetated, WUE remained relatively stable despite seasonal hydrometeorological variability. Here, stable WUE trends reflect well-developed rooting architecture of the plant community and a well-connected groundwater network between the two landscape units resulting in hydrological self-regulation sufficient to maintain adequate plant function during periods of water stress. In the upland, the growth and development of treed species resulted in a marked increase in latent heat flux, ET rates, CO_2 uptake and WUE, with seasonal trends mirroring plant phenology. However, at the conclusion of this study the upland was still functioning as a minor CO_2 source, but is expected to become a sink in the near future as trees continue to mature.

Overall, an examination of ecohydrological processes and feedbacks during early development suggests the constructed system is evolving towards a functional, self-sustaining ecosystem that's able to withstand periodic environmental stress. Furthermore, rates and seasonal trends of key ecohydrological indicators (ET, NEE, WUE) at the constructed

watershed were comparable to those observed at surrounding natural and post-disturbance boreal landscapes providing further support of ecosystem function. Results from this study provide insight to early ecosystem function and trajectories and can be applied to future designs and planting prescriptions to improve long-term reclamation success.

Acknowledgements

This PhD journey has been a wild ride, over the past six years much of the world has changed, and I've changed and grown with it. Completing the PhD would not have been possible without the immense support of many people - in fact I could write another thesis worth of gratitude.

First and foremost, I'd like to recognize my supervisor, Dr. Rich Petrone, for providing the opportunity to work on such an incredible project, the Nikanotee Fen, and for all the opportunities that have come along with being part of the Hydrometeorology Lab: field seasons, conferences, teaching courses and mentoring students. Thank you for your unwavering support and guidance. Your mentorship has played an integral role not only in this thesis, but in my growth as a scientist…and thank you for always being a calm sounding board when I've been frantic about science and life. But aside from the standard thank you's a supervisor deserves, Rich deserves a whole lot more acknowledgement - for being compassionate, understanding and more than anything patient during some of the hardest times that overlapped with the PhD.

I'd like to thank all the members of my committee for their helpful comments and support over the years. To Dr. Jon Price, thank you for conceptualizing Nikanotee and bringing her to life. It has been a great joy to work on this project, and truly inspiring to witness the evolution and growth. Our time together in the field during Nikanotee's 10^{th} growing season will forever stand out as one of the highlights of my PhD experience.

While not official committee members, I'm very grateful to have had the mentorship and friendship of two incredible women and bad ass scientists - Dr. Maria Strack and Dr. Merrin Macrae. You've both been instrumental in making this PhD happen. Thank you for all the life chats and for always helping to find a way to make my ridiculous field and sampling plans happen.

To everyone in the Hydrometerology, Wetlands Hydrology, Biogeochemistry and GHG exchange labs at UW, thank you for all the support and friendship in the lab and field over the years. I'd like to specially thank: Hilary, for being the best field partner one could ask for; Janina, for the painstaking amount of biogeochem analysis; our lab techs and managers, James, Adam, Eric, Myroslava, Suyuan and Eric; and the original sky dungeon gang - Brandon, Jess, Matt Morison, Tasha-Leigh, Owen and Nicole. I'd also like to thank Jeremy Cameron and Colin Skinner, our field services supervisors at Suncor who made so much of the field work possible and enjoyable.

There are people who have entered my life during this journey that I absolutely could not have done this without, my AB's Sophie, Kelly and Erin. Thank you for all the support, good food, laughs and everything in between. For making this whole experience so much more than just science. Regardless of where life and academia may take us, I am forever grateful for our little girl-gang family, and I will always save us a table at banquet night. A huge thank you to my pal Scott, for allllllll the stoop chats and figure discussions. And to Alana, for always showing up, and whose voice notes, love and encouragement gave me life during the final push.

To Maja Cholich and my kumovi Angela and Ogi, thank you x 100 for being the constant positivity and stability in my life. And to my SFE KOLO fam, for being my weekly dose of laughter, exercise and Scout.

I would like to wholeheartedly thank my entire family… kumovi, cousins and everyone in between. Your support during this time, not only of me but of the whole Popović-Kekerić clan helped make this possible. The biggest thank you goes out to Melanija and Marko, for your unconditional love, for always believing in me and for giving me the strength to push forwards.

Lastly, an immense thank you to my parents, I cannot even really put into words the role you've played in getting me here – thank you for all your sacrifices, for leading by example and for continuously supporting me throughout this journey…from ESL to PhD. To my mama for the daily hugs and sliced fruit. Thank you for always finding the energy be supportive, even throughout your own turbulent journey during this time. To my tata, the original Dr. Popović, it is bittersweet that you're not physically here to see this to the end.

Dedication

To my parents, Goran and Aleksandra Popović, whose own story mirrors that of reclamation: fleeing their war-torn home with me in tow, immigrating to Canada, and starting a new and different life from scratch…where they created something out of nothing…and planted all the seeds of opportunity so that I could grow and flourish into the woman and scientist I am today.

Table of Contents

Examining Committee Membership ii
Author's Declaration iii
Statement of Contributions iv
Abstract vi
Acknowledgements x
Dedication xii
List of Figures xvii
List of Tables xxiii
List of Abbreviations xxv
Chapter 1 : Introduction 1
1.1 Objectives 4
1.2 Organization of thesis 5
Chapter 2 : A temporal snapshot of ecosystem functionality during the initial stages of reclamation of an upland-fen complex 7
2.1 Introduction 7
2.2 Study Site 10
2.3 Methods 15
2.3.1 Micrometeorological Setup 16
2.3.2 Eddy Covariance Data Processing 17
2.3.3 Edaphic Conditions and Hydrometric Network 18
2.3.4 Vegetation 19
2.4 Results 22
2.4.1 Environmental Conditions 22
2.4.2 Carbon Dynamics 31
2.4.3 Water Dynamics 34
2.5 Discussion 39
2.5.1 Ecosystem Performance of NFW 39
2.5.2 Drivers of ecosystem functionality and interannual variability 46

2.5.3 Comparison of NFW net ecosystem exchange rates to natural and post-disturbance landscapes 51
2.6 Conclusions 58
Chapter 3 : Evolution of ecosystem-scale surface energy fluxes of a newly constructed boreal upland-fen watershed 61
3.1 Introduction 61
3.2 Methods 63
3.2.1 Study Site: Nikanotee Fen Watershed 63
3.2.2 Micrometeorological setup 68
3.2.3 Eddy covariance processing and energy balance 68
3.2.4 Ecophysiological Parameters 69
3.2.5 Edaphic conditions and hydrometric network 71
3.2.6 Vegetation and surface conditions 72
3.3 Results 74
3.3.1 Environmental Conditions (2013-2019) 74
3.3.2 Evolution of Surface Energy Fluxes (2013-2019) 80
3.3.3 Changes in surface ecophysiological parameters 84
3.4 Discussion 87
3.4.1 Changes in surface energy partitioning (2013-2019) 87
3.4.2 Implications for oil sands reclamation and regional climate 99
3.5 Conclusions 102
Chapter 4 : An assessment of carbon dioxide exchange following vascular plant establishment in a constructed boreal watershed 104
4.1 Introduction 104
4.2 Methods 105
4.2.1 Study Site and Sample Design 105
4.2.2 Environmental Conditions 109
4.2.3 CO_2 Chamber Fluxes 111
4.2.4 Data analysis 113
4.3 Results 114

4.3.1 Environmental conditions 114
4.3.2 Carbon Fluxes 120
4.3.3 Environmental controls on CO_2 and H_2O fluxes 124
4.4 Discussion 128
4.4.1 Biotic and abiotic controls on CO_2 dynamics 128
4.4.2 Comparison to early reclamation at NFW 140
4.4.3 Comparison to natural and post-disturbance boreal landscapes in the region 141
4.4.4 Implications for AOSR reclamation 145
4.5 Conclusions 146
Chapter 5 : Evapotranspiration dynamics during the ecosystem development of a constructed upland-fen watershed 148
5.1 Introduction 148
5.2 Methods 151
5.2.1 Study Site 151
5.2.2 Study Design 152
5.2.3 Environmental Conditions 155
5.2.4 Ecosystem-scale measurements: Micrometerology and evapotranspiration 156
5.2.5 Community-scale, instantaneous chamber evapotranspiration 158
5.2.6 Data Analysis 160
5.3 Results 160
5.3.1 Environmental Conditions 160
5.3.2 Ecosystem-scale Evapotranspiration Trends 165
5.3.3 Instantaneous Chamber Evapotranspiration 169
5.3.4 Environmental Controls 172
5.4 Discussion 175
5.4.1 Drivers and controls of surface-atmosphere moisture exchanges 175
5.4.2 Implications for AOSR reclamation and future work 187
5.5 Conclusions 189
Chapter 6 : Summary of ecohydrological function during ecosystem development 190

Chapter 7 : Conclusions 197
References 201
Appendices 232
Appendix A: Utilizing vegetation indices to capture ecosystem recovery 232
Appendix B: Spatial variability in environmental conditions and fluxes from 2017 to 2019 236

List of Figures

Figure 1-1: A) Depiction of thesis organization. B) Methods and key variables collected to capture the spatial and temporal ecosystem evolution and ecohydrological function discussed in this thesis. Here, both an ecosystem- and community-scale approach were used. **6**

Figure 2-1: A) Map of the Nikanotee Fen Watershed depicting the regions of interest (Fen and Upland) and the locations of soil moisture pits, eddy covariance and meteorological towers and water monitoring wells. B) Summary of key changes and milestones in site development over the first seven years following construction. C) Satellite imagery of site (plant) development. D) Stratigraphic cross-section along a central transect (A-A', shown in Figure **2-**1C-2013) depicting the layering of substrate materials and general groundwater flow direction. The thickness of each layer is indicated in parentheses. Note that the thickness of the clay liner in the diagram is not to scale (illustrated thicker than the actual 0.05 m thickness). **12**

Figure 2-2: Footprint of tower fetch for fen and upland from 2013 - 2019. Fetch decreases as the system develops. Increase in plant height results in an increase in surface roughness (thus, decrease in fetch). Note the similar extent of flux footprint in the fen from 2016 onwards once vegetation becomes stable. **19**

Figure 2-3: Seven-year time series of seasonal meteorological characteristics for the Fen (green) and Upland (grey). A) Daily precipitation (P, mm). B) Mean daily air temperature (T_{air}, °C). C) Mean daily relative humidity (rH, %). D) Mean daily vapour presser deficit. (VPD, kPa). E) Mean daily mid-day (10:00 – 16:00) photosynthetically active radiation (PAR, umol m^{-2} s^{-1}). F) mean daily net radiation (Q*; Wm^{-2}). Note the significant overlap between fen and upland values. Due to the close proximity of the landscapes (and thus towers; <300 m apart) atmospheric conditions were largely similar. Missing data in 2016 is due to Horse Creek Wildfire. Missing data from the upland in 2017 Upland is due to instrumentation malfunction. **23**

Figure 2-4: Time series of edaphic and water table conditions in the Fen (green) and Upland (grey) from 2013 – 2019). A) Daily precipitation (mm). B) Mean daily soil temperature (C) at 5 cm below ground surface. C) Mean daily water table levels (cm below ground surface). D) soil moisture conditions (volumetric water content) at 5 (light blue), 15 (blue) and 30 (dark blue) cm below ground surface. **26**

Figure 2-5: Temporal snapshot of plant development in the fen and upland from 2013-2019. A) Ecosystem scale mean peak season (DoY 170-220) Enhanced Vegetation Index (EVI). B) Timeseries of EVI values from the mean of a pixel grid (60 x 60 m) located at the epicenter of flux tower footprints (white square). Light green and grey shading depict values from nearby natural sites with similar plant compositions. **29**

Figure 2-6: Seven-year time series of gap-filled mean daily gross primary productivity (GEP, green), respiration (R_{eco}, red) and net ecosystem exchange (NEE, blue) for the fen (top) and upland (bottom). Negative NEE values indicate carbon uptake from atmosphere. **33**

Figure 2-7: Gap-filled half-hourly net ecosystem exchange (NEE) fluxes from 2013 – 2019 for the fen (top) and upland (bottom). Each square is a half-hourly measurement, each row a full day. Fingerprint plots show seasonal (May-Sept, y-axis) and diurnal (hourly, x axis) trends. Note clear diurnal trends of C uptake once vegetation becomes established (2015 Fen, 2017 Upland). Positive values indicate a source of carbon to the atmosphere, negative values indicate carbon uptake by the surface. 2016 missing data is due to Horse Creek Wildfire. 2013 Fen: July-Aug and 2017 Upland: August missing data is due to instrumentation malfunction. **34**

Figure 2-8: Daily evapotranspiration (ET) rates for the fen (green) and upland (grey). Black line indicates the median ET rate, the box represents the 25th to 75th quartile, the whiskers include 95% of the range, and the black circles are outliers. **35**

Figure 2-9: Daily water use efficiency (WUE, bottom) compared to peak season EVI (middle) and growing season rainfall(top). Black line indicates the median WUE, the box represents the 25th to 75th quartile, the whiskers include 95% of the range, and the black circles are outliers. **36**

Figure 2-10: Relationship between total growing season net ecosystem exchange of CO_2 and site age at NFW-fen compared with natural and post disturbance Canadian peatlands with eddy covariance data sets. Blue band represents the range of NEE observed at natural sites, where the small dashed line depicts mean growing season NEE of all natural sites. In the legend n is the number of study years. * represents annual NEE. 10B: Relationship between total growing season net ecosystem exchange of CO_2 and site age at NFW-upland compared with mature and post disturbance (fire and harvest) boreal forests with eddy covariance data sets. Blue band represents the range of NEE observed at natural sites, small dashed line depicts mean growing season NEE of natural sites. In the legend n is the number of study years. **53**

Figure 3-1: Study site and visual depiction of temporal evolution. A) Map of the Nikanotee Fen Watershed (NFW) depicting the regions of interest (Fen and Upland) and the locations of soil moisture pits, eddy covariance and meteorological towers and water monitoring wells. B) Stratigraphic cross-section along a central transect (A-A', shown in Figure **3-**1A) depicting the layering of substrate materials and general groundwater flow direction. The thickness of each layer is indicated in parentheses. Note that the thickness of the clay liner in the diagram is not to scale (illustrated thicker than the actual 0.05 m thickness). C) Satellite imagery of site evolution from year 1 (2013) to year 7 (2019). Imagery was acquired using Google Earth Engine (GEE) via Maxar Technologies satellite data. D) Field photos depicting surface conditions initially

(2014) and following plant development (2018). Upper row: focused on fen (taken from east slope). Bottom row: focused on upland (taken from west slope). **66**

Figure 3-2: Split violin plots depicting the magnitude and distribution of meteorological (A-E) and surface (F-J) conditions for the fen (left, dark green) and upland (right, light green) during the growing season (May – September). White dot represents the median, black bar the interquartile range. A) mean daily air temperature (Tair, °C); B) total daily precipitation (P, mm); C) mean daily incoming shortwave radiation (Rg, Wm^{-2}); D) mean daily vapour pressure deficit (VPD, kPa); E) mean daily relative humidity (rH, %); F) mean daily soil temperature at 5 cm below the ground surface (Tsoil, °C); G) mean daily soil volumetric water content (VWC, %); H) mean daily water table depth (WT, cm below ground surface); I) mean weekly enhanced vegetative index (EVI); J) mean daily mid-day (10:00 – 16:00) albedo. **76**

Figure 3-3: Spatial and temporal changes to surface conditions from 2013 to 2019. A) Satellite imagery of site evolution from year 1 (2013) to year 7 (2019). B) Results of the supervised land use/land classification (LULC) analysis where each pixel is 30m x 30 m. C) Distribution of land class (%) for each year during the study period for the fen (top) and upland (bottom). Legend corresponds to both B and C. **79**

Figure 3-4: Fingerprint plot depicting gap-filled, half-hourly surface energy fluxes from 2013 – 2019 for the fen. Each square is a half-hourly measurement, and each row represents a full day. Plots show seasonal (May-Sept, y-axis) and diurnal (hourly, x axis) trends of A) Net radition (Q*); B) Latent heat flux (Q_E); C) Sensible heat flux (Q_H); D) Ground heat flux (Q_G) in Wm^{-2}. 2016 missing data is due to Horse Creek Wildfire. 2013 Fen: July-Aug and 2017 Upland: August missing data is due to instrumentation malfunction. **82**

Figure 3-5: Fingerprint plot depicting gap-filled, half-hourly surface energy fluxes from 2013 – 2019 for the upland. Each square is a half-hourly measurement, and each row represents a full day. Plots show seasonal (May-Sept, y-axis) and diurnal (hourly, x axis) trends of A) Net radition (Q*); B) Latent heat flux (Q_E); C) Sensible heat flux (Q_H); D) Ground heat flux (Q_G) in Wm^{-2}. 2016 missing data is due to Horse Creek Wildfire. 2013 Fen: July-Aug and 2017 Upland: August missing data is due to instrumentation malfunction. **83**

Figure 3-6: Growing season averages of A) aerodynamic conductance (g_a, circles) and surface conductance (g_s, crosses); B) decoupling factor (Ω); C) Bowen ratio (β) and D) frictional velocity (u*) from 2013 - 2019. ..... **86**

Figure 3-7: Mean growing season latent heat flux (Q_E) normalized to net radiation (Q*) based on age since disturbance for peatland (A) and forest (B) sites in a Canadian boreal setting. NFW (this study) is represented by black points. Box and jitter plots represent the range of values for natural or mature (> 30 years post-disturbance) sites. **89**

Figure 4-1: Map depicting the Nikanotee Fen Watershed (NFW) fen and upland landscapes and the location of instrumentation (meteorological towers and soil pits) as well as chamber flux plot locations. B: Field photographs depicting the fen (top row) and upland (bottom row) and the whole-plant, single and stacked chamber flux technique. **108**

Figure 4-2: Meteorological conditions from 2016 to 2019. A) Monthly total precipitation (mm). B) Mean daily air temperature (°C). C) Mean daily daytime (07:00 – 20:00) photosynthetically active radiation (PAR; μmol m^{-2} s^{-1}). Black line indicates the median, the box represents the 25th to 75th quartile, the whiskers include 95% of the range, and the black circles are outliers **116**

Figure 4-3: Edaphic conditions measured at each flux plot from 2016 to 2019 for the fen (dark green) and upland (light green). A) Water table depth (WTD; cm), negative value indicates below ground. Note the break in the y axis. B) soil moisture measured at 5 cm depth (volumetric water content (VWC, %). C) soil temperature measured at 5 cm depth. Black line indicates the median, the box represents the 25th to 75th quartile, the whiskers include 95% of the range, and the black circles are outliers. **117**

Figure 4-4: Summary of dominant vegetation in the fen and upland. Based on surveys from each flux plot. A) Mean peak growing season (July) leaf area index (LAI) for each species. B) Mean plant height and litter (yellow rectangle) height for each species. **119**

Figure 4-5: Partitioning of CO_2 fluxes (g CO_2 m^{-2} d^{-1}) by species A) net ecosystem exchange (NEE). B) gross ecosystem productivity (GEP). C) respiration (R). Compact letter display depicts results from post-hoc Dunn statistical analysis representing significant differences between species. Black line indicates the median, the box represents the 25th to 75th quartile, the whiskers include 95% of the range, and the black circles are outliers. **122**

Figure 4-6: Seasonal variability in CO_2 fluxes based on monthly means by species from 2016 to 2019 for the fen and upland. A) net ecosystem exchange (NEE). B) gross ecosystem productivity (GEP). C) respiration (R). **123**

Figure 4-7: Graphical summary of significance from linear mixed effect model for NEE, GEP and R versus environmental variables per each species in the A) Fen and B) Upland. Variables are ordered by significance from left to right. Significance is denoted by . for $p<0.10$, * for $p < 0.05$, ** for $p < 0.01$, *** for $p < 0.001$. **127**

Figure 4-8: Temporal variability in environmental conditions (i.e., wetter versus drier growing seasons) and its effect on CO_2 fluxes in the A) Fen and B) Upland. Spearman rank coefficient (R_S) depicting the relationship between fluxes (GEP, R) and environmental variables between years (2017, 2018, 2019). Significance denoted by p-value . for $p<0.10$, * for $p < 0.05$, ** for $p < 0.01$, *** for $p < 0.001$. **128**

Figure 5-1: A) Map depicting the Nikanotee Fen Watershed (NFW) fen and upland landscapes and the location of instrumentation (towers and soil pits) as well as chamber flux plot locations; B) Field photographs depicting the fen (top row) and upland (bottom row) and the whole-plant, single and stacked chamber flux technique; C) Landscape-scale field photographs of biophysical surface characteristics in 2014 (year 2) compared to 2018 (year 6); D) Satelitte imagery of NFW capturing ecosystem evolution from 2013 – 2019; E) Summary of surface biophysical conditions for each year, based on the results of land cover spectral analysis, adapted from Popović et al. (2023)..... **154**

Figure 5-2: Cumulative seasonal AET (mm, green), PET (mm, dashed) and P (mm, black) for the fen (top) and upland (bottom) from 2013 to 2019. Nikanotee Fen Watershed, Fort McMurray, Alberta, Canada. Light green bands represent periods of missing data due to instrument malfunction. **167**

Figure 5-3: Fingerprint plot depicting gap-filled, half-hourly evapotranspiration (ET, mm) from 2013 – 2019 for the fen (top) and upland (bottom)at Nikanotee Fen Watershed, Fort McMurray, Alberta, Canada. Each square is a half-hourly measurement, and each row represents a full day. Plots show seasonal (May-Sept, y-axis) and diurnal (hourly, x axis) trends. 2016 missing data is due to Horse Creek Wildfire, other gaps are due to instrumentation malfunction. **168**

Figure 5-4: Sensitivity of gs to VPD from 2013 to 2019 in the fen (top) and upland (bottom). **169**

Figure 5-5: Results from chamber-based measurements, Nikanotee Fen Watershed, Fort McMurray, Alberta, Canada. A) ET fluxes by species in the fen (left, 2017 – 2019) and upland (right, 2018 – 2019). Compact letter display depicts results from post-hoc Dunn statistical analysis representing significant differences between species within each landscape. Black line indicates the median, the box represents the 25th to 75th quartile, the whiskers include 95% of the range, and the black circles are outliers. B) Partitioning of ET and E_S (surface evaporation) by species and year. C) Seasonal variability in chamber-based ET fluxes based on monthly means by species. **171**

Figure 5-6: Temporal snapshot of Spearman rank coefficient (RS) depicting the relationship between environmental conditions and ET fluxes in the A) fen and B) upland from 2013 to 2019. ..... **174**

Figure 5-7: Graphical summary of results from the linear mixed effect model depicting the interaction between ET and environmental variables per each species in the A) fen and B) upland. Significance is denoted by * for $p < 0.05$, ** for $p < 0.01$, *** for $p < 0.001$. $p < 0.10$ is not significant but exhibited some relationship and has been left in for discussion/context. **175**

Figure 6-1: Graphical summary of temporal changes in key ecohydrological variables measured in this study in the fen (green) and upland (grey). Letters highlight key moments and are described in the text. **192**

Figure 6-2: Conceptual diagram of ecohydrological interactions driving ET, CO_2 and WUE during two distinct phases of ecosystem development, A) bare ground and B) established vegetation. **193**

Figure 6-3: Conceptual diagram depicting the interaction of ecosystem components and key drivers of ecosystem evolution and function. **195**

Figure 6-4: Summary of controls driving surface-atmosphere exchanges during the different phases of ecosystem evolution. **196**

Figure A-1: Temporal snapshot of plant development in the fen and upland from 2013-2019. Ecosystem scale mean peak season (DoY 170-220) satellite imagery (top), Normalized Difference Vegetation Index (NDVI; middle) and Enhanced Vegetation Index (EVI; bottom). **233**

Figure A-2: Timeseries of NDVI and EVI values from the mean of a pixel grid (60 x 60 m) located at the epicenter of flux tower footprints (white square). Note the overestimation of NDVI in the fen and underestimation in the upland during early development. Values greater than 0.2 represent a plant signal. **234**

Figure A-3: Relationship between NDVI and GEP (left), and EVI and GEP (right) from 2013 to 2019. Based on mean daily GEP for weeks when spectral imagery is collected (every 8-16 days). Values greater than 0.2 represent a plant signal. Note that NDVI indicates a plant signal when there is limited to no GEP (2013,2014, red orange) confirming the overestimation of wet dark peat as plant matter. **235**

Figure A-4: Spatial interpolation of mean peak season edaphic conditions and CO_2 and ET fluxes from 2017 to 2019. A) water table depth (cm) where a negative value indicates below ground, B) soil moisture (%), C) soil temperature (°C), D) net ecosustem exchange (g CO_2 m^{-2} d^{-1}), E) evapotranspiration (ET, mm/day). White circles represent flux plot measurement locations. In the upland, the mean of each quadrant (rather than plot) was used No measurements were taken in the upland in 2017. ..... **238**

List of Tables

Table 2-1: Soil and vegetation characteristics of the NFW fen and upland. Soil moisture and water table depths are mean values from 2013-2019. **15**

Table 2-2: Summary of growing season means (±SD) of NFW environmental variables: air temperature, precipitation, relative humidity, vapour pressure deficit, photosynthetically active radiation, net radiation, water table depth, soil temperature, volumetric water content (at 5, 15 and 30 cm depths), electrical conductivity (E_c), and sodium concentration (Na^+). E_c and Na^+ are presented here as they depict changes in water quality during ecosystem development. Methods and a detailed analysis of solute transport and water quality changes at NFW are discussed by Kessel et al. (2018). **27**

Table 2-3: Summary of average (± SD) vegetation biometrics for the NFW fen and upland from 2013-2019 including seasonal aboveground biomass (measured in the fen only), leaf area index (LAI), enhanced vegetation index (EVI) for the growing season and peak season (DoY 170 – 220), vegetation or tree height, diameter at breast height (dbh) and litter thickness. – represents years where measurement was unavailable due to juvenile plant size (fen 2013; upland 2013-2016) and/or incomplete data due to instrument malfunctions or unfavourable environmental conditions. **30**

Table 2-4: Cumulative (A) and daily (B) values for carbon and water fluxes. **A)** Cumulative growing season (gs) and peak season (ps: DoY 170-220) carbon and ET fluxes from the fen and upland (2013 – 2019). CO_2 uptake represents the number of days with CO_2 uptake (based off on daily NEE) over 120 growing season days **37**

Table 3-1: Biophysical characteristics of the NFW fen and upland. **67**

Table 3-2: Timeline of key events and instrumentation during the initial stages of reclamation. Here, n represents the number of days measured (EC measurements) out of 120 during the growing season. **67**

Table 3-3: Description of land use/land cover (LULC) classes used to define changing surface conditions. **73**

Table 3-4: Mean seasonal energy flux for each energy balance component and the ratio of energy flux components normalized to net radiation (Q*) for the fen and upland from 2013 – 2019. **84**

Table 4-1: Landscape specific specs and sampling design **109**

Table 4-2: Number of flux measurements per season after QA/QC to r2 greater than 0.80. Original number of flux measurements in brackets. **109**

Table 4-3: Mean CO2 fluxes for NWF-Upland converted from g CO2 m-2 day-1 to g C m-2. Here we used 120 days as it represents the average length of the growing season in

boreal forest studies. To normalize data between plant communities, fluxes were subsequently divided by mean LAI of each tree type. **143**

Table 5-1: Landscape specific whole plant chamber measurement specifications and sampling design, Nikanotee Fen Watershed, Fort McMurray, Alberta, Canada. **153**

Table 5-2: Summary of environmental variables from 2013 to 2019. Data presented as monthly means (except for precipitation which is a monthly cumulative sum). **163**

Table 5-3: Biophysical surface and edaphic conditions at chamber-measured plots by species. Values represent averages from all years measured (2017 – 2019 fen, 2018 – 2019 upland). Negative WTD represents inundated conditions (above ground water table). **165**

List of Abbreviations

Ω	Surface – atmosphere decoupling factor	P	Precipitation
β	Bowen ratio	PAR	Photosynthetically active radiation
AET	Actual evapotranspiration	PET	Potential evapotranspiration
AOSR	Athabasca oilsands region	PET_{PM}	Penmen-montieth PET equation
As	Aspen	Q*	Net radiation
bgs	Below ground surface	Q_E	Laten heat flux
Bp	Balsam poplar	Q_G	Ground heat flux
Ca	*Carex aquatilis*	Q_H	Sensible heat flux
CO_2	Carbon dioxide	R	Respiration
dbh	Diameter at breast height	R_{eco}	Ecosystem respiration
EC	Eddy covariance	Rg	Incoming shortwave radiation
E_S	Surface evaporation	rH	Relative humidity
ET	Evapotranspiration	R_S	Spearman Coefficient
EVI	Enhanced vegetation index	Sp	Spruce
g_a	Aerodynamic conductance	Tair	Air temperature
g_s	Surface conductance	Tsoil	Soil temperature
GEP	Gross ecosystem productivity	u*	Friction velocity
H_2O	water	Us	Understory
ha	Hectare	VPD	Vapour pressure deficit
IRGA	Infrared gas analyzer	VWC	Volumetric water content
Jn	*Juncus balticus*	WBP	Western boreal plains
Jp	Jack pine	WT	Water table
LAI	Leaf area index	WTD	Water table depth
LULC	Land use land classification	WUE	Water use efficiency
Mx	Mixed		
NEE	Net ecosystem exchange		
NFW	Nikanotee Fen Watershed		

Chapter 1: Introduction

Resource extraction in the Athabasca Oilsands Region (AOSR) results in significant land disturbance, including land cover change (e.g., removal of vegetation), disruption of ecosystem services (e.g., loss of carbon sink capacity and storage), and alterations to the hydrological regime (e.g., disrupted water transmission and storage capacity). Reclamation aims to restore these disturbed areas to conditions that approach their natural functionality and is critical to responsible resource development and sustainable land use practices.

The AOSR is located within the Boreal Plains (BP) ecozone where the pre-disturbance landscape comprises mixed boreal forests, peatlands, and open-water regions. Boreal landscapes have long been recognized for their important ecohydrological and biogeochemical roles (Volik et al., 2021; Helbig et al., 2020; Thom and Seidl, 2016; Bonan, 2008; Ruckstuhl et al., 2008; IPCC, 2007). In particular, these landscapes play a significant role in global carbon cycling where boreal forests sequester large amounts of atmospheric CO_2 and subsequently store it in above and below ground biomass (Kurz et al., 2013) and northern peatlands serve as substantial reservoirs of soil carbon (Strack et al., 2022; Roulet et al., 2007; Syed et al., 2006). While individually these landscapes provide vital ecosystem services, in the AOSR, their hydrologic interconnectivity plays a pivotal role in maintaining ecosystem function as the region experiences frequent moisture-deficits (Ireson et al., 2015; Price et al., 2013; Bothe and Abraham 1993). Here, wetlands capture and conserve excess water during periods of surplus (Wells et al., 2017; Waddington et al., 2015; Devito et al., 2012; Spence et al., 2011) which then becomes available for redistribution (facilitated by the rooting architecture of forests) particularly during drought conditions (Depante et al., 2019; Petrone et al., 2015; Brown et al., 2014). Moreover, the geologic and topographic setting of the

region results in uplands often feeding groundwater to down-gradient fens, providing a consistent input to fens (Elmes and Price, 2019; Wells et al., 2017). As water availability is the primary driver of ecosystem function (Rodriguez-Iturbe, 2000) it is imperative that reclamation design can satisfy water requirements under both current and anticipated future climatic conditions to ensure successful ecosystem evolution, performance and ultimately longevity.

Reclamation efforts in the region have been ongoing since 1971, and to date less than 10% of previously disturbed land has been permanently reclaimed (64 km^2 of 1055 km^2; Alberta Environment and Parks, 2022). While the primary focus of reclamation has been on recreating forested upland landscapes, recognition of the vital ecohydrological role played by peatlands in the region (Volik et al., 2021; Elmes and Price 2019; Devito et al., 2012; Price et al., 2010) has prompted a concerted effort to integrate peatland ecosystems into the broader reclamation strategy. In natural settings, peatlands are created and maintained under specific hydrologic conditions (i.e., near surface water-table, persistent inundation) allowing for the slow decay of plant matter and eventual peat-accumulation. These requirements further highlight the importance of continuous water-availability and hydrologic connectivity in constructed systems. Fens are the prevalent peatland type within the AOSR (Volik et al., 2020), and are characterized by their specific soil properties, hydrology and nutrient status. The Canadian Wetland Classification System (CWCS) defines fens as having a minimum of 0.4 m of organic soil (peat), with hydrological inputs primarily from sources other than precipitation, such as surface water and groundwater, resulting in minerotrophic nutrient status. This input of nutrients via ground water typically leads to a more diverse plant community including sedges, grasses, reeds, and brown mosses, compared to other peatland types (e.g. moss-dominated bogs). As such, fen reclamation endeavours have been recently initiated, marked by the construction of two novel pilot projects: the Sandhill Fen

Watershed and the Nikanotee Fen Watershed. While the two watersheds exhibit variable design components, both were built upon a foundation of recycled, post-processed oil sands materials (i.e., tailing sands) and represent the first attempts to construct fen peatlands and recreate the mosaic of hydrologically connected land units prevalent in the region (Ketcheson et al., 2016). Since their initiation over a decade ago, extensive research has been produced particularly on individual ecosystem components such as the hydrological function (Biagi et al., 2021; Ketcheson et al., 2017), hydrochemistry (Yang et al., 2022; Biagi et al., 2019, Kessel et al., 2018, Simhayov et al., 2017), soil processes and evolution (Sutton and Price, 2020a, Sutton and Price, 2020b; Gingras-Hill et al., 2018, Nwaishi et al., 2015), carbon dynamics (Prystupa et al., 2023; Davidson et al., 2021; Clark et al., 2019; Nwaishi et al., 2016) and plant communities (Hartsock et al., 2021; Messner et al., 2019; Borkenhagen et al., 2019; Vitt et al., 2016) of these constructed landscapes. To date only a handful of studies (Clark et al., 2022; Fettah et al., 2022; Scarlett and Price, 2019; Scarlett et al., 2017; Strilesky et al., 2017; Nicholls et al., 2016) have examined soil-plant-water-atmosphere interactions of constructed landscapes and have been largely limited to the initial, post-construction stage (<3 years) due to the juvenile nature of these projects and generally focus on a single landscape unit. This work aims to build upon these previous studies and link together ecosystems components through an ecohydrological approach - by examining how biophysical factors, such as vegetation and edaphic conditions during various phases of ecosystem evolution and under variable hydroclimatic conditions affect the distribution of energy, carbon and water resources and in turn, influence ecosystem performance.

Moreover, the enactment of the Environmental Protection and Enhancement Act (EPEA) imposes a legal obligation on companies involved in oil sands development to restore mined areas to their pre-disturbance capacity, emphasizing the necessity for well-defined criteria for

reclamation targets. Reclamation targets have been broadly defined to entail the creation of functional, self-sustaining ecosystems that are resilient to periodic environmental stress (Alberta Environment and Sustainable Resource Development, 2013). Thus, quantifiable metrics for assessing ecosystem function are required. Preliminary research (Clark et al., 2022; Strilesky et al., 2017; Nwaishi et al., 2015) suggests utilizing key ecohydrological indicators (e.g., water-use efficiency, carbon sequestration) as integrated measures of reclamation performance as these metrics encompass a suite of ecosystem conditions and processes. Thus, this research provides a case-study opportunity to evaluate the viability of using ecohydrological indicators and their respective monitoring methods (e.g., eddy covariance, remote sensing) as a means to provide meaningful assessments of reclaimed AOSR landscapes.

1.1 Objectives

The primary goal of this thesis is to provide a comprehensive overview of ecohydrological functionality of both the upland and fen landscapes of the Nikanotee Fen Watershed during the initial, and likely most dynamic, stages of ecosystem evolution following construction. The main objectives are to:

1) Evaluate ecosystem performance by quantifying temporal patterns and rates of energy, carbon, and water fluxes during the first seven years following construction;
2) Illustrate ecosystem development and evolution through changes in biophysical surface properties;
3) Examine the role of developing vascular vegetation on surface-atmosphere interactions;
4) Delineate key ecohydrological feedbacks and controls during ecosystem evolution.

These objectives are addressed as key themes throughout the chapters outlined below.

1.2 Organization of thesis

This thesis comprises seven chapters that have been structured to conform to the manuscript option at the University of Waterloo. Here, key words and (graphical) abstracts have been removed to aid thesis structure and flow. To best capture the temporal evolution and functionality of the constructed landscapes, this thesis applied a multi-scale, multi-method approach. Figure 1-1 depicts thesis structure and highlights methods applied. Due to the nature of the project, some methods are recurrent across chapters such as eddy covariance measurements and remote sensing techniques capturing ecosystem development and biophysical surficial changes. The thesis begins with an examination of ecosystem-scale exchanges of carbon, water and energy during the first seven years post-construction (Chapter 2, 3 and 5) followed by a progression to community-scale carbon and water dynamics (Chapter 4 and 5) and finally a summary of surface-atmosphere feedbacks (Chapter 6) based on results presented in chapters 2-5. Chapter 1 provides context for this research by briefly outlining the ecohydrological significance of boreal landscapes in the region, the necessity for reclamation as well as defining the overarching goals and objectives of the thesis. Chapter 2 defines benchmarks for reclaimed landscape performance and evaluates ecosystem functionality through net ecosystem exchange (NEE) and water-use efficiency (WUE). Additionally, it provides context to NFW performance through comparison of carbon dynamics at nearby natural and post-disturbance sites. Chapter 3 examines changes in energy partitioning during ecosystem evolution and quantifies land cover change from bare ground to wide-spread vegetation. Chapter 4 assesses species-specific CO_2 fluxes following the widespread establishment of vascular vegetation and examines environmental controls. Chapter 5 examines evapotranspiration (ET) dynamics both at the ecosystem and community scale. Chapter 6

amalgamates the key findings and ecohydrological feedbacks discussed in chapters 2-5 into a timeline of ecosystem evolution and function. Finally, Chapter 7 provides conclusions and highlights the broader implications of this work for future reclamation endeavors in the region.

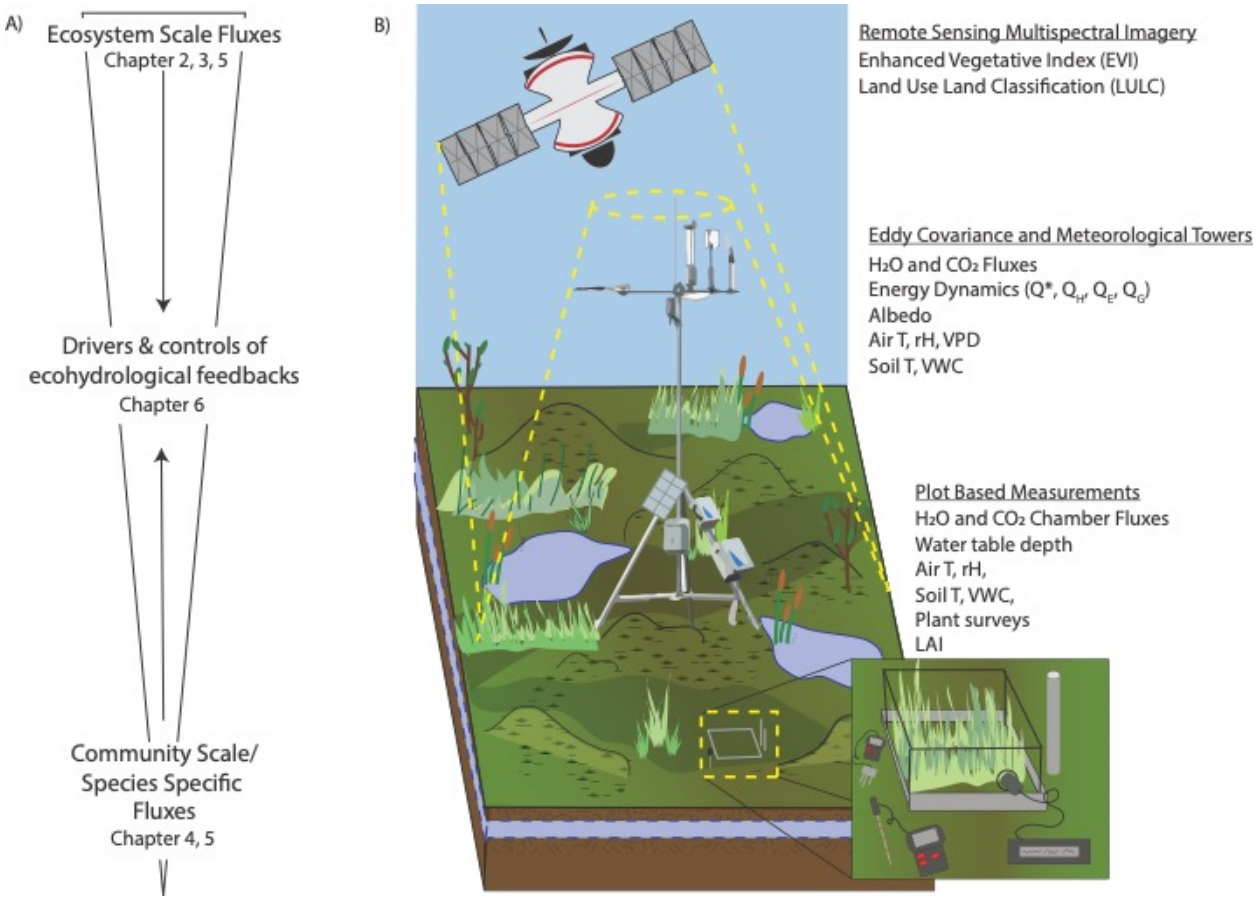


Figure 1-1: A) Depiction of thesis organization. B) Methods and key variables collected to capture the spatial and temporal ecosystem evolution and ecohydrological function discussed in this thesis. Here, both an ecosystem- and community-scale approach were used.

Chapter 2: A temporal snapshot of ecosystem functionality during the initial stages of reclamation of an upland-fen complex

2.1 Introduction

The Western Boreal Plains (WBP) ecozone provides important economic (via natural resource extraction) and environmental ecosystem services (EES) on regional and global scales. EES provided by landscapes in the region include: i) the regulation of regional hydrological regimes; ii) providing niche, diverse ecosystems; iii) nutrient transformation through biogeochemical cycling; and perhaps most importantly, iv) carbon sequestration and long-term carbon storage in soils (Lamothe et al., 2019; Kurz et al., 2013; Yu, 2012; Limpens et al., 2008; Blodau, 2002). The Athabasca Oil Sands Region (AOSR) encompasses an area of 93,259 km^2 within the WBP of northeastern Alberta, of which 5% (4800 km^2) is considered minable for oilsands extraction (ABMI, 2017). Here, one method of resource extraction consists of widespread surface mining, where up to 75 m of substrate below the ground surface are removed, resulting in a fully altered, disturbed landscape and subsequent loss of vital EES (Nwaishi et al., 2015a). Notably, Rooney et al. (2012) estimate AOSR mining activities will result in a potential net loss of 11.4 – 47.3 Tg of stored soil carbon. As of 2016, 901 km^2 of land in the AOSR has been impacted by mining activities. (Government of Alberta, 2017). Companies operating in the AOSR have a statutory obligation to return leased land to pre-disturbance equivalent land capability, defined as post-reclamation landscapes that can support ecosystem services and functions similar to what existed prior to disturbance (Alberta Environment, 2008). However, the resulting reclaimed landscape may not necessarily be identical to the pre-disturbance landscape (Poscente and Charette, 2012; Alberta Environment, 2008). As reclamation efforts in the region typically use mine waste materials (i.e., tailing sand, petroleum coke) as construction substrates, the trajectory and end-result of reclaimed systems is likely to result in a hybrid, or novel landscape. These landscapes may be physically different, but functionally similar to natural, pre-disturbance landscapes as the structural and hydrogeochemical characteristics of construction materials used in AOSR reclamation endeavours are

vastly different than those found in natural systems (Nwaishi et al., 2015a; Daly et al., 2012). The pre-disturbance landscape of the AOSR comprises a mosaic of upland forests (23%) and wetlands (54%) (AEP, 2018; Rooney et al., 2012), which are largely fen peatlands (Daly et al., 2012; Chee and Vitt, 1989). Initially, reclamation endeavours in the AOSR focused solely on reclaiming to upland forests. However, due to the extensive occurrence of peatlands, their specific ecosystem services (i.e., carbon storage) and hydrologic interconnectivity between uplands and peatlands, fens have begun to be integrated into regional reclamation efforts (Ketcheson et al., 2016). Due to the magnitude of disturbance, reclamation endeavours require the complete reengineering of surface topography and subsurface stratigraphy in addition to the initiation of vegetation through planting campaigns.

Reestablishment of hydrological connectivity is critical to the evolution and success of reclaimed landscapes, due to water requirements of key ecohydrological and biogeochemical functions – particularly in peatlands (i.e., inundated conditions, stable, near surface water table; Daly et al., 2012; Elshorbagy et al., 2005). Ensuring adequate water for ecosystem function in the AOSR is further complicated by the sub-humid climate of the region, where annual evapotranspiration commonly exceeds precipitation, resulting in frequent periods of water stress (Bothe and Abraham, 1993). Moreover, this water stress is expected to worsen in the area according to climate projections (Thompson et al., 2017; Ireson et al., 2015; Devito et al., 2012). The availability (and use) of water in an ecosystem is critical to successful development and function and is controlled mainly by the storage capacity of soils and vegetation (Rodriguez-Iturbe and Porporato, 2004). Thus, reclamation design in the AOSR needs to ensure adequate water availability for successful ecosystem development and function while accounting for the limited water availability.

The overarching goal of reclamation in the region is to create functional, self-sustaining, resilient ecosystems. As such, benchmarks encompassing ecologic, hydrologic and industry perspectives of ecosystem performance have been defined (Daly et al., 2012) and successful reclamation requires an ecosystem to be: 1) capable of supporting a representative assemblage of species; 2) carbon accumulating; and 3) able to withstand periodic environmental stress.

As AOSR fen reclamation is a relatively new endeavor, quantifiable metrics for evaluating the trajectory, success and long-term sustainability of reclamation projects is required. As it is difficult to directly measure ecosystem function through a single metric, the evaluation of reclamation performance has typically relied on the measurement of a large number of ecosystem variables (e.g., soil properties and geochemistry, vegetation surveys, biomass, water use), under the premise that in aggregate these variables will reflect ecosystem function and land capability. However, this approach has limitations, such as: data on a large number of variables can be onerous to collect and impossible to appropriately integrate; variables may be poor indicators of actual function; measured variables may reflect current site performance but fail to provide information on site stability under changing conditions, and on broader landscape-level performance. Alternatively, a focus on fewer biologically integrative factors or on emergent properties may be more effective (Straker et al., 2019; Strilesky et al., 2017; Nwaishi et al., 2015a).

Ecosystem water and carbon dynamics are integrative indicators of a suite of supporting ecosystem processes and characteristics. For example, water use efficiency (WUE), which links photosynthesis with water use, provides a useful metric to evaluate the use of water and carbon resources by plants. As such, assessment of the efficiency of ecosystem water use provides important insight on resiliency to climatic variation, and on landscape-level water storage and yield. Net ecosystem exchange (NEE) captures the net exchange (i.e., photosynthesis and respiration) of carbon between an ecosystem and the atmosphere and is a primary gauge of ecosystem carbon sink capacity. The overall carbon sink capacity of an ecosystem is dependent on edaphic conditions, water availability and plant community composition. Thus, integration of ecosystem-scale measurements of carbon exchange coupled with remote sensing metrics for plant development provides an efficient integrative measure of reclamation performance and early successional trajectory.

To date, only two pilot projects assessing reclamation design and performance have been constructed in the AOSR. Considerable research on early hydrological functioning (Biagi et al., 2021; Ketcheson et al., 2017), hydrochemistry (Biagi et al., 2019; Kessel et al., 2018; Simhayov et al., 2017), soil

dynamics (Sutton and Price (2020a, 2020b); Scarlett and Price, 2019; Gingras-Hill et al., 2018; Nwaishi et al., 2015b), ecology (Messner et al., 2019; Borkenhagen et al., 2019; Vitt et al., 2016) and plot-scale, seasonal carbon and water exchanges (Davidson et al., 2021; Scarlett et al., 2017; Nwaishi et al., 2016) has been conducted on reclaimed AOSR systems. However, there are limited long-term, assessments of performance based on ecosystem-scale metrics such as carbon and water dynamics in reclaimed, post-mining landscapes.

This study evaluates ecosystem development and performance during the initial stages of reclamation at the Nikanotee Fen Watershed (NFW; a constructed upland-fen complex) through the use of ecosystem scale techniques (e.g., eddy covariance towers, remote sensing). Specifically, the objectives were to: (a) provide a temporal snapshot of ecosystem evolution by using plant development, net ecosystem exchange (NEE) and WUE as metrics; b) evaluate ecosystem functionality and c) provide context to NFW performance through the comparison of carbon dynamics at surrounding natural and post-disturbance sites.

2.2 Study Site

The Nikanotee Fen Watershed (NFW) is a 32-ha constructed watershed located within an oil sands mining operation approximately 30 km north of Fort McMurray, Alberta (56°55.944′N, 111°25.035′W; Figure 2-1)). NFW consists of three previously reclaimed slopes (18.7 ha), an undisturbed natural slope (2.8 ha), a newly reclaimed upland (7.7 ha) and fen peatland (2.9 ha). This study focuses only on the newly reclaimed upland and fen landscapes of the system (Figure 2-1).

WBP climate is sub-humid, with thirty-year climate normals (1981-2010) having a mean July temperature of 17.1 °C, and an average of 419 mm of precipitation annually, of which ~70% occurs as rainfall (Environment Canada, 2015; Smerdon et al., 2008). Evapotranspiration (ET) commonly exceeds precipitation (P), resulting in periods of water stress (Petrone et al., 2007; Marshall et al., 1999; Bothe and Abraham, 1993).

NFW was designed based on numerical modeling of ideal geometries and substrate materials for successful ecosystem function within the WBP climate, while satisfying vegetation water requirements and facilitating peat accumulation (Price et al., 2010). Moreover, the system is designed to function in a simplified, but analogous manner to fen-upland ecosystems common in undisturbed landscapes of the WBP, where uplands supply groundwater to downgradient peatlands (Wells et al., 2017; Elmes and Price, 2019). As such, there is no manual manipulation of the water table at NFW. Hydrological inputs to the system include precipitation and surface runoff from the surrounding, previously reclaimed hillslopes (Figure 2-1A) and fen hydrology is dependent on the down-gradient transport of water from the upland aquifer (Sutton and Price, 2020a; Ketcheson et al., 2016). Surface water is discharged through an outflow located in the northeastern corner of the fen. A complete account of NFW hydrological functioning is given in Ketcheson et al. (2017).

Construction of the upland-fen complex began in 2012 and concluded in January 2013. Planting and revegetation were initiated in June 2013. In 2014, additional peat was added to the fen, in an attempt to counter ponding, and additional tamarack (*Larix laricina*) seedlings were planted in the upland. The upland surface was subsequently modified through tillage to create furrows perpendicular to flow, to limit excessive overland flow, increase recharge to the upland aquifer, and better facilitate development of plant rooting architecture (Sutton and Price, 2020a; Gingras-Hill et al., 2018; Ketcheson et al., 2017; Daly et al., 2012). In June 2015, a subsequent upland planting campaign occurred to actualize desired stand density (~10,188 additional tree and shrub saplings; Gingras-Hill et al., 2018).

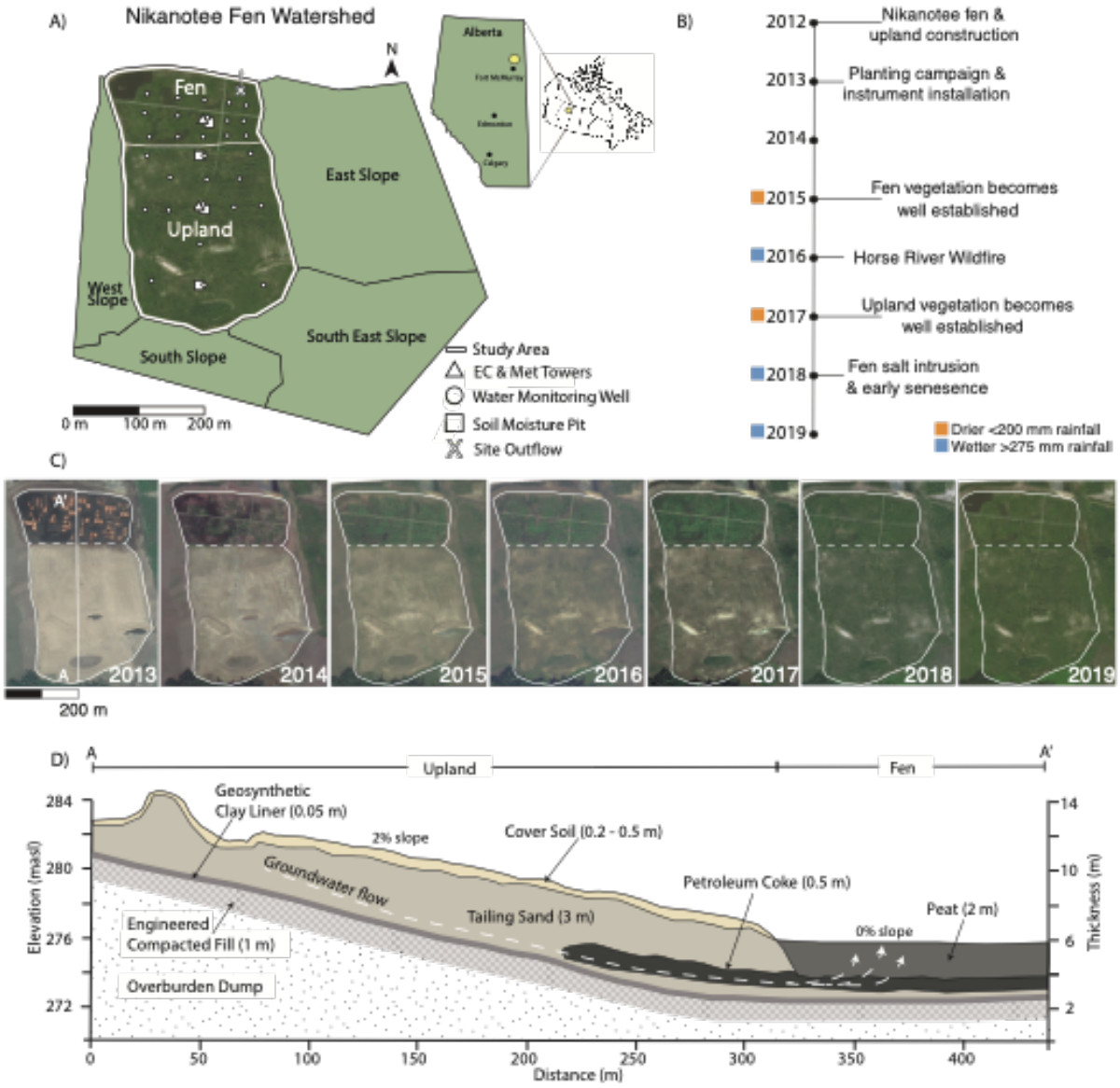


Figure 2-1: A) Map of the Nikanotee Fen Watershed depicting the regions of interest (Fen and Upland) and the locations of soil moisture pits, eddy covariance and meteorological towers and water monitoring wells. B) Summary of key changes and milestones in site development over the first seven years following construction. C) Satellite imagery of site (plant) development. D) Stratigraphic cross-section along a central transect (A-A', shown in Figure **2-**1C-2013) depicting the layering of substrate materials and general groundwater flow direction. The thickness of each layer is indicated in parentheses. Note that the thickness of the clay liner in the diagram is not to scale (illustrated thicker than the actual 0.05 m thickness).

Materials used in construction included locally and readily available recovered materials from mining operations, such as by-products of the bitumen extraction process (tailing sand, petroleum coke) and salvaged overburden (peat and forest mineral soils) from the initial clearing of natural landscapes on oil sands leases (Daly et al., 2012). In addition to being abundantly available, these recovered materials were used as they had the appropriate hydrophysical properties for recreating the requisite hydrologic connectivity (Price et al., 2010). The constructed upland-fen complex is underlain by an impermeable, engineered geotextile clay liner (0.05 m thick), which encourages lateral flow while limiting deep water loss to the regional water table (Figure 2-1D). Above the liner is a 0.5 m thick layer of tailing sand overlain by a 0.5 m thick layer of petroleum coke, which extends beneath the fen and partway into the upland, acting as a highly permeable underdrain to improve hydrological connectivity and more evenly distribute water and solute flows beneath the fen (Figure 2-1D; Simhayov et al., 2017; Daly et al., 2012). The entire system was constructed on, and due to the clay liner is hydrologically isolated from, a fine-textured over burden dump (Figure 2-1D).

In the upland, 2-3 m of tailing sand creates an aquifer to support transport of water from upland to fen due to its relatively high hydraulic conductivity (Sutton and Price, 2020a). However, these physical properties also result in poor moisture retention, which in turn impedes plant growth and development (Fung and Macyk, 2000). Moreover, as a by-product of bitumen extraction, tailing sand contains residual amounts of highly mobile solutes, namely sodium (Na^+), amongst other constituents (Simhayov et al., 2017; Rezanezhad et al., 2012), which can affect water quality (Biagi et al., 2019; Kessel et al., 2018; Simhayov et al., 2017; Rezanezhad et al., 2012) and plant function and diversity (Vitt et al., 2020; Nwaishi et al., 2016; Pouliot et al., 2012; Trites and Bayley, 2009). As such, a capping layer of salvaged forest soil (LFH, sandy loam to loam) was

placed on top of the tailing sand to better promote plant growth and function by limiting the degree of solutes in the rooting zone and improving rooting zone water retention (Naeth et al., 2013). Cover soil thickness is variable throughout the upland and ranges between 20 to 50 cm thick. Planting prescriptions followed procedures outlined by the Cumulative Environmental Management Association revegetation manual (Alberta Environment, 2008). Revegetation used native species common to WBP uplands such as black spruce *(Picea mariana*), jack pine (*Pinus bankstana*), willow (*Salix sp*.), Labrador tea (*Ledum rhododendron*), bunch berry (*Cornus stolonifera*), and bog cranberry (*Vaccinium oxycoccos*) and is classified as a 'b/d' ecosite - consisting of tree and shrub species (Beckingham et al., 1996). The upland is characterized by its deep water table (~2 m bgs) and drier surface conditions (Table 2-1).

The fen consists of 2 m of donor peat salvaged from newly developed lease areas, which was well decomposed, and intentionally derived from lower horizons lacking living roots, seeds or rhizomes. The fen was revegetated using an experimental factorial design that included mulching and weeding treatments on plots that had control (bare), moss, seedlings, seedling and moss and seeds (Borkenhagen and Cooper, 2019). In anticipation of pulses of Na^+-rich upland water, planting prescriptions incorporated both freshwater and saline sedge and graminoid species (*Carex aquatilis* (water sedge), *Calamagrostis stricta* (narrow reed grass), *Juncus balticus* (wire rush), *Triglochin maritima* (seaside arrow grass)), as well as a combination of *Sphagnum* and brown moss species harvested from a local rich fen via the moss transfer method (Rochefort et al., 2003). Ponds were not part of the original design, but the fen has had permanent standing water since 2013 and much of these ponded regions have become robust with invasive *Typha latifolia*. The fen is classified as a 'j' ecosite – rich fen dominated by sedge species (Beckingham et al., 1996). In contrast to the upland, the fen is characterized as a much wetter environment with a near

surface water table and high volumetric water content (Table 2-1). During the study period, NFW experienced several biophysical changes driven by autogenic and allogenic factors. Figure 2-1B provides a summary of milestones in site development.

Table 2-1: Soil and vegetation characteristics of the NFW fen and upland. Soil moisture and water table depths are mean values from 2013-2019.

		Fen	**Upland**
Size (ha)		2.9	7.7
Substrate (m)		2 m salvaged peat 0.5 m petroleum coke 0.5 m tailing sand	0.2 – 0.5 m salvaged forest floor material (LFH; cover soil) 0.5 m petroleum coke 3 m tailing sand
Planted		June 2013	June 2013 July 2015
Dominant (as of 2019)	**Species**	*Carex aquatilis* *Juncus balticus* *Typha latifolia* *Ptychostomum pseudotriquetrum*	*Populus tremuloides* *Populus balsamifera* *Picea mariana,* *Pinus banksiana*
Volumetric Soil Moisture (5 cm) (%)		84	20
Volumetric Soil Moisture (30 cm) (%)		87	32
Water Table Depth (cm bgs)		8	209

2.3 Methods

This study focuses on the upland and fen landscapes of the NFW system (Figure 2-1) during the snow-free, growing season period (May – September; DoY 135-255, n = 120 days) from time of construction (2013) to present (2019). Here, peak season is defined as end of June to early August (DoY 170 – 220), based on plant dynamics and meteorological trends. 2016 has limited data (covering only DoY 178 – 230 (n = 52) in the fen and DoY 178 – 256 (n = 78) in the upland) due to the Horse Creek wildfire evacuation that affected Fort McMurray and surrounding region.

2.3.1 Micrometeorological Setup

Both upland and fen meteorological systems had similar sensor configurations. Ground heat flux (Qg, Wm^{-2}) was calculated using ground heat flux probes (HFT3; Campbell Scientific: Logan, Utah, USA) inserted horizontally at depths of 5 cm below the ground surface, several meters apart and facing south. Air temperature (Tair, ^{o}C) and relative humidity (rH, %) were measured using a Rotronic HC2S3 (Campbell Scientific: Logan, Utah, USA), while precipitation (P, mm) with a tipping bucket (Texas Instruments TR-525M) placed within a clearing near the tower to avoid canopy and tower influences. 2016 precipitation data was gap-filled using nearby environment canada records. Vapour pressure deficit (VPD, kPa) was calculated using saturated vapor pressure (es), actual vapor pressure (ea), relative humidity (rH) and air temperature (Tair), (Howell and Dusek, 1995). Net radiation (Q*, Wm^{-2}) was measured using a CNR4 (Kipp Zonen; Delft, Netherlands). All meteorological data was sampled at 1-minute intervals and averaged every 30-min on a CR1000 datalogger (Campbell Scientific: Logan, Utah, USA). Each site had coupled eddy covariance systems, consisting of a closed path CO_2/H_2O gas analyzer (LI-7200: LI-COR: Lincoln, Nebraska, USA) and 3D sonic anemometer (Windmaster Pro: Gill Instruments: Lymington, Hampshire, UK) from 2013-2014, and an open path CO_2/H_2O gas analyzer (LI-7500: LI-COR: Lincoln, Nebraska, USA) with a 3D sonic anemometer (CSAT3 3D: Campbell Scientific: Logan, Utah, USA) from 2015-2019. Half-hourly values of photosynthetically active radiation (PAR) were derived from measured incoming shortwave radiation (CNR4 (Kipp Zonen; Delft, Netherlands) using a numerical coefficient (Britton and Dodd 1976) and the LakeMetabolizer package in RStudio (Winslow et al., 2016; R Core Studio, 2021). Due to developing vegetation in the upland, the height of the eddy covariance system increased from 2 m (2013-2017) to 3 m (2018-2019) to maintain representative flux footprints (Figure 2-2).

2.3.2 Eddy Covariance Data Processing

Raw eddy covariance (EC) data were collected at 20 Hz and averaged every 30-min where corrections for coordinate rotation (double rotation; Kaimal and Finnigan, 1994), time lag and sensor separation (Leuning and Judd, 1996) and density effects (Burba et al., 2012) were applied, following common Fluxnet protocols (Webb et al., 1980; Leuning and Judd, 1996; Foken and Leclerc, 2004; Aubinet et al., 2012). Resulting half-hour fluxes were then processed to ensure each half-hour flux record had 80% of the high-frequency records to maintain data quality. Data collected from open path systems (2015 – 2019) had additional filtering to remove periods that experienced precipitation or had the potential for dew formation on the infrared gas analyser lenses. Further outliers were removed by comparing a moving average for 10 half-hour means ± 3 standard deviations of neighboring values, as well as comparing each half-hour for each year to remove any outliers that were outside of a ± 3 standard deviations. A final manual check was completed to remove any physically improbable values. The Kljun et al. (2004) footprint analysis was used to constrain the measured fluxes to be within 80% of the desired site boundaries; this was also used to determine flux distances used in this study (Figure 2-2). Periods of low friction velocity (u*) were removed following methods outlined in Wutzler et al. (2018), using a 50% u* threshold for all flux data. Filtered NEE were gap-filled using MDS method outlined in Reichstein et al. (2005) and then partitioned into respiration (R_{eco}) and gross ecosystem production (GEP) using the relationship between night-time respiration and Tair (Reichstein et al., 2005). In this study, negative NEE indicates net ecosystem CO_2 uptake from the atmosphere. Latent heat flux (Qe) was gap-filled by scaling potential evapotranspiration (PET) to actual evapotranspiration (AET) by calculating the ratio between AET and PET, where α is the scaling variable, for each available half-hour. This ratio was then gap-filled using the MDS method

outlined in Reichstein et al. (2005) where Q*, VPD, and u* were used as the gap-filling conditions. Sensible heat flux (Qh) was then gap-filled by solving the energy balance equation, using measured and gap-filled Q*, Qe and Qg. Water-use efficiency (WUE) was calculated as a ratio between gross ecosystem productivity (GEP) and AET (Volik et al., 2021).

2.3.3 Edaphic Conditions and Hydrometric Network

Continuous measurements of volumetric water content (VWC) were collected at soil moisture pits along a north-south transect across both landscape units (three in upland, one in fen) (Figure 2-1A). VWC was measured over depths of 5 – 100 cm, however, only the 5, 15, 30 cm depths are reported here, as they represent the zone of most root biomass. Soil moisture pits were instrumented with dielectric impedance reflectometry soil moisture probes (Stevens Hydra Probe II) at each respective depth and recorded dielectric permittivity at one-minute intervals. Measurements were temperature and salinity corrected and converted to VWC based on a calibration (Seyfried et al., 2005) specific to the substrate material the probes were located in. Values were subsequently averaged to daily intervals. Soil temperature was measured at the meteorological stations using thermocouples (Type k thermocouple (2013-2018), CS-109 soil temperature probes (2019)) at 5 cm depth.

An extensive monitoring network of wells and piezometers was installed across NFW (Figure 2-1). WTD was logged automatically through pressure transducers (HOBO MX2001-S, Onset, Massachusetts, USA) and coupled with weekly manual measurements. Wells were 2.54 cm inner diameter (I.D.) polyvinyl chloride (PVC) pipes that were fully slotted and wrapped with well screening (Ketcheson et al., 2017). Well depths were 1.5 m in the fen and 2.75 m in the upland (initially). In 2014, upland wells were lengthened to capture water table positions below 3 m.

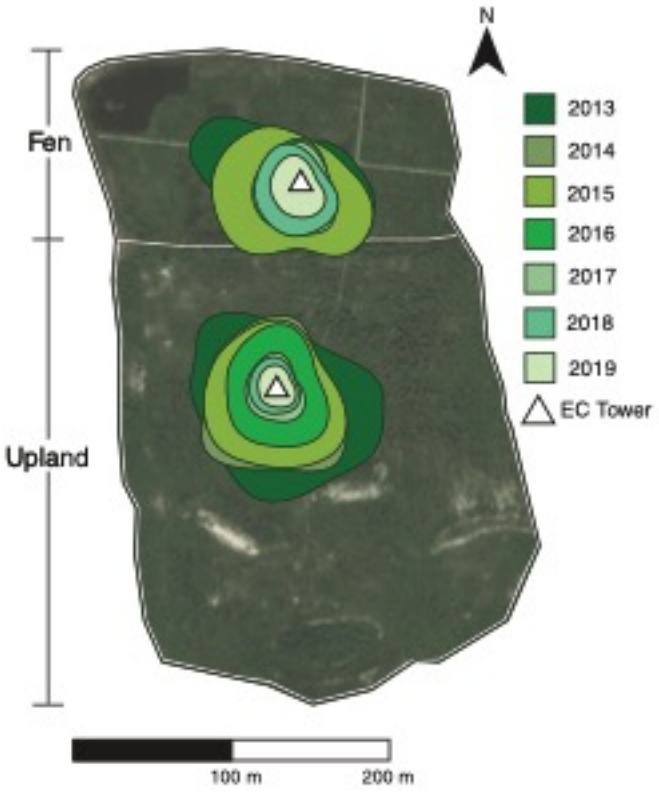


Figure 2-2: Footprint of tower fetch for fen and upland from 2013 - 2019. Fetch decreases as the system develops. Increase in plant height results in an increase in surface roughness (thus, decrease in fetch). Note the similar extent of flux footprint in the fen from 2016 onwards once vegetation becomes stable.

2.3.4 Vegetation

2.3.4.1 Field-based measurements

Leaf area index (LAI) was measured monthly along transects across both landscapes using LP-80 (2014-2018) and LI-2200C (2019) LAI probes. Two readings were taken at each measurement location: one at, or near, the ground surface and another above the understory vegetation. This allowed LAI results to be calculated for the understory and canopy layers, as well as the sum total. LAI was corrected for canopy clumping, needle-to-shoot, woody-to-total area ratios, and sun-scattering effects (Chen, 1996; Chen et al., 1997; Li-Cor, 2013). The sparse nature of the upland

canopy made it difficult to measure LAI of the canopy without large uncertainty and error. As such, LAI measurements are supplemented with other vegetation metrics to provide a more accurate description of vegetation characteristics.

Non-destructive vegetation surveys were conducted annually during peak growing season. In the fen, 60 x 60 cm collars installed for chamber-based CO_2 flux measurements were used as the survey area (n=32), where percent cover of vascular plant species, litter, bare ground, and water were estimated, along with measurements of plant height and litter thickness. In the upland, tree surveys were completed using 10 randomly placed 10 m x 10 m plots, where species, height, and diameter at breast height (DBH) were measured. Trees less than 1.37 m in height were classified as saplings. Understory vegetation surveys were completed within these large plots (n=5 within each 10 x 10 plot), using a randomly placed 1 x 1 m quadrat.

2.3.4.2 Enhanced Vegetation Index

Enhanced vegetation index (EVI) was derived to supplement field-based measurements and capture spatial and temporal vegetation development. While many vegetation indices are available (e.g., Normalised Difference Vegetation Index (NDVI); Red Edge Position (REP); Photochemical Reflectance Index (PRI) and EVI; see Lees et al. (2018) for more details), EVI best fit the "open" canopy nature of NFW, as it includes the blue band and background canopy correction, which helps better discern vegetation from wet, dark soils and leaf litter (Huete et al., 2002) - both of which are common in peatland settings. Additionally, EVI adjusts for atmospheric interference (clouds and aerosol particulates; Huete et al., 2002) and has been successfully applied in settings where biomass burning results in increased aerosol particulates (Ben-Ze'ev et al., 2006; Miura et al., 1998) and in regions with high pollution (Tariq et al., 2021; Zhang et al., 2016). Aerosol

interference is amplified at NFW, compared to natural settings, due to its proximity to mining operations (e.g., mine dust) and frequent forest fire haze.

EVI consists of reflectance from the near infrared (NIR), red (R) and blue (B) bands within the short-wave spectrum and is calculated using:

$$EVI = G \frac{NIR - RED}{NIR + C_1 \times RED - C_2 \times BLUE + L} \quad (1)$$

where *L* is the canopy background adjustment that addresses nonlinear, differential *NIR* and *RED* radiant transfer through a canopy, and *C1, C2* are the coefficients of the aerosol resistance term, which uses the blue band to correct for aerosol influences in the red band. Coefficients adopted in the EVI algorithm are, *L*=1, *C1* =6, *C2* = 7.5, and *G* (gain factor) = 2.5 (Huete et al., 2002; Huete, et al., 1997; Huete et al., 1994).

Here, satellite-derived, 30-m resolution EVI provides an ecosystem scale snapshot of vegetation development using Landsat 8 imagery acquired through USGS (Vermote et al., 2016). Temporal resolution of Landsat 8 is 8-16 days and had complete coverage during the study period. EVI was derived using the Google Earth Engine (GEE) application processing interface (API; Gorelick et al., 2017) and post-processed using a cloud masking script (modified by authors from GEE API Guides) to further remove effects of cloud cover, forest fire haze and mine dust (correcting for 75% of interference). Mean, peak-season (DoY 170-220) EVI values are presented here as a metric to spatially characterize the extent and development of vegetation in years following construction. Additionally, the mean of a 60 x 60 m pixel grid located at the epicenter of flux tower footprints was calculated to create a time series spanning 2013-2019. In order to provide context to EVI results, the grid method was applied to two nearby natural systems comprised of similar plant communities as well (saline fen and mixed wood upland).

2.4 Results

2.4.1 Environmental Conditions

As the two landscapes are adjacent to one another, meteorological variables (such as Tair and P) were consistent between the two landscapes. Differences between the two landscapes were most apparent in edaphic conditions and vegetation.

2.4.1.1 Climatic Conditions

Tair throughout the growing seasons varied between -4 to 36 ^{o}C (Figure 2-3B), while average seasonal temperatures ranged between 15.5 – 19.3 ^{o}C and were consistently above the 30-year climate normal (13.3 ^{o}C; Table 2). June, July, August (JJA) average temperatures ranged from 17.4 to 20.3 ^{o}C (again, above the 15.7 ^{o}C 30-year normal), with 2016 being the warmest and 2019 the coolest. Based on Tair and P trends, 2015 and 2017 were considered warmer, drier years (<200 mm year^{-1}), while 2018, 2019 were cooler and wetter (Table 2-2).

P ranged between 168 (2017) and 310 mm (2016), and all years except 2016 and 2019 had less rainfall than the 30-year average (283.4 mm; Figure 2-3A). Interannual variability in the timing, frequency and intensity of rain events was also present throughout the study period. Generally, most rainfall occurred during the months of June and July with the exception of 2019, where 126 mm (44% of seasonal rainfall) occurred in August. Over the seven-year study period, 75% of rain events were < 5 mm day $^{-1}$. Large/intense rain events (>30mm day^{-1}) typically occurred towards the end of July and into August (2018, 2019). Of note is July 2018, where 86 mm of rain fell over 4 days (30% of 2018 total rainfall), resulting in extensive ponding within the fen.

Maximum photosynthetically active radiation (PAR) typically occurred in mid to late June (between DoY 155-180), ranging between 1590 to 2042 μmol m^{-2} s^{-1}. During peak season, PAR

was highest between 11h00-17h00, with an interannual average of 947 µmol m^{-2} s^{-1}. By mid-August, PAR begins its

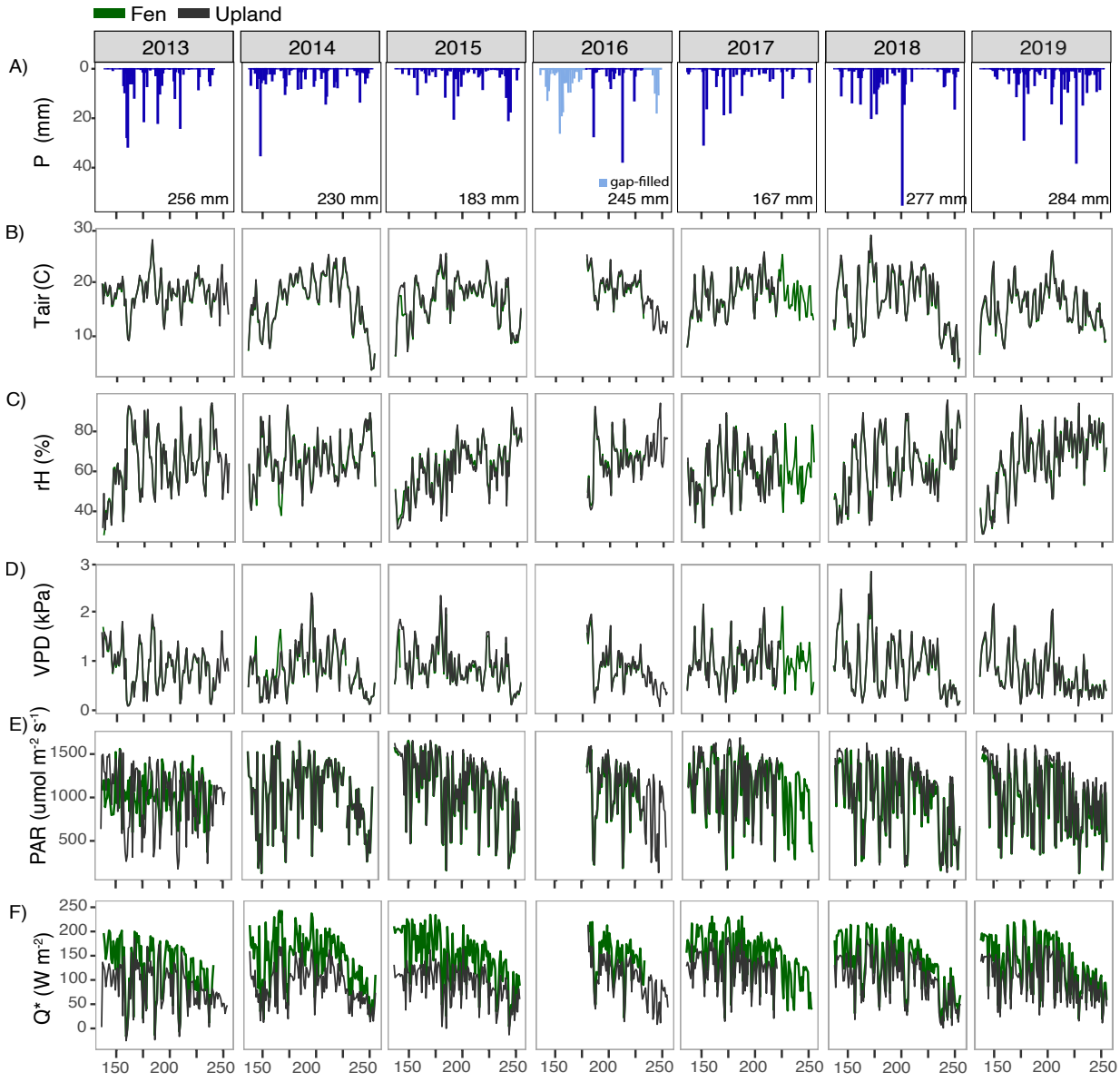


Figure 2-3: Seven-year time series of seasonal meteorological characteristics for the Fen (green) and Upland (grey). A) Daily precipitation (P, mm). B) Mean daily air temperature (T_{air}, °C). C) Mean daily relative humidity (rH, %). D) Mean daily vapour presser deficit. (VPD, kPa). E) Mean daily mid-day (10:00 – 16:00) photosynthetically active radiation (PAR, umol m^{-2} s^{-1}). F) mean daily net radiation (Q*; Wm^{-2}). Note the significant overlap between fen and upland values. Due to the close proximity of the landscapes (and thus towers; <300 m apart) atmospheric conditions were largely similar. Missing data in 2016 is due to Horse Creek Wildfire. Missing data from the upland in 2017 Upland is due to instrumentation malfunction.

autumn decline with daytime values averaging 731 μmol m^{-2} s^{-1}. A wide range of daily relative humidity values with an interannual average of 64% (Figure 2-3C) was observed. Of note, was the relatively large VPD, which remained relatively constant both intra and inter seasonally and reflected a large atmospheric demand for ET. Average seasonal VPD ranged between 0.75 (2019) to 0.97 (2017) kPa, with fluctuations in seasonal variability mirroring rainfall events (lower during wet periods/years) (Figure 2-3D). Interannual net radiation (Q*) varied between the fen (137 Wm^{-2}) and upland (99 Wm^{-2}). Fen Q* had remained relatively constant from 2014 onwards, whereas upland Q* exhibited an increasing trend as vegetation continued to mature. A more detailed examination of the surface energy balance is discussed in Chapter 3.

2.4.1.2 Edaphic Conditions

Water table (WT) position varied significantly between the two landscapes, being generally near the surface (interannual mean 8 cm bgs) in the fen and much deeper (interannual mean 209 cm bgs; Figure 2-4C) in the upland. Seasonally, mean water table depth (WTD) fluctuated slightly in the fen between wetter (2014, 2018, 2019) and drier years (2015, 2017). The largest range in fen WTD was in the year following construction (2013, -13 to 45 cm bgs); however, the initially low WT was during the wetting-up period of the fen. Mean upland WTD ranged between 158 cm bgs in 2014 to 257 in 2019. In both landscapes, smaller scale (<10mm), sporadic rain events appear to have a negligible impact on WTD position, however, larger or recurring rain events (2018) or prolonged dry periods (2017) influenced WTD (Figure 2-4A, C).

Edaphic conditions between the two landscapes varied significantly due to differences in substrate that affect the soil water holding capacity and the aforementioned differences in WTD. Fen soil temperatures varied from -4 (Sept 2014) to 29 ºC (June 2015) (Figure 2-4B). Seasonally, mean peat temperatures decreased over time from 16.6±4 (2013) to 12.1±4 ºC (2019). Warmest

mean seasonal peat temperatures occurred in 2014 (18.6±7 ºC). Mean seasonal upland soil temperature varied less across all years, decreasing only slightly over time from 20.5±7 (2013) to 18.3±5 ºC (2019).

Soil volumetric water content (VWC) was measured at 5, 15, and 30 cm bgs. In both landscapes, 30 cm values were consistently wettest (87% fen, 33% upland) and upper 5 cm driest (83% fen, 19 % upland) (Figure 2-4D). Fen VWC remained high throughout all years, ranging between 72 to 92 % (Figure 2-4D). Moreover, fen VWC appeared to remain relatively stable, with only slight increases occurring during large rain events. However, prolonged dry periods in the fen led to a decline in moisture content in the near surface (top 5 cm), as exhibited in 2017 when values dropped from 85% down to 72 % (Figure 2-4D). During wetter years, fen VWC measured at 15cm depth was 2-6% drier than the upper, near surface peat, while the opposite trend emerged during drier years (5cm typically drier than deeper peat). Upland soil layers exhibited larger differences between depths and were generally much drier. Mean daily VWC ranged from 10 – 40 % (Figure 2-4D). In contrast to the fen, upland VWC showed rapid responses to rain events, resulting in values fluctuating up to 20% over a few days (see years 2018, 2019 in Figure 2-4D).

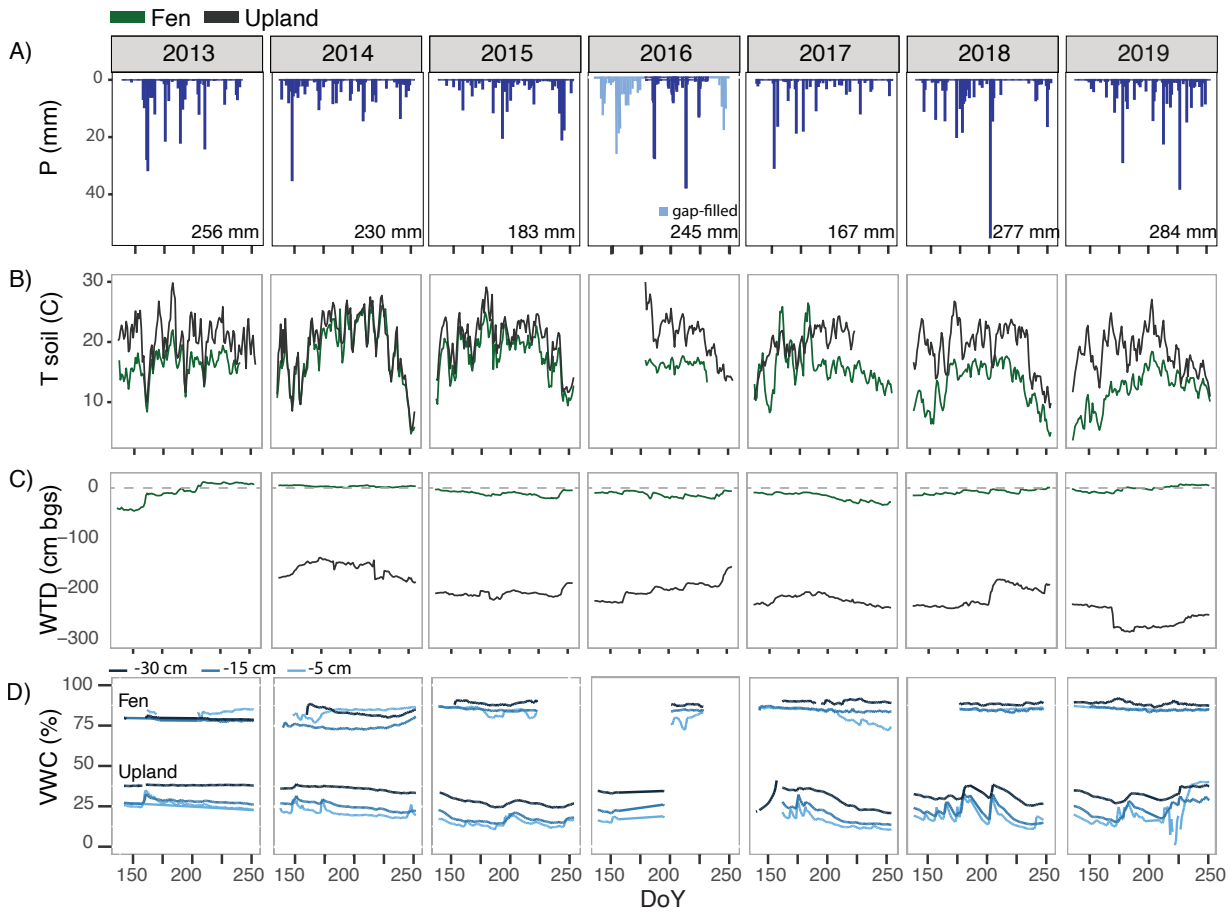


Figure 2-4: Time series of edaphic and water table conditions in the Fen (green) and Upland (grey) from 2013 – 2019). A) Daily precipitation (mm). B) Mean daily soil temperature (C) at 5 cm below ground surface. C) Mean daily water table levels (cm below ground surface). D) soil moisture conditions (volumetric water content) at 5 (light blue), 15 (blue) and 30 (dark blue) cm below ground surface.

Table 2-2: Summary of growing season means (±SD) of NFW environmental variables: air temperature, precipitation, relative humidity, vapour pressure deficit, photosynthetically active radiation, net radiation, water table depth, soil temperature, volumetric water content (at 5, 15 and 30 cm depths), electrical conductivity (E_c), and sodium concentration (Na^+). E_c and Na^+ are presented here as they depict changes in water quality during ecosystem development. Methods and a detailed analysis of solute transport and water quality changes at NFW are discussed by Kessel et al. (2018).

	T_{air}	P	rH	VPD	PAR mid-day	Q*	WTD	T_{soil}	VWC 5 cm	VWC 15 cm	VWC 30 cm	E_c[2]	Na^{+2}
	°C	mm	%	kPa	umol m^{-2} s^{-1}	Wm^{-2}	cm bgs	°C	%	%	%	µs cm^{-1}	mg L^{-1}
Fen													
2013	18±5	256	64±22	0.86±0.71	1034±620	123±200	8±19	16±4	83±3	78±1	79±1	2051±635	96±51
2014	17±6	230	66±21	0.81±0.71	1091±480	143±212	-3±1	19±7	84±2	75±2	83±2	2524±832	79±59
2015	17±6	183	62±22	0.85±0.72	1138±490	146±213	11±5	18±7	84±2	85±1	89±1	2606±708	157±89
2016	19±5	310[1]	66±19	0.91±0.72	1115±461	147±205	12±5	16±2	79±3	84±0	88±1	2954±1376	158±99
2017	17±6	168	60±22	0.97±0.77	1161±459	146±207	18±8	16±4	82±5	85±1	9±2	2914±885	179±80
2018	17±7	278	63±22	0.89±0.84	1006±480	130±189	8±4	13±4	85±0	85±1	88±1	2440±767	219±114
2019	15±6	285	65±23	0.75±0.72	1027±461	130±186	1±6	12±4	85±1	85±1	89±1	--	112±99
Upland													
2013	18±5	257	64±22	0.88±0.73	1150±476	85±169	--	21±7	26±2	28±1	38±0	2623±1090	269±162
2014	17±6	231	66±21	0.81±0.74	1109±476	90±168	158±19	20±8	21±3	25±3	36±1	2131±901	132±107
2015	17±6	183	61±22	0.93±0.79	1193±487	91±173	207±7	21±6	15±2	17±2	27±2	2332±812	241±152
2016	18±5	310[1]	67±20	0.81±0.7	1044±484	100±181	200±17	21±5	16±1	22±1	34±0	2522±887	131±72
2017	18±6	141	59±22	0.99±0.77	1200±489	124±197	220±10	20±4	15±4	19±5	29±6	3254±1195	180±66
2018	17±7	278	63±22	0.9±0.85	1073±511	103±175	213±20	19±5	18±5	21±5	31±3	2596±997	184±148
2019	16±6	285	65±23	0.76±0.73	1106±493	106±176	257±19	18±5	22±9	23±5	33±3	--	--

[1] Fen and upland 2016 P gap-filled due Horse River fire evacuations using Environment Canada data
[2] Mean value from all well and piezometer depths, methods and values reported by Kessel et al., 2018.

2.4.1.3 Vegetation Dynamics

Fen plant community was dominated by *Carex aquatilis*, with smaller regions of *Typha latifolia* and *Juncus balticus*, with *Typha latifolia* dominating ponded regions. The greatest increase in fen plant foliage occurred from 2014 to 2015, with aboveground biomass and LAI increasing from 395.38±46 g m^{-2} and 0.4±0.14 to 518.20±29 g m^{-2} and 1.21±0.08, respectively (Table 3; Messner, 2019). 2015 onwards, LAI remained relatively constant (interannual mean of 1.53±0.21) and values were typically largest in August. 2018 exhibited lowest foliage yields out of all developed years (aboveground biomass: 412.14±38, LAI: 0.59±0.07). As of 2019, mean plant height was 54 cm (*Carex aquatilis*), 105 cm (*Typha latifolia*) and 41 cm (*Juncus balticus*). *Carex aquatilis* and *Typha latifolia* both produce large amounts of seasonal litter, resulting in litter thickness at the fen varying between 5 to 27 cm thick (18 cm average) as of 2019 (Table 3).

Upland trees developed slowly during initial years and became robust by 2017. Prior to 2017, the upland was dominated by patches of bare ground, understory vegetation (shrubs and dry grasses) and juvenile trees. Upland LAI ranged from 0.02 (2013) to 2.56 (2019; Table 3). Typically, peak LAI values were observed in July with broadleaf species senescing by mid-August. As of 2019, mean tree height of all species ranged between 1.14 and 1.87 m (Table 3). Variability in tree height and DBH was large for *Populus balsamifera* due to the significant abundance of tree saplings in the transect area (excluding saplings, average height and DBH are 1.9 m, 4.2 cm).

Seasonal mean EVI values for the fen illustrate the rapid increase from bare ground in 2013 (0.18±0.04) to expansive plant coverage by 2015 (0.36±0.1) (Figure 2-5A), with an EVI >0.2 representing a vegetative signal (Huete et al., 2002). From 2015 onwards, mean seasonal EVI fluctuated between 0.32±0.09 (2019) to 0.47±0.16 (2017). Mean peak season EVI values varied

between early years (2013-2014) and later years (2015-2019), after vegetation became established, from 0.25 to 0.48, respectively. 2017 exhibited the highest mean peak season EVI of 0.59±0.06.

Upland EVI values increased annually, but at a slower rate, compared to the fen, with values remaining low from 2013-2016 (interannual mean 0.23±0.0; Figure 2-5A). As trees matured, EVI increased from 2017 onwards (interannual mean 0.44±0.02h; Figure 2-5A; Table 2-3).

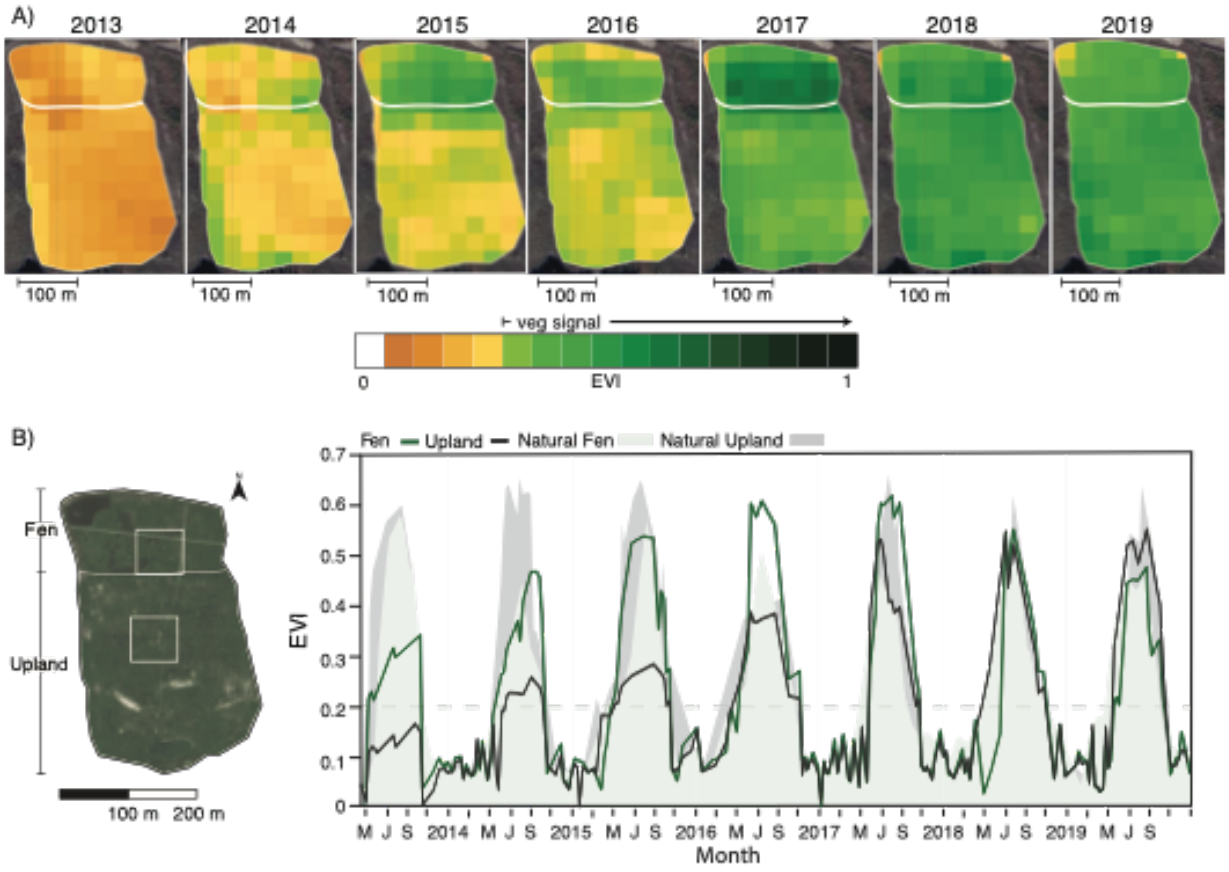


Figure 2-5: Temporal snapshot of plant development in the fen and upland from 2013-2019. A) Ecosystem scale mean peak season (DoY 170-220) Enhanced Vegetation Index (EVI). B) Timeseries of EVI values from the mean of a pixel grid (60 x 60 m) located at the epicenter of flux tower footprints (white square). Light green and grey shading depict values from nearby natural sites with similar plant compositions.

Table 2-3: Summary of average (± SD) vegetation biometrics for the NFW fen and upland from 2013-2019 including seasonal aboveground biomass (measured in the fen only), leaf area index (LAI), enhanced vegetation index (EVI) for the growing season and peak season (DoY 170 – 220), vegetation or tree height, diameter at breast height (dbh) and litter thickness. – represents years where measurement was unavailable due to juvenile plant size (fen 2013; upland 2013-2016) and/or incomplete data due to instrument malfunctions or unfavourable environmental conditions.

	Aboveground Biomass[1]	**LAI**	**EVI**	**EVI**	**Vegetation Height** cm			**Litter Thickness**
	g m^{-2}		growing season	peak season	*Carex*	*Juncus*	*Typha*	cm
Fen								
2013	--	--	0.18±0.04	0.21±0.03	--	--	--	--
2014	395±46	0.4±0.14	0.24±0.06	0.26±0.03	8.6±5.0	8.2±2.8	--	--
2015	518±29	1.21±0.08	0.36±0.11	0.44±0.01	--	--	--	2.7±1.6
2016	557±38	--	0.45±0.12	0.49±0.07	--	--	--	--
2017	521±34	1.77±0.18	0.47±0.16	0.57±0.06	51.3±10	45.5±5	95±26	12±6.2
2018	412±38	0.59±0.07	0.38±0.14	0.49±0.03	46±7	47±9	101±28	16.2±7.6
2019	442±31	1.63±0.26	0.32±0.09	0.39±0.02	54±14	41±12	105±23	17.8±9.5

					Deciduous		**Coniferous**		
					height (m)	dbh (cm)	height (m)	dbh (cm)	
Upland									
2013	--	--	0.16±0.03	0.17±0.02	--	--	--	--	--
2014	--	--	0.21±0.03	0.23±0.02	--	--	--	--	--
2015	--	0.62±0.07	0.23±0.03	0.22±0.03	--	--	--	--	<1
2016	--	0.79±0.12	0.31±0.04	0.31±0.03	--	--	--	--	<1
2017	--	0.82±0.30	0.35±0.09	0.42±0.04	1.17±68	1.67±0.44	--	--	2.7±0.30
2018	--	0.75±0.02	0.34±0.14	0.44±0.05	1.70±0.61	2.12±0.67	1.47±0.40	1.3±0.58	3.2±0.50
2019	--	2.57±0.20	0.41±0.09	0.47±0.01	1.85±0.45	4.46±1.2	1.58±0.38	1.35±0.25	3.8±0.75

[1] Collected and analyzed by Messner, 2019

2.4.2 Carbon Dynamics

2.4.2.1 Gross Ecosystem Production (GEP)

Total GEP in the fen increased significantly, with total growing season values of 24 g C m^{-2} in 2013 to 279 g C m^{-2} in 2019 (Table 4A). Following planting (2014 onwards), seasonal fen GEP has remained above 279 g C m^{-2} (2019). Highest seasonal GEP occurred in 2015 at 512 g C m^{-2}, coinciding with the first year that vegetation was robust and expansive across the entire fen. Peak season (DoY 170-220) daily average GEP ranged from 0.7±0.8 g C m^{-2} day^{-1} (2013) to 5.6±1.5 g C m^{-2} day^{-1} (2015) (Table 4B). Peak season interannual average daily GEP was 4.4±1.3 g C m^{-2} day^{-1}. 2019 had the lowest peak season average at 3.4±0.7 g C m^{-2} day^{-1} and overall lowest trends in GEP out of the years with vegetation (2014 onwards). Highest daily GEP typically occurred in July (between DoY 180-210) and ranged between 2.6 (2013) to 8.4 (2015) g C m^{-2} day^{-1}. Average seasonal daily GEP ranged between 0.5±0.5 to 5.2±1.6 g C m^{-2} day^{-1} (Table 4B).

In the upland, total seasonal GEP increased from 65 in 2013 to 439 g C m^{-2} in 2019. Lowest average daily upland GEP was in 2013 at 0.5±0.3 g C m^{-2} day^{-1}, followed by an increase in 2014 (2±1.3g C m^{-2} day^{-1}), likely due to emergence of sparse understory vegetation (Table 4A). Moreover, there was a substantial increase in upland daily GEP in 2018 and 2019 (3.7±1.7 and 3.7±1.4 g C m^{-2} day^{-1}; Table 4B), when tree and understory vegetation were more established. 2017 onwards, seasonal GEP begins to exhibit a typical parabolic shape that follows foliation, peak season, and senescence in deciduous tree dominated ecosystems (Figure 2-6B). Similar to the fen, highest rates of GEP in the upland occurred between DoY 171 – 215, with later years all occurring before day 200 (191, 171, 181). Maximum daily GEP ranged from 1.4 (2013) to 7.9 (2018) g C m^{-2} day^{-1}.

2.4.2.2 Respiration (R_{eco})

Total seasonal fen ecosystem respiration (R_{eco}) also fluctuated during the first three years (2013-2015) ranging between 94 g C m^{-2} (2013) to 404 g C m^{-2} (2014, Figure 2-5A; Table 2-4A). From 2016 onwards, total R_{eco} remained relatively stable, ranging between 102 – 268 g C m^{-2} seasonally (Figure2- 6; Table 2-4A). Daily average R_{eco} ranged between 1.3±0.4 to 3.4±1.6, 2 g C m^{-2} day^{-1} (Table 2-4B).

Overall, upland R_{eco} was greater than in the fen across all years, with totals ranging from 207 (2016) to 620 g C m^{-2} (2014). Lower totals in 2016 and 2017 (246, 267 g C m^{-2}) were the result of missing data from tower malfunctions and fire evacuation. Higher R_{eco} in the upland compared to the fen corresponds to the higher upland soil temperatures and lower soil moisture (Figure 2-4).

2.4.2.3 Net Ecosystem Exchange (NEE)

The fen quickly developed from a carbon source (70, 2013) to a steady sink by 2015 (-243 g C m^{-2}) after which NEE remained a relatively stable sink of CO_2 (Table 2-4A, Figure 2-7). Average daily NEE ranged from 1.5±0.4 (2013) to -3.3±1.4 g C m^{-2} day^{-1} (2015), with highest NEE rates typically occurring in early July (Figure 2-6). The highest daily rate of NEE occurred in 2016 at -6.2 g C m^{-2} day^{-1}. Peak NEE occurred between DoY 185-206 in all years except for 2014 (DoY 243). Daily peak season uptake from 2015 – 2019 ranged between -1±1 (2019) to -3.3±1.4 (2016) g C m^{-2} day^{-1} (Table 2-4B). In 2015 the fen was a daily C sink throughout the observation period (Figure2- 7). From 2017 onwards, the start of daily CO_2 uptake occurred later each season. The timing of when net CO_2 uptake became prominent at the site followed plant green-up, with the latest date (post-2015) occurring in mid-June (DoY 160) in 2019.

In the upland, as vegetation became more established and GEP increased, a notable improvement in C sink capacity and daily C uptake occurred. Highest upland C emissions occurred during 2013, with 519 g C m^{-2} released. This subsequently decreased to an annual source of only 46 g C m^{-2} in 2019 (Figure 2-7, Table2- 4A). Average daily seasonal rates decreased from 4.4±1.0 g C m^{-2} day^{-1} in 2013 to 0.4±0.9 g C m^{-2} day^{-1} in 2019 (Table 4B). From 2017 onward, daily C uptake begins to occur more frequently throughout the season (Figure 2-7) from 0 days of uptake (2013-2016) to 21 days in 2017 (-8 g C m^{-2} sequestered) and 44 days in 2019 (-22 g C m^{-2} sequestered), equivalent to 0, 17 and 37% of growing season days with carbon uptake, respectively.

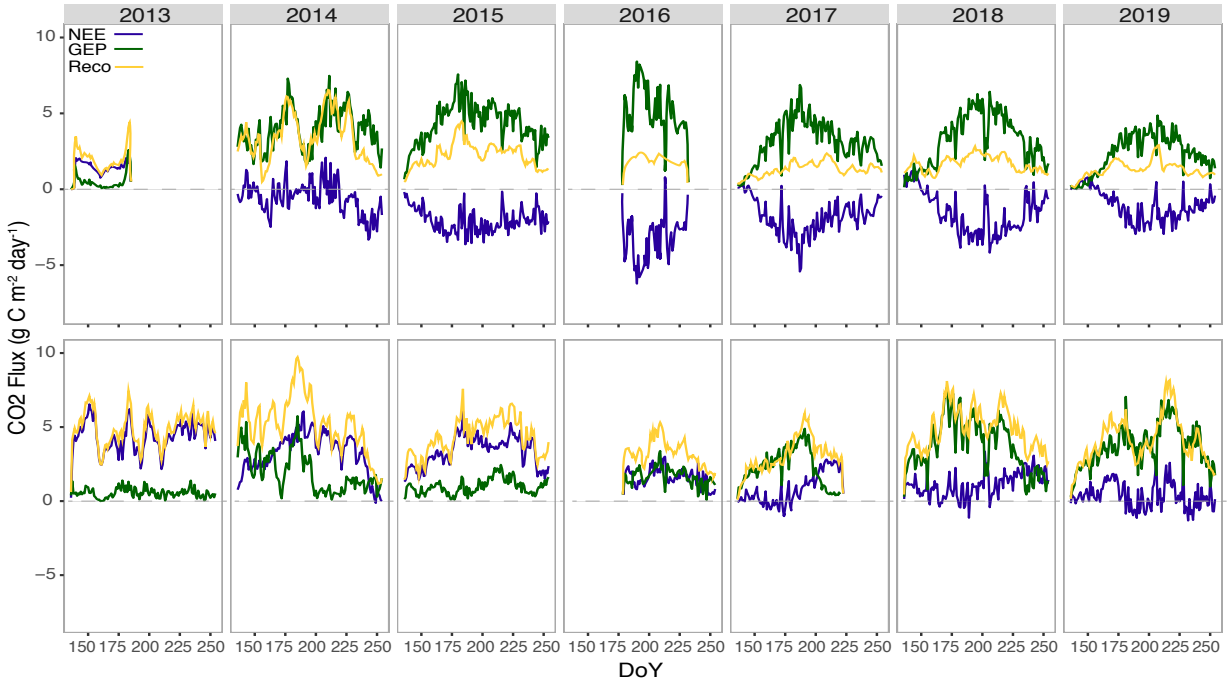


Figure 2-6: Seven-year time series of gap-filled mean daily gross primary productivity (GEP, green), respiration (R_{eco}, red) and net ecosystem exchange (NEE, blue) for the fen (top) and upland (bottom). Negative NEE values indicate carbon uptake from atmosphere.

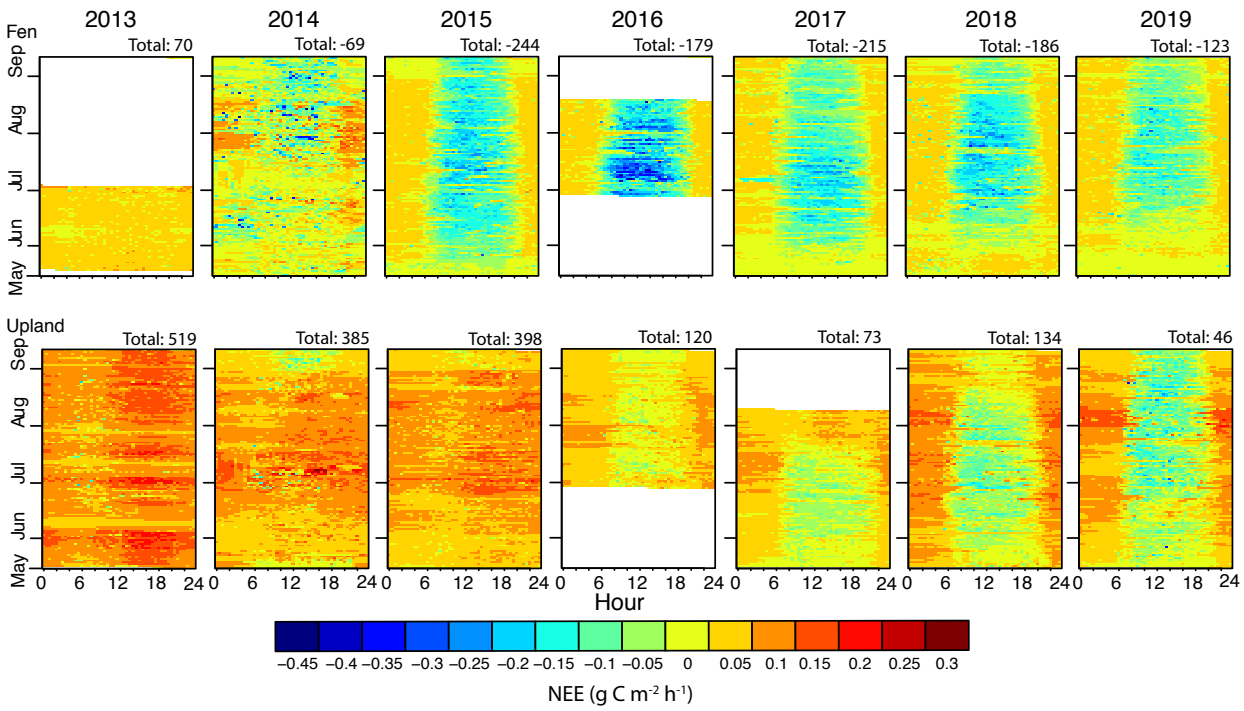


Figure 2-7: Gap-filled half-hourly net ecosystem exchange (NEE) fluxes from 2013 – 2019 for the fen (top) and upland (bottom). Each square is a half-hourly measurement, each row a full day. Fingerprint plots show seasonal (May-Sept, y-axis) and diurnal (hourly, x axis) trends. Note clear diurnal trends of C uptake once vegetation becomes established (2015 Fen, 2017 Upland). Positive values indicate a source of carbon to the atmosphere, negative values indicate carbon uptake by the surface. 2016 missing data is due to Horse Creek Wildfire. 2013 Fen: July-Aug and 2017 Upland: August missing data is due to instrumentation malfunction.

2.4.3 Water Dynamics

2.4.3.1 Evapotranspiration (ET)

Fen ET rates were higher in early years (2013-2015), in contrast to later years (2017 – 2019; Figure 2-8; Table 2-4B). Highest daily rates typically occurred between DoY 171 – 207 (slightly earlier than peak GEP), with the highest daily ET occurring in 2014 (7.8 mm day^{-1}, DoY 185). In later years, once vegetation growth had ensued, maximum daily ET ranged between 4.4 – 5.9 mm day^{-1}. Fen total seasonal ET exceed precipitation in all years during the study period (Table 4A).

Upland ET had remained relatively constant, with only a slight increase from 2014 to 2019. Mean daily ET rates ranged from 1.2±1.1 mm day^{-1} (2016) to 2.2±0.9 mm day $^{-1}$ (2018). Total seasonal ET remained relatively stable from 2013 – 2019 ranging between 147 and 260 mm (Table 2-4A) and exhibited a slight increase from 2017 onwards, coinciding with more mature vegetation. Upland ET exceeded seasonal precipitation in years 2015, 2016, and 2017 (Table 4A).

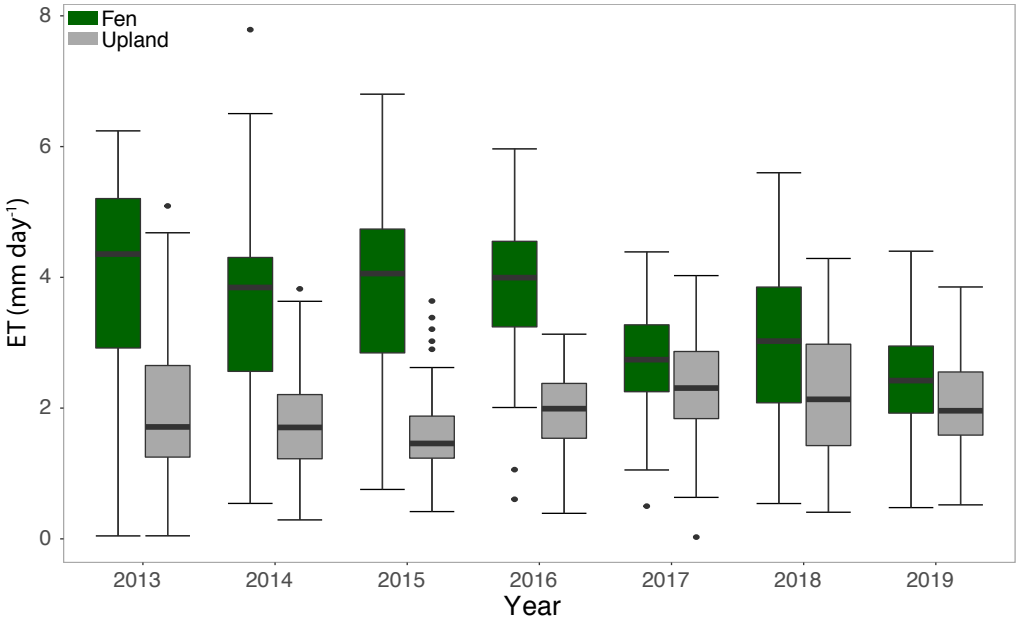


Figure 2-8: Daily evapotranspiration (ET) rates for the fen (green) and upland (grey). Black line indicates the median ET rate, the box represents the 25th to 75th quartile, the whiskers include 95% of the range, and the black circles are outliers.

2.4.3.2 Water-Use Efficiency (WUE)

Fen WUE increased from 0.6±1.0 in year 1 (2013) to 1.5±1.65 (2014) g C kg H_2O^{-1} day^{-1} in the first full growing season (Table 4B). This was followed by a relative stabilization in WUE across later (vegetated) years (2015 onwards) with an interannual mean of 1.7±0.5 (Figure 2-9, Table 2-4B). Following the development of vegetation, even in drier years (2015, 2017) WUE rates remained relatively stable. Upland WUE has been steadily increasing as vegetation continues to mature from 1.0±0.8 (2013) to 2.3±0.74(2019) g C kg H_2O^{-1} day^{-1}.

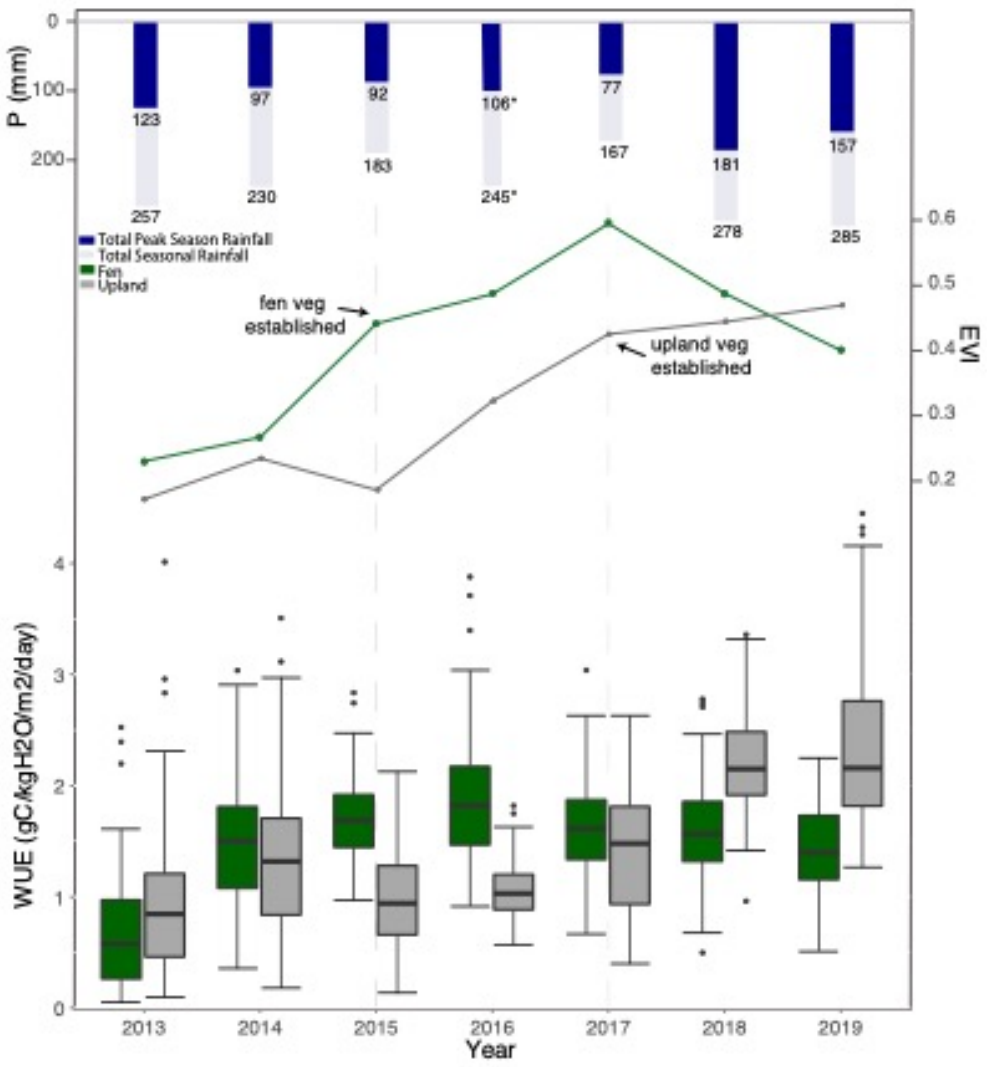


Figure 2-9: Daily water use efficiency (WUE, bottom) compared to peak season EVI (middle) and growing season rainfall(top). Black line indicates the median WUE, the box represents the 25th to 75th quartile, the whiskers include 95% of the range, and the black circles are outliers.

Table 2-4: Cumulative (A) and daily (B) values for carbon and water fluxes. **A)** Cumulative growing season (gs) and peak season (ps: DoY 170-220) carbon and ET fluxes from the fen and upland (2013 – 2019). CO_2 uptake represents the number of days with CO_2 uptake (based off on daily NEE) over 120 growing season days

A) Totals	**NEE**		**R_{eco}**		**GEP**		**CO_2 Uptake**	**ET**		**P-ET**
	gC m^{-2}		gC m^{-2}		gC m^{-2}		days	mm		mm
	gs	**ps**	**gs**	**ps**	**gs**	**ps**		**gs**	**ps**	
Fen										
2013[1]	70	24	94	35	24	11	0	326	164	-70
2014	-69	-1	404	225	474	226	86	424	212	-193
2015	-244	-123	269	145	512	268	114	452	207	-268
2016*	-179	-151	102	84	281	235	53	207	166	-87
2017	-215	-131	158	85	373	216	109	328	159	-160
2018	-186	-128	202	111	388	239	100	348	184	-71
2019	-123	-86	156	86	279	172	95	296	148	-12
Upland										
2013	519	208	585	240	65	32	0	243	131	14
2014	385	221	620	312	235	92	0	210	103	21
2015	398	201	514	256	117	55	0	188	94	-5
2016*	120	73	247	151	126	78	1	147	94	-27
2017[2]	73	67	267	191	194	123	21	207	118	-66
2018	134	46	579	303	445	257	17	260	140	18
2019	46	25	485	249	439	224	43	248	127	37

[1] Fen 2013: incomplete data due to EC tower instrument malfunction (n = 47; where n = number of days measured out of 120, see Figure 7)

[2] Upland 2017 incomplete data due to EC tower instrument malfunction (n=87)

***** Fen and upland 2016 incomplete data due Horse River fire evacuations (n = 54 (fen), 79 (upland))

Table 2-4: B) Daily growing season (gs) and peak season (ps) mean (± SD) carbon (NEE, R_{eco}, GPP) and water fluxes (ET, WUE) from 2013 – 2019.

B) Daily	NEE		R_{eco}		GEP		ET		WUE	
	g C m^{-2} day^{-1}		g C m^{-2} day^{-1}		g C m^{-2} day^{-1}		mm day^{-1}		g C kg H_2O^{-1} day^{-1}	
	gs	**ps**	**gs**	**ps**	**gs**	**ps**	**gs**	**ps**	**gs**	**ps**
Fen										
2013[1]	1.5±0.4	1.5±0.4	2±0.8	2.2±1	0.5±0.5	0.7±0.8	3.8±1.8	4±1.9	0.6±1.0	0.6±0.6
2014	-0.6±1.1	0±0.9	3.4±1.6	4.4±1.3	4±1.4	4.4±1.5	3.6±1.4	4.2±1.2	1.5±1.7	1.5±0.7
2015	-2±0.8	-2.4±0.8	2.3±0.8	2.8±0.7	4.3±1.4	5.2±1	3.8±1.3	4.1±1.3	1.8±1.3	1.8±0.4
2016*	-3.3±1.4	-3.6±1.4	1.9±0.4	2±0.3	5.2±1.6	5.6±1.5	3.8±1.1	3.9±1.2	2.1±1.7	2.1±0.7
2017	-1.8±1.2	-2.6±1.1	1.3±0.4	1.7±0.3	3.1±1.4	4.2±1.1	2.8±0.8	3.1±0.9	1.7±1.3	1.7±0.4
2018	-1.6±1.4	-2.5±1	1.7±0.5	2.2±0.3	3.3±1.7	4.7±1	2.9±1.2	3.6±1.2	1.8±1.3	1.8±0.4
2019	-1±1	-1.7±0.8	1.3±0.5	1.7±0.5	2.3±1.3	3.4±0.7	2.5±0.9	2.9±0.9	1.5±1.1	1.5±0.3
Upland										
2013	4.4±1	4.1±0.9	4.9±1.1	4.7±1	0.5±0.3	0.6±0.3	2±1.1	2.6±1.2	1.0±0.8	1.1±0.8
2014	3.2±1.4	4.3±0.6	5.2±1.9	6.1±1.8	2±1.3	1.8±1.5	1.8±0.7	2±0.7	1.5±0.8	1.2±0.8
2015	3.3±1	3.9±0.6	4.3±1.2	5±0.9	1±0.5	1.1±0.6	1.6±0.6	1.8±0.7	1.0±0.4	1.0±0.5
2016*	1±0.9	1.4±0.9	2.1±1.7	3±1.6	1.1±0.9	1.5±0.9	1.2±1.1	1.8±1	1.1±0.3	1.1±0.3
2017[2]	0.6±1	1.3±1.1	2.2±1.7	3.7±0.9	1.6±1.5	2.4±1.5	1.7±1.3	2.3±0.8	1.3±0.6	1.4±0.7
2018	1.1±0.8	0.9±0.9	4.9±1.4	5.9±1	3.7±1.7	5±1.3	2.2±1	2.7±0.9	2.2±0.5	2.3±0.5
2019	0.4±0.9	0.5±1	4.1±1.6	4.9±1.5	3.7±1.4	4.4±1.3	2.1±0.7	2.5±0.8	2.3±0.7	2.2±0.8

[1] Fen 2013: incomplete data due to EC tower instrument malfunction (n = 47; where n = number of days measured out of 120, see Figure 7)

[2] Upland 2017 incomplete data due to EC tower instrument malfunction (n=87)

* Fen and upland 2016 incomplete data due Horse River fire evacuations (n = 54 (fen), 79 (upland)

2.5 Discussion

2.5.1 Ecosystem Performance of NFW

The overarching goal of reclamation in the region is to create functional, self-sustaining, resilient ecosystems. As there is no singular metric or definition for ecosystem function, benchmarks encompassing ecologic, hydrologic and industry perspectives of ecosystem performance have been defined for NFW (Daly et al., 2012). Here, successful reclamation requires an ecosystem to be: 1) capable of supporting a representative assemblage of species; 2) carbon accumulating; and 3) able to withstand periodic environmental stress.

2.5.1.1 Capacity for supporting representative species assemblage

Plants play a fundamental role in nutrient, carbon and water cycling as the central conduit between surface-atmosphere exchanges driven by climatic and hydrological conditions (Brümmer et al., 2012; Limpens et al., 2008; Bubier et al., 2003). Particularly in peatlands, plant community composition and species-specific phenologies control carbon uptake through plant productivity (Peichl et al., 2018) and quality of litter deposited, ultimately affecting rates of peat formation (Trites and Bayley 2009). Specific to reclaimed AOSR landscapes, planting prescriptions must ensure efficient water use and ability to function under the expected range of environmental (i.e., saline) conditions during ecosystem evolution.

In the fen, both vascular and bryophyte species were introduced through a number of planting treatments (see Borkenhagen and Cooper, 2019). By year 3 (2015) fen vascular vegetation was widespread and robust, consisting predominantly of *Carex aquatilis* and to lesser extents *Juncus balticus*, *Typha latifolia*, *Calamagrostis inexpansa* and *Triglochin martima.* A similar rapid expansion of sedge species has also been observed at a nearby reclaimed fen (Sandhill Fen (SFW);

Clark et al., 2018, Vitt et al., 2016) and several post-disturbance fen landscapes in Alberta, including restored seismic lines (Davidson et al., 2021) and well pads (Lemmer et al., 2020). Bryophyte establishment following moss-transfer did occur at NFW, but at a much lesser rate than expected, likely due to the rapid expansion of sedge species. Due to its tolerance of saline conditions, *Ptychostomum pseudotriquetrum* has become the dominant bryophyte species occurring throughout NFW fen, although other bryophyte species (*Calliergon giganteum, Campylium stellatum, Drepanocladus aduncus, Drepanocladus polygamus, Leptobryum pyriforme*) are also present (Borkenhagen and Cooper, 2019). Similar to nearby natural saline fens (Volik et al., 2018) and Sandhill Fen Watershed (Hartsock et al., 2021; Vitt et al., 2016), the spatial extent of plant assemblages at NFW-fen was driven largely by water table position and salinity. As observed in other restored and reclaimed peatland landscapes (Poulin et al., 2013; Vitt et al., 2016), *Typha latifolia* colonized most of the ponded, standing water regions of the fen. Widespread establishment of invasive *T. latifolia* may be problematic for reclamation performance, as it decays quickly and is not a peat-forming species, which may affect long term peatland function (Borkenhagen and Cooper, 2019; Trites and Baylay, 2009; Shih and Finklestein, 2008).

Between 2014 and 2019, fen plant assemblages evolved, coinciding with changes in soil and water salinity. Fresh-water sedge and grass species in the fen such as *Carex aurea, Carex disperma* and *Hierochloe hitra* peaked in 2015, but were then rare or absent following increased levels of mobile sodium (Borkenhagen and Cooper, 2019). Species with a larger range of salt tolerance, such as *Juncus balticus*, *Calamagrostis inexpansa* and *Triglochin martima,* persisted and even expanded in some plots with increased salinity. In 2018, the fen experienced the highest in-flux of sodium during the study period (Table 2; Kessel et al., 2018; Sutton, 2021), resulting in visible salt-stress in *Carex aquatilis* and *Typha latifolia* (observed yellowing in foliage) and early

senescence of some plots. In recent years, clusters of *Betula pumila* and *Salix pedicellaris* have developed in persistently drier regions of the fen. Overall, the fen plant community at NFW was representative of natural (saline) fens in the region (Volik et al., 2018; Purdy et al., 2005; Chee and Vitt, 1989) however, plant succession and trajectory towards herbaceous or more marsh-like vegetation may occur and could have implications on long term carbon dynamics for this site in the future.

Evolution of upland vegetation occurred at a much slower rate than the fen. Use of salvaged forest floor materials as a capping layer is common practice in forest reclamation efforts in the region (Rowland et al., 2009, Prentice 2020; Irving 2020) as it supports soil water retention necessary for plant growth (Sutton and Price, 2020a) and provides propagules of species common to natural boreal forests (Pinno and Hawkes, 2015; Mackenzie and Naeth, 2010). Early successional upland species at NFW were markedly different than that of other naturally regenerating forests (e.g., post-fire, post-harvest) due to dry conditions and hydrochemistry. However, similar to other reclaimed uplands (Strilesky et al., 2017; Mackenzie and Naeth, 2010; Rowland et al., 2009), the initial 5 years following construction, NFW upland consisted of a patchy understory comprising invasive forbs and grasses (*Sonchus arvensis* and *Agropyron tracycaulum*) and dry, bare ground. Although counter intuitive, these non-native, early successional species were critical to the emergence and development of planted tree species. They facilitated improved soil structure through rhizosphere development as well as litter layer establishment, which resulted in the addition of labile organic matter and nutrients (Padilla et al., 2006; Gómez-Aparicio et al., 2004; Maestre et al., 2001). Trees became prominent by year 5 (2017) and consisted of both broadleaf (*Populus tremuloides, Populus balsamifera*) and coniferous (*Picea mariana, Pinus banksiana*) species native to the region. As of 2019, the understory consisted of shrubs,

graminoids, and forbs, and trees were becoming the dominant vegetation type. Notably, *Populus tremuloides* was never planted in the upland, however wind-blown seeds were likely dispersed from the nearby previously reclaimed slopes. Growth and timing of development of NFW upland tree species was similar to that of other reclaimed uplands in the region (Strilesky et al., 2017).

Remote sensing has been increasingly applied to peatland and post-disturbance studies as a means to identify plant community development and succession following disturbance (Chasmer et al., 2020; Lees et al., 2018). In this study, the derivation of remotely sensed EVI provided a more complete temporal and spatial record of plant emergence and development than fields methods alone. Once plant communities were established, EVI values measured at NFW were comparable to that of surrounding natural sites (Figure 2-5) and on par with other post-disturbance landscapes (e.g., restored peatland; Nugent et al., 2018), or those composed of similar plant communities (e.g., sedge fens: Schubert et al., 2010; Helbig et al., 2019; mixed wood boreal forest: Jahan and Gan 2011) ranging between 0.3 and 0.6 during peak season.

Although the timing of vegetative development varied between the two landscapes, planting campaigns paired with adequate edaphic conditions resulted in establishment of a diverse plant community comprising largely native species. While saline fens are uncommon, they do exist in the WBP and are within the scope of acceptable reclamation targets (Province of Alberta, 2017). Due to the specific, altered hydrochemical and physical state of the substrate materials used in reclamation (e.g., unstratified, compressed or dried peat, presence of naphthenic acids/mobile sodium in tailing sand; Nicholls et al., 2015a; Nwaishi et al., 2015b; Kessel et al., 2018; Biagi et al., 2021), plant succession and system evolution may take on a transformed, novel trajectory from the pre-disturbance landscape (Nwaishi et al., 2015a). Assigning common landscape classification

to these novel ecosystems is less relevant in reclamation, and of greater importance is the functionality of plant assemblages under present and future environmental conditions.

2.5.1.2 Carbon accumulation

One of the key ecosystem functions performed by peatlands is net uptake of atmospheric CO_2 via photosynthesis, and the long-term storage of carbon as organic matter in peat and litter (Vasander and Kettunen, 2006, Blodau, 2002; Gorham, 1991,). As NEE is typically the largest component of northern peatland annual carbon budgets (Limpens et al., 2008; Nilsson et al., 2008; Roulet et al., 2007) it was used here as a metric to quantify NFW's annual carbon function. Growing season results show significant progress towards ecosystem functionality from a CO_2 perspective. The fen quickly evolved from a bare-ground, growing season source of CO_2 in 2013 to an extensively vegetated, sink by 2015 (-243 g C m^{-2}). Moreover, from 2015 onwards, the fen has been sequestering CO_2 at rates comparable to nearby natural sites (see section 5.3). While the upland was still a growing season source of CO_2 in 2019 (46 g C m^{-2}), there has been an increase in plant CO_2 uptake that is expected to continue as the canopy continues to develop. As a result, the NFW upland is on a trajectory towards becoming a net carbon sink in the near future.

2.5.1.3 Response to periodic environmental stress

In the seven years following inception, NFW has demonstrated resilience to periodic hydrologic stress as observed during wet and dry periods, as well as during changes in water quality (e.g., migration and influx of salts).

2.5.1.3.1 Resilience to hydrologic stress

The WPB sub-humid climate presents an additional challenge to reclamation in the region with moisture deficits and decadal dry cycles (Chasmer et al., 2018; Devito et al., 2017; Bothe and

Abraham 1993). Climate change predictions for the region project an increase in both temperature and precipitation, which may further exacerbate moisture deficits (Thompson et al., 2018; Ireson et al., 2015; Devito et al., 2012). While increased precipitation will provide more water to the system, increased temperatures will likely lengthen the growing season and enhance ET. Additionally, variability in the intensity, frequency and amount of rainfall may have unknown effects on current ecohydrological feedbacks. As such, water availability and use are critical to the long-term sustainability and performance of reclaimed systems in the AOSR. In all seven years during the study period, fen ET rates exceeded precipitation, yet vegetation was able to grow, develop and uptake CO_2 at rates comparable to natural sites (see 5.3 below). Notably, fen WUE rates remained relatively stable (Figure 2-9) from 2015 onwards even during seasons with significantly less rainfall (seasonal rainfall ranging from 168 to 285 mm season^{-1}).

Stable WUE is indicative of a well-connected groundwater network between the upland and fen which resulted in sufficient hydrological self-regulation during times of hydrologic stress. Additionally, because fen vegetation developed significant rooting architecture (>1m depth in places; Messner 2019) it was able to access water even during prolonged dry periods that resulted in water table drawdown (e.g., 2017). As a result, the system had adequate plant-water availability, and plant function was not solely dependent on P inputs – ultimately increasing resilience to (future) moisture deficits. Moreover, fen WUE rates, once vegetation became established (2015-2019 average 1.8±1.3 g C kg H_2O^{-1} day^{-1}), were comparable to those observed at nearby natural fens (c.f. 1.7 to 3.0 g C kg H_2O^{-1} day^{-1} in Volik et al., 2021). Currently, the upland is supplying the fen with adequate water for ecohydrological functioning, however it is uncertain if this will continue as the upland canopy continues to develop, requiring more water, and water deficits continue to worsen. As trees continue to mature, ET rates are expected to increase (Strilesky et

al., 2017) and will likely lead to ET > P more frequently (to date, ET > P occurred only during dry years (2015,2017)). Moreover, as the canopy develops, more water is expected to be lost through evaporation of intercepted water, resulting in less direct inputs into the soil (Fettah, 2020). However, studies of boreal aspen stands during drought conditions describe an efficient redistribution of water via aspen rooting systems (Petrone et al., 2015; Brown et al., 2014), which may ensure enough water for plant function during periods of water stress in the upland. Furthermore, Sutton and Price (2020a) modelled the hydrologic effects of upland plant growth in NFW and concluded the system will likely be capable of providing sufficient groundwater to the fen and support the development and function of an upland forest. However, the system will likely be operating just within the margins of adequate water availability. Overall, the current ecohydrological functioning of NFW is capable of adapting and coping with the climatic regime of the AOSR.

2.5.1.3.2 Resilience to salt stress

Mitigating the effects of salinization from waste materials used in reclamation in the AOSR is an ongoing challenge (Biagi et al., 2019; Kessel et al., 2018; Simhayov et al., 2017). To date, fen and upland vegetation have been able to develop and persist under current concentrations of Na^+ and electrical conductivity values (Table 2). However, in 2018, *Carex aquatilis* and *Typha latifolia* exhibited signs of salt stress (yellow foliage, early senescence). While NEE in 2018 remained within the range of previous years and that of natural sites, there was an observable decrease (Figure 2-6, 2-7; Table 2-4A and B). Additionally, there was a decrease in biomass (Messner, 2019), LAI and EVI values (Table 3). Current hydrochemical conditions of NFW are still well within the range of levels observed at natural saline sites (Volik et al., 2021; Volik et al., 2019; Hartsock et al., 2021; ESRD 2015). Planting and establishment of species ranging in salt tolerance

likely helped the fen continue functioning (i.e., carbon uptake) at a comparable rate to other years. However prolonged exposure to saline conditions will likely result in a shift in the plant community and a decrease in carbon uptake capacity (Volik et al., 2018). Moreover, a number of ecohydrological and biogeochemical processes (decay rates, nutrient acquisition, plant water uptake etc.) may be affected by prolonged soil and water salinity, which may ultimately affect the long-term functionality of these landscapes (Nwaishi et al., 2015a).

2.5.2 Drivers of ecosystem functionality and interannual variability

Results indicate that ecosystem function, during the initial stages of development of a constructed, reclaimed landscape, is directly linked to the establishment and growth of vegetation**.** However, system design and construction are critical first steps as appropriate abiotic conditions, such as substrate quality and water availability, are required to initiate vegetation growth and persistence. Studies of boreal watersheds (natural, restored and constructed) indicate that water table dynamics, nutrient availability and hydrochemistry play a critical role in determining plant community composition (Volik et al., 2020a; Borkenhagen and Cooper, 2019; Spannato et al., 2018; Vitt et al., 2016; Dieleman et al., 2015; Koropchak et al., 2012, Trites and Bayley, 2009; Eppinga et al., 2009a; Strack et al., 2006; Lavoie et al., 2005). The relatively quick initiation of a widespread and robust sedge community in the fen was likely facilitated by planting and initial growth occurring in relatively wet years (2013, 2014, Figure 2-3A), as well as the relatively quick initiation of stable, near surface water table conditions following construction (Figure 2-4C). In reclaimed AOSR uplands, growth and persistence of plants is driven by available soil moisture, which is facilitated largely by cover soil composition and thickness (Sutton and Price, 2020a; Gingras-Hill et al., 2018). Spatial variability in the timing of plant emergence in the NFW upland (Figure 2-5A) was linked to the heterogeneity of soil conditions (i.e., moisture and nutrient availability). Soil

moisture and capping layer thickness maps created by Sutton and Price (2020a) of NFW correspond strongly to EVI imagery presented in this study (Figure 2-5A), particularly during early development (2014-2016), where areas of thicker capping materials (>30 cm) and in turn higher VWC promoted earlier plant establishment and more consistent robust growth.

2.5.2.1 Interannual variability of carbon fluxes

Results from peatland restoration (Strack et al., 2014; Strack and Zuback, 2013; Samaritani et al., 2011; Waddington et al., 2010; Petrone et al.,2001) and post-disturbance afforestation efforts (Strilesky et al., 2017; Dhar et al., 2018; Petrone et al., 2015; Mhkabela et al., 2009) indicate revegetation activities greatly reduce carbon losses and can return degraded ecosystems to carbon sinks over time. In both NFW landscapes, carbon uptake improved substantially with development of vegetation (Figure 2-7, Table 2-4). In established plant communities, seasonal variability in carbon fluxes is largely controlled by plant physiology, growing season length, PAR and meteorological conditions (Baldocchi et al., 2018; Charman et al., 2013; Brümmer et al., 2012; Barr et al., 2007; Falge et al., 2002; Law et al., 2002; Bubier et al., 1998). Examination of interannual variability in carbon fluxes in years following plant establishment (fen, 2015-2019, Figure 2-6 and 2-7) suggests a response to environmental changes. Notably, in 2017, the fen received only 61 mm of rainfall between July – September (compared to 154 mm in 2018, and 208 mm in 2019) resulting in a decrease in water table position and VWC (Figure 2-3). As such, there was a decrease in daily GEP rates (and NEE; Figure 2-6A; 2-7A) in 2017 during this dry period compared to wetter years (e.g., 2018 and 2019). However, it's important to note that carbon uptake continued during this time, albeit at a lesser rate, likely due to stomatal closure to limit water loss. Daily GEP rates during the 2017 dry period (3.6±1.4 g C m^{-2} day^{-1}) were comparable to those of nearby (within 40km) natural sites in the region experiencing similar meteorological conditions at

the time (daily GEP between 1.5 – 4.1 g C m^{-2} day^{-1}; Volik et al., 2021). Moreover, a similar GEP decrease under warming or drying conditions has been reported in rich fens (Adkinson et al., 2011) and sedge-dominated microforms in a poor fen (Strack et al., 2006). However, other studies in open-treed fens have shown contradictory results, where GEP increased under warming or drying conditions (Flanagan et al., 2010; Cai et al., 2010). Moreover, bryophyte dominated microforms showed less response to changing conditions (Strack et al., 2006) Thus, the response of GEP in peatlands to changing environmental conditions is complex, non-linear, and likely controlled by site-specific variables (i.e., plant community and edaphic conditions) and the overall amplitude of change (Smeraro et al., 2019). Moreover, the timing and frequency of rain events produced interseasonal variability in carbon fluxes. In 2018 rainfall events were intense, but less frequent (including 28 days with no rain between DoY 206 – 234; Figure 2-2, Table 2-2), which contrasted with 2019, where there was weekly, and, for some parts of the season, daily, smaller rainfall events. As a result, there was variability between the two years in the number of overcast days, which limited PAR and ultimately, plant productivity. As such, 2018 exhibited higher daily GEP rates than 2019 (Figure 2-6) even though both years received a similar amount of total precipitation. In particular, there was a clear decrease in CO_2 uptake in the afternoon hours of 2019 (Figure 2-7) due to lower PAR and overcast conditions (compared to the same time of year in 2017 and 2018). Similarly, Nijp et al. (2015) examined the effects of daytime rain events on NEE during an 11-year study in northern Sweden and found that reduced light availability, due to cloud cover during rain events, reduced net ecosystem CO_2 uptake on average by 0.23–0.54 g C m^{-2} day^{-1} or ~4.4% decrease in GEP throughout a growing season.

Growing season length coupled with the timing of plant emergence also affects seasonal carbon fluxes (Charman et al., 2013). There was a distinct temporal trend in the timing of plant

emergence throughout fen evolution. In earlier years (2015), plant emergence, green-up and subsequent carbon uptake occurred quickly (by DoY 136; Figure 2-7) due to low plant competition, adequate edaphic conditions and little to no litter layer. From 2017 onwards a delay in plant emergence was observed with daily carbon uptake beginning later each year (DoY 146, 150, 160 for 2017, 2018, 2019). This delay is likely attributed to persistence of winter conditions and ice lenses (Pulliainen et al., 2017; Charman et al., 2013; Aurela et al., 2004) and accumulation of a relatively thick litter layer (mean litter layer thickness 12±6.2 cm (2017) and 17.8±9.5 (2019; Table 3) resulting in new growth requiring more energy (and time) to emerge. Moreover, there was variability in the timing of plant emergence (and thus plant productivity and CO_2 sequestration) between the fen and upland (Figure 2-7AB - timing of NEE signal 2017-2019) due to differences in plant community composition.

2.5.2.2 Interannual variability in ET

NFW ET was strongly coupled to water availability and development of vegetation, as was previously noted at NFW (Scarlett et al., 2017), and related boreal studies (Brown et al., 2010; Petrone et al., 2001; Price et al., 1998; Lafleur 1990). Early in its development (2013, 2014), the fen surface was bare and dominated by dark, wet peat and large ponded areas (Figure 2-1). As a result, ET was high (326 and 424 mm growing season^{-1}), and close to PET. Here, ET rates were largely driven by high surface evaporation (similar to those measured off a boreal pond; Petrone et al., 2007). As vegetation developed and became widespread, ponded and bare regions were reduced and ET rates were subsequently driven by plant transpiration. 2015 onwards, fen ET began to decrease and stabilize as vegetation became established and fully developed (Figure 2-8). Furthermore, similar to the straw mulch technique used in peatland restoration (Petrone et al., 2004; Rochefort 2000; Price et al., 1998), development of a thick fen litter layer was likely limiting

large fluctuations in surface soil temperatures and impeding surface evaporative losses (2017 onwards). The slight increase in fen ET in 2018 was attributed to the large, intense rain fall event (86 mm over 4 days; Figure 2-3A), which resulted in extensive flooding and an increase in surface evaporation. While 2018 and 2019 were both wetter years (total growing season rainfalls of 278 and 285 mm), the frequency and intensity of events differed: 2018 had less frequent, more intense events, whereas 2019 consisted of frequent, small rain events. Differences in ET trends between these two years were a clear example of how changes in intensity, timing and frequency of rainfall can impact ecohydrological dynamics. Upland ET rates increased from 2017 onwards as trees matured (five years post construction and planting (Figure 2-8). Strilesky et al. (2017) reported an increase in ET by 62% as tree cover became established within the first ten years of a nearby reclaimed forest. Amiro et al. (2006a, 2006b) describe a similar increase in ET coinciding with growth of regenerating boreal forests post wildfire.

Drivers of ecosystem functionality varied during development. Initially, abiotic factors such as soil and water chemistry, availability of water and nutrients, and adequate substrate quality, paired with climatic conditions, dictated the timing, growth, success and type of plant community development. Once a plant community became established, plant physiology and phenology drove early carbon and water fluxes. Notably, successful development of these early plant communities is likely to dictate future trajectories and overall success of the system as these early plant communities initiate and control key ecohydrological and biogeochemical feedbacks (i.e., nutrient input, litter quality, decay rate, carbon uptake) necessary for ecosystem function. Once vegetation was well established, interannual fluctuations in carbon and water fluxes were once again driven by environmental factors. Similar to natural ecosystems, NFW was able to continue functioning through interannual fluctuations in environmental conditions (see 5.1.3. Response to periodic

stress). However, prolonged environmental stressors may lead to a plant successional shift (Scheffer, 2010; Eppinga et al., 2009) in the future at which point carbon and water fluxes would again be largely impacted by changes in plant form and function.

2.5.3 Comparison of NFW net ecosystem exchange rates to natural and post-disturbance landscapes

To contextualize the results and performance of NFW, NEE results were compared to natural and post-disturbance AOSR peatlands and forests. Figure 2-10 summarises total growing season NEE versus age following disturbance, while providing a mean range of values recorded at natural sites (blue band). Following plant emergence (2014), the NFW fen has remained a CO_2 sink throughout the study period with growing season NEE ranging between -69 to -215 g C m^{-2} (Table 4). Currently, only two upland-wetland pilot ecosystems (this study (Nikanotee Fen Watershed (NFW)) and Sandhill Fen Watershed (SFW)) have been constructed to test the design and feasibility of reclamation projects in the region. The two systems were guided by different conceptual approaches and test differing designs (Ketcheson et al., 2016). Briefly, NFW utilized numerical modelling for landscape optimization, while SFW was designed to mimic the water conserving function of natural fen systems based on their low-lying landscape position. Both systems were constructed using similar materials (i.e., by-products of the bitumen extraction process) albeit at variable thicknesses (e.g. peat thickness of 2 m at NFW vs 0.5 m at SFW) and included planting campaigns. A notable difference between the two systems is water transport and storage. In an attempt to combat the frequent periods of water stress common to the region and ensure ample inundated conditions for fen evolution, SFW was built with pumps to allow for the active management of water inputs and withdrawals, as such the system has no natural outflow for

surface and near surface water (Ketcheson et al., 2016; Biagi et al., 2021). Contrastingly, there is no manual water table manipulation at NFW, fen groundwater inputs are solely supplied from the upgradient upland, and water is discharged gravitational through a natural-flowing outlet. Remarkably, these two reclaimed peatlands follow a similar (carbon) trajectory despite differences in conceptual designs and water management techniques (Clark et al.,2018; Ketcheson et al., 2016), likely due to the rapid initiation of plant growth immediately following construction. At both sites, the peatlands become growing season CO_2 sinks within 3 years following construction at uptake rates comparable to nearby natural sites (Figure 2-10A). Clark et al. (2018) report a growing season net CO_2 uptake of -194 g C m^{-2} and -112 g C m^{-2} in the lowland and midland of SFW by year 3 (Figure 2-10A). Natural fens across the boreal exhibit a wide range of NEE values (both between sites and interannually within a single site) attributed to differences in plant community composition, edaphic conditions, and responses to hydrological dynamics and meteorological influences (Volik et al., 2021; Loisel and Yu, 2013; Charman et al., 2013; Gažović et al., 2013; Adkinson et al., 2011; Lund et a., 2010; Strack et al., 2006). A variety of natural nearby (within 40km of NFW) fens have been concurrently monitored during the study period, including a moderately-treed poor fen (Pauciflora Fen), heavily treed moderate-rich fen (Poplar Fen) and a saline fen system (Saline Fen). Growing season NEE values for these nearby natural sites (Pauciflora, Poplar and Saline), ranged between -92 to -196 g C m^{-2} (Pauciflora), -25 to -207 g C m^{-2} (Poplar) and 89 to

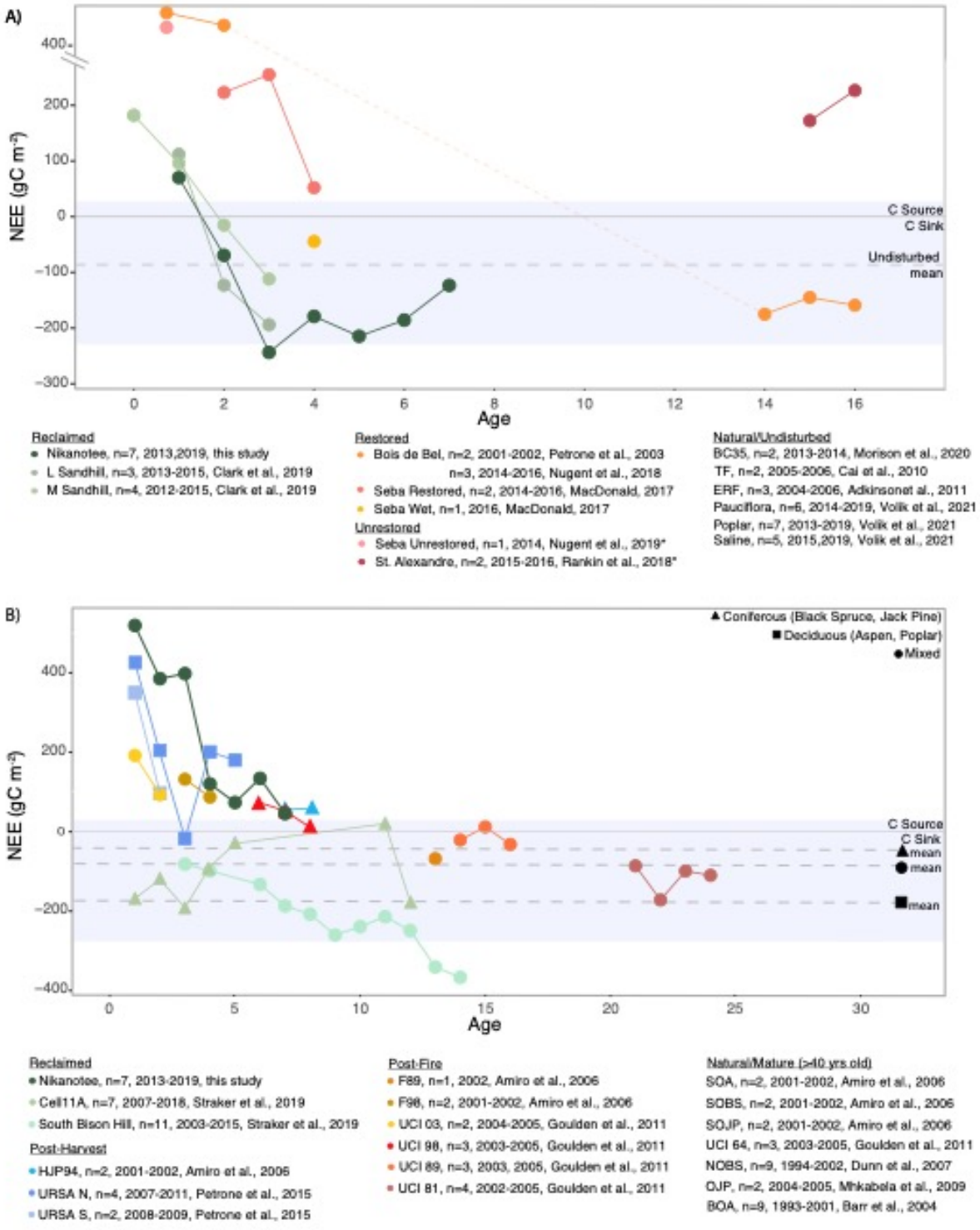


Figure 2-10: Relationship between total growing season net ecosystem exchange of CO_2 and site age at NFW-fen compared with natural and post disturbance Canadian peatlands with eddy covariance data sets. Blue band represents the range of NEE observed at natural sites, where the

small dashed line depicts mean growing season NEE of all natural sites. In the legend n is the number of study years. * represents annual NEE. 10B: Relationship between total growing season net ecosystem exchange of CO_2 and site age at NFW-upland compared with mature and post disturbance (fire and harvest) boreal forests with eddy covariance data sets. Blue band represents the range of NEE observed at natural sites, small dashed line depicts mean growing season NEE of natural sites. In the legend n is the number of study years.

-54 g C m^{-2} (Saline; Volik et al., 2021). Here, variability between sites is attributed largely to differences in plant community (treed with moss vs sedge) and hydrochemistry, with the saline site exhibiting lower rates of GEP due to salinity inhibiting plant productivity (Volik et al., 2021). Similarly, Morison et al. (2020) report NEE values of -25 and -130 g C m^{-2} in a two-year study of an undisturbed, poor fen in north-central Alberta within this time frame (2013-2014). Adkinson et al. (2011) also report interannual variability in NEE in a sedge dominated, extreme rich fen in northern Alberta (-35, -154, -42 g C m^{-2}), while NEE from a nearby moss-dominated poor fen was similar across the study period (-110.1 ± 0.5 g C m^{-2}), further depicting the range of plant communities found in the region and their varying responses to fluctuating environmental conditions. Typically, vascular vegetation is more sensitive to environmental changes (such as WT drawdown) than mosses, due to the high water-holding capacity of moss (Kokkonen et al., 2019; Laine et al., 2020). Cai et al. (2010) measured (June – September) NEE in an Alberta treed fen over two years and reported higher values of -282 and -207 g C m^{-2}, likely attributed to the prominent robust, mature woody vegetation. NFW-fen growing season NEE falls well within the range of values reported at natural, undisturbed sites (Figure 2-10A).

While peatland reclamation is a novel concept, peatland restoration is not and numerous, ongoing peatland restoration endeavours provide suitable analogies of ecosystem recovery. Results from both NFW and SFW depict the importance of plant community development and emergence on ecosystem function and evolution.

Initially following construction prior to plant emergence, both NFW and SFW functioned as carbon sources (70 (NFW), 112 (SFW-lowland), 96 (SFW-midland) g C m^{-2})). Waddington et al. (2010), measured NEE in a cutover bog in Quebec (Bois de Bel) pre- and post-restoration and reported a seasonal net CO_2 loss of 245 g C m^{-2} prior to restoration. Petrone et al. (2003) reported on the first two years post-restoration of the aforementioned site, at which point CO_2 emissions remained high (478 and 468 g C m^{-2}) due to the lack of a complete cover of carbon fixing vegetation and high respiration rates from decomposing mulch. Similarly, high CO_2 losses were observed during the initial year of study at adjacent restored and unrestored peatlands (445, 504 g C m^{-2}; Nugent et al., 2019) in northern Alberta. Furthermore, Rankin et al. 2018 reports that an unrestored peatland continues to function as a net CO_2 source (173 and 259 g C m^{-2}) 15- and 16-years post-disturbance. Moreover, timing of the return to carbon sink capacity varies amongst post-disturbance sites and has been observed by year 3 in a restored cut-away peatland (Tuittila et al., 1999) and year 14 at Bois de Bel (Nugent et al., 2018). Strack and Zuback (2013) measured CO_2 fluxes at Bois de Bel ten years following restoration, however, the system was still functioning as a carbon source due to WT drawdown and drier conditions resulting in increased rates of respiration. Differences in the rate and timing of carbon uptake in post-disturbance landscapes is largely driven by vegetation dynamics (i.e., vegetation emergence and establishment, plant community composition) and environmental conditions (particularly edaphic conditions, where dry conditions exacerbate respiration). Rapid emergence of wide-spread vascular vegetation, stable edaphic conditions and development of a thick litter layer resulted in GEP rates continually exceeding respiration at NFW-fen, resulting in a return to carbon sink capacity comparable to natural and restored sites. Natural (Saline fen, Volik et al., 2021) and restored (Strack and Zuback, 2013) peatlands exhibit periods of seasonal, or short-term carbon losses typically prompted by

changes in water availability or hydrochemistry, which can each inhibit plant productivity. As of 2019, NFW-fen has shown resilience to environmental stressors and is expected to continue functioning (in terms of carbon uptake) like natural sites, barring any major successional shifts in vegetation.

Although there have been numerous studies assessing upland reclamation treatment materials (Mackenzie and Naeth, 2010; Naeth et al., 2013; Pinno and Hawkes, 2015) and soil structure and function (Sutton and Price, 2020b; Gingras-Hill et al., 2018; Dietrich et al., 2017; Rowland et al., 2009), there have been limited long-term studies of carbon and water dynamics of AOSR reclaimed uplands (Straker et al., 2019; Strilesky et al., 2017). Moreover, mature stand dynamics can vary from that of juvenile or regenerating forest systems (Goulden et al., 2011). As such, here, post-disturbance (i.e., fire, harvest) regenerating boreal forests are discussed to provide context of early results and trajectory of our NFW upland. Upland WBP forests range from broadleaf leaf, aspen dominated to coniferous forests comprised of black spruce, jack pine and tamaracks, and less frequently, mixed forest comprised of both tree types. Forest type is a key driver of carbon dynamics as broadleaf forests typically have higher leaf area, GEP and ultimately CO_2 uptake than coniferous species (Brümmer et al., 2012). Of the seven mature (<40 years old) forests summarised in Figure 2-10B, broad leaf forests had the highest mean growing season uptake (-182 ± 104 g C m^{-2}), followed by mixed –tree stands (-73±57 g C m^{-2}) and coniferous stands (-7±40 g C m^{-2}; Figure 2-10B). As of 2019 (year 7), NFW upland was still a source of CO_2, emitting 46 g C m^{-2}. However, it is on a trajectory to becoming a carbon sink in the next 3-5 years, which is on par with the assessments of carbon dynamics in regenerating forests. For example, Amiro et al. (2010; 2006a) examined a number of mature, post-harvest and post-fire forests across boreal regions of North America and reported that most sites became carbon sinks ten years

following disturbance. Goulden et al. (2011) examined CO_2 exchanges in stands ranging in age from 1 to 154 years post disturbance and found a similar temporal trend where 1- to 6-year-old sites were losing carbon (emitting between 11 to 192 g C m^{-2}), 15 year old sites were beginning to gain carbon (-21 to -32 g C m^{-2} sequestered) and any sites over 25 were sequestering carbon (-40 to -110 g C m^{-2}) at rates comparable to mature, natural sites. The lag in carbon sequestration rates in juvenile forests is attributed to the small stature and low LAI of saplings as well as respiration losses from bare forest floor. Previously reclaimed uplands in the AOSR (South Bison Hill and Cell11A on Figure 2-10B) exhibited an increase in CO_2 uptake almost immediately following planting, due to the emergence and rapid expansion of understory vegetation. Once trees mature, these uplands perform on par or better than mature forests (mean total seasonal NEE of -216 g C m^{-2} for a mixed forest and -107 g C m^{-2} for a jack pine dominated landscape; Straker et al., 2019). Similar to AOSR wetlands, forest carbon function is sensitive to environmental changes, particularly hydrologic stress. Petrone et al. (2015) examined two regenerating, aspen dominated stands and reported a return to carbon sink function by year 3 (from 425 to -17 g C m^{-2} between years 1-3), followed by subsequent CO_2 losses in years 4-5 (201 and 180 g C m^{-2}) due to the persistence of drought like conditions. A significant increase in tree growth and foliage in the NFW-upland from 2017 onwards resulted in a marked increase in GEP and overall CO_2 uptake. However, due to the sparse understory and rather dry edaphic conditions, respiration rates remained high throughout the study period. This was in contrast to juvenile, post-fire sites, where respiration rates are typically lower in the initial years following fire as burnt soil and fire residue take longer to decompose (Czimczik et al., 2006, Litvak et al., 2003). Nevertheless, as the canopy continues to mature, GEP is expected to increase and eventually overtake respiration as the dominant carbon flux at our upland site. Currently, the upland is following a similar trajectory to

other regenerating forested systems and is expected to regain function as a carbon sink within the next 3-5 years.

2.6 Conclusions

This study captured what was likely the most dynamic period of NFW evolution, characterized by the rapid transition from a barren landscape to a flourishing ecosystem comparable to natural analogues in the region. Beginning in the first-year post-construction to the present, the system experienced rapid growth and establishment of vegetation (by 2015 in the fen, and 2017 in the upland) and changing hydrochemical conditions. Results indicate ecosystem functionality, namely carbon and water fluxes were largely controlled by plant growth and establishment. The fen quickly evolved from a carbon source in 2013 to a stable carbon sink by 2015 (total seasonal NEE of 70 to -243 g C m^{-2}). The slower growth rate of trees, coupled with dry edaphic conditions in the upland, resulted in net carbon losses during the study period (NEE of 519 to 46 g C m^{-2} from 2013-2019). Similarly, WUE rates in both the fen and upland showed a marked increase once vegetation became established. Moreover, plant function and carbon uptake were able to persist throughout dry years indicating sufficient hydrological connectivity between the two landscapes and ecosystem resilience to intervals of periodic water stress. Interannual variability of fluxes suggested that plant communities are exhibiting typical responses to environmental changes, as these responses mirror those of natural sites in the surrounding area experiencing similar conditions. Barring a successional shift caused by prolonged saline or dry conditions, water and carbon fluxes of both landscapes are expected to stabilize, and future fluctuations are predicted to be controlled by meteorological influences. Assessment of CO_2 and water exchanges provided sufficient evidence that the system is currently operating as intended and functioning comparably to undisturbed landscapes (fen) or post disturbance landscapes of a similar age and plant

community (upland). Persistent saline conditions will likely result in a shift to more salt-tolerant species in the future which may decrease rates of plant productivity and carbon sequestration. While it is difficult to definitively predict future abiotic conditions and thus ecosystem trajectories, the fen will likely evolve towards a plant community and ecosystem functionality similar to that of fens in the region. The upland will likely be capable of supporting a forest of similar density to undisturbed sites and continue supplying adequate water to the down-gradient fen.

A limitation of this research is that NFW is a pilot project and thus the only current example of this design. As such it may not reflect the only successional path of future reclamation endeavours, particularly if designs are adjusted or baseline environmental conditions change. Thus, as future reclamation endeavours are initiated, carbon and water fluxes along with plant development should continue to be monitored to improve our knowledge base. Moreover, as the NFW is still in a juvenile phase and hydrochemistry is expected to continue changing, future work should include continued monitoring, particularly if there is a shift in plant communities. Lastly, as this study only focused on CO_2 fluxes future work should include a complete carbon balance for the site to accurately assess carbon accumulation and storage.

This study is currently the longest reported record of carbon and water dynamics of a reclaimed upland-fen complex in the AOSR. Assessment of ecohydrological dynamics during early-development suggests that the constructed system is evolving towards becoming a self-sustaining, carbon-accumulating, functional ecosystem. This study demonstrates that (fen) reclamation is possible and can be successful in the AOSR. Moreover, this study applied a functional-based approach focused on a few, critical ecohydrological variables (CO_2 and WUE) measured using ecosystem scale techniques (eddy covariance and remote sensing analysis). The methods used here provide a feasible approach for capturing temporal ecosystem evolution and

functionality following construction and could prove useful especially for large-scale or remote reclamation endeavours where field work is not possible. This research provides a unique opportunity to assess surface-atmosphere interactions during the early successional stage of ecosystem development ultimately, improving our understanding of ecohydrological processes.

Ecohydrological insights gained from this study on the function and evolution of constructed landscapes will aid reclamation practitioners, regulatory decision-makers, and mine operators in the future design of reclamation endeavours in the region. Moreover, the rapid return of carbon sink capacity illustrated in this study paired with the ability for ecosystem functionality to persist in the water-limited setting of the AOSR may prove useful outside of the realm of reclamation as peatlands are increasingly becoming recognized as viable, nature-based solutions to climate change.

Chapter 3: Evolution of ecosystem-scale surface energy fluxes of a newly constructed boreal upland-fen watershed

3.1 Introduction

Surface energy dynamics are driven by atmospheric forcing and biophysical surface properties (Helbig et al., 2020b; Betts and Ball., 1997), which influence the exchange of energy, momentum, and water between the surface and atmosphere (Laguë et al., 2019; Bonan 2019). These exchanges are pivotal to ecosystem function as they drive ecohydrological and biogeochemical processes and feedbacks including the energy available for evapotranspiration (ET) and carbon assimilation. Surface biophysical properties, such as plant community composition and structure (Thompson et al., 2004; Bonen, 2008) and soil moisture (Wilson et al., 2002), affect both radiative (e.g., albedo) and non-radiative (e.g., aerodynamic and surface conductance, surface roughness) drivers of surface-atmosphere exchanges (Helbig et al., 2020; Devaraju et al., 2015; Bonen, 2008; Bonen, 2019; Raupach, 1995; Schulze et al., 1995; Green et al., 2021). As such, landcover change, whether through natural or anthropogenic drivers, results in localized, and often rapid, changes to energy partitioning (IPCC, 2021; Lagüe et al., 2019; Halim et al., 2019; Winckler et al., 2017; Waddington et al., 2015; Jin et al., 2012), which can have broader implication for local and regional surface-atmosphere feedbacks, such as atmospheric boundary layer (ABL) thickness, cloud formation, and surface temperature and precipitation trends (Beamesderfer et al., 2022; Helbig et al., 2020; Rigden and Li, 2017). Moreover, biophysical changes to the surface can alter biogeochemical processes (particularly carbon dynamics; IPCC 2021) with bare or degraded landscapes attributing to significant anthropogenic greenhouse gas emissions (Strack et al., 2022; Arias et al., 2021; Harper et al., 2018).

Boreal landscapes have been increasingly recognized for their important role in both regional and global carbon, water, and climate dynamics (Strack et al., 2022; Helbig et al., 2020ab; Jia et al., 2019; Bonan et al., 2008). The Athabasca Oil Sands Region (AOSR) encompasses a 93 258 km^2 section of the Canadian boreal ecozone in northern Alberta and is comprised of a mosaic of hydrologically connected upland forests and wetlands (where 25% of the wetland area is classified as swamp, and 64% as peatland (24% bogs, 40% fens); Alberta Merged Wetland Inventory; Volik et al., 2020; Ficken et al., 2019; Elmes and Price, 2019; Vitt et al., 1996). However, as of 2020, approximately 1055 km^2 of natural boreal landscapes in the region have been disturbed (Alberta Environment and Parks, 2020) due to large-scale resource extraction of bitumen which has been ongoing since 1967 (Alberta Environment, 2008). Land disturbance via resource extraction has resulted in altered surface conditions due to the removal of vegetation and excavation of tens of meters of substrate (Johnson and Miyanishi, 2008) and a substantial loss of ecosystem functions and services (Rosa et al, 2017; Ficken et al., 2019; Rooney et al., 2012).

Under the Alberta Environmental Protection and Enhancement Act (EPEA) mine operators are obligated to return disturbed landscapes to pre-disturbance equivalent land capacity (Province of Alberta, 2021). However, unlike restoration efforts where typically only planting and/or rewetting are required, due to the intensity of land disturbance during surface mining, reclamation requires the complete reconstruction and reengineering of surface and subsurface properties. Moreover, reclamation efforts are further complicated as the AOSR experiences decadal-dry cycles and evapotranspiration frequently exceeds precipitation in the region (Bothe and Abraham, 1993). As water availability is critical for ecosystem function (Rodriguez-Iturbe et al., 2004) understanding ecohydrological drivers, controls, and feedbacks of reclaimed boreal landscapes is necessary to

ensure adequate ecosystem evolution, longevity, resilience to periodic environmental stressors and capability to function under future climate scenarios.

As reclamation in the AOSR is still a relatively novel endeavour there is currently limited research on reclaimed landscape function, evolution, and trajectory. Recent AOSR reclamation studies have been largely focused on hydrologic function (Clark et al., 2022; Biagi et al., 2021; Sutton and Price, 2020ab; Ketcheson et al., 2017) and carbon exchanges (Chapter 2; Davidson et al., 2021; Clark et al., 2019). Only a few studies have examined the energy balance of reclaimed forested uplands (Strilesky, 2019; Strilesky et al., 2017; Carey, 2008), but to date no studies have examined the surface-atmosphere energy exchanges of reclaimed peatlands during ecosystem evolution in the AOSR region.

In this study, surface energy fluxes of a reclaimed upland-fen complex were examined during the initial seven years (2013 – 2019) following construction. Ecosystem-scale energy exchanges were measured using the eddy covariance method while land cover change was derived via remote sensing. The objective of this study was to quantify energy partitioning during ecosystem evolution from bare ground to a robustly vegetated landscape and compare these results to nearby natural and post-disturbance boreal landscapes for context.

3.2 Methods

3.2.1 Study Site: Nikanotee Fen Watershed

The Nikanotee Fen Watershed (NFW) is a 32-ha mosaic of reclaimed landscapes constructed in a previously mined section within an oil sands lease, approximately 30 km north of Fort McMurray, Alberta (56°55′59” N, 111°25′00” W). NFW design is based on numerical modelling (Price et al., 2010), which identified appropriate substrate materials, ideal thicknesses, and landscape

geometries to ensure adequate water movement and storage throughout the system to maintain ecosystem function even under prolonged drought conditions. Detailed descriptions of site design, construction and characteristics have been previously reported (Popović et al., 2022; Ketcheson et al., 2016; Daly et al., 2012). Briefly, in terms of hydrologic function, NFW was designed to be self-sufficient, with no manual manipulation of the water table through dams or pumps. Hydrological inputs to the system are precipitation and surface runoff from the surrounding, previously reclaimed hillslopes (Figure 3-1A), and groundwater inflow to the fen from a constructed upland aquifer (Sutton and Price, 2020a; Ketcheson et al., 2016). Surface water is discharged through an outflow located in the northeastern corner of the fen (Figure 3-1A). Hydrologic connectivity and function are aided through the subsequent design aspects (Figure 3-1B). A 0.05 m-thick, impermeable, engineered geotextile clay liner underlies the entire upland-fen complex, which encourages lateral and down-gradient flow while isolating the system from the regional water table. Moreover, to further improve hydrologic connectivity, a 0.5 m thick, highly permeable layer of petroleum coke extends partway into the upland to beneath the fen peat (Figure 3-1B; Simhayov et al., 2017; Daly et al., 2012). A full account of NFW hydrological functioning is described by Ketcheson et al. (2017).

This study focuses on the treed upland (7.7 ha) and fen peatland (2.9 ha) components of the watershed (Figure 3-1A), whose construction was completed in January 2013. The upland consists of a 3 m thick coarse tailings sand aquifer, with a high hydraulic conductivity (Sutton and Price, 2020a) and 3% basal slope (Figure 3-1B; Ketcheson et al., 2017). A 20-50 cm thick cover soil, composed of salvaged forest materials (sandy loam to loam LFH) overlies the tailings sand aquifer. Planting prescriptions in the upland followed procedures outlined by the Cumulative Environmental Management Association revegetation manual (Alberta Environment, 2008) and

consisted of native species common to WBP uplands, including black spruce *(Picea mariana*), jack pine (*Pinus bankstana*), balsam poplar (*Populus balsamifera*), labrador tea (*Ledum groenladicum*) and bunch berry (*Cornus stolonifera*). The fen consists of 2 m of salvaged, donor peat overlying the petroleum coke underdrain. While not part of the original design, the fen has had permanent standing water ("ponds") since 2013. The fen was revegetated using an experimental factorial design described in detail by Borkenhagen and Cooper (2019). Planting prescriptions incorporated both freshwater and saline sedge and graminoid species (*Carex aquatilis* (water sedge), *Juncus balticus* (wire rush), *Triglochin maritima* (seaside arrow grass)), as well as moss species harvested from a local rich fen, using the moss transfer method (Rochefort et al., 2003). In 2014, invasive *Typha latifolia* infilled many of the ponded regions, followed by removal campaigns from 2014-2016. Table 3-1 provides a summary of biophysical characteristics for each landscape respectively.

Field measurements were conducted during the snow-free growing season (May – September, DoY 135-255, n = 120 days), during the first seven years post-reclamation (2013 – 2019). Table 3-2 highlights key milestones, such as surface amendments, planting campaigns, and the timing of site evolution during the initial stages of reclamation.

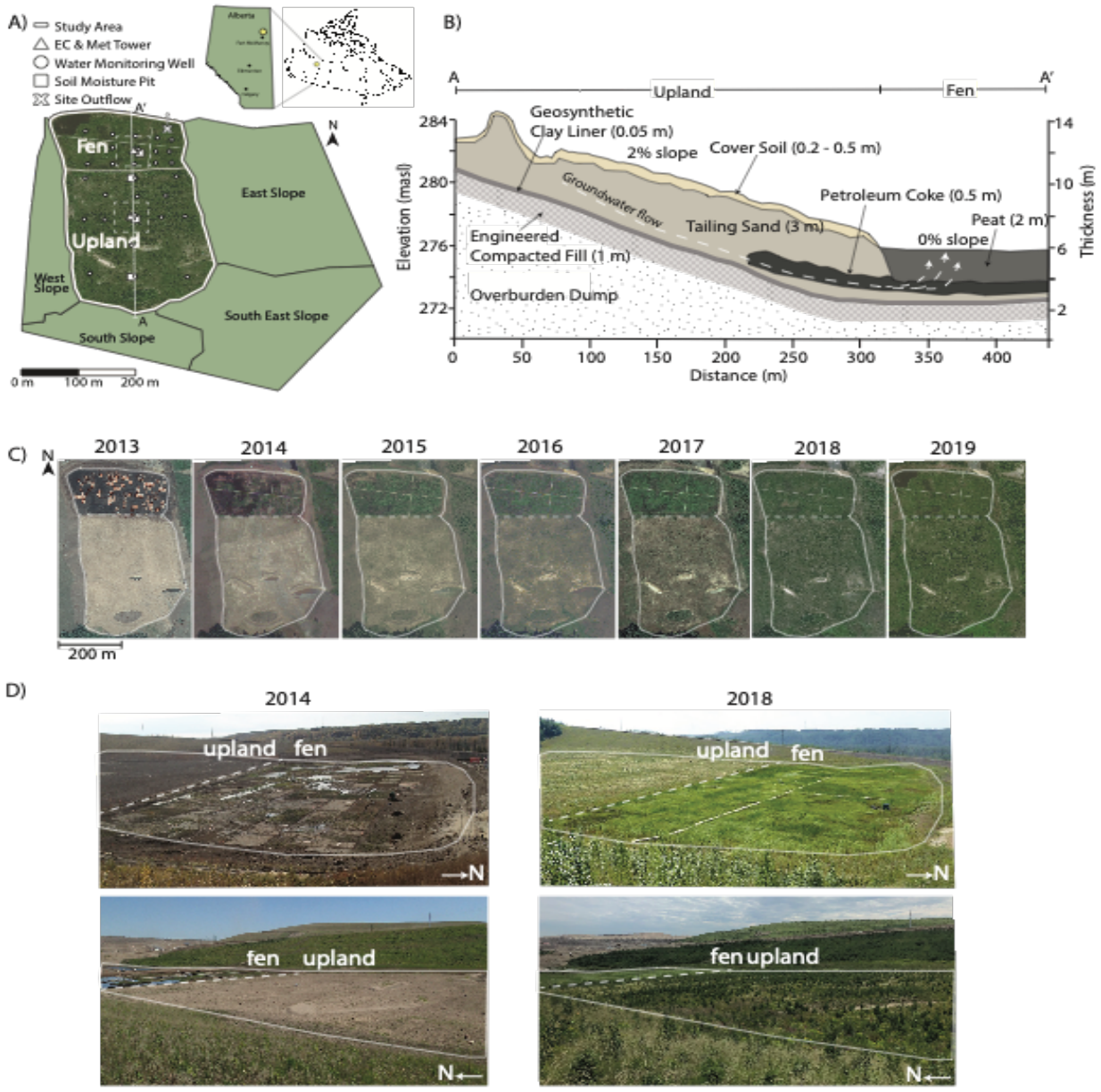


Figure 3-1: Study site and visual depiction of temporal evolution. A) Map of the Nikanotee Fen Watershed (NFW) depicting the regions of interest (Fen and Upland) and the locations of soil moisture pits, eddy covariance and meteorological towers and water monitoring wells. B) Stratigraphic cross-section along a central transect (A-A', shown in Figure **3-**1A) depicting the layering of substrate materials and general groundwater flow direction. The thickness of each layer is indicated in parentheses. Note that the thickness of the clay liner in the diagram is not to scale (illustrated thicker than the actual 0.05 m thickness). C) Satellite imagery of site evolution from year 1 (2013) to year 7 (2019). Imagery was acquired using Google Earth Engine (GEE) via Maxar Technologies satellite data. D) Field photos depicting surface conditions initially (2014) and following plant development (2018). Upper row: focused on fen (taken from east slope). Bottom row: focused on upland (taken from west slope).

Table 3-1: Biophysical characteristics of the NFW fen and upland.

	Fen	**Upland**
Size (ha)	2.9	7.7
Substrate (m)	2 m salvaged peat 0.50 m petroleum coke 0.50 m tailing sand	0.2 – 0.5 m salvaged forest floor material (LFH) 0.50 m petroleum coke 3 m tailing sand
Dominant Species (as of 2019)	*Carex aquatilis* *Juncus balticus* *Typha latifolia* *Ptychostomum pseudotriquetrum*	*Populus tremuloides* *Populus balsamifera* *Picea mariana,* *Pinus banksiana*
Ecosite classification (Beckingham)	'j' ecosite - rich fen dominated by sedge species	'b/d' ecosite - mixed treed forest and shrubland

Table 3-2: Timeline of key events and instrumentation during the initial stages of reclamation. Here, n represents the number of days measured (EC measurements) out of 120 during the growing season.

2013	**2014**	**2015**	**2016**	**2017**	**2018**	**2019**
Completed construction	Additional peat added to ponded areas (fen)	Robust, widespread vegetation (fen)	Horse Creek Wildfire (limited field season)	Robust, widespread vegetation (upland)	Large rain event (July) – 86 mm over 4 days	Additional peat added to northwest corner (fen)
Initial planting & instrument installation	Removal of *Typha latifolia* (fen)	Removal of *Typha latifolia* (fen)	Removal of *Typha latifolia* (fen)	EC tower malfunction (upland)		
Additional tillage (furrows) of upland cover soil (autumn)	Additional planting of tamarack seedlings (upland)	Subsequent planting campaign (upland)				
EC tower malfunction (fen)						
← Closed-path EC system →		← Open-path EC system →				
n = 47 (fen) n = 120 (upland)	n = 120 (fen, upland)	n = 120 (fen, upland)	n = 54 (fen) n = 87 (upland)	n = 120 (fen) n = 87 (upland)	n = 120 (fen, upland)	n = 120 (fen, upland)

3.2.2 Micrometeorological setup

Each landscape was configured with a meterological station with an eddy covariance (EC) system. Identical instrumentation was set-up in both landscapes, differing only in sensor height as vegetation developed. Initially tower height in both landscapes was 2 m, with upland tower height increasing to 3 m (2018-2019) to maintain representative flux footprints.

Meteorological stations measured air temperature (Tair, ^{o}C) and relative humidity (rH, %) using a Rotronic HC2S3 sensor (Campbell Scientific; Utah, USA). Net radiation (Q*, Wm^{-2}), shortwave and longwave incoming and outgoing radiation components were measured using a CNR4 sensor (Kipp Zonen; Delft, Netherlands). Albedo was computed using CNR4 measurements. Ground heat flux (Q_G, Wm^{-2}) was calculated using ground heat flux probes (HFT3; Campbell Scientific: Utah, USA), inserted horizontally at depths of 5 cm below the ground surface. Precipitation (P, mm) was measured with a tipping bucket gauge (Texas Instruments TR-525M), placed within a clearing near the tower to avoid canopy and tower influences. Vapour pressure deficit (VPD, kPa) was calculated using saturated vapor pressure (e_s) and actual vapor pressure (e_a), using measurements of Tair and rH, following methods of Howell and Dusek, 1995. All meteorological data were sampled at 1-minute intervals and averaged every 30-min on a CR1000 datalogger (Campbell Scientific: Logan, Utah, USA).

3.2.3 Eddy covariance processing and energy balance

Eddy covariance (EC) systems consisted of a closed path CO_2/H_2O gas analyzer (LI-7200: LI-COR: Lincoln, Nebraska, USA) and a 3D sonic anemometer (Windmaster Pro: Gill Instruments: Lymington, Hampshire, UK) from 2013-2014, and an open path CO2/H2O gas analyzer (LI-7500: LI-COR: Lincoln, Nebraska, USA) with a 3D sonic anemometer (CSAT3 3D: Campbell Scientific: Logan, Utah, USA) from 2015-2019 (Table 2). Raw EC data were collected at 20 Hz

and averaged every 30-min. Corrections for coordinate rotation (double rotation; Kaimal and Finnigan, 1994), time lag and sensor separation (Leuning and Judd, 1996) and density effects (Burba et al., 2012) were applied, following common Fluxnet protocols (Webb et al., 1980; Leuning and Judd, 1996; Foken and Leclerc, 2004; Aubinet et al., 2012). Resulting half-hour fluxes were then quality checked and further processed using a custom R-Software script. Data collected from open path systems (2015 – 2019) had additional filtering to remove periods that experienced precipitation or had the potential for dew formation on the infrared gas analyser lenses. For further data processing details see (Popović et al., 2022). The Kljun et al. (2004) footprint analysis was used to constrain the measured fluxes to be within 80% of the desired site boundaries. NFW flux footprint is depicted in Popović et al (2022).

The surface energy balance of NFW was defined as,

$$Q^* = Q_H + Q_E + Q_G \quad (1)$$

where net radiation (Q*) was partitioned between turbulent latent (Q_E) and sensible (Q_H) heat fluxes, and conductive, ground heat flux (Q_G). The energy fluxes were forced closed, where the additional energy was partitioned based on the Bowen ratio (β) following methods of Wilson et al., 2002). Gap-filling of data is described in Volik et al. (2021). Following filtering 68% of the fen and 64% of the upland data remained (total data across all years) and 16% and 25% of the data was gap filled. Energy fluxes were then normalised by Q* to investigate energy partitioning and adequately compare between years.

3.2.4 Ecophysiological Parameters

Ecophysiological parameters were derived from half-hourly flux data and calculated using the bigleaf package (Knauer et al., 2018) in R (R Core Team, 2021). Aerodynamic conductance

describes how effective an ecosystem is at transferring mass and energy to the atmosphere (i.e., sensible and latent heat exchange; Raupach, 1995) via,

$$g_a = \frac{1}{(r_a + r_b)} \quad (2)$$

where r_a is the aerodynamic resistance for momentum transfer and r_b is the canopy (quasi-laminar) boundary layer resistance to heat transfer (Knauer et al., 2018; Peichl et al., 2013; Mölder and Kneller, 2002). Surface conductance (g_s), which regulates the transport of water vapour from the land surface to the atmosphere (Schulze et al., 1995) was calculated by inverting Penman-Monteith (Knauer et al., 2018; Monteith 1965) and in this study encapsulated the entire surface - coupling soil and plant components,

$$g_s = \frac{Q_E g_a \gamma}{\Delta(Q^* - Q_G) + \rho C_p g_a VPD - Q_E(\Delta + \gamma)} \quad (3)$$

As in other studies of boreal landscapes (Alekeychik et al., 2018; Peichl et al., 2013), g_s was calculated using daytime values (8h00 – 18h00), where $Q^* > 100$ Wm^{-2} and during precipitation-free periods, with at least 6 hours precipitation free before the measurement. Conductances (g_a and g_s) were then combined to assess the degree of interaction between the surface vegetation and the atmosphere into a vegetation-atmosphere decoupling factor (Ω; Jarvis and McNaughton, 1986,

$$\Omega = \frac{\frac{\Delta}{\gamma} + 1}{\frac{\Delta}{\gamma} + 1 + \frac{g_a}{g_s}} \quad (4)$$

Vegetation-atmosphere decoupling (Ω) ranges between 0 and 1. An Ω value near 0 indicates a well-coupled ecosystem, where evapotranspiration (ET) is typically constrained by stomatal controls on transpiration and affected by VPD. Conversely, in uncoupled systems, Ω is closer to 1 and available energy controls ET (McNaughton and Jarvis, 1991). Water-limited, or aerodynamically rougher ecosystems, such as forest, tend to exhibit a higher degree of coupling,

whereas wetter environments are typically more uncoupled (Knauer et al., 2018; Runkle et al., 2014).

3.2.5 Edaphic conditions and hydrometric network

Continuous measurements of volumetric water content (VWC) were collected at soil moisture pits along a north-south transect spanning both landscape units (Figure 3-1A). VWC was measured between 5 to 100 cm bgs, however only the near surface (5 cm depth) values are reported here. A summary of VWC at other depths has been previously reported by Popović et al. (2022) and Sutton and Price (2020b). Each soil moisture pit was instrumented with dielectric impedance reflectometry soil moisture probes (Stevens Hydra Probe II) and recorded dielectric permittivity at one-minute intervals. Measurements were temperature and salinity corrected and converted to VWC, based on a calibration (Seyfried et al., 2005) specific to the substrate material. Soil temperature was measured at the meteorological stations using thermocouples (Type k thermocouple (2013-2018), CS-109 soil temperature probes (2019)) at 5 cm depth.

Water table depth (WTD) was logged automatically through pressure transducers (HOBO MX2001-S, Onset; Massachusetts, USA), using the extensive monitoring network of wells and piezometers installed across NFW (Figure 3-1A). Wells were 2.54 cm inner diameter (I.D.) polyvinyl chloride (PVC) pipes that were fully slotted and wrapped with well-screening (Ketcheson et al., 2017). Well depths were 1.5 m in the fen and 3 m in the upland. No values are reported for the upland in 2013 due to installation delays. Here, positive values indicate a water table below the soil surface (cm below ground surface (bgs)) and negative values indicate a water level above the soil surface. Further details about the hydrometric network are described in Ketcheson et al. (2017).

3.2.6 Vegetation and surface conditions

Using Landsat 8 satellite imagery acquired through the USGS (Vermote et al., 2016), which has a 30-m spatial resolution and 8 to 16 day temporal resolution spanning the entirety of the study period, enhanced vegetation index (EVI) was derived using the Google Earth Engine (GEE) application (API; Gorelick et al., 2017) and post-processed using a cloud masking script, modified by authors from GEE API Guides, to further remove the effects of cloud cover, forest fire haze and mine dust. EVI was calculated via,

$$EVI = G \times \frac{NIR - RED}{NIR + C_1 \times RED - C_2 \times BLUE + L} \quad (5)$$

where infrared (NIR), red (R) and blue (B) are the shortwave spectrum bands and L is the canopy background adjustment that addresses nonlinear, differential *NIR* and *RED* radiant transfer through a canopy. *C1, C2* are the coefficients of aerosol resistance term, which uses the blue band to correct for aerosol influences in the red band. Coefficients adopted in the EVI algorithm here were: L=1, *C1* =6, *C2* = 7.5, and G (gain factor) = 2.5 (Huete et al., 2002; Huete, et al., 1997; Huete et al., 1994). As the timing of plant development varied, both spatially and temporally, the mean EVI of a 60 x 60 m pixel grid located at the epicenter of flux tower footprints (dashed box, Figure 3-1A) was calculated for the study period. This ensured EVI values were representative and related to tower flux measurements.

To capture the spatial heterogeneity of evolving surface conditions, a supervised land use/land classification (LULC) was derived using the Landsat 8 imagery (Vermote et al., 2016) for the month of July (i.e., during peak vegetation) for each year. Multispectral imagery was processed using the semi-automatic classification plugin (SCP; Congedo, 2021) in QGIS (QGIS, 2021). Training points were defined based on reference data, including field measurements and

photographs, aerial imagery, satellite imagery and EVI spatial analysis results. Four macro-classes, including water, bare, vegetated, and mixed, were defined based on spectral signatures and the aforementioned field metrics. Bare and mixed macro-classes were further subdivided to capture variability between the two landscapes (Table 3), in particular during periods of plant emergence when many pixels contained some degree of vegetation, bare ground and/or surface water. Accuracy assessment of the supervised classification produced a kappa coefficient of 0.84.

Throughout the study period, field-based plant community measurements (LAI, non-destructive surveys) were collected and described in Popović et al. (2022), Messner (2019) and Borkenhagen and Cooper (2019). Table 1 in supplemental materials provides a summary of field-based results from the aforementioned NFW studies.

Table 3-3: Description of land use/land cover (LULC) classes used to define changing surface conditions.

Macro-Class	Sub-class	Description
Bare	Bare peat	Wet, dark, bare peat, substrate of fen
	Bare soil	Light coloured, sandy loam, cover soil of upland
Mixed	Bare + Veg (Fen)	Plant emergence, but not full coverage, mix of bare peat and plant coverage
	Veg + Water (Fen)	Ponded regions infilled with *Typha latifolia* and/or other veg, mix of plant cover and ponded water
	Bare > Veg (Upland)	Dominated by bare ground with some early plant emergence (juvenile trees and understory)
	Bare < Veg (Upland)	Mix of plant coverage and bare ground with greater plant coverage
Veg	Full Veg	Total plant coverage, no bare ground or ponded water detected
Water	Surface Water	Ponded or flooded regions

3.3 Results

3.3.1 Environmental Conditions (2013-2019)

3.3.1.1 Microclimatic Variability

Mean daily air temperature (Tair, °C) ranged between 4 and 29 °C throughout the growing season, and seasonal averages for both landscapes ranged between 15°C (2019) to 19°C (2016), consistently above the 30-year climate normal (13 °C; Environment Canada, 2020) (Figure 3-2A). On average, September was typically the coolest month (average of 11°C) and July the warmest (average of 19°C), with the exception of June 2016 (average of 23°C). Temperature trends in the early growing season (i.e., May) fluctuated interannually with some years exhibiting cooler temperatures (monthly mean of 13 °C in 2014 and 2015) and others warmer (monthly means of 17 – 18 °C in 2013 and 2018). Total seasonal precipitation (P) ranged between 168 mm (2017) to 310 mm (2016), and all years except 2016 and 2019 (285 mm) had less rainfall than the 30-year average (283 mm, Environment Canada, 2020). Most rainfall occurred during the months of June and July apart from 2019 where 126 mm (44% of seasonal rainfall) occurred in August. Over the seven-year study period, 75% of rain events were < 5 mm day^{-1} (Figure 3-2B). Incoming shortwave radiation (Rg, Wm^{-2}) between the two landscapes was largely similar with only slight variation on some days (±20 Wm^{-2}), likely due to instrument position and cloud cover (Figure 3-2C). Highest daily rates of Rg were observed between the hours of 11h – 15h (mean of 530 ± 240 Wm^{-2}). Mean monthly Rg was typically highest in May, however, insolation remained high until the end of July when it began to decline. September had the lowest mean monthly rates (ranging from 111 – 205 Wm^{-2}) across all years. Vapour pressure deficit (VPD, kPa) was relatively large, reaching a daily maximum of up to 4.9 kPa and reflecting the large atmospheric demand for ET in the region. Daily

averages ranged between 0.1 - 2.8 kPa (Figure 3-2D). Daily mean relative humidity (rH, %) ranged from 28 to 92% (Figure 3-2E) with an interannual average between 60 and 67%.

3.3.1.2 Edaphic Conditions

Fen mean daily peat temperatures ranged from 3.6 - 26.9 ºC (Figure 3-2F) throughout the study period. Interannually, mean peat temperatures decreased over time from 16.6 (2013) to 12.1 ºC (2019; Figure 3-2F). Upland soil temperature was consistently higher than fen's (Figure 3-2F) and varied less between years, with seasonal averages ranging from 18.3 (2019) to 20.5 (2013) ºC.

Soil volumetric water content (VWC, at 5cm depth) was drastically different between the two landscapes (Figure 3-2G) with the fen being consistently wetter across all years than the upland (cf. 84% vs 20%).

Fen daily VWC averages during the study period ranged between 70 - 87% (Figure 3-2G). Overall fen VWC remained relatively stable, with seasonal means between 82 - 85% and only slight fluctuations (1-2%) in response to rain events. However, during dry periods, VWC decreased throughout the growing season (2015 and 2017). Notably, mean fen VWC in 2017 decreased from 86% in May to 72% by the end of August. In the upland daily average VWC ranged between 10 - 40 % (Figure 3-2G) with seasonal means between 15 (2015) to 26% (2013). In all years except 2019, monthly upland VWC decreased throughout the growing season by approximately 5% on average, apart from 2017, which had the steepest decline (~10% from May to August). In contrast to the fen, upland VWC showed rapid responses to rain events, resulting in values fluctuating up to 20% over a few days.

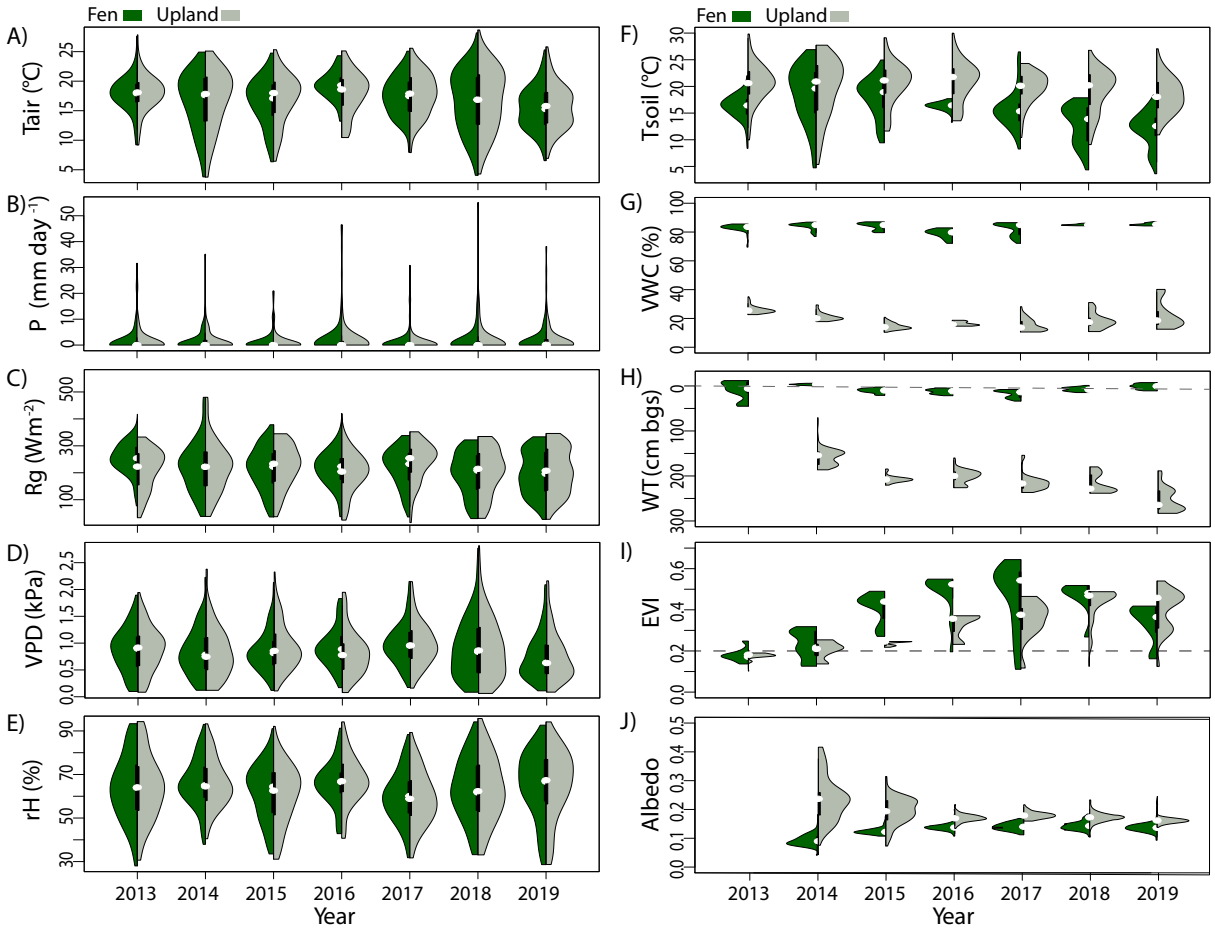


Figure 3-2: Split violin plots depicting the magnitude and distribution of meteorological (A-E) and surface (F-J) conditions for the fen (left, dark green) and upland (right, light green) during the growing season (May – September). White dot represents the median, black bar the interquartile range. A) mean daily air temperature (Tair, °C); B) total daily precipitation (P, mm); C) mean daily incoming shortwave radiation (Rg, Wm^{-2}); D) mean daily vapour pressure deficit (VPD, kPa); E) mean daily relative humidity (rH, %); F) mean daily soil temperature at 5 cm below the ground surface (Tsoil, °C); G) mean daily soil volumetric water content (VWC, %); H) mean daily water table depth (WT, cm below ground surface); I) mean weekly enhanced vegetative index (EVI); J) mean daily mid-day (10:00 – 16:00) albedo.

Water table position between the two landscapes was markedly different, with a near surface water table prominent in the fen (interannual mean 8cm bgs) and a much deeper (interannual mean 209 cm bgs) water table in the upland (Figure 3-2H). Once a stable and high WT position was established post-2013, the largest seasonal variability in fen WT position was during the drier

summer of 2017. Other notable seasonal variability included an increase in monthly average WTD in both 2018 and 2019 from July (from 6 and 7 cm bgs) to September (1 and -6 cm bgs, respectively), following large rain events (> 90 mm over four days, 2018) and increased precipitation frequency (2019). Upland WT position decreased from 2014 (158 cm bgs) to 2015 (207 cm bgs), after which it remained relatively stable (2015-2018), with seasonal means ranging between 200 to 220 cm bgs (Figure 3-2H). Mean seasonal WT saw a marked decrease in 2019, the deepest during the entire study period (257 cm bgs). In both landscapes, smaller scale (<5mm), sporadic rain events appear to have a negligible impact on daily WT position, however, larger (2018), or recurring rain events (2019) or prolonged dry periods (2017) effected overall WT trends.

3.3.1.3 Vegetation growth and changes in surface conditions (2013-2019)

During the seven years following construction, NFW evolved from a barren landscape to a robustly vegetated ecosystem (Figure 3-1C-D; Figure 3-3). EVI values depict plant development and expansion, with values >0.2 representing a vegetative signal (Figure 3-2I). In both the fen and upland, the 2013 EVI signal was indicative of bare ground (seasonal means of 0.18 (fen) and 0.16 (upland), Figure 3-2I). Following planting campaigns in 2013, some plant establishment had begun in the fen (0.24) as well as upland understory development of grasses (0.21). By 2015, plant development between the two landscapes began to diverge, with fen vegetation becoming wide-spread and robust (EVI: 0.36) and remaining relatively steady with seasonal EVI means ranging between 0.32 (2019) to 0.47 (2017). Upland values increased annually, but at a slower rate than those in the fen, with 2015 seasonal mean remaining low (0.23). EVI increased after 2016 as trees and understory vegetation continued to mature and become more widespread (0.31, 0.35, 0.34, 0.41from 2016 – 2019; Figure 3-2I). Interannual variability is present within both landscapes (Figure 3-2I) and is representative of low EVI values during the shoulder seasons (May and

September). Furthermore, surface conditions evolved as vegetation developed due to the production of a litter layer. In the fen, *Carex aquatilis* and *Typha latifolia* both produce large amounts of seasonal litter, resulting in the rapid accumulation of litter from 2015 (seasonal mean of 2.7 cm) to 2019 (seasonal mean of 17.8 cm; data from Chapter 2). In the upland, the litter layer developed at a slower rate due to the lower volume of plant matter deposited seasonally (i.e., juvenile aspen trees and conifers), but still increased from <1 cm in 2015 to 3.8 cm in 2019.

Complementary to plant development was the change in the proportion of surface water and bare ground over time. Results from the simplified land cover classification reveal that initially in the fen, surface water covered 47% and 41% of the fen surface in 2013 and 2014, respectively (Figure 3-3). The remainder of the surface was dominated by wet, dark, bare peat (53% in 2013) or a mix of bare peat and juvenile vegetation (18% bare, 41% mixed bare + veg in 2014; Figure 3-3; Table 3). By 2015, fen vegetation had become widespread (62%) and previously ponded regions had become infilled by rapidly expanding, invasive *Typha latifolia*, creating regions of mixed veg + water (23%; Figure 3-3; Table 3-3), and only 15% bare peat. From 2016 onwards, the fen surface was dominated by full plant coverage, ranging from 53 to 68%, which fluctuated depending on environmental and meteorological conditions (Figure 3-3). Similarly, the proportion of bare ground in the upland decreased over time from >95% in 2013, to 34% in 2016 (Figure 3-3). From 2014 to 2016, upland surface conditions consisted of regions with varying degrees of mixed bare ground and vegetation cover (Figure 3-3; Table 3-3). By 2017 there were regions of full vegetation coverage (22%), followed by an increase in 2018-2019 to almost complete vegetation cover (77 and 87% respectively; Figure 3-3).

Above mentioned surface changes, due to plant emergence and growth, were mirrored in changes in albedo values over the seven year study period (Figure 3-2J). During bare ground

conditions, the two landscapes had larger differences in albedo (0.09 and 0.25, for the fen and upland, respectively). As vegetation became more expansive, mean seasonal albedo values shifted in both landscapes (Figure 3-2J) and ranged between 0.12 - 0.14 (fen) and 0.16 - 0.18 (upland) from 2017 to 2019.

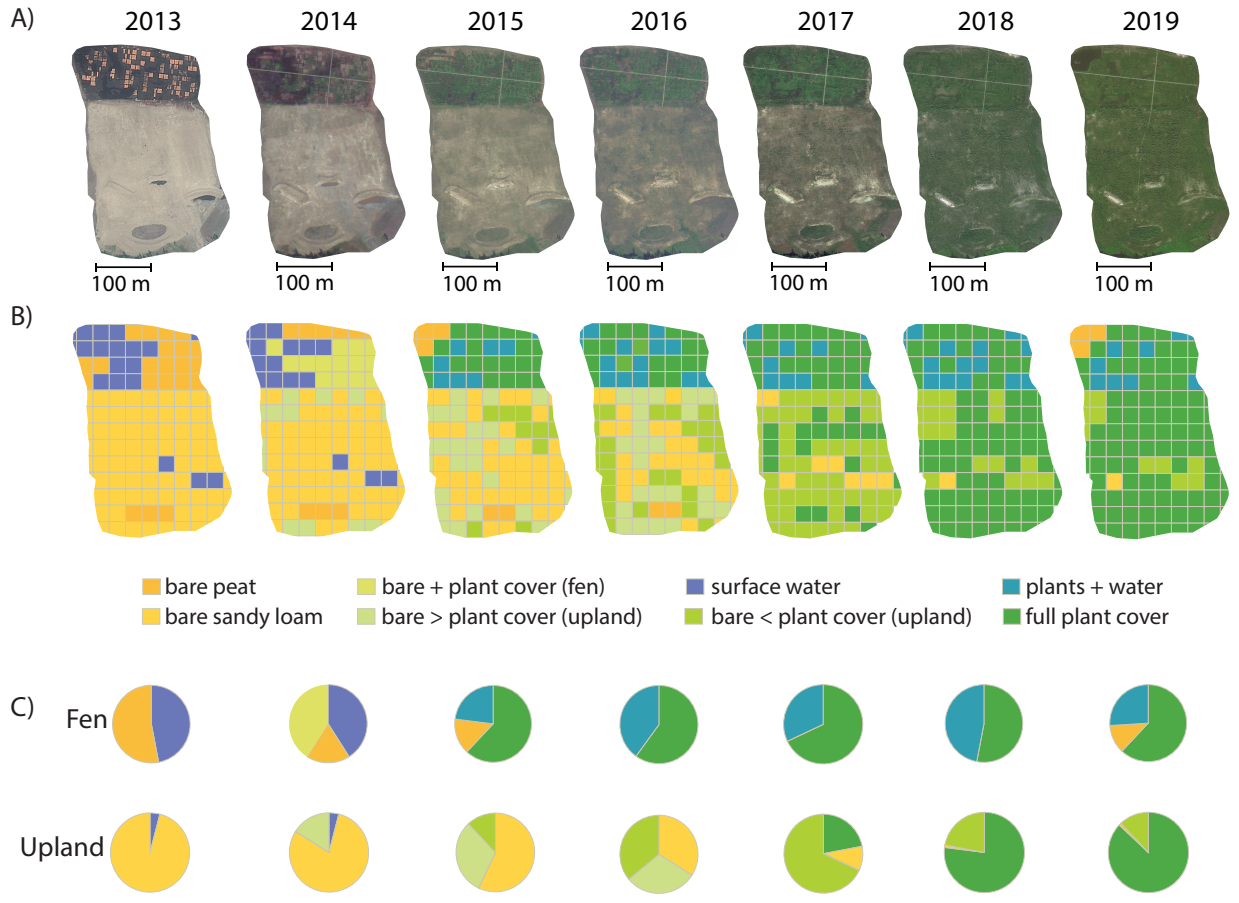


Figure 3-3: Spatial and temporal changes to surface conditions from 2013 to 2019. A) Satellite imagery of site evolution from year 1 (2013) to year 7 (2019). B) Results of the supervised land use/land classification (LULC) analysis where each pixel is 30m x 30 m. C) Distribution of land class (%) for each year during the study period for the fen (top) and upland (bottom). Legend corresponds to both B and C.

3.3.2 Evolution of Surface Energy Fluxes (2013-2019)

Available energy (Q*) varied between the two landscapes with the fen consistently exhibiting slightly higher Q* than the upland (interannual means of 130 and 100 Wm^{-2} respectively; Figure 3-4, Table 3-4). Latent heat (Q_E) was the dominant energy flux in the fen, consuming at least 50% of available energy across all years (Figure 3-4; Table 3-4). Q_E decreased over time from 113 Wm^{-2} in 2013 to 68 Wm^{-2} in 2019 (Table 4). During the day, positive Q_E values occurred between 6h-22h, with peak values between 12h – 18h (Figure 3-4B). In contrast, sensible heat (Q_H) steadily increased as the fen developed from 28 Wm^{-2} in 2013 to 54 Wm^{-2} in 2019 (Table 3-4). During the day, positive Q_H fluxes occurred during a narrower daytime window than Q_E (from 8h-19h) with highest values occurring between 10h-16h (Figure 3-4C). Mean seasonal ground heat flux (Q_G) in the fen was low in 2013 (1 Wm^{-2}), followed by an increase from 2014 onwards (between 8-12 Wm^{-2}; Table 3-4). Fen's diurnal Q_G trends showed a clear difference between night and day in early years (2013-2015), while in later years the diurnal Q_G signal became more muted (Figure 3-4D). Moreover, there was a shift in the timing of peak daily Q_G between 2013 and mid-2014, aligning with the transition from bare ground to vegetated surface. Seasonally, Q_E was typically highest during peak season (July) in the fen (Figure 3-4B), while Q_H and Q_G peaked in May and decreased throughout the growing season (Figure 3-4C,D). Mean seasonal midday (10h to 16h) Bowen ratio (β) in the fen ranged between 0.50 (2016) to 1.21 (2017) (Figure 3-6C) and was typically higher earlier in the season (May to mid-June), followed by a steady decrease throughout the growing season.

Upland partitioning of available energy was less dynamic than the fen's, with Q_E and Q_H making up almost equal parts in all years except 2013 (Figure 3-5). Notably, 2015 was the only year that Q_H made up a larger portion of the available energy (Table 3-4). Interannually, Q_E increased

slightly over time in the upland from 42-52 Wm^{-2} in early years (2013-2015) to 58-65 Wm^{-2} in later years (2017-2019; Table 4; Figure 3-5B). Q_H was typically highest in May/June apart from 2017, where highest values were observed in mid-July and into August (Figure 3-5C). In early years (2013-2015), upland's daily peak Q_G ranged between 70 to 100 Wm^{-2}, whereas in later years (2017 onwards), it ranged between 50 to 70 Wm^{-2}. Unlike the fen, diurnal peaks occurred during the same time frame (10h-16h) across all years and fluxes (Figure 3-5). Moreover, there was greater diurnal oscillation in upland Q_G compared to the fen, with larger daytime gains followed by rapid losses at night (Figure 3-5D), which resulted in low mean Q_G (<5 Wm^{-2}). Upland mean seasonal midday β was consistently above 1 and ranged between 1 and 1.6 (Figure 3-6C). However, monthly averages show that midday β was typically higher during the shoulder season, ranging from 1.4 to 2.8 in May and September, and lower during peak season (0.6 to 1.2 in mid-June – early August), with later years (2017) exhibiting the lower end of peak season β values.

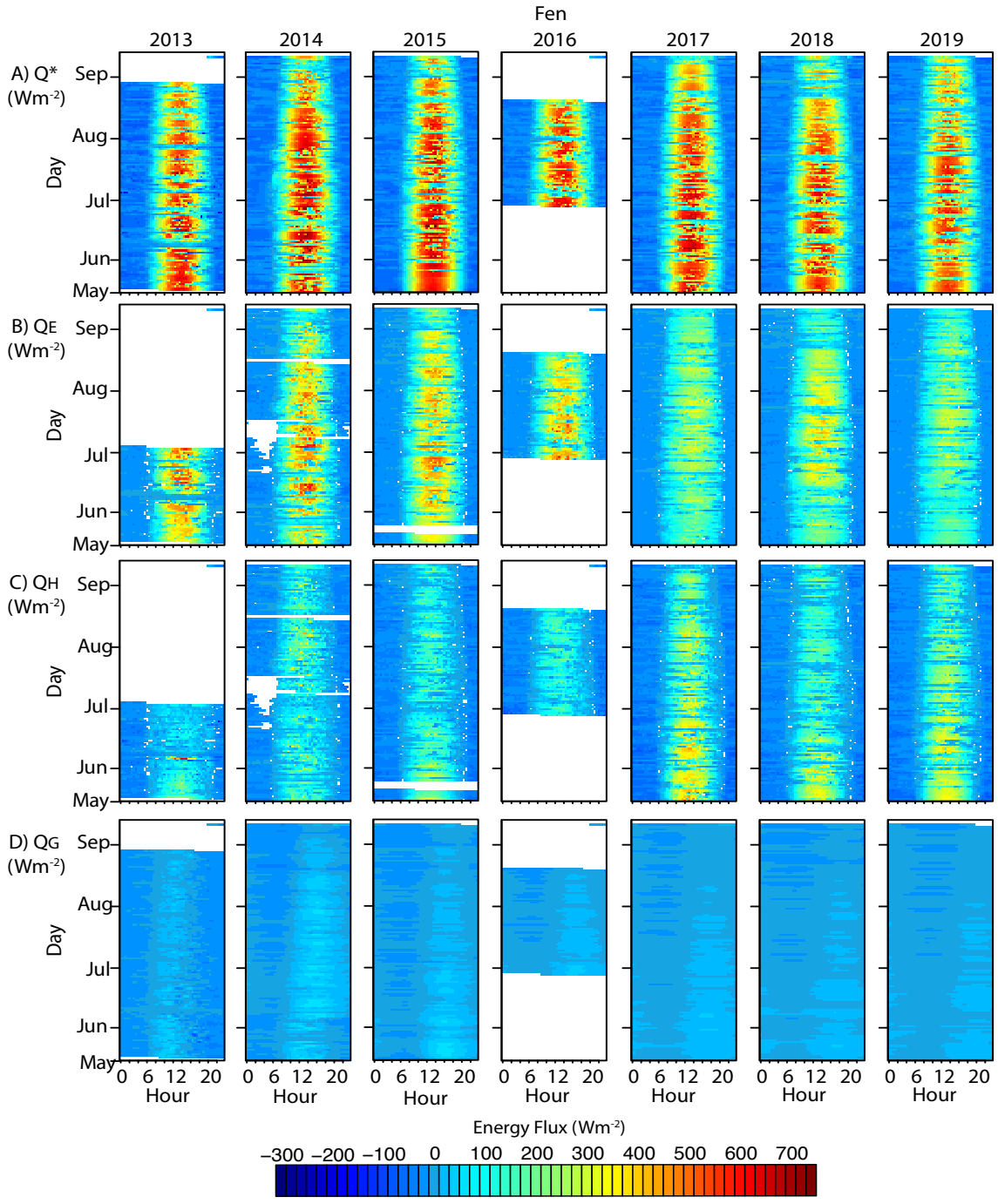


Figure 3-4: Fingerprint plot depicting gap-filled, half-hourly surface energy fluxes from 2013 – 2019 for the fen. Each square is a half-hourly measurement, and each row represents a full day. Plots show seasonal (May-Sept, y-axis) and diurnal (hourly, x axis) trends of A) Net radition (Q*); B) Latent heat flux (Q_E); C) Sensible heat flux (Q_H); D) Ground heat flux (Q_G) in Wm^{-2}. 2016 missing data is due to Horse Creek Wildfire. 2013 Fen: July-Aug and 2017 Upland: August missing data is due to instrumentation malfunction.

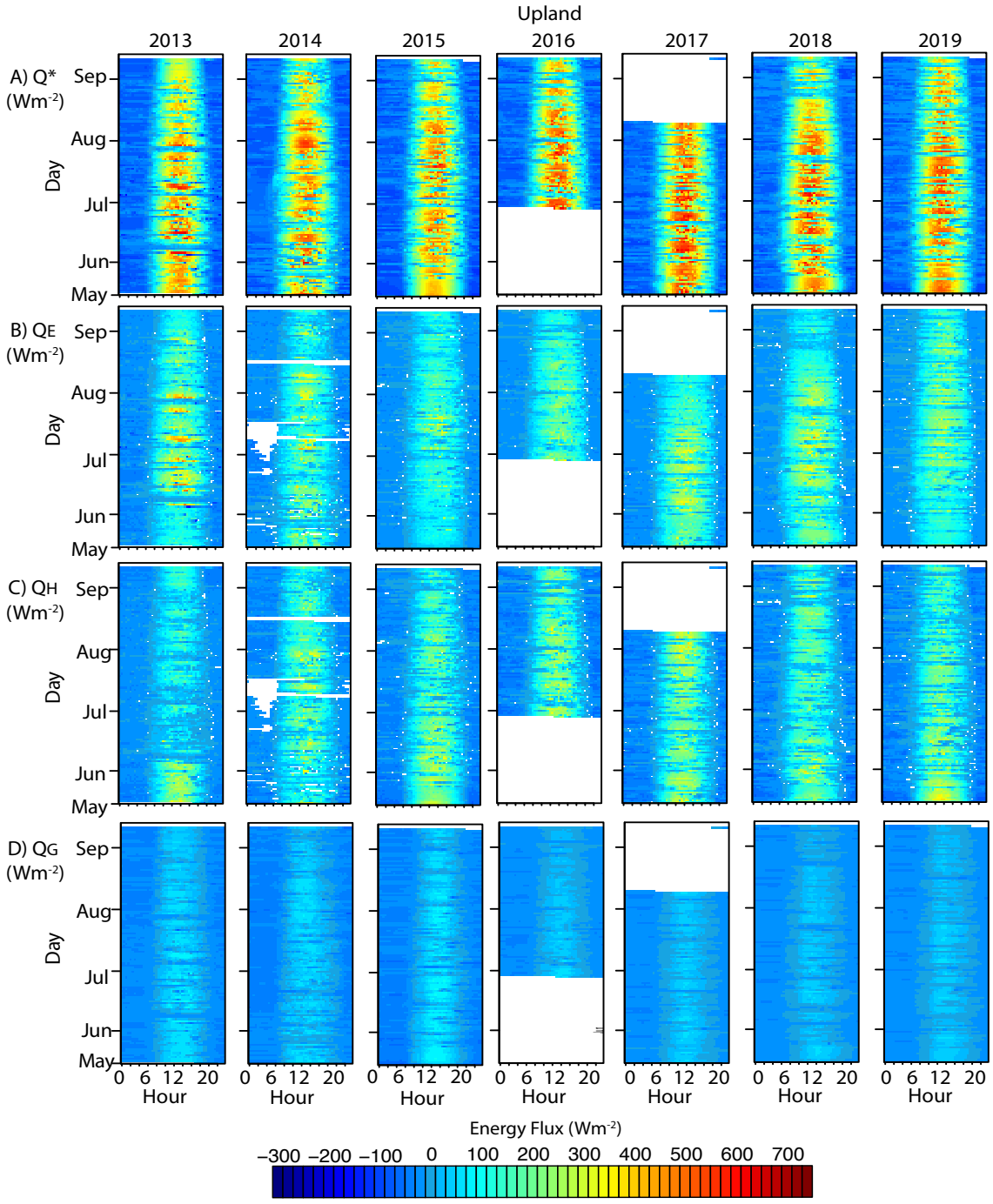


Figure 3-5: Fingerprint plot depicting gap-filled, half-hourly surface energy fluxes from 2013 – 2019 for the upland. Each square is a half-hourly measurement, and each row represents a full day. Plots show seasonal (May-Sept, y-axis) and diurnal (hourly, x axis) trends of A) Net radition (Q*); B) Latent heat flux (Q_E); C) Sensible heat flux (Q_H); D) Ground heat flux (Q_G) in Wm^{-2}. 2016 missing data is due to Horse Creek Wildfire. 2013 Fen: July-Aug and 2017 Upland: August missing data is due to instrumentation malfunction.

Table 3-4: Mean seasonal energy flux for each energy balance component and the ratio of energy flux components normalized to net radiation (Q*) for the fen and upland from 2013 – 2019.

Year	Q* Wm^{-2}	Q_E Wm^{-2}	Q_H Wm^{-2}	Q_G Wm^{-2}	Q_E/Q^*	Q_H/Q^*	Q_G/Q^*
Fen							
2013	125	113	28	1	0.91	0.22	0.01
2014	143	106	37	12	0.74	0.26	0.09
2015	146	104	32	9	0.72	0.22	0.06
2016	149	111	30	10	0.74	0.2	0.07
2017	146	77	59	10	0.53	0.41	0.07
2018	130	81	42	8	0.62	0.32	0.06
2019	130	68	54	9	0.53	0.41	0.07
Upland							
2013	84	52	30	3	0.62	0.4	0.04
2014	91	50	48	1	0.54	0.51	0.01
2015	91	42	48	2	0.46	0.53	0.03
2016	102	54	48	0	0.53	0.47	0.00
2017	123	65	56	4	0.53	0.45	0.03
2018	103	60	43	1	0.59	0.42	0.01
2019	105	58	47	2	0.55	0.44	0.02

3.3.3 Changes in surface ecophysiological parameters

Conductance terms (g_a, g_s) exhibited temporal changes over the study period (Figure 3-6A). g_a mirrored vegetation development, with lowest season average occurring in 2013 (22 mm s^{-1}) and then remained relatively steady from 2015 onwards (27 to 33 mm s^{-1}). 2014 had the highest g_a and corresponds with the rapid invasion and growth of *Typha latifolia*. g_a had a wide range of values throughout the growing season (22 to 157 mm s^{-1}) and typically lower values occurred during the shoulder season (May, September), with larger values coinciding with peak plant growth. In contrast to g_a, early years exhibited higher g_s values (seasonal mean of 8 to 9 mm s^{-1}) than later years (4 to 6 mm s^{-1}). Mean seasonal decoupling factor (Ω) in the fen ranged from 0.32 to 0.49

and exhibited a slight decrease over time (Figure 3-6B). 2017 exhibited the lowest means (Figure 3-6A,B) and range of values for both g_s (maximum of 29 mm s^{-1} in 2017 vs. 40-50 mm s^{-1} in other years) and Ω (maximum of 0.74, vs other years (0.8-0.9)). Friction velocity (u*) changed over time (Figure 3-6D) with lowest seasonal mean u* occurring in 2013 (0.14) followed by an abrupt increase in 2014 (0.26) coinciding with the invasion and rapid quick growth of *Typha latifolia*. After 2015 u* remained relatively stable, ranging between 0.19 – 0.23 (Figure 3-6D).

Similar to the fen, upland g_a increased over the study period with early years (2013-2015) exhibiting similar seasonal mean of 24-25 mm s^{-1}, followed by an increase to 31-41 mm s-1 from 2016 onwards, with 2019 having the largest mean g_a (Figure 3-6A). Overall upland g_s was lower than in the fen and seasonal means ranged between 2.5 to 4.5 mm s^{-1}(Figure 3-6A). Mean seasonal Ω values in the upland ranged between 0.23 to 0.30 (Figure 3-6B), and were generally lower than in the fen. Upland u* slowly increased over time with similar values from 2013 – 2016 (seasonal means between 0.19-0.22), followed by an increase in 2017 – 2019 (0.23, 0.26, 0.28 respectively; Figure 3-5D).

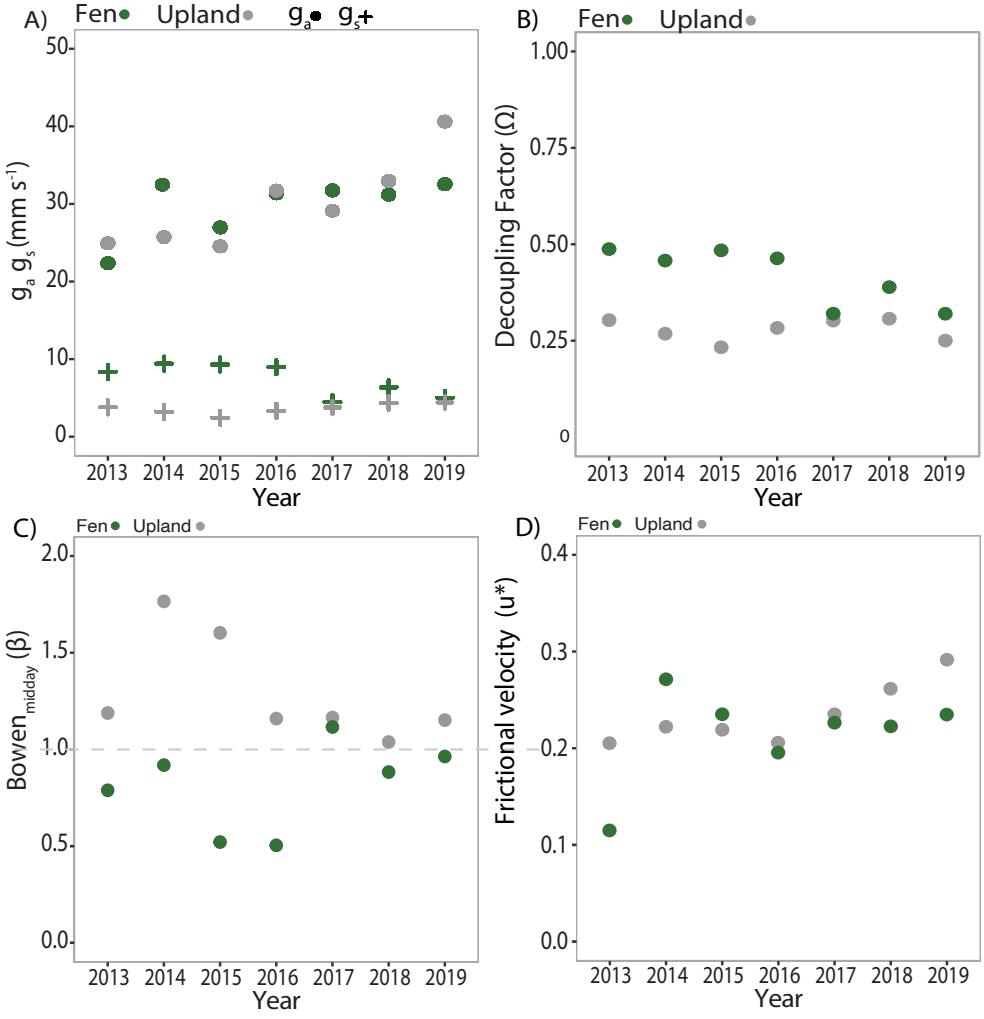


Figure 3-6: Growing season averages of A) aerodynamic conductance (g_a, circles) and surface conductance (g_s, crosses); B) decoupling factor (Ω); C) Bowen ratio (β) and D) frictional velocity (u*) from 2013 - 2019.

3.4 Discussion

3.4.1 Changes in surface energy partitioning (2013-2019)

Surface energy and moisture exchanges are largely controlled by the coupled interactions between surface characteristics and atmospheric forcings, such as radiation and VPD (Helbig et al., 2020a; Worral et al., 2019; Brümmer et al., 2012, Baldocchi et al., 2000). Distinct temporal changes to intra and interannual growing season surface energy partitioning were observed at our study site in the first seven years post construction and coincided with the biophysical development of NFW from a barren landscape to a robustly vegetated ecosystem. To provide context, results from this study were compared to those from natural and post-disturbance (e.g., post-fire, harvest, drainage) boreal landscapes (Figure 3-7). Due to the heterogeneity of boreal ecosystems and the hydroclimatology of the WBP (sub-humid with decadal dry cycles and periods of water stress; Brown et al., 2010; Bothe and Abram 1993) Figure 3-7 is largely focused on studies from a Canadian (western) boreal setting with similar ecohydrological conditions.

3.4.1.1 Fen

Following construction in 2013, the fen surface consisted of wet, dark, bare peat with large regions of ponded water. Low albedo and the large amount of available surface water, paired with the high evaporative atmospheric demand common to the region, resulted in Q_E dominating available energy (Q_E/Q^* 0.91), with a corresponding $\beta < 1$ (Table 3-4). During this time, energy partitioning is interpreted to have been driven largely by available water and radiative forcing (Q^*), as g_s and Ω were high (relative to other years; Figure 3-6A,B), suggesting decoupling between the surface and atmosphere. High Q_E/Q^* (>0.85) values have been reported at unrestored (Petrone et al, 2004) and abandoned (Waddington and Price, 2000) peatlands with similar surface conditions (i.e. wet

and barren). Moreover, in a review of peatland ecohydrological feedbacks post-wildfire, Nelson et al. (2021) describes a decrease in both albedo and plant-mediated shading as key feedbacks for changes to energy partitioning immediately following severe burns. However, under drier conditions unrestored peatlands had reduced Q_E/Q^* (0.67-0.69; Petrone et al., 2004; Waddington and Price 2000; Price et al., 1998). Moreover, Morison et al. (2020) reported lower values (Q_E/Q^* 0.47 and 0.45), with more energy being partitioned towards Q_H than Q_E (β of 1.19) in the second and third-year post-fire, due to dry surface conditions, post-fire soil hydrophobicity and limited water availability, further depicting the role of site-specific biophysical conditions on surface-atmosphere interactions.

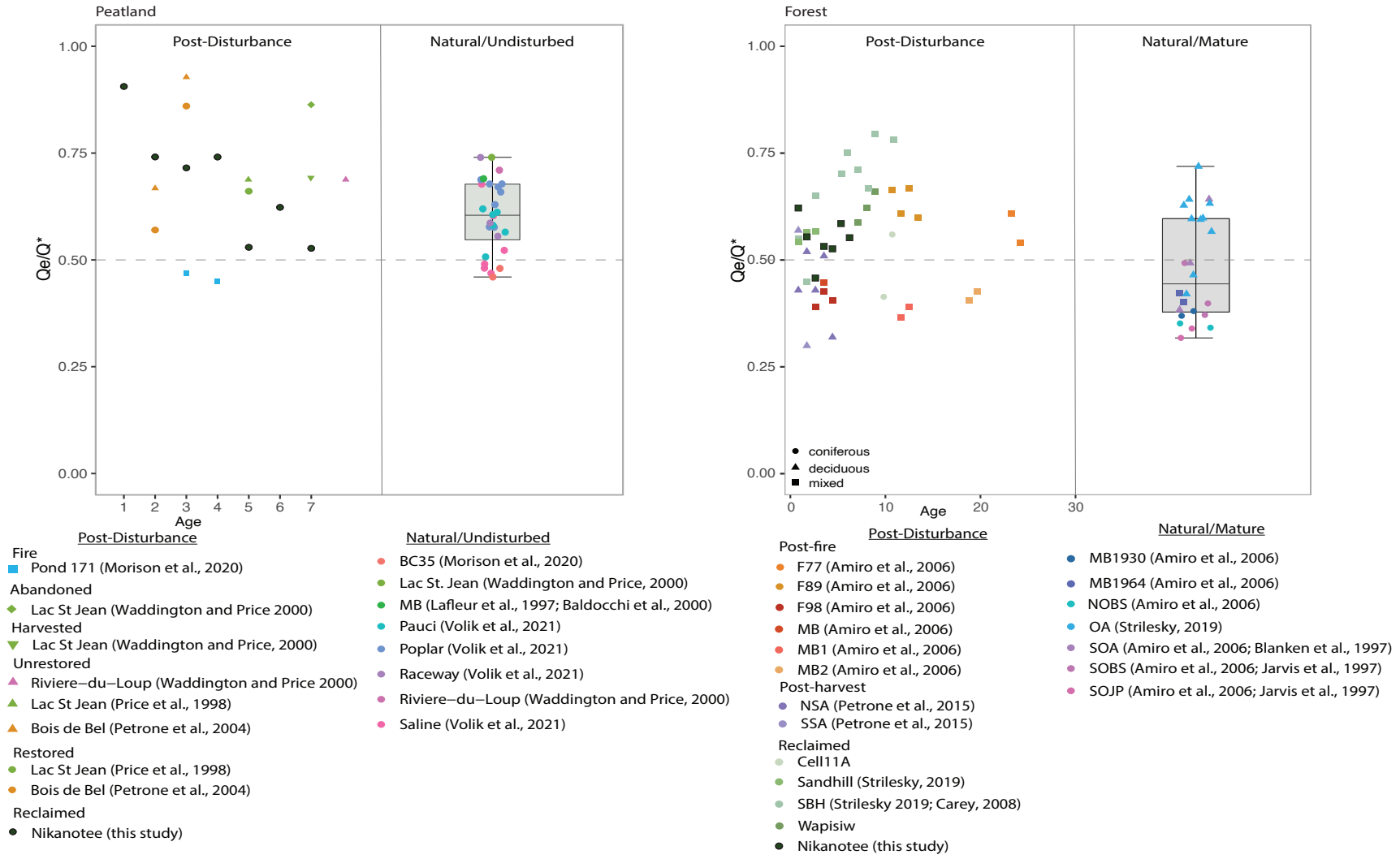


Figure 3-7: Mean growing season latent heat flux (Q_E) normalized to net radiation (Q*) based on age since disturbance for peatland (A) and forest (B) sites in a Canadian boreal setting. NFW (this study) is represented by black points. Box and jitter plots represent the range of values for natural or mature (> 30 years post-disturbance) sites.

The effects of plant emergence on energy exchange are complex as it results in changes to surface roughness and albedo (Lee et al., 2021; Worrall et al., 2019; Thompson et al., 2015; Admiral and Lefleur, 2008). As fen vegetation became more widespread (2014 - 2016), the proportion of bare ground and ponded areas significantly decreased (Figure 3-1C-D, Figure 3-3). However, water table and soil moisture remained high (Figure 3-2G,H). The emergence of vegetation resulted in an increase in albedo from 0.09 to 0.14 by 2016, as well as increases in surface roughness, g_a and u*, which resulted in less absorption of incoming radiation by the peat surface and more longwave re-radiation and likely further enhanced Qe through turbulent transport (Green et al., 2020). Q_E continued to make up the largest component of energy partitioning (0.72-0.74), albeit less than during bare ground conditions. Moreover, shade from rapidly growing, tall vascular vegetation (*Typha latifolia* and *Carex aquatilis*), paired with the increase in albedo, resulted in a decrease in peat temperature over time (Figure 3-2F) and likely less evaporative loss directly from the surface compared to bare ground conditions in 2013 (Chapter 5). During this period there was a decrease in negative Q_G observations, an increase in daily amplitude (Figure 3-4D, Table 3-4), and a 1-3 hour lag in diurnal trends with respect to Q*, reflective of the change in surface conditions, which is attributed to higher heat capacity of wet, peat soils (Alekseychik et al., 2018; Wu et al., 2021). Notably, during this period, energy partitioning remained similar between years (2014 – 2016), Figure 3-4, Table 3-4) even though the site experienced variable meteorological inputs (i.e., dry vs wet years; timing and frequency of P). This is attributed to the relatively consistent high water table and VWC, resulting in limited surface stomatal control over energy fluxes. As a result, Q_E was likely largely driven by Q* and VPD, as indicated by high decoupling (mean seasonal $\Omega > 0.45$; Figure 3-6B). An intermediate to high degree of surface-atmosphere decoupling (Ω) has been reported across boreal peatland landscapes (Ω of 0.34 to 0.74;

Alekseychik et al., 2018 Runkle et al., 2014; Brümmer et al., 2012; Kurbatova et al., 2002), with variability largely driven by plant community composition, water availability and edaphic conditions.

From 2017 – 2019, there was a shift in energy partitioning, compared to earlier years, where Q_E was still the dominant energy flux, but a larger proportion of available energy was partitioned to Q_H (Q_H/Q^* of 0.32 to 0.41, compared to 0.20 to 0.26 in earlier years; Figure 3-4; Table 3-4). In terms of biophysical changes during this period, vegetation was well-established and widespread with extensive belowground biomass formation - rooting depth extended >50 cm bgs (Messner, 2019), and a relatively thick litter layer (mean: 12 to 17 cm from 2017 to 2019, but reaching a maximum of 27 cm thick in some areas) was formed. The litter layer altered the feedbacks between surface and atmospheric energy and moisture exchanges by providing radiative sheltering and shading of the surface, thus further limiting the amount of energy reaching the peat surface, resulting in a decrease in soil temperature (Figure 3-2F) and ultimately, a reduction in evaporative surface losses (Figure 3-4B). Similar feedbacks associated with plant sheltering and shading have been described by Waddington et al. (2015) and Green et al. (2020) and extensively in peatland restoration literature, where straw mulch is commonly applied to the peat surface during early restoration to limit water losses and large fluctuations in soil temperature, and aid in revegetation (Xu et al, 2021; Rowland et al., 2021; Chimner et al., 2017; Petrone et al., 2004; Rochefort 2000; Price et al., 1998). Following litter development at NFW-fen Q_G daytime signal was dampened (Figure 3-4D). Moreover, there was an increase in Q_H particularly in the early season, compared to earlier years. This is attributed to the timing and lag in plant emergence in later years (2017 onward), as new growth required more energy and time to break through the litter layer to the surface, resulting in the delay of plant transpiration. Moreover, the litter surface had a higher

albedo than green plant matter resulting in less absorption of incoming energy while also heating up faster (less water content). As a result, mean monthly β was >1 during the month of May to early June in later years compared to <1 in earlier years. In contrast to earlier years, there was a reduction in Ω and g_s, which is indicative of stronger surface-atmosphere coupling. During the 2017 season, plants had developed deeper roots and were able to access deeper stores of soil moisture during dry periods of watertable drawdown. As a result, Q_E was largely driven by surface controls in later years of this study, unlike radiative energy in previous years. This was further evident from the overall decrease in Ω (seasonal mean of 0.32), denoting a higher degree of coupling between the surface and atmosphere. Moreover, there was a decrease in g_s (Figure 3-6A), likely due to stomatal closure during periods of water stress or high VPD providing further evidence of stronger surface – atmosphere coupling. A decrease in g_s is well documented in literature to represent regulation of plant mediated moisture exchanges (Runkle et al., 2014; Oren et al., 1999; Schulze et al., 1994). The decrease in g_s observed during the 2017 season, coincided with WT drawdown - a coupled relationship which has been described in several peatland studies, particularly those with continuous vascular plant coverage (Peichl et al., 2013; Raddatz et al., 2009; Acreman et al., 2003). For example, Alekseychik et al. (2018) describe a relationship between WT drawdown and a subsequent decrease in Ω, and g_s showing stronger coupling between the surface and atmosphere as WT position deepens as well as a relative increase in β. Other studies at boreal peatlands have shown similar relationships, following a significant decrease in water table, resulting in a decrease in Q_E with an increase in Q_H (Worrall et al., 2015; Wu et al., 2010; Wilson et al., 2002). However the degree that fluctuations in soil moisture and WT position affect energy partitioning and moisture fluxes is also dependant on ecophysiological controls such as the dominant plant community (ex. vascular vs bryophyte; Admiral and Lafleur, 2007).

2018 and 2019 were wetter years with similar total P, but differences in P timing, frequency, and intensity. As a result, energy partitioning rates varied between the two years. 2018 was warm and wet, and the growing season was punctuated by a large rain event in July (86 mm over four days) that resulted in extensive ponding for the remainder of the season. Moreover, 2018 had the largest range and highest values of VPD (maximum of 4.9 kPa, Figure 3-2D). Thus, water availability was high and able to sufficiently satisfy high atmospheric demands. This likely explains the increase in Q_E and decrease in Q_H in July-August of 2018 (Figure 3-4B). In contrast, 2019 was wet and cool with increased cloud cover resulting in an overall decrease in available energy (Figure 3-4A, particularly towards the end of the season). Although there was ample available water, similar to that of 2018, lower Tair and limited available energy resulted in a surplus of water that could not be evaporated or transpired. As such, 2019 observed the lowest Qe rates during the study period, even though it was one of the wettest years, further depicting the complexity of feedbacks between surface-atmosphere exchanges.

As a result of wet surface conditions Q_E is typically the dominant energy flux in boreal peatland ecosystems, with β typically <1 (Lafleur, 2008). However due to regional climate variability, as well as plant community composition and edaphic conditions, natural and post-disturbance fens throughout the boreal experience a large range of values for energy and moisture exchanges both between sites and interannually within a single site. (Figure 3-7; Volik et al., 2021a; Helbig et al., 2020a; Alekseychik et al., 2018; Brümmer et al., 2012; Lafleur, 2008). At nearby fens, within 60km of NFW, Q_E/Q^* ranged between 0.4-0.6 for an open, sedge-dominated fen to 0.55 – 0.73 for treed fens (Volik et al., 2021). Following the emergence of vegetation, NFW-fen values fell within the range of Q_E/Q^* and β values described in natural settings (Figure 3-7). NFW-fen surface

albedo, values were also within range of natural peatlands (0.9-0.16; Helbig et al., 2020a; Lafleur et al., 2008).

3.4.1.2 Upland

Initially following construction during the early 2013 growing season, the upland surface consisted of dry bare ground and limited available surface water, resulting in a higher albedo, a larger proportion of long wave reradiation and lower Q* values compared to the fen (Table 3-4). These surface conditions were further reflected in Q_E and Q_H signals (Figure 3-4B, Q_E and Q_H, May to June), with Q_H exceeding Q_E. Moreover, as the upland is a more water-limited system compared to the fen, P inputs produced short-term (i.e., hourly to daily) edaphic responses in VWC. High intensity P events at the beginning of June resulted in large amounts of overland flow and ponding, due to limited infiltration capacity of the capping layer (Ketcheson, 2015). Following this event there was a shift in energy partitioning with Q_E exceeding Q_H (Figure 3-5). To increase infiltration and aquifer recharge, furrows were tilled perpendicular to the slope of the upland in 2013, prior to upland planting (Table 3-2). In 2013, Q_E comprised a larger proportion of energy fluxes (Table 3-4), however due to the dry edaphic conditions and limited water-availability, seasonal mid-day β remained >1 (Figure 3-6C). Mean seasonal Ω was 0.30 (Figure 3-6B) suggesting some degree of surface-atmosphere coupling. From 2014 to 2016 early successional understory vegetation emerged, consisting of forbs and grasses. However, the timing of emergence and spatial distribution of vegetation was uneven and sparse, due to the heterogeneity of edaphic conditions such as variability in capping layer thickness and soil moisture (Sutton and Price 2020a,b; Popović et al., 2022). A large proportion of the surface continued to be dominated by bare ground (80 to 34% from 2014 to 2016; Figure 3-3). Moreover, trees planted in 2013 and 2015 were small seedlings with low leaf area, and began significant growth and development beginning in 2016

(Figure 3-2I; Figure 3-3). Moreover, the development of soil macropores, paired with the effects of tillage, resulted in higher infiltration rates and a larger percentage of P inputs partitioned to groundwater recharge rather than surface evaporation (Sutton and Price, 2020b). During this time, mean seasonal Ω was low (0.23 to 0.28) and mean β remained >1, indicating coupling between the surface and atmosphere. Here, energy partitioning was largely driven by limited water availability and surface conditions (i.e. bare ground, sparse veg, higher albedo).

In the first 1-3 years post-reclamation, surface characteristics of NFW upland differed from that of other post-disturbance landscapes. Immediately following harvest or fire disturbance (0-2 years), albedo is typically reduced due to the removal of vegetation and the presence of charcoal residue, scorched soil and/or coarse woody debris (Halim et al., 2019; Chambers and Chapin, 2002). Moreover, natural landscapes typically have a higher proportion of organic matter, and thus darker appearance, and some remnant live or dead vegetation compared to salvaged forest soils used in reclamation (Quideau et al., 2013; Naeth et al., 2013; Rowland et al., 2009)). Amiro et al. (2006b) reported a summertime albedo immediately post-fire of ~0.05 in a synthesis of post-fire energy dynamics of 22 boreal forest sites. Similar decreases in albedo (to 0.07, 0.08) have been reported post-fire in boreal stands (Jin et al. 2012; Chambers et al., 2005). Post-harvest summertime albedo reduction, compared to pre-disturbance values, have also been reported, with generally a smaller decrease than post-fire (albedo ~ 0.09-0.11; Halim et al., 2019). In contrast to these values, NFW upland albedo in years 2 and 3 was higher (0.25 and 0.20) due to the barren and dry, light coloured sandy-loam cover soil and sparse patches of understory vegetation, dominated by forbs and grasses that began emerging at this time. Similar albedo values have been reported for dry, bare agricultural sandy loam soils (0.18 – 0.25; Cellier et al., 1996). Moreover, previous studies of grasslands and forest successional species indicate higher reflectance and

increased albedo of grasses and deciduous shrub species (~0.2; Randerson et al., 2006; Baldocchi et al., 2000; Betts and Ball 1997). These differences in post-disturbance surface conditions (i.e. albedo) correspond to variability in Q* between these landscapes, with post-fire sites exhibiting a 3-20% increase in Q* (Amiro et al., 2006a; Chambers et al., 2005). Similarly, Petrone et al. (2015) reported a post-harvest mean Q* ranging between 103 to 140 Wm^{-2}. This contrasts with reclaimed AOSR uplands (NFW upland and South Bison Hill), which exhibited lower mean Q* in early years (between 70 to 91 Wm^{-2}, Strilesky, 2019; Table 4). However, as vegetation became more wide-spread and robust, NFW albedo decreased (0.16-0.18; and mean Q* increased (105 to 125 Wm^{-2})) and was similar to that of other vegetated boreal uplands (Helbig et al., 2020a; Jin et al., 2012; Amiro 2006b; Baldocchi et al., 2000).

From 2017 onwards, vegetation became more widespread, and the proportion of bare ground decreased (Figure 3-1C-D, Figure 3-3) along with trees developing in terms of height, rooting architecture and leaf area, and the formation of a thin litter layer (1 – 3 cm thick; Supplementary Table 1). These biophysical changes resulted in a decrease and stabilization of surface albedo as well as an increase in both g_a and u*. Due to surface changes, particularly the reduction of bare ground and increased radiative shading by vegetation, Q_G losses were also reduced (Figure 3-5D). During this time, mean midday β remains > 1, but is closer to one than in previous years (Figure 3-6C) and energy fluxes were likely controlled by surface (plant/stomatal) controls, as indicated by low Ω (0.25 – 0.31). Energy partitioning varied intraseasonally as well, with monthly β >1 during the shoulder season (May, September, sometimes August) and <1 during peak season, defined by maximum leaf out, further highlighting the control of vegetation on energy partitioning. Similar intraseaonsal β trends, highlighting the role of plant phenology on energy fluxes, have

been described in a nearby reclaimed upland (Carey, 2006), as well as in natural sites (Amiro et al., 2006; Blanken et al., 1997).

Boreal forest ecosystems exhibit a large range of values in terms of energy and water exchanges, due to the heterogeneity of these systems, which is driven by variable climate (Brümmer et al., 2012; Eugster et al., 2000; Baldocchi et al., 2000), water availability (Petrone et al., 2015), edaphic conditions (Brown et al., 2014) and stand architecture. Stand architecture includes variability in LAI (i.e. open vs. closed canopy), understory characteristics, successional stage, forest type (i.e., mixed, coniferous, deciduous) (Lukeš et al., 2013; Ni-Meister and Gao, 2011; Liu et al., 2008; Amiro et al., 2006ab; Thompson et al., 2004). Figure 3-7B captures the heterogeneity of these systems, depicted by the wide range of energy partitioning during post-disturbance recovery, with Q_E/Q^* ranging between 0.3 to 0.8 during the first 30 years post-disturbance. NFW upland values fell within this range (0.46 to 0.62) and exhibited a response in Q_E/Q^* under varying environmental conditions as the system evolved.

Variability in energy fluxes between reclaimed AOSR sites is attributed to different edaphic conditions (i.e. soil moisture and salvaged soil quality) and the timing of plant emergence, where both Sandhill Fen and South Bison Hill had higher soil moisture content in early years (<30% Strilesky et al., 2017; Carey, 2008), higher organic matter (~17% (Biagi et al., 2021) vs 4.5% NFW upland (Irving 2020)) and faster, more widespread emergence of understory vegetation than NFW (Strilesky, 2019). These differences in surface properties were reflected in energy partitioning, particularly with regard to Q_H in early years, where NFW Q_H/Q^* ranged between 0.40 to 0.53, compared to less than 0.40 for both Sandhill Fen and South Bison Hill (Strilesky, 2019). However, similar to other natural and reclaimed recovering uplands (Strilesky et al., 2017; Amiro et al., 2006b), once vegetation became more robust and trees matured (year 4-7), a slight decrease in β

was observed at NFW upland, likely due to an increase in leaf and root area, water uptake and thus transpiration. Amiro et al. (2006b) found that β was typically >1 in the first 10 years post-disturbance, followed by a decrease and steadying once trees matured. Strilesky et al. (2017) described water and energy dynamics during the initial twelve years following reclamation at a nearby site in the AOSR (South Bison Hill) and similarly observed a decrease in β with plant evolution from 1.1 to 0.4.

Environmental forcings such as climate and water-availability also affect ecosystems recovery, function and ultimately surface-atmosphere exchanges. Petrone et al (2015) examined two regenerating boreal aspen stands within the first five years post-harvest. They found wet conditions propelled rapid understory and stand recovery in the first 2 years, resulting in a higher proportion of energy partitioned to Q_E than Q_H. However, due to lower water availability following drought, Q_E/Q^* decreased and β subsequently increased. Carey (2008) observed a comparable response between wet and dry years during the initial three years of reclamation, with the wetter year exhibiting the highest Q_E/Q^* (0.65). Moreover, Amiro et al (2006b) describe local moisture limitations and climate effects as a key driver of annual Q_E variability in recovering uplands. A similar response to drier conditions was observed at NFW upland in 2015 and 2017, with increased β and decreased Ω. Ω values at NFW were higher than those reported for mature coniferous and deciduous forests, likely due to the juvenile nature of vegetation, particularly in early years, and dry edaphic conditions, however, they were comparable to a boreal mixed wood forest (ranging between 0.16-0.25; Brümmer et al., 2012). NFW upland g_a values were lower than at mature sites, due to the smoother surface of the understory, which dominated at the time (2013 – 2016). However, as trees matured, g_a increased and Ω decreased slightly. By year seven, g_a at NFW (44 mm s^{-1}) remained slightly lower than at mature sites (46 – 61 mm s^{-1}). In the initial years following

reclamation, NFW upland differed compared to natural, post-disturbance sites, due to biophysical differences such as albedo, edaphic conditions, and timing of plant emergence. However, once the plant community became established, energy partitioning and ecophysiological responses to climatic conditions mirrored that of natural, recovering ecosystems in the region. Several post-disturbance chronosequence studies (Strilesky et al., 2019; Amiro et al., 2006ab; Jin et al., 2012) state a period of 8-10 years post-disturbance is required for boreal forested ecosystems to mature and recover to pre-disturbance function. As such, based on the evidence presented here, and assuming sufficient future water availability, energy fluxes of NFW upland are on a trajectory to match nearby natural upland ecosystems.

By year seven (2019), ecophysiological properties and energy fluxes in both NFW landscapes were comparable to natural systems. From an energy partitioning perspective, intra and inter seasonal β trends aligned with those summarised in Helbig et al. (2020a), with the fen exhibiting $\beta < 1$, with lowest values in July and upland β remaining >1 early in the season and approaching 1 or less during peak season. Albedo values of NFW (fen 0.12-0.14; upland 0.16-0.18) were similar to values presented in Helbig et al. (2020a; peatlands 0.9 – 0.17; forests 0.08-0.14), although the slightly higher NFW-upland albedo is attributed to the system being a mixed broad and needle leaf forest compared to solely needleleaf systems described in Helbig et al. (2020a). Based on these results, NFW surface energy exchanges are comparable to natural and post-disturbance boreal landscapes, indicating the system is evolving towards a functional ecosystem.

3.4.2 Implications for oil sands reclamation and regional climate

Currently, there are limited studies of upland surface energy exchanges in a reclaimed AOSR setting and none capturing the energy dynamics following peatland reclamation. Moreover, the sub-humid climate of the WBP makes the region a further unique niche where boreal landscapes,

such as peatlands, exist despite frequent water limitations. Surface-atmosphere exchanges are important to overall ecosystem function as they influence the amount of energy and water available for key ecohydrological feedbacks and processes, such as energy for photosynthesis and evapotranspiration. From a reclamation standpoint, examining energy exchanges during landscape evolution provides further insight into the outcomes of ecosystem design and planting as well as the feasibility of reclamation endeavours providing information on the ecohydrological trajectory and stability of the system.

Results from this study indicate that within the first seven years of site establishment, NFW energy fluxes and ecophysiological responses to changing environmental conditions were comparable to natural and post-disturbance landscapes in the region, which is encouraging from a reclamation perspective. Results from this study add to our knowledge of the coupled dynamics of soil-plant-atmosphere-water dynamics and processes by providing a temporal snapshot of energy and water fluxes under varying surface and meteorological conditions. For example, our results provide further evidence of surface-atmosphere coupling and the important role of vegetation in regulating water losses. These results are particularly relevant for reclamation endeavours in the AOSR, as the region is expected to experience increased water-stress (Thompson et al., 2017; Ireson et al., 2015), and the question of ecosystem evolution, through plant succession and function under drought conditions, is a prominent issue. This work also provides a spatial snapshot of land cover change following reclamation, using ecosystem scale, remote sensing techniques, which could be a useful and feasible tool to apply to future studies of reclamation endeavours, especially for larger scale projects. However, this work only provides an initial (seven year) snapshot of energy dynamics – future work should include continued monitoring of energy exchanges as the NFW system evolves and trees mature. Moreover, a limitation of this study is that it only includes

the results from a single pilot site – variation to site design or even environmental conditions (e.g., air temperature and precipitation) during initial years following construction could result in a different successional trajectory and energy partitioning, particularly during early years. Thus, ecosystem scale monitoring at future reclaimed sites is recommended. Furthermore, this study only quantifies growing season measurements. Future work examining the effects of reclamation on winter albedo values and energy exchanges may be beneficial to understanding annual energy balance and climate interactions, as recent studies have indicated boreal wetlands may have a warming effect in winter but a cooling effect in summer (Wu et al., 2021). Overall, similar monitoring campaigns of future reclamation sites are recommended to improve and further reclamation practices, designs and assessments.

From a broader perspective, reclamation (i.e., land cover change) and the subsequent changes to surface-atmosphere exchanges could have implications and effects on regional climate and carbon balance (Mahmood et al., 2014). To date, an approximate area of 1055 km^2 has been impacted by open-pit oil sands mining in the AOSR (Alberta Environment and Parks, 2020) drastically altering surface conditions resulting in albedo changes, decreased surface roughness, drier surface conditions and ultimately a change in energy partitioning, all of which can impact surface temperatures, water and carbon dynamics as well as boundary layer thickness and cloud formation (Helbig et al., 2020b; Bonan, 2008; Chamber and Chapin, 2002). Increasingly boreal landscapes (in particular peatlands) are being proposed as nature based solutions (NbS) to climate change due to their water storage capacity, biogeochemical cooling effect and long-term sequestration of carbon dioxide (Strack et al., 2022; Helbig et al., 2020; Worral et al., 2019; Nugent et al., 2019; Frolking and Roulet, 2007). Firozjaei et al. (2021) found reclamation of a portion of the Hambach mine in Germany resulted in a decrease in mean land surface temperature (LST) by

up to 13°C. Similarly, Cao et al. (2020) found that for every 0.1 increase in EVI plant coverage, LST decreased by approximately 0.75°C in the mining city of Jixi, China. Worral et al. (2019) observed a significant decrease in LST in an 18-year study following the restoration and rewetting of a drained peatland. While LST was not directly examined in our NFW study, we did observe changes in soil temperature, energy partitioning, aerodynamic and surface conductance as well as ET fluxes (Chapter 2, Chapter 5) as the system evolved from a bare to vegetated system. Moreover, in Chapter 2 and Clark et al. (2019) observed a rapid return to carbon sink function at AOSR constructed fens within three years of reclamation. We infer that current energy and water exchanges at NFW are similar to that of nearby natural (or post-disturbance) landscapes and are an improvement compared to the bare, disturbed (pre-reclamation) landscape. Reclamation efforts in the AOSR could potentially help mitigate or lessen future climate change impacts by altering (i.e., returning) surface conditions to pre-disturbance radiative properties, which could affect the regional energy balance and ultimately temperature and precipitation trends.

3.5 Conclusions

This study quantified surface-atmosphere exchanges during the initial seven years following reclamation – from barren landscape to a flourishing, vegetated ecosystem. The fen and upland exhibited varying rates of ecosystem evolution, as well as energy partitioning, due to different biophysical conditions. Both landscapes exhibited a temporal shift in controls on energy partitioning linked to the establishment of robust plant coverage. Initially abiotic factors, such as available energy, meteorologic and edaphic conditions, dictated energy partitioning as well as the timing and type of plant emergence. Plant growth resulted in altered surface conditions (i.e., change in albedo, surface roughness, shading) and a subsequent shift in energy dynamics. Once vegetated, plant phenology and physiology along with environmental conditions, largely

controlled energy partitioning. Moreover, with the establishment of vegetation, surface-atmosphere exchanges became more coupled, and water loss was regulated by plant stomatal processes. By year seven, energy and moisture exchanges were comparable to that of natural and other post-disturbance landscapes in the region suggesting this particular constructed system is on a trajectory to becoming a functional, self-sustaining ecosystem.

Chapter 4: An assessment of carbon dioxide exchange following vascular plant establishment in a constructed boreal watershed

4.1 Introduction

Ecohydrological feedbacks are driven by complex, coupled dynamics between biotic and abiotic elements (Brümmer et al., 2012; Morris et al., 2011). While environmental conditions strongly dictate the structure and composition of plant communities (Trites and Bayley, 2009; Vitt and Chee, 1990; Tilman, 1988; Bazzaz 1979), vegetation itself alters the biophysical environment and performs a critical role in the redistribution of resources including energy, carbon, water and nutrients (Caylor et al., 2005). The patterned landscape of forests, wetlands and open-water regions that comprise the Boreal biome have been increasingly recognized for their important ecosystem services, particularly carbon sequestration and storage (Strack et al., 2022; Mazziotta et al., 2022; Helbig et al., 2020). The Athabasca Oil Sands Region (AOSR) in the Boreal Plains ecozone is an area of interest in this regard due to the large-scale removal of these natural ecosystems in the extraction of bitumen, resulting in the loss of the carbon sequestration function. Over the past decade, pilot-scale endeavours assessing the feasibility of reclamation efforts in the AOSR have been on-going. Metrics for assessing ecosystem design, development, function, and trajectory of these constructed systems are still being assessed. Preliminary research suggests utilizing carbon, water, and nutrient fluxes as integrated measures of reclamation performance as these indicators provide meaningful assessments of ecosystem function (Clark et al., 2022). To date, limited studies assessing community-scale plant function and response to evolving environmental conditions have been conducted at reclaimed sites due to the juvenile nature of these pilot projects and the use of largely ecosystem-scale (e.g., eddy covariance and remote sensing) monitoring techniques. Capturing species-specific CO_2 dynamics provides vital insight for future reclamation

endeavours in terms of planting campaigns as well as the longevity and self-sustainability of these constructed ecosystems under periodic environmental stress. Moreover, species-specific studies of reclaimed AOSR landscapes have been largely limited to the initial or early (<3) years post-construction and largely focused on wetland landscapes (Prystupa et al., 2023; Hartsock et al., 2021; Clark et al., 2019; Murray et al., 2017; Scarlett et al., 2017; Nwaishi et al., 2015) or are greenhouse/laboratory based (Glaeser et al., 2021; Vitt et al., 2020). This study builds upon these earlier studies by providing insight to plant dynamics and function following the initial developmental years after construction and also provide insight into ecohydrological dynamics of upland species. The main objective of this study was to quantify species-specific CO_2 fluxes following the widespread establishment of vascular vegetation for constructed fen and upland landscapes. Secondly, we aimed to determine atmospheric and edaphic controls on CO_2 fluxes and whether they controls varied among species in the fen and in the upland.

4.2 Methods

4.2.1 Study Site and Sample Design

This study was conducted at the recently constructed (2013) upland and fen landscapes of the Nikanotee Fen Watershed (NFW), located approximately 30 km north of Fort McMurray, Alberta (56°55′59” N, 111°25′00” W). Construction, site design, and planting campaigns are described in detail in Ketcheson et al. (2017), Borkenhagen and Cooper (2019) and Popović et al. (2022). Hydrologically, NFW was designed to be self-sustaining and mimic the mosaic of forested upland-wetland landscapes of the AOSR where uplands supply water to downgradient fens (Elmes and Price, 2019). The upland (7.7 ha) was constructed at a ~3% slope to encourage groundwater flow towards the fen and consists of a 3 m thick coarse tailings sand aquifer with high hydraulic conductivity (Sutton and Price, 2020a) overlain by a 20-50 cm thick cover soil composed of

salvaged forest soil (sandy loam to loam). As of 2019, the upland was a mixed broadleaf-coniferous forest and dominant tree species include black spruce *(Picea mariana*), jack pine (*Pinus bankstana*), balsam poplar (*Populus balsamifera*) and aspen (*Popules tremuloides*). The understory is composed of forbs and grasses including thistle (*Sonchus arvensi*), slender wheat grass (*Agropyron tracycaulum*), bunch berry (*Cornus stolonifera*), showy aster (*Eurybia conspicua*) and yarrow (*Achillea millefolium* L.). Understory coverage was not continuous and quite sparse in some areas and characteristically similar to 'dry brush' (see Figure 4-1B, bottom row). Moreover, as trees were still juvenile, the overstory was open. Additionally, due to planting campaigns, growth rates, and variability in edaphic conditions, upland species can be grouped into three zones (Figure 4-1): i) *low slope*: dominated by broadleaf (>140 m in height) with some coniferous (generally smaller and less abundant) species; ii) *mid-slope*: mix of broadleaf and coniferous species, most trees are greater than 140 cm in height; and iii) *high slope*: dominated by coniferous trees with few to rare broadleaf species, where all trees are larger than 140 cm in height. The fen (2.9 ha) is composed of a 2 m thick layer of salvaged, donor peat and while not part of the initial design has had regions of standing water ("ponds") since construction in 2013. While initially an experimental factorial design consisting of various treatments was applied (Borkenhagen and Cooper, 2019) and both freshwater and saline-tolerant sedge and moss species were planted, by 2015 fen vegetation was widespread and largely dominated by *Carex aquatilis* with smaller pockets of *Juncus balticus* occurring in drier regions. From 2014 onwards, invasive *Typha latifolia* infilled many of the ponded regions.

This study focused on community-scale (i.e., species specific), whole plant chamber fluxes. Measurements were taken weekly at each flux location (hereafter referred to as a plot) during the snow free growing season (May – August). Each plot contained a dominant species (Table 4-1).

In the fen, a mixed group was also added (for plots containing both *Carex aquatilis* and *Juncus balticus*). Fen measurements span from 2016 to 2019 and a total of 32 plots were measured each week (Table 4-1). Evacuations in 2016 during Horse Creek wildfire resulted in a shortened field season, with measurements from mid-July and early August only (and have been omitted from any statistical analysis here). Due to slower plant development, upland measurements were only collected in 2018 and 2019 (once trees became more robust). Due to its size, heterogeneity and to adequately capture trends, the upland was divided into nine quadrants (Figure 4-1) and within each quadrant one plot of each species was measured (Table 4-1) for a total of 45 upland plots. Note that Latin species names are used in this manuscript; however, colloquial or shorthand versions (e.g., Carex (Ca) or Aspen (As)) are used in figures to simplify legends and axis labels.

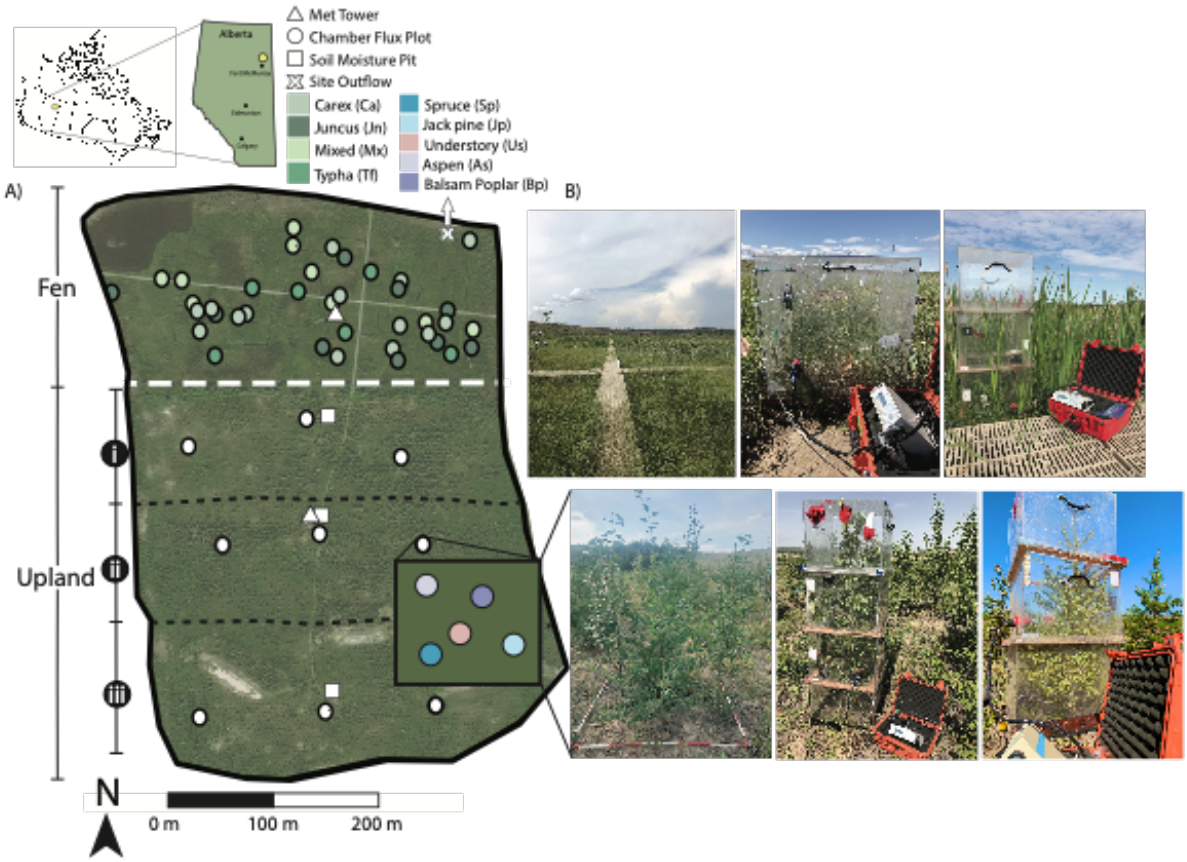


Figure 4-1: Map depicting the Nikanotee Fen Watershed (NFW) fen and upland landscapes and the location of instrumentation (meteorological towers and soil pits) as well as chamber flux plot locations. B: Field photographs depicting the fen (top row) and upland (bottom row) and the whole-plant, single and stacked chamber flux technique.

Table 4-1: Landscape specific specs and sampling design

	Dominant Species	Number of Plots	Chamber Dimensions (cm)	Chamber Type	Tube Length (cm)	Metal Collar
Fen	*Carex aquatilis*	12	60 x 60 x 60	single	75	yes
	Juncus balticus	7	60 x 60 x 60	single	75	yes
	Typha latifolia	6	50 x 50 x 40	stacked (x3)	200	no
	Mixed	7	60 x 60 x 60	single	75	yes
	Total	**32**				
Upland	*Populus tremuloides*	9	50 x 50 x 40	stacked (x4)	200	no
	Populus balsamifera	9	50 x 50 x 40	stacked (x4)	200	no
	Picea mariana,	9	50 x 50 x 40	stacked (x3)	200	no
	Pinus banksiana	9	50 x 50 x 40	stacked (x4)	200	no
	Understory	9	50 x 50 x 40	single	75	no
	Total	**45**				

Table 4-2: Number of flux measurements per season after QA/QC to r2 greater than 0.80. Original number of flux measurements in brackets.

	2016*	2017	2018***	2019***
Fen	72 (76)	378 (385)	272 (281)	261 (266)
Upland	--	--	264 (272)**	289 (294)

* field season shortened due to Horse Creek Fire evacuation (measurements from mid July – early August only)
** no measurements in May (due to installation delays)
***fewer measurements (due to inclement weather)

4.2.2 Environmental Conditions

Meteorological towers were installed in each landscape following construction (2013) with identical instrumentation. Air temperature and relative humidity were measured using ROTRONIC HCTS3 (Campbell Scientific: Logan, Utah, USA) probes while precipitation was measured with a tipping bucket rain gauge (TR-525M; Texas Electronics, Texas, USA) placed within a clearing near the tower to avoid canopy and tower influences. Mean daytime (07:00 – 20:00) photosynthetically active radiation (PAR) was derived from incoming shortwave radiation

(CNR4) (Kipp Zonen; Delft, Netherlands) using a numerical coefficient (Britton and Dodd, 1976) and the LakeMetabolizer package in RStudio (Winslow et al., 2016). All data were collected on a CR1000 (Campbell Scientific: Logan, Utah, USA) datalogger at a sampling frequency of 1 minute and averaged every half-hour. Half-hourly values were subsequently calculated into daily averages. Here, tower measurements provide an overview of ecosystem-scale atmospheric conditions during the study period. Instantaneous chamber measurements of air temperature, relative humidity and PAR were used in flux calculations and statistical analysis.

Water table depth (WTD) measurements were collected via the extensive hydrometric network using a combination of both manual and automatic (HOBO MX2001-S; Onset: Massachusetts, USA) measurement techniques. Complete details about the hydrometric network are described in Ketcheson et al. (2017). Wells were constructed using polyvinylchloride (PVC) pipes with an inside diameter of 2.54 cm, fully slotted, wrapped with well screening and installed at depths of 1.5 m (fen) and 3 m (upland). Here, positive WTD values indicate a water table above the soil surface. In the fen, additional wells were installed adjacent to measurement plots. Near surface (5 cm) soil moisture (VWC) and soil temperature (Tsoil) were manually measured using a WET-2 Sensor/HH moisture meter (Delta-T Ltd: Cambridge, UK) calibrated for each soil type (i.e., peat vs mineral soil). At times, dry conditions in the upland (<10% VWC) limited the ability to use the WET-2 Sensor accurately and data was corroborated and gapfilled using instrumented soil moisture pits (Figure 4-1) located throughout the upland (described in Popović et al., 2022). Edaphic conditions were measured adjacent to (and outside of) the flux collar (see below) as to not distort gas exchanges. Measurements were taken concurrently with flux measurements to capture accurate environmental conditions.

Leaf area index (LAI) was measured monthly at flux plots using LP-80 (2016-2018; Hoskin Scientific, Oakville, Canada) and LI-2200C (2019; LI-COR: Lincoln, Nebraska, USA). LAI probes as described in Popović et al., 2022. Briefly, dual readings were taken at each measurement location to derive understory and canopy layer LAI. Standard LAI corrections were applied according to literature (Chen et al., 1997). Non-destructive vegetation surveys were conducted yearly during peak season foliage to supplement the description of vegetation. In the fen, the 60 x 60 cm collars installed for chamber-based flux measurements were used as the survey area (n=32), where percent cover of vascular plant species, litter, bare ground, and water were estimated, along with measurements of plant height and litter thickness. In the upland, similar methods were applied at each understory flux plot (n=9) along with measurements (species, height, and diameter at breast height (DBH), litter thickness) of all treed flux plots (n=36).

4.2.3 CO_2 Chamber Fluxes

Carbon dioxide (CO_2) exchanges were measured using the portable closed-chamber flux method (Petrone et al., 2011; Nwaishi et al., 2016) via a portable infrared gas analyser (EGM–4; PP Systems: MA, USA). Table 4-1 describes chamber dimensions and sample design. Notably, stackable plexiglass chambers were used in the upland (and *Typha latifolia* fen plots; Figure 4-1) to adequately fit vegetation under the chamber without breakage or bending. Chamber measurements of air temperature (Tair), relative humidity (rH), photosynthetic radiation (PAR) and CO_2 were taken every 15 seconds for a 3 minute interval on the EGM-4. At each plot, both a light and dark run were completed to partition respiration (R) from net ecosystem exchange (NEE) and calculate gross ecosystem photosynthesis (GEP). Here, R includes both autotrophic and heterotrophic respiration. Dark conditions were simulated by covering the clear plexiglass

chamber with a black, opaque tarp. To achieve equilibrium in CO_2 concentrations between measurements, chambers were lifted and aired out until CO_2, rH and temperature readings returned to ambient levels. Moreover, two small battery-operated fans were installed in each chamber to continuously circulate air during measurements. Plots were measured in random order on each sample day to capture a range of day-time values and conditions at each plot. Plexiglass chambers were placed on a perforated metal collar (permanently inserted in the ground, ~ 15 to 20 cm deep) and water was poured around the edges to create a seal. In the fen, metal collars were installed prior to this study period (following site construction). In the upland, metal collars were not installed following construction, thus at the time of this study as treed species had already established rooting systems, steel collars were not inserted as too not sever roots (and affect tree health and productivity). Instead, a 5-10 cm deep groove spanning the perimeter of a chamber was carefully cut into the ground around each tree to place the chamber in. Due to the short measurement period (3 minutes) and large chamber volume, leakage is assumed negligible (based on testing by Pérez-Priego et al., 2010). CO_2 fluxes (net ecosystem exchange (NEE)) were calculated from the linear change in concentration over time. Lines of best fit were derived and any samples where the flux change over time resulted in an r^2 less than 0.8 were rejected as suggested by Pelletier et al. (2007). Exceptions were made when instances of low NEE flux were probable (e.g., early growing season). Here, a negative CO_2 flux indicates carbon uptake by the surface from the atmosphere. The number of flux measurements varied across years (Table 4-2) as measurements are limited to fair-weather conditions and cannot be taken during precipitation events, low PAR (<200) or high relative humidity (>80%) due to sensor function. As such, years with more precipitation events typically result in fewer available measurement days. CO_2 fluxes

were partitioned into NEE, respiration (R) and gross ecosystem productivity (GEP). GEP was calculated as the difference between (chamber measured) NEE and R,

$$GEP = NEE - R \quad (1)$$

4.2.4 Data analysis

For statistical analysis, only measurements spanning from the last week of June to the first week of August from 2017-2019 were used as this time frame: a) represented peak leaf out for vegetation in the region and limited interference caused by varying plant emergence rates and LAI; and b) had a consistent amount of data points between years. 2016 was omitted from statistical analysis due to the shortened field season and limited measurements. Note that no data was collected in the upland in 2017. The accepted significance level used for all statistical tests was $p < 0.05$ and significance is denoted by . for $p<0.10$, * for $p < 0.05$, ** for $p < 0.01$, *** for $p < 0.001$ in figures. All statistics were completed using RStudio (RStudio Team, 2020). A Kruskal-Wallis with post-hoc Dunn test was conducted to evaluate differences in CO_2 fluxes between species for each landscape. A linear mixed effect model (LME) was run for each landscape to delineate environmental controls. To evaluate species-specific relationships between edaphic (i.e., water table depth, soil moisture, soil temperature,) and atmospheric (PAR and Tair) environmental variables and fluxes (NEE, GEP, R) LME were run for each species. All LME's were run using the nlme package (Pinheiro et al., 2014) with year and plot as the random factor. To examine environmental controls on fluxes between years a spearman rank correlation was conducted for each year. Here, only R and GEP are analyzed against environmental variables to reduce model redundancy and results repetition as NEE is a sum of R and GEP. Correlations were generated using the Performance Analytics package (Peterson and Carl, 2020) paired with GGally package (Schloerke et al., 2020) producing a p-value between each pair of parameters and a Spearman rank

coefficients (R_S), ranging from -1 to 1, where values with absolute value closer to 1 indicate a stronger correlation and values closer to zero indicate less correlation.

4.3 Results

4.3.1 Environmental conditions

During the study period a range of meteorological conditions were observed (Figure 4-2) from warm and dry (2017: mean seasonal Tair = 17 °C, 162 mm total P), warm and wet (2018: mean Tair = 17 °C, 253 mm total P) and cool and wet (2019: mean seasonal Tair = 15 °C, 263 mm total P). 2016 was also classified as warm and wet based on Environment Canada records for the region for the growing season when paired with site measurements (July, August 2016 site measurements: mean seasonal Tair = 19 °C, 202 mm total P). Tair exceeded seasonal 30-year climate normals for the region (14 °C, 247 mm P; Environment Canada, 2020) across all years, while 2016, 2018, 2019 experienced P in excess of normals. Air temperature ranged between -4 °C (May, 2019) and 35 °C (July, 2018) throughout the study period and exhibited typical seasonal trends of higher temperatures in June, July (average 18 °C) and lower temperatures in May and August (average 15 °C; Figure 4-2B). Notably, the frequency, intensity and timing of precipitation events varied among years (Figure 4-2A), with 2017 being the driest year. Photosynthetically active radiation (PAR) was typically higher from May to mid-July and slowly decreased in August towards the end of the growing season (Figure 4-2C). Seasonally, PAR was similar throughout 2016 – 2018, however a slight decrease was observed in 2019 (Figure 4-2C), reflective of (frequent) overcast conditions that year.

Due to differences in substrate composition (peat in the fen versus mineral soil in the upland) and site design, edaphic conditions varied between the two landscapes (Figure 4-3). Generally, the fen

was wetter and characterized by a stable, near-surface (± 20 cm of the ground surface) water table and high soil moisture (seasonal means ranging between 78-87%), while the upland exhibited drier conditions consisting of a deeper (>200 cm below ground surface) water table and lower soil moisture (10-25%; Figure 4-3A,B). Moreover, edaphic response to meteorological conditions varied between the fen and upland with fen WTD and soil moisture remaining relatively stable following smaller, less intense precipitation events. However, prolonged dry periods (e.g., 2017 July-August) or intense rainfall (e.g., 2018 July) resulted in an edaphic response in the fen (Figure 4-3). Notably, between June and August 2017 mean water table depth in the fen decreased from 1 cm above ground surface to 14 cm below ground surface and mean soil moisture decreased by 15% (from 85 to 70%). By mid-August 2017, some inundated regions were no longer ponded (although WT remained at or near the surface, ± 2cm). Similarly, highest mean monthly VWC (93%; Figure 4-3) was observed in August 2019, coinciding with frequent P events and the wettest month during the study period (Figure 4-2). Upland edaphic response was much more rapid resulting in soil moisture fluctuating between 5-15% over several hours to days following precipitation events. Due to substrate composition, wetter conditions and more widespread plant (and litter) coverage, soil temperature was lower in the fen than the upland across all years (seasonal means of 17.8 °C (fen) and 23.5 °C (upland); Figure 4-3C). Moreover, there was less diurnal Tsoil fluctuation in the fen than upland.

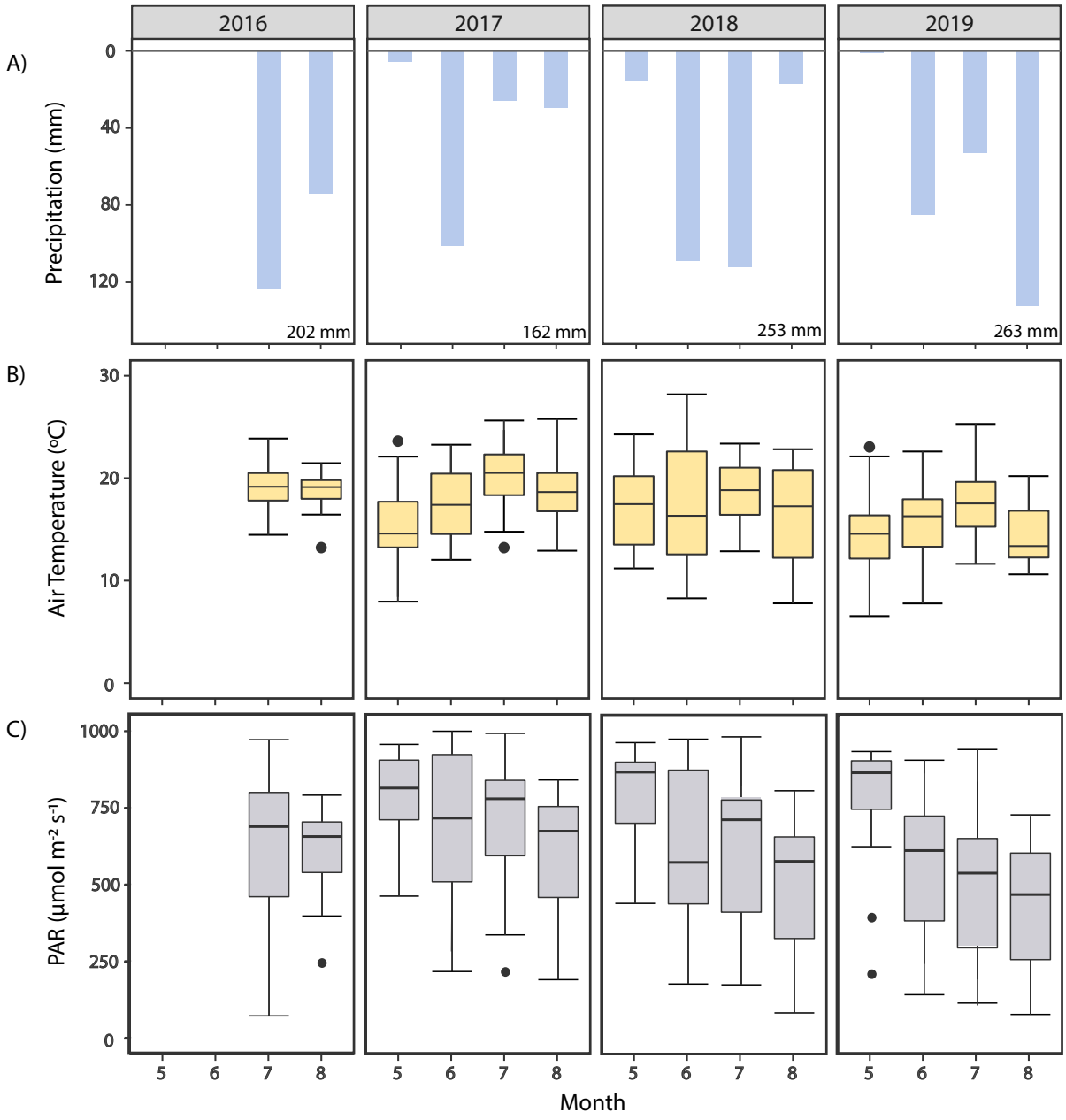


Figure 4-2: Meteorological conditions from 2016 to 2019. A) Monthly total precipitation (mm). B) Mean daily air temperature (°C). C) Mean daily daytime (07:00 – 20:00) photosynthetically active radiation (PAR; µmol m^{-2} s^{-1}). Black line indicates the median, the box represents the 25th to 75th quartile, the whiskers include 95% of the range, and the black circles are outliers

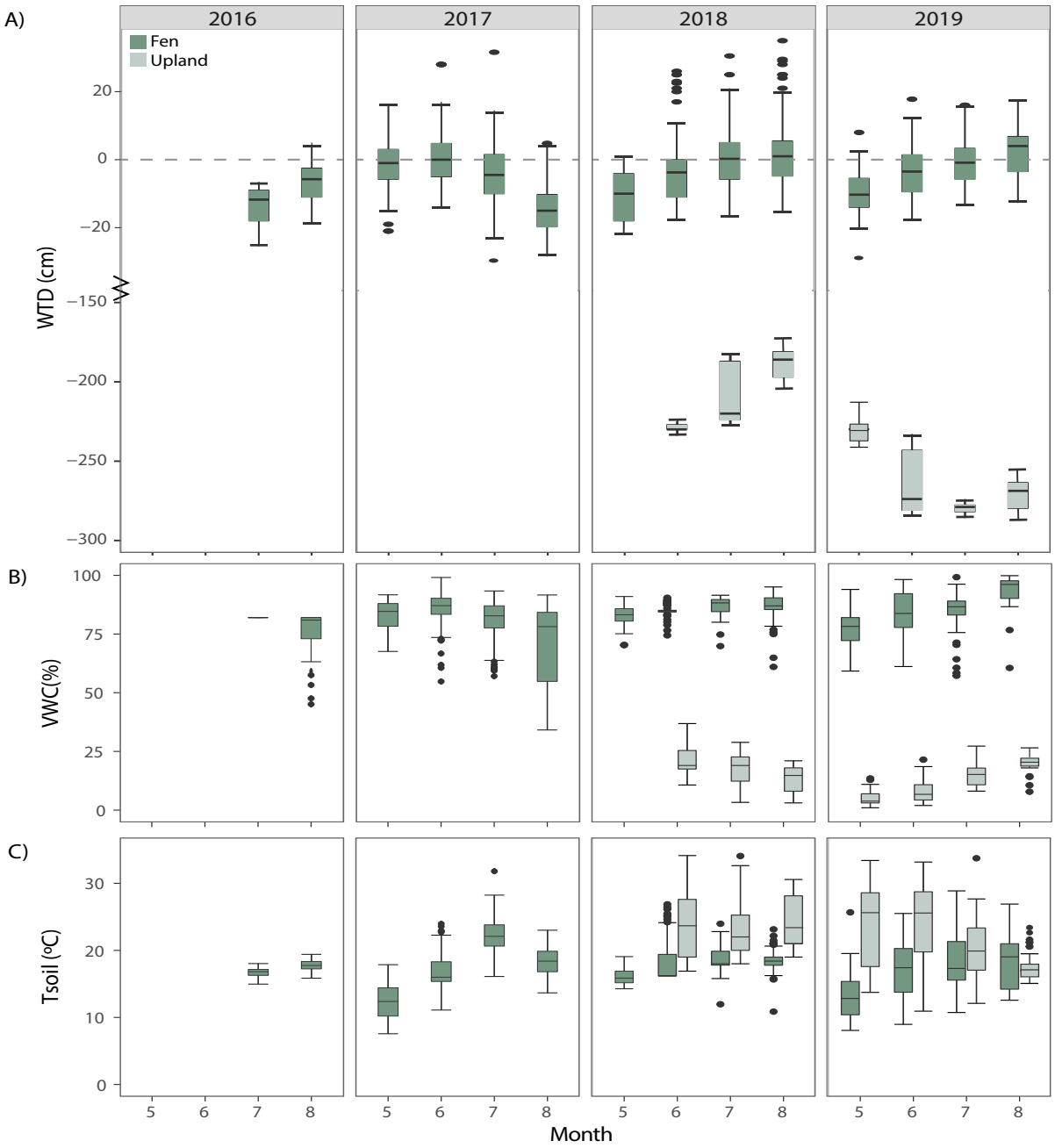


Figure 4-3: Edaphic conditions measured at each flux plot from 2016 to 2019 for the fen (dark green) and upland (light green). A) Water table depth (WTD; cm), negative value indicates below ground. Note the break in the y axis. B) soil moisture measured at 5 cm depth (volumetric water content (VWC, %). C) soil temperature measured at 5 cm depth. Black line indicates the median, the box represents the 25th to 75th quartile, the whiskers include 95% of the range, and the black circles are outliers.

In the fen edaphic conditions varied between species-specific plots. *T. latifolia* plots were typically wettest and most stable with near-constant ponding (seasonal mean WTD of 12±11 cm above ground; VWC of 87± 6%; Tsoil of 16.8±5°C). Highest water table position during the study period was observed at *T. latifolia* plots in 2018 (maximum of 38 cm above ground surface), which was also the tallest in the fen (Figure 4-4) (average height of 101 cm) with a seasonal mean LAI of 1.4 and created a moderate amount of litter seasonally (average thickness 11 cm; but often submerged). *J. balticus* plots were generally drier compared to other species (seasonal mean WTD of 9±7 cm below ground surface; VWC of 80±9%; Tsoil of 19±7°C) and experienced a more rapid, and at times more frequent, response to changing environmental conditions (i.e., frequent wetting and drying). *J. balticus* plants were generally the shortest with a seasonal mean height and LAI of 45 cm and 1.65 (Figure 4-4), were typically less dense than *C. aquatilis* plots and accumulated less litter (than species with wider or larger plant morphologies and biomass). *C. aquatilis* plots were wetter than *J. balticus* (seasonal mean WTD of 5±5 cm below ground surface; VWC of 84±6%; Tsoil of 17±4°C) and experienced less variability throughout the growing season. Interannual mean height and LAI of *C. aquatilis* plots were 54 cm and 1.9 (Figure 4-4), which were also typically the densest amongst fen species and had the thickest litter layer on average at 16 cm. Mixed plots exhibited a range of edaphic conditions between *C. aquatilis* and *J. balticus* plots (interseasonal mean WTD of 6±9 cm below ground surface; VWC of 82± 6%; Tsoil of 18±5°C) depending on plot location and the proportion of each species within the plot.

In the upland edaphic conditions were largely similar between species. Litter formation was significantly less compared to the fen (Figure 4-4) with broadleaf species and understory plots accumulating a marginally thicker litter layer than coniferous species. Average height and LAI of the upland understory was 36 cm and 0.9 (Figure 4-4). *P. balsamifera* trees were on average tallest

(Figure 4-4) in the upland and had a mean dbh of 4.8 cm and an average LAI of 2.1. *P. tremuloides* trees were slightly shorter with thinner dbh (mean 3.5 cm) and lower LAI than their broadleaf counterparts (1.8; Figure 4-4). Coniferous species differed from one another with *P. banksiana* being the larger of the two (Figure 4-4). *P. banksiana* generally had the thickest dbh (mean 5.4 cm), widest basal area and largest LAI (2.3; Figure 4-4) of all upland species. *P. mariana* trees were on average the smallest tree species measured in the upland (Figure 4-4).

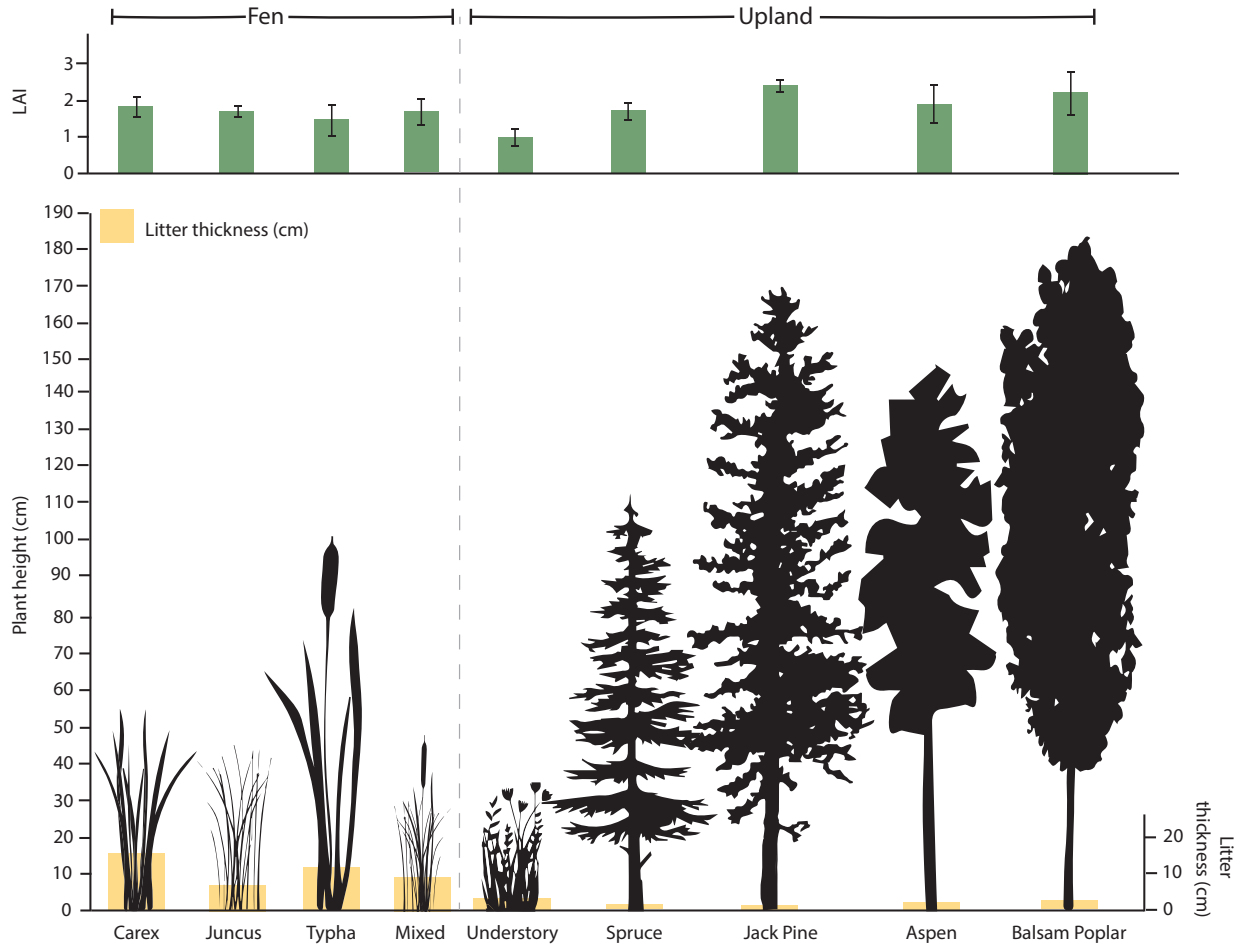


Figure 4-4: Summary of dominant vegetation in the fen and upland. Based on surveys from each flux plot. A) Mean peak growing season (July) leaf area index (LAI) for each species. B) Mean plant height and litter (yellow rectangle) height for each species.

4.3.2 Carbon Fluxes

Seasonally, both landscapes were on average net sinks for CO_2 during daytime conditions, albeit at varying magnitudes (interseasonal mean NEE of -14 and -25 g CO_2 m^{-2} day^{-1} in the fen and upland, respectively; Figure 4-5). In the fen, some variability between years was observed with mean seasonal NEE ranging between -9 to -18 g CO_2 m^{-2} day^{-1} (in 2017 and 2018 respectively). Moreover, lowest mean seasonal fen GEP and R were observed in 2019 at -28 and 15 g CO_2 m^{-2} day^{-1}, respectively (Figure 4-6). The upland exhibited less variability between years with mean seasonal NEE ranging between -26 and -24 g CO_2 m^{-2} day^{-1}. However, like the fen, mean seasonal GEP and R were lower in 2019 (-47 and 23 g CO_2 m^{-2} day^{-1}) compared to 2018 (-53 and 27 g CO_2 m^{-2} day^{-1}). GEP and R were higher in the upland than fen with means of -50 and 26 g CO_2 m^{-2} day^{-1} (upland) and -32 and 19 g CO_2 m^{-2} day^{-1} (fen). However, fen R showed greater fluctuation and range compared to the upland (Figure 4-6). Results of Kruskal-Wallis with post-hoc Dunn tests showed significant differences between species although to varying degrees between the two landscapes, with less variation between fen than upland species (Fen: p-value <0.05, Chi-squared of 8.2; Upland p-value < 0.001, Chi-squared of 95.3; Figure 4-5). In the fen, *C. aquatilis*, *J. balticus* and mixed plots had similar overall CO_2 dynamics while *T. latifolia* plots were significantly less productive, with lower R and less net uptake of CO_2 (less negative NEE) (Figure 4-5). *J. balticus* plots had the greatest uptake (seasonal mean NEE -19 g CO_2 m^{-2} day^{-1}, GEP -43 g CO_2 m^{-2} day^{-1}) and highest R (24 g CO_2 m^{-2} day^{-1}) of all fen species. In the upland, broadleaf species (*P. balsamifera* and *P. tremuloides*) generally had the largest GEP and R and sequestered more CO_2 (seasonal mean NEE of -42 and -39 g CO_2 m^{-2} day^{-1}, respectively; Figure 4-5) than coniferous or understory plots. Understory plots sequestered the lowest amount of CO_2 with mean seasonal NEE ranging between -1 and 1 g CO_2 m^{-2} day^{-1} (Figure 4-5). While understory plots had R rates

comparable to coniferous species, GEP was significantly lower (i.e. less negative) than tree species (Figure 4-5).

Both landscapes exhibited seasonal variability (Figure 4-6) with lowest NEE typically occurring in May (Figure 4-6). During the early growing season, many fen plots were a source of CO_2 with mean May NEE ranging between -6 to 9 g CO_2 m^{-2} day^{-1} among fen species (Figure 4-6). Notably in 2018, mean May R in the fen was almost double compared to other years at *C. aquatilis*, *J. balticus* and mixed plots (with 16, 17 and 11 g CO_2 m^{-2} day^{-1} in 2018 compared to 9, 8 and 6 g CO_2 m^{-2} day^{-1} in 2017 and 2019) but not at *T. latifolia* plots (Figure 4-6). Moreover, *J. balticus* plots typically experienced the greatest seasonality and sequestered more CO_2 earlier in the growing season (i.e., June) than *C. aquatilis* or mixed plots (Figure 4-6). In the upland, seasonal variability differed between tree types with coniferous plots exhibiting less seasonality and a smaller change in GEP (~5-20 g C m^{-2} day^{-1}) compared to broadleaf plots, which exhibited larger (~10-40 g C m^{-2} day^{-1}) changes in GEP throughout the season (Figure 4-6).

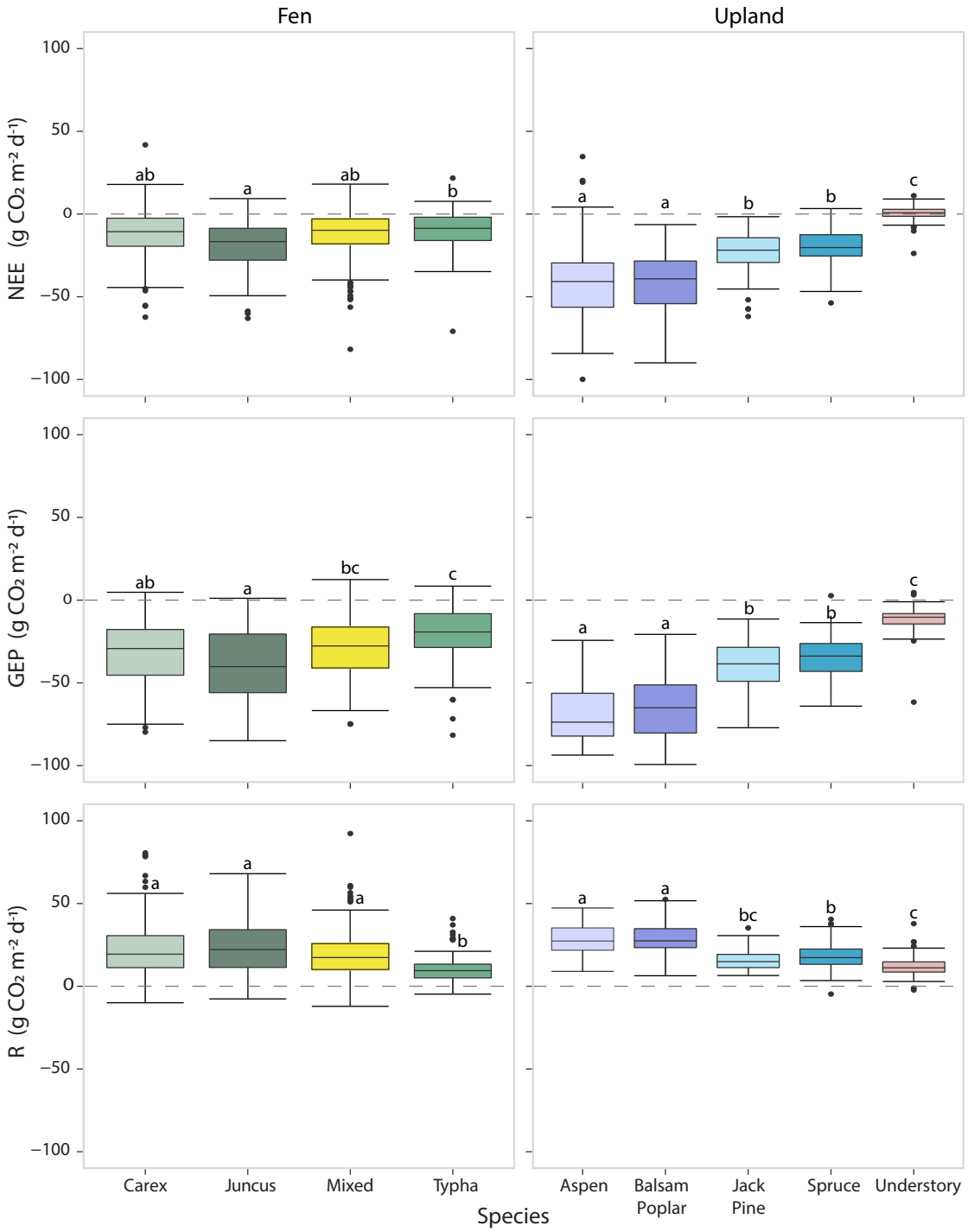


Figure 4-5: Partitioning of CO_2 fluxes (g CO_2 m^{-2} d^{-1}) by species A) net ecosystem exchange (NEE). B) gross ecosystem productivity (GEP). C) respiration (R). Compact letter display depicts results from post-hoc Dunn statistical analysis representing significant differences between species. Black line indicates the median, the box represents the 25th to 75th quartile, the whiskers include 95% of the range, and the black circles are outliers.

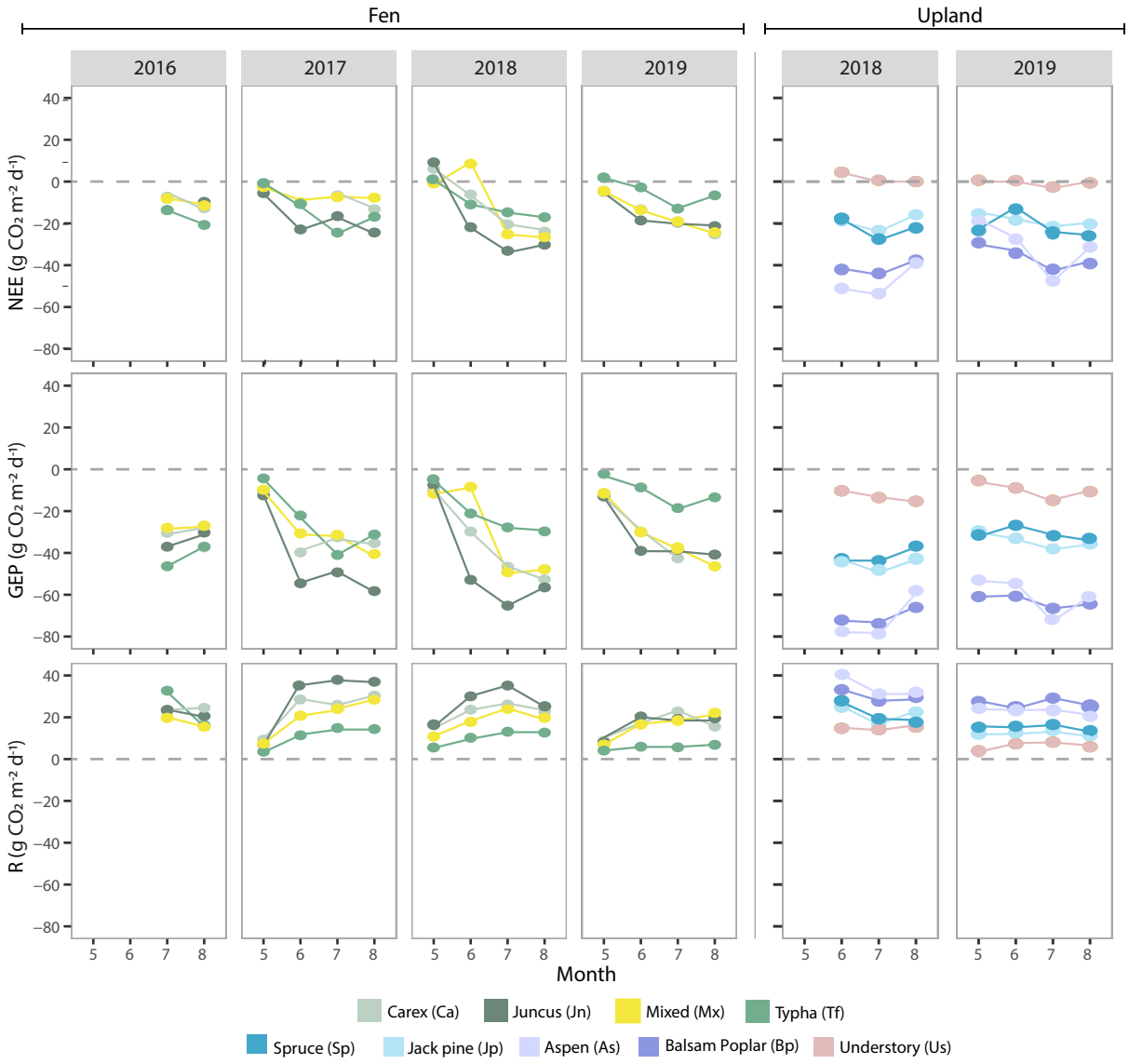


Figure 4-6: Seasonal variability in CO_2 fluxes based on monthly means by species from 2016 to 2019 for the fen and upland. A) net ecosystem exchange (NEE). B) gross ecosystem productivity (GEP). C) respiration (R).

4.3.3 Environmental controls on CO_2 and H_2O fluxes

As a result of differences in substrate material, edaphic conditions and plant communities' environmental controls and sensitivity to changing conditions varied between the two landscapes. Figure 4-7 summarises the relationship between edaphic (Tsoil, VWC, WTD) and atmospheric (PAR, Tair) variables and fluxes (NEE, GEP, R) for each species. Figure 4-8 depicts landscape-scale spearman rank coefficients (R_S) between environmental variables and CO_2 fluxes (GEP, R) for each year, providing insight into the strength of the relationship depending on the hydroclimatology of the season (i.e., in a wet versus dry year). Negative R_S between GEP and environmental variables is due to the sign convention used in this study where, as GEP increases the value becomes more negative.

At the landscape scale, results of LME model analysis showed atmospheric controls explained a significant amount of variation in GEP (PAR and Tair upland: p=0.0017, 0.021; fen: p=0.0016, 0.037) in both landscapes. WTD was not significant for explaining variation in upland fluxes and only weakly significant for fen GEP (p=0.0489). Edaphic conditions largely drove R but to varying degrees between the two landscapes with upland R strongly driven by Tsoil (p=0.0027) and VWC (p=0.0041), while fen R displayed weaker interactions with Tsoil (p=0.0361), VWC(p=0.0483) and to a lesser (non-significant) degree WTD (p=0.0722). Notably, upland R experienced a weak (but not significant) degree of atmospheric controls as well (p=0.0571).

Fen species saw a greater variability in controls between species due to the heterogeneity in surface conditions (Figure 4-7A) and plant physiology. In contrast to other fen species, as edaphic conditions were relatively stable and consistently wet (i.e., frequently ponded, high water-availability) atmospheric controls were found to be the only significant factors driving GEP and

NEE at *T. latifolia* plots (Figure 4-7A). Furthermore, no significant control was defined for R at *T. latifolia* plots. At *J. balticus* plots, where edaphic conditions frequently fluctuated between wetter and drier, R was strongly related to edaphic conditions (Tsoil, VWC and WTD; Figure 4-7A) and to a lesser extent Tair. Moreover, R was significantly related to WTD at *J. balticus* plots, unlike at other plots where WTD was not significant. As mixed and *C. aquatilis* plots were generally wetter (than *J. balticus* plots) R was controlled by Tsoil and VWC albeit to varying degrees of significance (Mixed plots p=0.0074 (Tsoil), p=0.0385 (VWC); *C. aquatilis* p=0.056 (Tsoil), p=0.057 (VWC); Figure 4-7A). Notably, there was no significant relationship between WTD and GEP in fen species although *C. aquatilis* and mixed plots did show a weak (non-significant) relationship (p=0.068 and 0.073, Figure 4-7A). Controls on NEE between the species largely reflected GEP and R trends. In wetter plots (*T. latifolia, C. aquatilis*) NEE was more strongly controlled by atmospheric variables (and those linked to GEP) compared to drier plots (or plots that exhibited frequent fluctuations in edaphic conditions; *J. balticus* and mixed plots) where edaphic controls (and R) played a larger role.

Upland species largely exhibited similar environmental controls, although there was some variability between tree types (e.g., broadleaf versus coniferous R; Figure 4-7B). WTD was not significant for any flux-species relationships in the upland. Controls on GEP were largely similar between treed species (driven by PAR, VWC and Tair) but differed for understory plots where Tsoil, VWC and to lesser extent PAR were dominant drivers (Figure 4-7B). Controls on upland R also varied between tree types with coniferous species exhibiting strong edaphic controls as well as a (non-significant) degree of atmospheric influence (Figure 4-7B).

Results from the spearman correlation analysis reinforced NLME results by depicting a strong relationship between GEP and atmospheric conditions across all years (Figure 4-8). Moreover,

spearman correlation results indicated that the strength of the relationship between environmental variables and fluxes varied depending on overall seasonal hydroclimatic conditions (i.e., wet versus dry years). For example, while Tsoil was positively correlated and significant to R across all years (Figure 4-8) there was a stronger and more significant correlation in the drier 2017 season (R_S=0.62, $p < 0.0001$) than wetter years (2018, 2019; R_S between 0.38 and 0.41, $p < 0.05$; Figure 4-8A). Similar trends (i.e., stronger correlation during the drier 2017 season than 2018 and 2019) were exhibited between VWC, WTD and R (Figure 4-8A). Moreover, Tair was significantly associated with R in 2017 but not 2018 or 2019. Additionally, there was a stronger correlation between WTD and GEP in dry years (2017; R_S= -0.38, $p<0.05$) compared to wetter, cooler years (2019; -0.17, $p > 0.10$; Figure 4-8A). Generally during warmer years, fen edaphic conditions were more strongly correlated to CO_2 fluxes while during wetter years with ample water availability, fluxes were more strongly correlated to atmospheric conditions. In the upland the degree of correlation was similar between years (2018 and 2019) with the largest difference observed in relation to VWC and GEP where in 2018 VWC was significant (R_S = -0.41, $p < 0.01$) but in 2019 it was not (R_S = -0.28, $p < 0.10$; Figure 4-8B). Moreover, it is worth noting the upland exhibited stronger edaphic (VWC and Tsoil) and atmospheric (PAR and Tair) controls on R (Figure 4-8) compared to the fen. Moreover, GEP was more strongly correlated to VWC in the upland than fen.

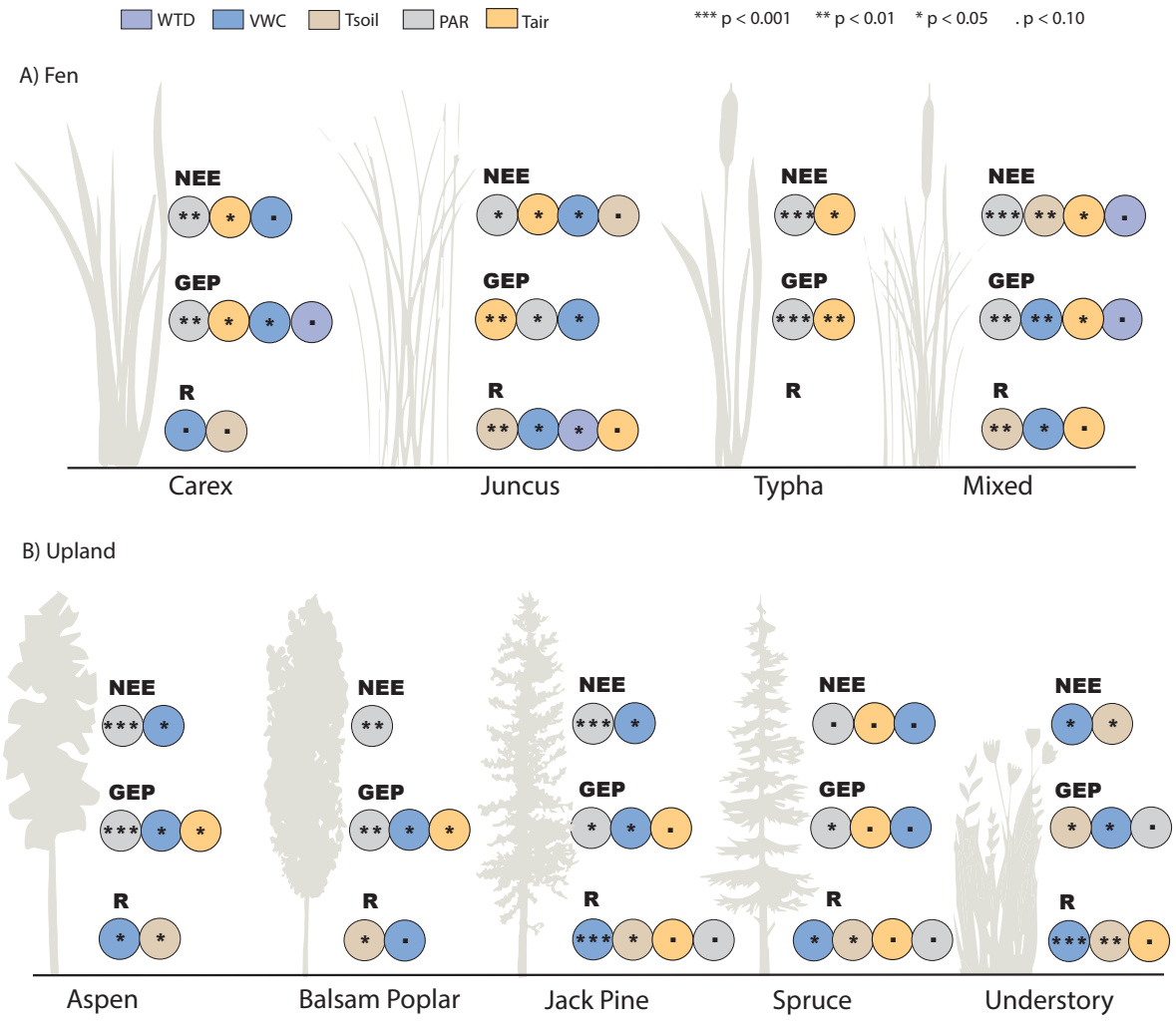


Figure 4-7: Graphical summary of significance from linear mixed effect model for NEE, GEP and R versus environmental variables per each species in the A) Fen and B) Upland. Variables are ordered by significance from left to right. Significance is denoted by . for p<0.10, * for p < 0.05, ** for p < 0.01, *** for p < 0.001.

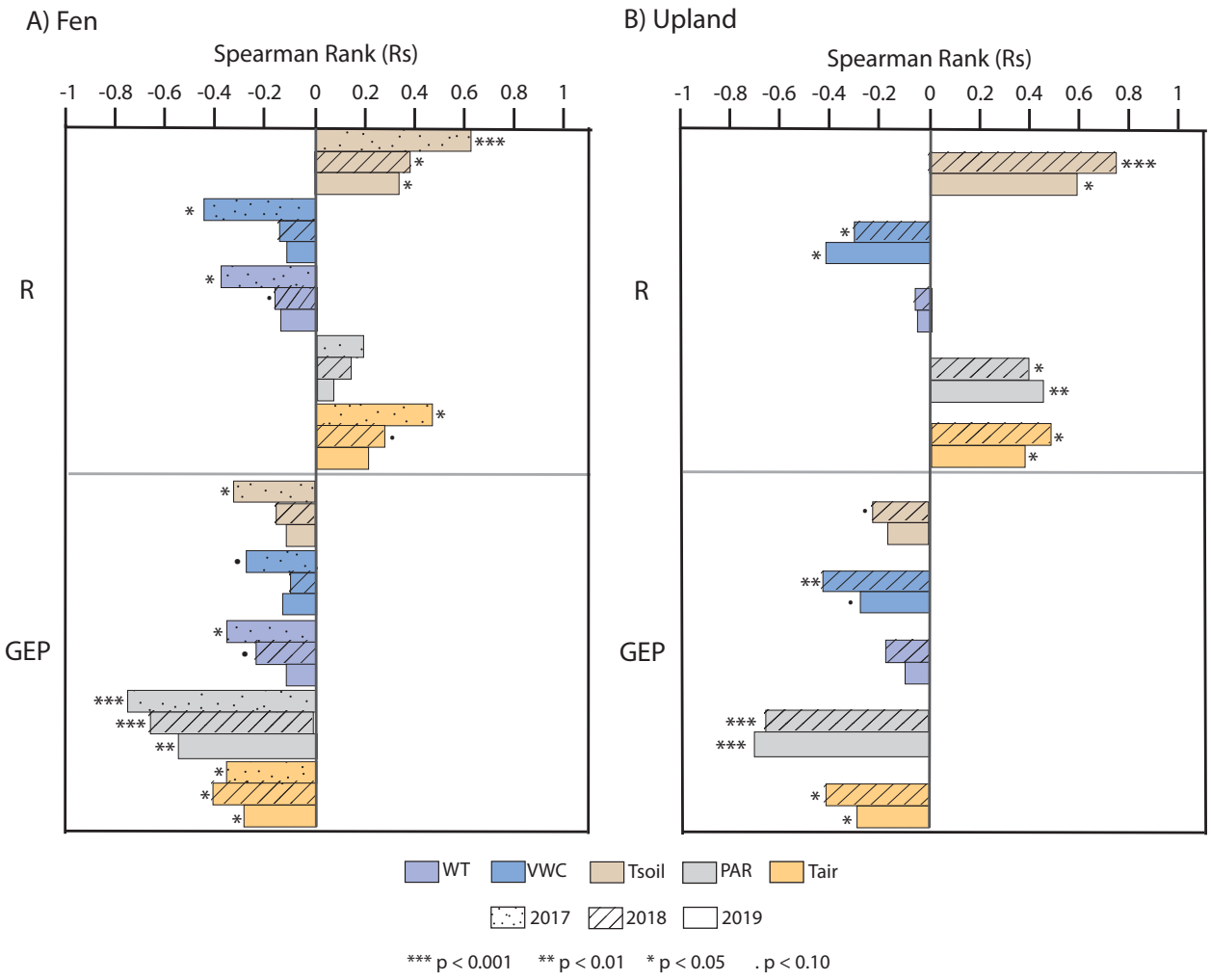


Figure 4-8: Temporal variability in environmental conditions (i.e., wetter versus drier growing seasons) and its effect on CO_2 fluxes in the A) Fen and B) Upland. Spearman rank coefficient (R_S) depicting the relationship between fluxes (GEP, R) and environmental variables between years (2017, 2018, 2019). Significance denoted by p-value . for p<0.10, * for p < 0.05, ** for p < 0.01, *** for p < 0.001.

4.4 Discussion

4.4.1 Biotic and abiotic controls on CO_2 dynamics

Drivers of CO_2 fluxes varied between the two landscapes, between species within a landscape (Figure 4-7) and also between years within a landscape (Figure 4-8). Temporally, seasonal trends largely followed plant phenology and growing season dynamics (i.e., hydroclimatology) with less CO_2 uptake in the early growing season prior to full green up, followed by an increase in CO_2

sequestration during peak leaf out (coinciding with abiotic conditions such as high PAR), and a subsequent decrease in CO_2 uptake later in the growing season due to decreasing Tair and PAR initiating the early stages of plant senescence (Figure 4-6). This is consistent with the well-established relationship between plant phenology (i.e., changing LAI) and CO_2 dynamics in both peatland and forested landscapes (Goud et al., 2017; Xia et al., 2015; Aurela et al., 2009; Bonan, 1993). A variable response in plant productivity under varying environmental conditions (i.e. wet versus dry periods) is also observed between species largely due to differences in plant physiology, highlighting the potential advantages of diverse planting regimes in reclaimed ecosystems.

4.4.1.1 Fen

In the fen, variability in fluxes and response to changing environmental conditions between species was linked to both plant physiology and abiotic controls. Abiotic conditions have been repeatedly shown to dictate species abundance and distribution (Vitt et al., 2022; Phillips et al., 2016; Hartsock et al., 2015; Trites and Bayley 2009; Tilman, 1988; Slack et al., 1980; Bazzaz 1979). While a systematic planting campaign followed construction (Borkenhagen and Cooper, 2019), by 2016, the 4th year post-construction, these plots were largely undiscernible, and the dominant species described in this study had become widespread. A coupling between species distribution and edaphic conditions is seen with *J. balticus* dominating generally drier regions and zones with frequent (edaphic) fluctuations following rain events. *C. aquatilis* plots were typically wetter (than *J. balticus)* with a more stable edaphic regime and invasive *T. latifolia* dominated ponded regions. Development of similar early successional plant communities has also been observed at the second, nearby, constructed pilot fen (Vitt et al., 2020; Hartsock et al. 2021). While each of the species are common across natural boreal wetlands, they have varying tolerance thresholds to drought, waterlogging and salinity (Zoltai and Vitt, 1995; Slack et al., 1980). As such, while

overall NEE rates are largely similar between fen species (Figure 4-5), species-specific response to (changing) environmental conditions varied due to species physiology and function (Figure 4-6). A slightly lower NEE is observed during drier conditions (2017) compared to wetter years (2018). Photosynthesis (GEP) does not appear to be limited by water table drawdown, drier surface conditions or high evaporative demand as all species remained productive during drier periods (e.g., August 2017, Figure 4-6-GEP). Moreover, during this drier year, GEP rates of all species remained well within the range of reported values in natural (-18 to -61 g CO_2 m^{-2} day^{-1}; Volik et al., 2020; Cai et al., 2010; Humphreys et al., 2006) and post-disturbance (-3 to -50 g CO_2 m^{-2} day^{-1}; Schmidt et al., 2021; Clark et al., 2019; Strack et al., 2014) boreal peatlands dominated by vascular vegetation in the region. *C. aquatilis* dominated plots (including some mixed plots) do exhibit slightly lower GEP during drier periods (see July-August *C. aquatilis* in 2017 versus 2018, Figure 4-6) and compared to *J. balticus* plots during drier periods (August 2017 versus August 2018). This decrease is attributed to plant-mediated stomatal closure, a physiological response to limit water loss during drier conditions (Otieno et al., 2012, Monteith, 1995) and due to *J. balticus* plants being more tolerant (than *C. aquatilis*) to drier or fluctuating edaphic conditions (Montemayor et al., 2008; Cooper, 1987). A similar response (i.e., decrease in GEP during drier conditions) has been reported in other boreal fens (Laine, 2019; Strack et al., 2014; Adkinson et al., 2011). However, peatland water table-CO_2-temperature feedbacks are complex and a contrasting response (i.e., GEP increases with decreased WT) has also been reported at other boreal peatlands (Munir et al., 2014; Flanagan and Syed 2011; Cai et al., 2010). This non-linear response and existence of alternate stable states under similar external forcings suggests that functional thresholds are likely site-specific and dependent on a multitude of variables (e.g., plant community, site age, nutrient status, water availability; Eppinga et al., 2009; Scheffer et al., 2001; Lewontin,

1969). At NFW (this study) sustained plant productivity in the fen during drier surface conditions is likely driven by biotic controls, namely the well-developed rooting architecture (>0.5 m below ground surface in places; Messner, 2019) of fen species, which allowed access to deeper water stores and maintained plant function. Previous studies have examined the influence of WT position on CO_2 dynamics in peatlands (Pugh et al., 2017; Minke et al., 2016; Chimner et al., 2017; Adkinson et al., 2011; Riutta et al., 2007; Strack et al., 2006; Oechel et al., 1998) and found that small variations in WTD (particularly when WT remains near the surface) are often negligible and do not significantly alter GEP or function of vascular plant communities. However, WT drawdown past a (site-specific) critical threshold paired with surface drying or prolonged drought conditions can negatively affect plant productivity. Results from this study support this finding with the limited relationship between WTD and fen species (Figure 4-7) as WT remained largely near the surface throughout the study period. While there is a stronger correlation between GEP and WTD in drier years (compared to wetter years, Figure 4-8), the degree of change in GEP is minor and plant function continued, indicating species are able to withstand periodic hydrologic stress. It is important to note that dry conditions in this study are only periodic, temporary perturbations, and while plant function is able to persist, at this time it is unclear how current fen species would respond to prolonged hydrologic stress.

Additionally, drier conditions in 2017 result in higher R across all fen species (Figure 4-6). *J. balticus* plots exhibit higher R (Figure 4-5 and 4-6) and greater edaphic and atmospheric controls than other species (Figure 4-7) due to the drier (and thus warmer) near surface conditions. This differs from *T. latifolia* plots, which are nearly continuously inundated resulting in anoxic conditions and the lowest R rates across all years (Figure 4-5 and 4-6). Peatland R rates are strongly controlled by wet, edaphic conditions and substantial increases in R have been linked to amplified

microbial activity during oxic conditions caused by warming and drying (Li et al., 2021; Volik et al., 2021; Jassey et al., 2017; Gažović et al., 2013). Recently, Allingham et al. (2022) assessed microbial function across AOSR peatlands and found a strong relationship between edaphic conditions and microbial activity. Moreover, they found substrate-induced (i.e., heterotrophic) respiration was higher at NFW (this site) than at three nearby natural peatlands likely due to deeper WT position. Like other peatland studies (Pearson et al., 2015; Gazović et al., 2013; Cai et al., 2010; Chivers et al., 2009; Riutta et al., 2007; Strack et al., 2006), the decrease in NEE during drier conditions observed in this study was more strongly driven by increased R rather than decreased plant productivity (Figure 4-6).

While edaphic conditions are a significant driver of R rates, the physical structure of aboveground biomass also (indirectly) drives R as it affects edaphic conditions and feedbacks through the establishment of a barrier between the surface and atmosphere - intercepting light, reducing soil temperature and limiting surface evaporative losses (Weltzin et al., 2005; Facelli and Pickett, 1991a). The thin, rod-type nature of *J. balticus* shoots and overall lower plant density in plots produced less litter seasonally (Figure 4-4), resulting in less sheltering and shading at the surface and in turn led to more rapid drying and warming at the surface (particularly during dry periods). Thus, the more prominent relationship between Tair and R at *J. balticus* dominated plots (Figure 4-7) is likely a result of closer coupling of Tair and Tsoil as more light (and energy) reaches the surface. Contrastingly, *C. aquatilis* and *T. latifolia* both produced a large amount of biomass resulting in a thicker litter layer (Figure 4-4) and when coupled with the generally wetter plot conditions resulted in slower rates of drying and warming at the surface, ultimately supressing R to some degree. This is evident in 2017 R (Figure 4-6), where drier, warmer conditions result in consistently high R at *J. balticus* plots, while R rates at *C. aquatilis* plots were similar to wetter

years and only exhibited an increase in August once significant (and prolonged) drying had occurred. While surface modification via litter deposition can limit water and heat exchanges between the surface and atmosphere, it can also impede or delay early growing season processes by limiting resources such as light (Holdredge and Bertness, 2011; Facelli and Pickett, 1991a,b). Observed earlier green up of *J. balticus* compared to *C. aquatilis* plots (e.g. May, June GEP 2018; Figure 4-6) is likely due to new plant emergence requiring less energy and time to break through the thinner litter to the surface. Moreover as *J. balticus* plots are typically drier with less surface sheltering than *C. aquatilis* and *T. latifolia* plots, soil temperature generally rise faster and the persistence of lingering winter conditions (e.g. ice lenses) in the early growing season (i.e. May) was reduced, further accelerating the timing of plant emergence as well as R (e.g. higher R in May 2018, Figure 4-7).

While surface conditions played a significant role in driving CO_2 dynamics, the influence of atmospheric controls is also observed as light availability (i.e., PAR) and Tair directly influence plant function and are key moderators of photosynthesis rates (Korrensalo et al., 2017; Frolking et al., 1998; Figure 4-7). Notably, GEP rates are lower across all fen species in 2019 (Figure 4-6), a considerably wetter year than 2017 with ample water availability, as a result of lower light availability (Figure 4-2) due to recurrent overcast conditions (Nijp et al., 2015). Moreover, more frequent, smaller precipitation events coupled with lower PAR and cooler conditions results in less energy available for surface evaporation resulting in the persistence of wetter surface conditions and thus lower R (Figure 4-3B - August; Figure 4-6 - 2019) (Radu et al., 2018; Aurela et al., 2007; Waddington & Roulet, 2000; Griffis & Rouse, 2001).

A comparison of CO_2 fluxes between 2017 (dry and warm) and 2019 (wet and cool) captures the complexity of ecohydrological feedbacks as mean seasonal NEE values are similar (-9 and -13 g

CO_2 m^{-2} day^{-1}) despite experiencing contrasting hydrometeorological conditions and varying (abiotic and biotic) controls. In 2017, CO_2 dynamics are largely driven by plant mediated controls (i.e, regulating water availability and losses) and positive abiotic feedbacks (i.e., increased drying → increased Tsoil → increased R) while in 2019 there is ample water available for plant function, but GEP is limited by atmospheric controls (i.e., lower PAR and Tair) resulting in negative abiotic feedbacks (cool wet conditions → less R, less energy available for surface ET → less surface drying and more stable moisture regime). This is also similar to other observations in peatlands where concurrent shifts in both GEP and R in response to wet or dry years results in little change to NEE (Sulman et al., 2010).

Additionally, species physiology coupled with environmental controls accounted for some of the trends observed. Notably, *T. latifolia* plots are more productive and sequester more CO_2 during a warmer, drier year (2017) than in wetter years (2018, 2019) due to abiotic controls, namely Tair and PAR (Sendall et al., 2015; Berry and Björkman 1980). *T. latifolia* plants are most (photosynthetically) efficient between 18 and 24°C (Gustafson, 1976) and require high light to function at optimal photosynthetic capacity, which is achieved through the morphology and density of its foliage (Ojanguren and Goulden, 2013). Hydrometeorologic conditions in 2017 are more favorable for *T. latifolia* (from a productivity perspective) than other (wetter) years as there is less rain and thus more consistent (high) PAR and Tair. Moreover, while both 2017 and 2018 are warm years, there is less variability in 2017 and July 2017 Tair largely falls within the aforementioned optimal temperature range (Figure 4-2).

While outside of the scope of this study, salinity is a concern for reclaimed systems in the AOSR due to the use of post-processed materials (e.g., tailing sand) during construction. Thus, the potential impact of salt-stress on plant function should be considered when interpreting results

presented here. Field and greenhouse experiments have explored salinity thresholds for plant function for the three species discussed here (Wang et al., 2022; Glaeser et al., 2021; Volik et al., 2020; Vitt et al., 2021; Mollard et al., 2013; Koropchak and Vitt., 2013). A decrease in plant structure and photosynthetic function has been observed in *C. aquatilis* plants when rooting zone sodium (Na^+) levels exceed 1500 mg L^{-1}(Vitt et al. 2021; Glaeser et al., 2021). Similarly, Wang (2022) found *J. balticus* photosynthetic capacity decreased when Na^+ concentrations exceed 2300 mg L^{-1} and Koropchak and Vitt (2013) found *T. latifolia* plant health declined substantially between 300 and 600 mg L^{-1}. At NFW average Na^+ in water from the top 35 cm of the fen in 2019 was 292 mg L^{-1} and reached up to 500 mg L^{-1} in some regions, particularly ponded areas where *T. latifolia* is dominant (Yang et al., 2022). Moreover, high rates of Na^+ are found within leaf biomass of *C. aquatilis* and *T. latifolia* (exceeding 2000 mg kg^{-1}) while less was present in *J. balticus* (unpublished data from NFW). Notably, *C. aquatilis* and *T. latifolia* plants did exhibit some degree of yellowing along leaf ends and earlier foliage senescence during the 2018 and 2019 growing seasons (field observations). Thus, photosynthesis inhibited by salt stress may further explain why *J. balticus* plots were more productive and sequestered more CO_2 than *C. aquatilis* and *T. latifolia* at times (i.e., warm periods with ample water available, see 2018, Figure 4-6) as *J. balticus* is generally more salt-tolerant (Tang, 2022; Montemayor et al., 2008; Cooper, 1987). Further examination of the effects of salt accumulation in plant organs on plant function and photosynthetic capacity at reclaimed sites is currently being investigated.

4.4.1.2 Upland

Upland CO_2 dynamics exhibit clear trends linked to tree type (Figure 4-5, Figure 4-6) as broadleaf species typically have higher photosynthetic capacity than coniferous species due to leaf morphology (Brümmer et al., 2012; Dang et al., 1997) and have been found to sequester up to two

times more CO_2 than coniferous species (Arain et al., 2002; Popović et al., 2022). Furthermore, plant phenology and LAI dynamics are captured in the shape (i.e., variability) of seasonal GEP and NEE trends between tree types. Conifer species exhibit less seasonal variability (i.e., amplitude) compared to broadleaf species, which follows a more parabolic shape mirroring changes in LAI and growing season conditions (Figure 4-6; Amiro et al., 2006; Baldocchi et al., 1997, 1996). Variability in seasonal trends between tree types is attributed to the amount and timing of leaf/needle chlorophyll content, which is coupled with LAI. While coniferous species reach a chlorophyll and LAI maximum early (May, June, ~25 μg cm^{-2}) and exhibit minimal change throughout the growing season compared to broadleaf species, which experience variable LAI throughout the season (i.e., budding, foliation and senescence) and typically reach peak chlorophyll content in July (>30 μg cm^{-2}) compared to lower rates during the shoulder season (~ 8 μg cm^{-2}; Middleton et al.,1997).

Upland fluxes responded more strongly to edaphic controls than the fen (Figure 4-7 and 4-8) due to drier conditions, open canopy and the discontinuous nature of the understory (see Figure 4-1), resulting in greater coupling between the surface and atmosphere and often a rapid edaphic response to changing meteorological conditions. This differs from mature forests where the understory and/or canopy are better established, providing some degree of sheltering and shading of the surface, dampening moisture loss and R (Hart and Chen, 2006). Moreover, edaphic controls at NFW are likely influenced by tree root morphology. Apart from *P. banksiana*, upland species at NFW are dominated by adventitious, laterally spreading, near-surface rooting architectures. *P. tremuloides* and *P. balsamifera* roots are clonal and can extend between 2 to 7 m laterally, while rarely exceeding 0.5 m depth during early growth, although over time tap and sinker roots may extend to >1 m depth (Adonsou et al., 2016; Strong and La Roi, 1983). *P. mariana* roots have been

observed to lateral extend up to 3 m and to a maximum depth of 0.30 m, albeit much of the rooting system is often located within the top 0.15 m (Walker et al., 2018; Strong and La Roi, 1983). *P. banksiana* exhibit some horizontal roots but tend to have more abundant vertical rooting structures (compared to the other species; Stamatinos, 2019, Rudolph and Laidley, 1990). Moreover, Strong and La Roi (1983) found a significant increase in rooting depth with age in *P. banksiana* trees from 0.3 m (age 3) to 1.1 m (age 9) and >2 m in mature trees (> 30 years). Thus, at NFW, at the time of this study, WT is not a significant control between years or species (Figure 4-7 and 4-8) likely due to the deep WT position (> 2 m) and near-surface rooting morphology. However, as trees continue to mature, sinker and tap roots of some species (e.g., *P. banksiana*) may extend deep enough to access deeper water stores, particularly during periods of surface drying and thus increase WT influence.

Although WTD did not significantly explain variation in upland CO_2 dynamics, soil moisture and soil temperature are key drivers (Figure 4-7 and 4-8), due to plant function being largely dependent on rooting zone water availability as a result of near-surface rooting architecture. Thus, it is worth noting that while only manual measurements of the top 5 cm are presented here (Figure 4-3), VWC measured at 15 and 30 cm below ground surface (i.e., within the rooting zone) ranged between 20-40% during the study period (Chapter 2) and likely provided water for plant function even during times of periodic surface (5cm) drying. However, a decrease in GEP was observed across all species in August 2018, likely the result of both drier edaphic and warm/dry atmospheric conditions as well as the early stages of senescence in broadleaf species. Persistent, or even increased carbon uptake in boreal forests under warming climate conditions has been strongly linked to (soil) water availability (Bonan 2008; Griffis et al., 2003; Arian et al., 2002). Moreover, the influence of soil moisture on GEP and NEE varies across boreal forest sites due to site-specific

heterogeneity (i.e., stand age and composition, soil characteristics), with broadleaf species exhibiting greater sensitivity to drier edaphic conditions due to high water needs compared to conifers, which can tolerate a wider range of moisture conditions during development (Arnup et al., 1988). At a mature *P. tremuloides* stand, GEP was able to persist during the first drought affected season as soil-moisture remained high within the lower regions of the rooting zone (up to 60 cm depth) but then declined by 13 and 15% following persistent drought conditions; however, GEP remained similar at mature *P. mariana* and *P. banksiana* stands during the same drought conditions even with changes in soil moisture (Krishnan et al., 2006; Kljun et al., 2007). The difference between tree types and clear decrease in *P. tremuloides* GEP was linked to lower broadleaf LAI driven by reduced water availability (Kljun et al., 2007; Barr et al., 2004) indicating feedbacks between soil, water and plant processes. Similarly, CO_2 uptake is found to be independent of soil moisture, despite experiencing a wide range of (wet and dry) conditions at a mature *P. banksiana* stand likely due to a well-established, deep-reaching rooting system able to access water at depth (Baldocchi et al., 1997; Reich et al., 2018; Petrone et al., 2015; Amiro et al., 2010). However, mature stands are typically less sensitive to drier conditions due to better established rooting systems, understory coverage and overall tree size (and LAI). Moreover, limited soil moisture or prolonged drought conditions during the juvenile phase can stunt the development of critical above and belowground plant organs further propagating lower CO_2 uptake and decreasing the ability to withstand periodic moisture stress. Petrone et al. (2015) observed a stunted response in stand height/growth (and thus GEP) during drought years compared to years with wetter soil moisture regimes. Moreover, in a recent experiment Reich et al. (2018) found soil moisture significantly affected the photosynthetic capacity of 11 juvenile (aged 3-5) boreal species with *P. tremuloides* exhibiting greater GEP sensitivity to lower VWC than *P. banksiana*. We

observe a similar response with a greater decrease in GEP at broadleaf compared to conifer plots during warm and dry conditions (Figure 4-6 August GEP). These results point to the importance of establishing adequate soil evolution and moisture regimes during construction in order to ensure successful ecosystem evolution, growth and function. Understory CO_2 dynamics are less influenced by atmospheric controls (Figure 4-7) likely due to the lower stature of the understory and periodic shading from surrounding trees.

R is strongly controlled by Tsoil and VWC (Figure 4-7 and 4-8). A decrease in R is observed in measurements taken days following the intense rainfall of July 2018, which results in wetter and cooler conditions. Moreover, the slightly lower R measured in 2019 across all species is attributed to more frequent rain events, resulting in wetter conditions (Figure 4-3, July-August 2019) and reduced soil microbial activity (Mkhabela et al., 2009; Khomik et al., 2006, Griffis et al., 2003). However, other boreal studies have exhibited a contrasting response (i.e., decrease in respiration with increasing soil temperature or dryness; Allison and Treseder, 2008; Bronson et al., 2008; Krishnan et al., 2006) due to (root or microbial) acclimation to persistent dry conditions, soil temperature exceeding the threshold for microbial activity or other edaphic limitations (i.e., nutrient availability).

Soil-plant-atmosphere feedbacks are also observed. Notably, there was greater atmospheric influence on R at *P. banksiana* and *P. mariana* plots than at broadleaf plots likely due to less surface coverage (i.e., thinner litter layer) and less surface shading (needles versus broad leaves) resulting in more incoming radiation reaching the surface and stronger coupling between atmospheric and edaphic conditions (Warmer Tair and more incoming radiation reaching the surface → greater warming/drying at the surface → increased R). Root morphology and plant (i.e., litter) composition also contribute to R in the upland. When paired with dry edaphic conditions,

near-surface rooting architecture can result in high amounts of autotrophic (root) respiration, particularly during recovery following disturbance, where it can comprise more than 35% of total R (Amiro, 2001; Striegl and Wickland 1998). High R rates have been found to offset GEP in juvenile or recovering forest ecosystems, resulting in a net source of CO_2 during the initial ~10 years of recovery (Watts et al., 2021; Amiro et al., 2006; Amiro 2001). Moreover, despite a slightly thicker litter layer and greater shading due to tree size and LAI (i.e., less direct surface warming) greater R rates are observed at broadleaf plots (Figure 4-5 and 4-6), likely linked to variability in litter composition and quality between broadleaf and coniferous species. Deciduous leaves are more labile and decay faster than coniferous needles (Preston et al., 2000) resulting in greater microbial activity via decay and soil respiration. Similar to results presented here, respiration rates have been observed to be two to three times higher in broadleaf compared to coniferous species in juvenile (Tjoelker et al. (2008) and mature (Griffis et al., 2003) stands. Moreover, Jílková (2020) observed litter composition was at times a stronger driver of forest respiration rates than soil temperature. The upland experiences greater coupling between atmospheric and edaphic conditions and plant function due to lower water availability, compared to the fen, and sparse surface coverage. Thus, atmospheric controls largely explain the variability in CO_2 fluxes between years, where similar to the fen, GEP was higher during a warm year punctuated by a few larger rain events (2018) compared to a wetter, cooler year with reduced incoming radiation (2019; Figure 4-6).

4.4.2 Comparison to early reclamation at NFW

Plot-scale CO_2 fluxes of NFW-fen were measured in years initially following construction and planting (2013 to 2015; Nwaishi et al., 2016). Plots were initially labelled based on planting prescriptions (control (unvegetated), moss, seedling, mulched and unmulched, open water).

However, by the time of this current study, initial naming conventions are no longer applicable as the above-described plant community has emerged. There has been a marked improvement at control (unvegetated) plots, from CO_2 loss (1-2 g CO_2 m^{-2} day^{-1}) in 2013 (Nwaishi et al., 2016) to net CO_2 uptake (interseasonal mean of -11 g CO_2 m^{-2} day^{-1}) following the development of vegetation at these plots. Moreover, an increase in mean seasonal GEP (from -23 to -32 g CO_2 m^{-2} day^{-1}) and R (from 11 to 19 g CO_2 m^{-2} day^{-1}) is observed since year two post-construction (2014; Nwaishi et al., 2016). Changes in CO_2 dynamics are attributed to higher LAI and widespread plant coverage (Nugent et al., 2018; Goud et al., 2017; Humphreys et al., 2006, Petrone et al., 2003). Corresponding with biophysical changes at the surface, an increase in mean near surface soil moisture from 73-79% in 2014 (Nwaishi et al., 2016) to 78-87% is observed during this study.

Species-specific, plot-scale CO_2 dynamics were not previously measured in the NFW-upland. However, a comparison to eddy covariance CO_2 measurements during the initial years (2013 – 2015; Chapter 2) following construction provides some context of ecosystem evolution and change over time. A substantial shift in CO_2 dynamics is observed as the upland evolved from a barren landscape to extensive plant coverage. During early years, the upland emitted 15 g CO_2 m^{-2} day^{-1} (interseasonal mean NEE 2013 – 2015; Chapter 2) due to high R (interseasonal mean of 18 g CO_2 m^{-2} day^{-1}; Chapter 2) and limited GEP (interseasonal mean GEP of 3 g CO_2 m^{-2} day^{-1}; Chapter 2) compared to this current study, where the presence of vegetation results in increased GEP (54 g CO_2 m^{-2} day^{-1}) and CO_2 sequestration (NEE of -25 g CO_2 m^{-2} day^{-1}).

4.4.3 Comparison to natural and post-disturbance boreal landscapes in the region

The ever-growing database of multiyear, multi-site studies captures the heterogeneity of boreal ecosystems due to varied edaphic conditions, plant communities (e.g., moss- versus sedge-dominated, treed versus open, mixed forest versus coniferous), growing season conditions (e.g.

incoming radiation based on latitude) and regional hydroclimatology. As such, comparison of CO_2 dynamics between studies even of the same landscape type (e.g., fens) can yield variable results. Natural, post-disturbance landscapes (e.g., post-fire or harvest) offer a comparable trajectory of ecosystem function during the initial stages of recovery. Moreover, post-disturbance, early successional plant communities (e.g., rapidly-establishing vascular species or juvenile trees) tend to mirror the current plant community at NFW more closely than mature, natural or undisturbed sites. Thus, to provide context to the results of this study, the discussion here is focused on natural and post-disturbance landscapes with similar plant communities (e.g., vascular species, sedge-dominated), age and/or hydroclimatological conditions to the AOSR.

NFW-fen mean seasonal NEE rates range between -9 to -18 g CO_2 m^{-2} day^{-1} and are within the wide range of values observed at a nearby, saline, sedge-dominated fen (-5 to -60 g CO_2 m^{-2} day^{-1}; Volik et al., 2021). NFW-fen exhibited greater GEP rates than some natural boreal fens (GEP of -9 to -15 g CO_2 m^{-2} day^{-1} Cai et al., 2010; Humphreys et al., 2006). Higher GEP rates at NFW-fen (interseasonal mean of -32 g CO_2 m^{-2} day^{-1}) are attributed to differences in plant community composition, where NFW-fen is dominated by sedges while the other landscapes have a mixed community of mosses, sedges and shrubs. NFW-fen CO_2 dynamics are similar to those measured in year three and four of a restored cutover peatland, particularly in plots with greater vascular plant coverage (Strack et al., 2014). To date, only two pilot fens have been constructed in the AOSR (this study (NFW) and Sandhill Fen (Ketcheson et al., 2016)). Slightly lower CO_2 uptake was reported by Clark et al. (2019) at Sandhill Fen (NEE -5 to -8 g CO_2 m^{-2} day^{-1}) compared to those provided here, although this is likely due to differences in site age as the Sandhill study reported only the initial 3 years following construction (versus years 5-7 in this study) as well as

measurement techniques (Eddy covariance versus chambers). It is hypothesized that Sandhill fen will demonstrate a similar increase in CO_2 uptake as the ecosystem continues to evolve.

The juvenile nature of trees in the NFW-upland provide a novel opportunity to measure individual, whole tree CO_2 dynamics. However, there are few chamber-based, studies of boreal forest species (Gaumount et al., 2006; Medhurst et al., 2006; Lavign et al., 1997), none of which examined juvenile or recovering stands. Most boreal forest studies are measured at the stand scale via eddy covairnce methods and report carbon dynamics in g C m^{-2}. As such, in this section we've converted our chamber measured values from g CO_2 m^{-2} day^{-1} to g C m^{-2} (Table 4-3). However, with upscaling comes a degree of error, and values presented in Table 4-3 are likely an over-estimate of net CO_2 uptake as they only encompass day-time measurements (versus full day measurements via eddy covariance). Moreover, at the time of this study, NFW-Upland trees ranged between four to seven years old. As mature stand dynamics often vary from juvenile stands due to size and abundance of above and belowground components, degree of understory development and canopy closure (Goulden et al., 2011) the discussion here is largely focused on post-disturbance, recovering uplands.

Table 4-3: Mean CO2 fluxes for NWF-Upland converted from g CO2 m-2 day-1 to g C m-2. Here we used 120 days as it represents the average length of the growing season in boreal forest studies. To normalize data between plant communities, fluxes were subsequently divided by mean LAI of each tree type.

	NEE (g C m^{-2})	GEP (g C m^{-2})	R (g C m^{-2})
Upland	419	838	435
Broadleaf species	474	1092	618
Coniferous species	314	726	412
Understory	109	619	474

Post-disturbance forests are typically a CO_2 source during the initial 1-5 years (Petrone et al., 2015; Goulden et al., 2011; Amiro et al., 2006) due to the slower initial growth and expansion of tree species and NEE being dominated by R. This is followed by a significant increase in CO_2 uptake and productivity as LAI increases during the initial 10-15 years following reclamation (Clark et al., 2022; Straker et al., 2019; Strilesky et al., 2017) or disturbance (i.e., post-harvest Petrone et al., 2015, Coursolle et al., 2012; post-fire Mkhabela et al., 2009, Amiro et al., 2006). Due to site heterogeneity, environmental conditions and the variable timing of tree and understory development, recovering (5-15 year old) western boreal forests exhibit a wide range in CO_2 dynamics. GEP of reclaimed uplands during the first 15 years post-construction range from 200 – 1400 g C m^{-2} (Clark et al., 2022; Straker et al. 2019; Strilesky et al., 2017) compared to a narrower range (500 – 1000 g C m^{-2}) for similarly aged recovering (post-fire and harvest) uplands (Petrone et al., 2015; Coursolle et al., 2012; Mkhabela et al., 2009; Amiro et al., 2006). NFW-upland values measured in this study fall within these ranges. However, NFW-upland R values differ from other natural and reclaimed sites. R was higher at post-harvest sites (>700 g C m^{-2}; Vestin et al., 2020; Petrone et al., 2015; Coursolle et al., 2012) compared to NFW-upland (400-600 g C m^{-2}; Table 2) likely due to the intact nature of the soil profile and plant remnants resulting in a higher degree of organic matter and microbial activity at post-harvest sites. Contrastingly, NFW-upland R is greater than that reported by Clark et al. (2022) for 5-9 year old broadleaf (300-500 g C m^{-2}) and conifer (<300 g C m^{-2}) reclaimed stands despite having less organic matter content, likely due to differences in biophysical/edaphic conditions between sites with NFW-upland exhibiting a greater degree of exposed bare ground and less understory development along with drier conditions resulting in greater R. This variability between recovering upland sites further points to the

complexity of ecohydrological feedbacks and the role/control of vegetation and biophysical conditions on CO_2 fluxes.

4.4.4 Implications for AOSR reclamation

This study highlights the importance of biodiversity in reclaimed landscapes as species have varying responses to (changing) environmental conditions. Results from this study are upon initial examination surprising, with *J. balticus* plots exhibiting higher GEP and more CO_2 sequestration than *C. aquatilis* and *T. latifolia*, two typically highly productive species. However, a closer examination of environmental conditions and controls showed that at times, conditions were more favorable for *J. balticus* as these plots displayed a greater threshold for drier or fluctuating edaphic conditions. Similar to results presented here, Volik et al. (2021) observe greater CO_2 uptake by *J. balticus* under drier or more saline conditions providing further insight into species-specific thresholds and their applicability in reclaimed AOSR landscapes. In a greenhouse monolith study, Ström et al. (2005) similarly observed greater GEP and NEE rates at *Juncus effecus plots* than *Carex rostrata* during drier conditions. Contrastingly, in a study examining CO_2 dynamics of a restored peatland, Wilson et al. (2007) found *T. latifolia* and *Carex rostrata* had higher GEP and NEE than *Juncus effecus* plots due to wetter edaphic conditions. Thus, variability across sites with similar plant communities highlights the complex relationship between biotic and abiotic environmental factors driving carbon exchanges. This information is valuable for planning appropriate planting prescriptions for reclamation under current and potential future hydroclimactic conditions. Moreover, an examination of species-specific trends provides valuable insight into understanding ecosystem-scale CO_2 trends observed via eddy covariance measurements. Popović et al. (2022) capture ecosystem scale carbon fluxes of the study area and as of 2019, the upland was still a minor source of carbon, on trajectory to becoming a sink in the

near future. This is largely attributed to the proportions of understory to trees. As observed in this current study, tree species sequester large amounts of CO_2, however, the dry edaphic conditions and discontinuous nature of the understory led to R exceeding GEP. Results here suggest the important physical role litter and plant cover have on controlling and mediating light, temperature and water at the surface and by extension important ecohydrological feedbacks pertaining to CO_2 exchanges. Moreover, Chi et al (2021) found GEP was similar across same-aged forested sites and that the greater driver of NEE variability across sites was R and forest floor dynamics. Studies by Dhar et al. (2022) and Brown and Naeth (2013) examined the effects of adding woody debris to AOSR reclamation cover soils and found an improvement to soil moisture and temperature trends particularly in forest-mineral mix cover soils further supporting our recommendations. Moreover, the rapid improvement in CO_2 sequestration at South Bison Hill (a nearby reclaimed upland) was largely attributed to the early establishment of a robust understory immediately following construction (Strilesky et al., 2017). Thus, future reclamation projects in the region would benefit from the addition of straw mulching and/or woody debris to the upland surface or amendments to soil quality or understory planting to help provide sheltering, decrease surface warming and decrease respiration losses while improving net CO_2 uptake.

4.5 Conclusions

This study examined community-scale CO_2 fluxes of a constructed upland-fen complex following plant establishment using the chamber method. Drivers of CO_2 fluxes varied between the two landscapes, as well as between species within a landscape and were largely regulated by environmental conditions. CO_2 fluxes in this study were similar to natural or recovering Boreal landscapes in the region. But perhaps more importantly, the constructed landscape exhibited similar dynamics, controls and ecophysiological responses to fluctuating environmental conditions

as those observed in natural landscapes, namely the ability to maintain function (i.e., carbon uptake) during periods of periodic hydrologic stress. Results from this study provide insights into the ecohydrological functioning of common boreal species in reclaimed systems once vascular vegetation becomes well-established. Pairing these results with ecosystem-scale measurements (e.g. EC monitoring) can aid in the design of future reclamation endeavours. More broadly, results from this study add to the knowledge base of species-specific function and thresholds under variable environmental conditions such as wetter versus drier seasons, information useful in the planning of planting prescriptions for reclamation under a changing climate.

Chapter 5: Evapotranspiration dynamics during the ecosystem development of a constructed upland-fen watershed

5.1 Introduction

Large-scale resource extraction in the Athabasca Oilsands Region (AOSR) has resulted in ~1055 km^2 of disturbed boreal landscapes (Alberta Environment and Parks, 2020). Located within the Boreal Plains ecozone, the pre-disturbance landscape is characterized by hydrologically connected boreal forests, fen peatlands and lakes that provide critical ecosystem services including regulation of the regional hydrological regime and carbon sequestration and storage (Strack et al., 2022; Helbig et al., 2020; McLaughlin and Cohen, 2013). In recognition of the importance of boreal ecosystems to regional ecohydrological processes, reclamation of these impacted landscapes to pre-disturbance equivalent land capacity is mandatory under the Alberta Environmental Protection and Enhancement Act (EPEA; Province of Alberta, 2021). Reclamation targets have been broadly defined to entail the creation of functional, self-sustaining ecosystems that are resilient to periodic environmental stress (Alberta Environment and Sustainable Resource Development, 2013). Ecosystem function and performance can be defined through numerous metrics (e.g., water use efficiency, carbon sink capacity, diverse plant communities) which are inherently driven by available water (Asbjornsen et al., 2011; D'Odorico et al., 2010; Rodriguez-Iturbe, 2000). Water availability is largely controlled by the storage capacity of soils, vegetation and hydroclimatology (Rodriguez-Iturbe et al., 2004). Thus, system design must first adequately satisfy water needs to ensure successful evolution, performance and longevity of reclamation endeavors. Creation and maintenance of such conditions in the AOSR is complex as the climate is sub-humid and the region experiences frequent moisture deficits and decadal wet/dry cycles (Chasmer et al., 2018; Devito et al., 2017; Bothe and Abraham 1993). Here, evapotranspiration (ET) is the dominant

hydrological flux in the regional water balance (Petrone et al., 2007; Devito et al., 2005), thus an understanding of the mechanisms by which (constructed) landscapes and specific native species retain and exchange water with the atmosphere is necessary for creating informed decisions on planting prescriptions and site design. ET is driven by available energy, (soil) water availability, atmospheric vapour pressure deficit and turbulence (Helbig et al., 2020). Many of the aforementioned drivers are strongly influenced by biophysical surface properties as they control the exchange of energy and water between the surface and atmosphere (e.g., surface albedo affecting energy partitioning; plant cover affecting surface roughness and soil moisture; Balandier et al., 2022; Lafleur and Rouse, 1988). Unlike natural or other post-disturbance landscapes (e.g., fire, harvest) where some remnants of pre-disturbance features remain (e.g., plant cover, rooting architecture, soil structure, established hydrology), constructed systems undergo an initial, bare-ground phase followed by the planting, emergence and succession of plant communities before becoming robust ecosystems. Understanding the dominant controls on hydrological fluxes during the different successional phases can help ensure successful ecosystem evolution from one phase to the next. For example, it is critical that during initial post-construction bare ground conditions, cover soils store and provide adequate water to help initiate and sustain plant growth while withstanding the region's high evaporative demand.

Previous studies have examined the ET dynamics of natural (Liu et al., 2022; Green et al., 2021; Volik et al., 2020a, b; Phillips et al., 2016; Thompson et al., 2015; Brown et al., 2014; Brown et al., 2010; Petrone et al., 2007; Humphreys et al., 2006) and recovering (Morison et al., 2021; Nelson et al., 2021; Petrone et al., 2015; Thompson et al., 2014; Mkhabela et al., 2009; Amiro et al., 2006) boreal ecosystems in the Boreal Plains improving our understanding of environmental drivers. These studies emphasize the interconnectivity between soil-water-plant-atmospheric

processes and delineate water availability, plant community composition and age, and climate to be key factors influencing ET in the region. Notably, many of these studies express the potential sensitivity to drought under changing climatic conditions (Thompson et al., 2017). In the AOSR, initial reclamation efforts have been largely focused on recreating upland landscapes with only a recent shift to attempt to incorporate peatlands (Daly et al., 2012) to mitigate potential water deficits. To date only two pilot-scale upland-peatland complexes have been constructed (Sandhill Fen Watershed and Nikanotee Fen Watershed). As reclamation in the region is still a relatively new endeavour, only a handful of water flux studies have been conducted at constructed sites (Clark et al., 2022; Fettah et al., 2022; Biagi et al., 2021; Scarlett and Price, 2019; Ketcheson et al., 2017; Scarlett et al., 2017; Strilesky et al., 2017; Nicholls et al., 2016), many which encompass only the initial phase post-construction (<3 years). Only recently has sufficient time passed and data been collected to evaluate moisture exchanges during further stages of ecosystem evolution. Moreover, most long-term boreal studies of water fluxes are measured at the stand to ecosystem-scale via the eddy covariance technique (Helbig et al., 2020; Volik et al., 2020; Straker et al., 2019; Mkhabela et al., 2009; Amiro et al., 2006). Less work has been conducted at the community/species scale on vascular vegetation (Scarlett and Price, 2019; Scarlett et al., 2017; Phillips et al., 2016), particularly of upland tree species (Fettah et al., 2022). Previous studies have highlighted the heterogeneity of boreal landscape plant communities and the influence species variability within a site can have on surface-atmosphere moisture exchanges (Volik et al., 2020; Brown et al., 2010; Coursolle et al., 2006; Barr et al., 2001). Additionally, it is well recognized that species biodiversity greatly improves an ecosystem's ability to withstand changing environmental conditions (Anderegg et al., 2018). Thus, evaluating species-specific responses to

variable environmental conditions in a constructed setting provides valuable insight for future planting and planning.

In this study a multi-scale approach (ecosystem and community) was applied to capture water fluxes at the constructed Nikanotee Fen Watershed (NFW). The aim of this study is to (i.) examine ecosystem-scale fen and upland growing-season ET dynamics during the initial seven years (2013 – 2019) following construction; (ii.) quantify community-scale ET of the dominant vascular vegetation in each landscape; and (iii.) determine environmental controls on ET fluxes and whether these controls varied among species in the fen and upland respectively.

5.2 Methods

5.2.1 Study Site

Nikanotee Fen Watershed (NFW; Figure 5-1), is a constructed landscape consisting of an upland (7.7 ha) and fen peatland (2.9 ha) created to assess the viability of (fen) reclamation endeavours in the AOSR. Construction of NFW was completed in January 2013 in a formerly surface-mined section within an oil sands lease approximately 30 km north of Fort McMurray, Alberta (56°55′59” N, 111°25′00” W). The design of NFW emulates the natural, undisturbed landscapes of the Western Boreal Plains, where uplands steadily supply groundwater to downgradient peatlands (Price et al., 2010). This hydrological connectivity is assumed to be a key mechanism for continued peatland functionality in the frequently moisture-limited regional climate (Devito et al., 2012). Additionally, from a reclamation design perspective, it provides a means for self-sufficient hydrological function allowing for self-design, and without engineering interventions (e.g., pumping, periodic drainage). Detailed descriptions of site design and construction were previously reported (Popović et al., 2022; Sutton and Price., 2020; Ketcheson et al., 2016; Daly et al., 2012).

The design follows recommendations based on a modelling exercise that tested the response of various configurations using locally available materials and historical climate (Price et al., 2010). Briefly, the upland consists of a 3 m thick coarse tailings sand aquifer placed at a 3% basal slope, overlain by a 20-50 cm thick cover soil composed of salvaged forest soil (sandy loam to loam). Planting prescriptions in the upland consisted of native species common to WBP uplands including black spruce *(Picea mariana*), jack pine (*Pinus bankstana*), balsam poplar (*Populus balsamifera*); Labrador tea (*Ledum groenladicum*) and bunch berry (*Cornus stolonifera*). The fen consists of 2 m thick layer of salvaged, donor peat and has had permanent standing water ("ponds") since following construction in 2013. The fen was vegetated using an factorial design described in detail by Borkenhagen and Cooper (2019). Planting prescriptions incorporated both freshwater and saline sedge and graminoid species (*Carex aquatilis* (water sedge), *Juncus balticus* (wire rush), *Triglochin maritima* (seaside arrow grass)), as well as brown moss species harvested from a local rich fen via the moss transfer method (Rochefort et al., 2003). In 2014, invasive *Typha latifolia* infilled many of the ponded regions.

5.2.2 Study Design

This study combines both ecosystem- and community-scale measurements. Ecosystem-scale, eddy covariance measurements were conducted during the snow-free growing season (May – September, DoY 135-255) during the first seven years post-construction (2013 – 2019). Community-scale, chamber-based measurements were conducted from 2017 – 2019 in the fen and 2018 – 2019 in the upland. Whole plant chamber measurements were taken weekly at each flux location (hereafter referred to as a plot) during the growing season (May – August). Each plot contained a dominant species (Table 5-1). In the fen, a total of 32 plots were measured each week (Table 5-1). Due to its size, heterogeneity and to adequately capture trends, the upland was divided

into nine quadrants (Figure 5-1A) and within each quadrant one plot of each dominant species was measured (Table 5-1) for a total of 45 upland plots. Latin species names are used in this manuscript; however, colloquial or shorthand versions (e.g., Carex (Ca) or Aspen (As)) are used in figures to simplify legends and axis labels.

Table 5-1: Landscape specific whole plant chamber measurement specifications and sampling design, Nikanotee Fen Watershed, Fort McMurray, Alberta, Canada.

	Chamber measurements per season	Dominant Species	Number of Plots	Chamber Dimensions (cm)	Chamber Type	Tube Length (cm)
Fen	378 (2017)	*Carex aquatilis*	12	60 x 60 x 60	single	75
	272 (2018)	*Juncus balticus*	7	60 x 60 x 60	single	75
	261 (2019)	*Typha latifolia*	6	50 x 50 x 40	stacked (x3)	200
		Mixed	7	60 x 60 x 60	single	75
		Total	**32**			
Upland	264 (2018)	*Populus tremuloides*	9	50 x 50 x 40	stacked (x4)	200
	289 (2019)	*Populus balsamifera*	9	50 x 50 x 40	stacked (x4)	200
		Picea mariana,	9	50 x 50 x 40	stacked (x3)	200
		Pinus banksiana	9	50 x 50 x 40	stacked (x4)	200
		Understory	9	50 x 50 x 40	single	75
		Total	**45**			

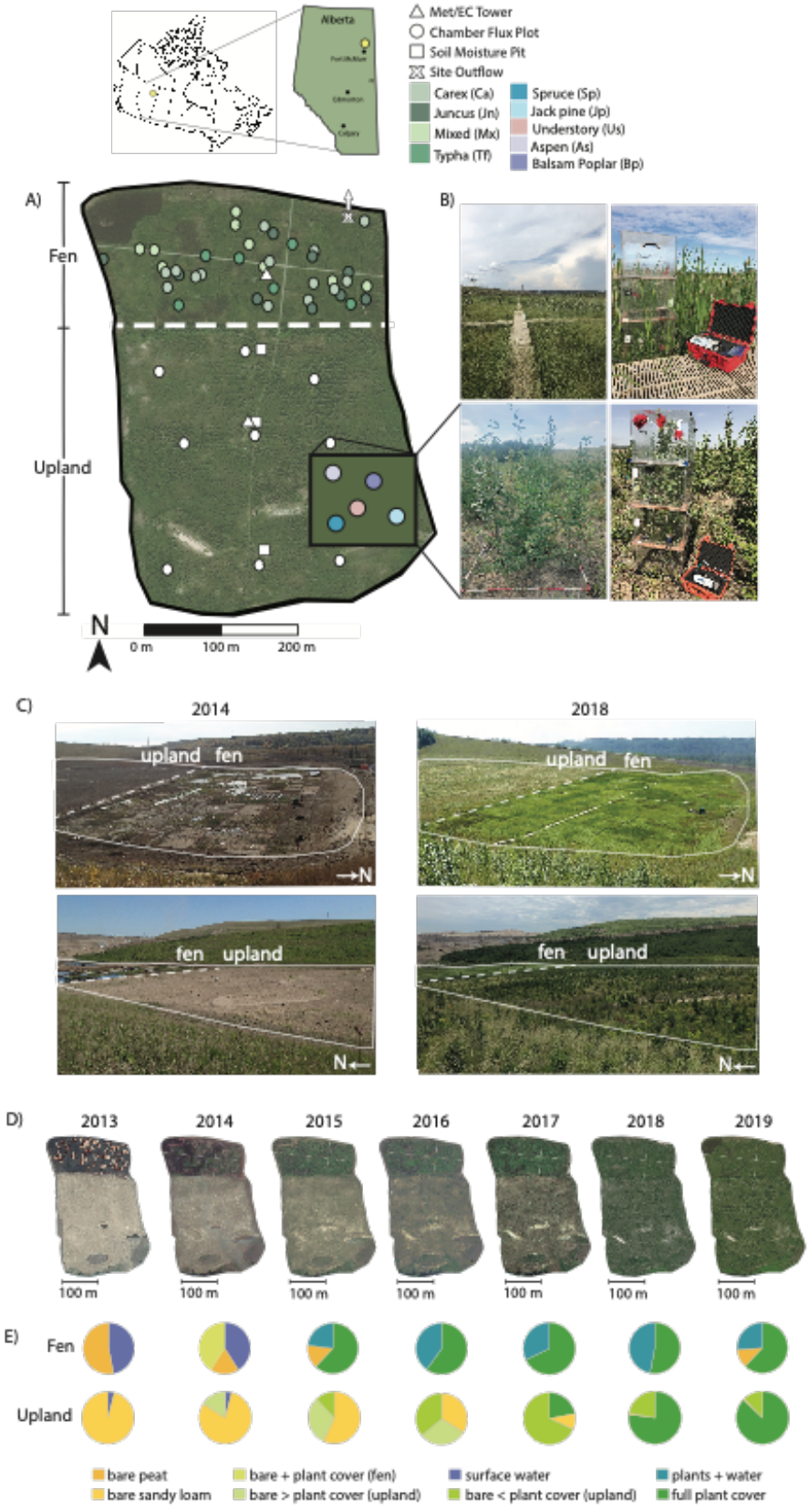


Figure 5-1: A) Map depicting the Nikanotee Fen Watershed (NFW) fen and upland landscapes and the location of instrumentation (towers and soil pits) as well as chamber flux plot locations; B) Field photographs depicting the fen (top row) and upland (bottom row) and the whole-plant, single and stacked chamber flux technique; C) Landscape-scale field photographs of biophysical surface characteristics in 2014 (year 2) compared to 2018 (year 6); D) Satelitte imagery of NFW capturing ecosystem evolution from 2013 – 2019; E) Summary of surface biophysical conditions for each year, based on the results of land cover spectral analysis, adapted from Popović et al. (2023)

.

5.2.3 Environmental Conditions

Water table depth (WTD) measurements were collected via the site's extensive hydrometric network that was installed at the time of construction using a combination of both manual and automatic (HOBO MX2001-S; Onset: Massachusetts, USA) measurement techniques (Ketcheson et al., 2017). Wells were installed at depths of 1.5 m (fen) and 3 m (upland). Volumetric water content (VWC) of the rooting zone (up to 50 cm below ground surface) was measured in soil moisture pits spanning a north-south transect across the site (three in upland, one in fen; Figure 5-1). Pits were instrumented with dielectric impedance reflectometry soil moisture probes (Hydra Probe II; Stevens Water Monitoring Systems, Portland, USA) at each 5, 15, 30 and 45 cm depths and recorded dielectric permittivity at one-minute intervals, which were subsequently converted to daily averages. All measurements were temperature and salinity corrected and converted to VWC based on a calibration specific to substrate material (organic vs mineral soil) as outlined in Seyfried et al. (2005). Soil temperature was measured at meteorological towers using thermocouples (Type k thermocouple (2013–2018), CS-109 soil temperature probes (2019)) at 5 cm depth.

Water table position and edaphic conditions were measured adjacent to chamber plots (as to not distort measurements) to capture environmental conditions at the time of flux measurement. Near surface (5 cm) soil moisture (VWC) and soil temperature (Tsoil) were manually measured using a WET-2 Sensor/HH moisture meter (Delta-T Ltd: Cambridge, United Kingdom) and calibrated for each soil type (organic vs mineral soil).

Evolution of surface biophysical conditions (plant emergence and development) at NFW during the study period have been previously reported (Chapter 2, Chapter 3)) using a range of techniques including remote sensing (enhanced vegetation index, land use land cover change) and

extensive plot-scale measurements (leaf area index and vegetation surveys). Results from the these studies are summarized in Table 5-2 and 5-3 and Figure 5-1 C-E and included in this current study to provide context to ET results.

5.2.4 Ecosystem-scale measurements: Micrometerology and evapotranspiration

Both the fen and upland were configured with identical instrumentation including a meterological station with an eddy covariance (EC) system. Meteorological stations were configued to measure air temperature (Tair, ^{o}C) and relative humidity (rH, %) using a Rotronic HC2S3 (Campbell Scientific, Logan, Utah, USA) and net radiation (Q*, Wm^{-2}) using a CNR4 (Kipp Zonen, Delft, Netherlands). Precipitation (P, mm) was measured with a tipping bucket rain gauge (Texas Instruments TR-525M) placed within a clearing near each tower to avoid tower interference. Vapour pressure deficit (VPD, kPa) was calculated via saturated vapor pressure (e_s) and actual vapor pressure (as outlined in Howell and Dusek, 1995). Photosynthetically active radiation (PAR, μmol m^{-2} s^{-1}) was derived from measured incoming shortwave radiation (CNR4 (Kipp Zonen; Delft, Netherlands) using a numerical coefficient (Britton and Dodd, 1976) and the LakeMetabolizer package in RStudio (Winslow et al., 2016; R Core Studio, 2021). Ground heat flux (Q_G, Wm^{-2}) was calculated using ground heat flux probes (HFT3; Campbell Scientific: Logan, Utah, USA) inserted horizontally at depths of 5 cm below the ground surface, several meters apart. All data were sampled at 1-minute intervals and averaged every 30-min on a CR1000 datalogger (Campbell Scientific: Logan, Utah, USA). Eddy covariance (EC) systems consisted of a closed path CO_2/H_2O gas analyzer (LI-7200: LI-COR, Lincoln, Nebraska, USA) and 3D sonic anemometer (Windmaster P ro: Gill Instruments, Lymington, Hampshire, UK) from 2013-2014, and an open path CO_2/H_2O gas analyzer (LI-7500: LI-COR, Lincoln, Nebraska, USA) with a 3D sonic anemometer (CSAT3 3D: Campbell Scientific, Logan, Utah, USA) from 2015-2019.

Detailed descriptions of tower and sensor set ups and data post procesing are described in Popović et al., 2022 and 2023.

Potential evapotranspiration (PET) was estimated using meteorological data and the Penman-Monteith equation (Allen et al., 1998; Monteith, 1965; Penman, 1948, Equation 1),

$$PET_{PM} = \frac{\Delta(Q^* - Q_G) + \rho_a C_p \frac{(e_s - e_a)}{r_a}}{\left(\Delta + \gamma \left(1 + \frac{r_s}{r_a}\right)\right)\lambda} \quad (5\text{-}1)$$

where Δ is the slope of the vapour pressure-temperature curve, γ is the psychrometric constant, ρ_a is the density of air, C_p is the specific heat of dry air, λ is the latent heat of vaporization. Aerodynamic (r_a) and surface (r_s) resistances terms were not directly measured and were calculated according to Allen et al. (1998). Saturation (e_s) and actual (e_a) vapour pressure were calculated using Tair and rH as outlined by Howell and Dusek (1995).

Surface conductance (g_s), which regulates the transport of water vapour from the land surface to the atmosphere (Schulze et al., 1995) was calculated by inverting Penman-Monteith (PET_{PM}; Knauer et al., 2018; Monteith 1965) as described in Chapter 3. Sensitivity of g_s to VPD, which can be used as an indicator of plant water-use was derived using a modified Lahammer's function fitted using a non-linear least-squares model (Oren et al., 1999; Equation 2):

$$g_s = -mln(VPD) + b \quad (5\text{-}2)$$

where *b* is the reference surface conductance at VPD = 1 kPa, and *m* is the sensitivity parameter of g_s to VPD. Generally, g_s decreases exponentially with increasing VPD (Oren et al., 1999) and transpiration rates increase until a species-specific VPD threshold (Grosslord et al., 2020; Monteith 1995). Thus, sensitivity (*m*) will typically decrease in response to plant water-regulation during

periods of water-stress or soil moisture decline (Novick et al., 2016). Wetter environments typically have a higher *m* and *b* compared to drier, water-limited settings (Novick et al., 2016).

5.2.5 Community-scale, instantaneous chamber evapotranspiration

Community-scale measurements were conducted using a portable closed-chamber system and infrared gas analyser (EGM–4; PP Systems, MA, USA). Table 5-1 describes chamber dimensions and sample design. In the upland and at *Typha latifolia* fen plots, stackable chambers were used (Figure 5-1) to measure taller species and avoid damage to plants.

Chamber measurements of air temperature (Tair), relative humidity (rH) and photosynthetic radiation (PAR) were taken every 15 seconds for a 3-minute interval on the EGM-4. At each plot, both a light and dark run were completed. Dark conditions were simulated by covering the clear plexiglass chamber with a black, opaque tarp. Plots were measured in random order on each sample day to capture a range of day-time values and conditions at each plot. The number of flux measurements varied across years (Table 5-1) as measurements were limited to fair-weather conditions and not taken during precipitation events, low PAR (<200) or high relative humidity (>80%) due to sensor function. As such, years with more precipitation events typically had fewer measurement days.

Instantaneous chamber evapotranspiration (ET) was calculated following methods described by McLeod et al. (2004) by deriving the slope of chamber vapour pressure over time via least squares regression. This calculated slope was then applied to a modified equation (Stannard, 1988),

$$ET = 3.6\frac{MVC}{A} \quad (5\text{-}3)$$

where ET is evapotranspiration (mm h^{-1}), M is the slope of the constant slope section (g $m^{-3}s^{-1}$), V is the volume inside the chamber (m^3), C is the calibration factor to account for vapour absorption by the chamber material (unitless, derived via calculations outlined in McLeod et al. (2004) and Hamel et al., 2015), A is the area of land surface covered by the chamber (m^2) and 3.6 is a factor to convert a volume of water per unit area (g H_2O m^{-2} s^{-1}) to an hourly flux rate (mm h^{-1}). In terms of the calibration factor (C), the EGM-4 used in this study passes sampled air through a filter of Sofnolime Granules (Sodium Hydroxide; Molecular Products, Essex, UK) before it is analyzed in the central system resulting in a (calculated/estimated) loss of water vapour of 0.036 and 0.083 g H_2O per 3-minute interval for the fen and upland respectively (based on chamber volume). Moreover, as water vapour tends to absorb to the internal wall of the sample tubes (between the chamber and EGM-4), tube length impacts the amount of absorption and can result in an over (or under) estimation (Hamel et al., 2015) of H_2O fluxes. Tube lengths varied between the upland and fen (200 cm versus 75 cm, respectively; Table 5-1) due to variation in chamber height and position of EGM on the ground (see Figure 5-1B). As such. the calibration factor (C) was adjusted for each landscape and species based on the above sources. Measurements from dark chamber runs were used to partition evapotranspiration and provide an estimate of surface evaporation (E_S), under the assumption that during dark conditions, stomata were closed, and minimal transpiration was occurring.

5.2.6 Data Analysis

For statistical analysis, only measurements spanning from the last week of June to the first week of August were used as this time frame represented peak leaf out for vegetation in the region and limited interference caused by varying plant emergence times in the spring, while also containing a relatively consistent amount of data points between years. The accepted significance level used for all statistical tests was $p < 0.05$ and significance is denoted by "." for $p<0.10$, "*" for $p < 0.05$, "**" for $p < 0.01$, "***" for $p < 0.001$ in figures. All statistics, were completed using RStudio (RStudio Team, 2020). A Kruskal-Wallis with post-hoc Dunn test was conducted to evaluate differences in ET fluxes between species within each landscape. To examine landscape-scale environmental drivers on ET between years a Spearman rank correlation was conducted for each year (2013 – 2019, EC data). Correlations were generated using the Performance Analytics package (Peterson and Carl, 2020) paired with GGally package (Schloerke et al., 2020) producing a p-value between each pair of parameters and Spearman rank coefficients (RS), ranging from -1 to 1, where values with absolute value closer to 1 indicate a stronger correlation and values closer to zero indicate less correlation. To evaluate species-specific relationships between edaphic and atmospheric variables and ET a linear mixed effect model (LME) was run for each species using nlme package (Pinheiro et al., 2014) with year and plot as the random factor. LME was also run for each landscape as a whole, where species was included as a fixed factor. LME was run using only chamber-measured data.

5.3 Results

5.3.1 Environmental Conditions

Environmental conditions have been previously summarised as a time series of growing season daily means (Chapter 2) and yearly boxplots in (Chapter 3). Seasonal average mean daily air temperature (Tair) ranged between 15 ºC (2019) to 19 ºC (2016) with September typically being the coolest and July the warmest of the measurement period. Total seasonal precipitation (P) ranged between 168 mm (2017) to 310 mm (2016), and all years except 2016 and 2019 (285 mm) had less rainfall than the 30-year average (283 mm, Environment Canada, 2020). Most rainfall occurred during the months of June and July apart from 2019, where 44% of seasonal rainfall occurred in August (126 mm). Furthermore, while 2016, 2018 and 2019 were all wetter years with similar amounts of rainfall (total growing season rainfalls of 310, 278 and 285 mm, respectively), the timing and intensity of events differed greatly (Figure 5-2). VPD was variable between years, and ranged between 0-5 kPa reflecting the large atmospheric demand for ET in the region. Daily averages ranged between 0.1 - 2.8 kPa. Daily mean relative humidity (rH) ranged from 28 to 92% with an interannual average between 60% and 67%. PAR was highest between 11h00–17h00, with an interannual average of 947 µmol m^{-2} s^{-1}. PAR was typically higher from May to mid-July and slowly decreased in August towards the end of the growing season. PAR was similar across years; however, a slight decrease was observed in 2019 reflective of (frequent) overcast conditions that year. Interannual mean fen soil moisture (volumetric water content, VWC) was 84% with daily averages ranging between 70 – 87%. Fen mean daily peat temperatures ranged from 3.6 - 26.9 ºC over the study period. Interannually, mean peat temperatures decreased over time from 16.6 (2013) to 12.1 ºC (2019). Fen had a near-surface water table position (interannual mean 8 cm bgs). Upland interannual mean VWC was 20% with daily means ranging between 10 – 40%. Upland soil temperature was warmer and varied less between years, with seasonal averages ranging from 18.3 (2019) to 20.5 (2013). ºCUpland had a much deeper WT position compared to the fen with season

means ranging from 158 to 220 cm bgs. In both landscapes, smaller scale (<10 mm), sporadic rain events appear to have a negligible impact on (daily) WT position, however, larger or recurring rain events or prolonged dry periods (2017) affected overall edaphic trends. Table 5-3 summarizes biophysical attributes of chamber plots for each species. Ecosystem development and biophysical characteristics have been previously described (Chapter 2, Chapter 3) and are summarised in Figure 5-1 C-E. Surface conditions rapidly evolved from bare ground to robustly vegetated plant communities within the initial seven years following construction (Figure 5-1C-E). In the fen, vegetation was widespread by 2015. Upland plant establishment was slower and became robust in 2017.

Table 5-2: Summary of environmental variables from 2013 to 2019. Data presented as monthly means (except for precipitation which is a monthly cumulative sum).

	P (mm)	T (°C)	VPD (kpa)	PAR (µmol $m^{-2}s^{-1}$)	WT (cm bgs)		VWC 5 cm (%)		VWC 30 cm (%)		Tsoil (°C)		EVI	
					Fen	Upland	Fen	Upland	Fen	Upland	Fen	Upland	Fen	Upland
2013														
5	1	18.0	1.2	1017	42.3			25.1	79.5	37.6	14.8	21.7	0.15	0.17
6	139	17.8	0.8	916	19.2		80.6	28.7	80.3	38.1	16.1	20.1	0.17	
7	91	17.8	0.9	954	2.6		82.1	26.1	79.5	38.0	16.5	20.4	0.23	0.17
8	26	18.6	0.8	968	-9.5		83.4	24.3	78.8	38.2	16.9	20.9	0.19	0.18
9	0	17.6	1.0		-8.1		85.1	23.2	78.7	38.1		19.4	0.14	0.10
2014														
5	65	13.2	0.7	649	-5.2	170.8	81.5	23.7		36.8	14.4	16.3	0.13	0.14
6	43	17.0	0.7	703	-3.6	145.3	80.9	23.1	86.4	37.5	18.5	19.8	0.21	0.21
7	66	20.2	1.1	771	-2.9	143.5	85.0	19.9	82.6	36.7	22.4	23.3	0.30	0.22
8	42	18.1	0.9	572	-2.2	169.9	85.2	18.8	81.1	34.5	20.2	20.7	0.29	0.21
9	14	7.6	0.3	374	-3.5	182.5	86.4	21.0	83.9	33.5	8.5	9.4	0.32	0.23
2015														
5	5	14.2	1.2	901	5.0	207.1	86.5	15.4	89.5	31.5	15.9	19.1	0.23	0.20
6	30	18.1	1.1	834	9.7	209.0	85.0	13.4	89.2	27.6	20.0	22.4	0.37	0.24
7	68	18.8	0.9	676	11.0	209.2	83.2	15.8	88.3	26.6	19.7	21.9	0.44	0.18
8	59	17.8	0.9	539	16.6	209.6	80.7	13.4	90.0	25.6	17.7	20.6	0.49	0.28
9	22	10.5	0.3	289	4.7	189.8		16.0		25.7	11.0	12.4	0.36	0.24
2016														
5	20				9.0	223.6		16.0		33.6			0.20	0.23
6	79	23.2	1.7	930	8.2	212.5		17.1		33.5	16.6	26.5	0.53	0.32
7	140	19.5	0.9	628	16.3	199.0	76.7	18.3	87.5	34.3	16.3	22.8	0.45	0.30
8	59	17.6	0.8	624	16.5	190.3	81.2		87.8		16.3	19.9	0.53	0.37
9	24	12.3	0.4		6.8	164.5						14.4	0.34	

Table 2: continued

	P (mm)	T (°C)	VPD (kpa)	PAR (µmol $m^{-2}s^{-1}$)	WT (cm bgs)		VWC 5 cm (%)		VWC 30 cm (%)		Tsoil (°C)		EVI	
					Fen	Upland	Fen	Upland	Fen	Upland	Fen	Upland	Fen	Upland
2017														
5	6	15.2	1.1	855	10.7	228.1	86.1				12.4	16.1	0.17	0.22
6	101	16.6	0.8	708	10.1	212.6	85.6	21.0	90.0	35.8	18.9	19.3	0.41	0.38
7	26	20.2	1.1	703	15.7	211.7	84.0	15.6	90.4	32.4	16.5	22.0	0.57	0.44
8	9	18.1	0.9	593	26.7	226.8	77.1	12.1	90.5	23.8	14.6	21.2	0.59	0.34
9				458	31.3	235.4	73.4	10.9	89.6	21.3	12.5		0.48	0.30
2018														
5	15	17.6	1.3	845	13.6	231.9		17.8		31.3	9.3	19.7	0.17	0.24
6	109	17.2	0.9	673	9.9	233.3	85.1	21.5	88.5	30.8	13.3	19.7		
7	112	18.9	0.9	676	6.0	212.6	84.7	21.5	88.2	34.8	16.1	20.6	0.49	0.44
8	17	16.6	0.8	481	6.0	192.5	85.3	13.6	88.1	29.1	13.1	19.5		
9	25	8.3	0.3	362	1.1	197.3	86.0	17.4	89.2	26.5	6.8	11.3	0.27	0.13
2019														
5	1	15.2	1.2	896	6.4	230.2	86.7	17.0	89.3	33.7	7.1	17.8	0.18	0.29
6	85	15.7	0.8	692	7.2	250.1	85.9	16.5	90.1	29.1	10.5	19.1	0.40	0.39
7	53	17.9	0.9	490	0.9	275.6	85.1	19.3	87.9	31.7	14.7	20.7	0.39	0.46
8	125	14.6	0.5	447	-4.5	263.2	84.7	28.3	88.5	34.1	13.6	16.8	0.37	0.48
9	21	12.8	0.4	323	-5.8	249.3	84.6	40.0	87.5	37.5	12.3	14.5	0.31	0.44

Table 5-3: Biophysical surface and edaphic conditions at chamber-measured plots by species. Values represent averages from all years measured (2017 – 2019 fen, 2018 – 2019 upland). Negative WTD represents inundated conditions (above ground water table).

	Plant Height (cm)	Litter Height (cm)	LAI	WTD (cm bgs)	VWC (%)	Tsoil (°C)
Fen						
Carex aquatilis	54	16	1.9	5 ± 5	84 ± 6	17 ± 4
Juncus balticus	45	6	1.6	9 ± 7	80 ± 9	19 ± 7
Typha latifolia	101	11	1.4	-12 ± 11	87 ± 6	16 ± 5
Mixed	56	8	1.8	6 ± 9	82 ± 6	18 ± 5
Upland						
Populus tremuloides	152	2	1.8	211 ± 17	14 ± 9	22 ± 4
Populus balsamifera	186	3	2.1	211 ± 17	17 ± 6	23 ± 3
Picea mariana,	112	1	1.4	211 ± 17	15 ± 4	24 ± 5
Pinus banksiana	171	1	2.3	211 ± 17	12 ± 4	23 ± 7
Understory	36	4	0.9	211 ± 17	14 ± 9	21 ± 4

5.3.2 Ecosystem-scale Evapotranspiration Trends

Total seasonal ET in the fen ranged between 296 to 452 mm, and decreased over time as the system developed (Figure 5-2 and 5-3). Highest seasonal rates occurred in 2014 and 2015 with 424 and 452 mm, respectively, while the lowest season total occurred in 2019 (296 mm). In early years (2013 – 2015) ET approached or was equal to the calculated value of PET, whereas from 2017 onwards, ET was less than PET (Figure 5-2). Furthermore, fen total ET exceeded total seasonal precipitation six out of seven years. Typically, the largest amount of ET occurred in July (interannual mean of 113 mm) apart from 2013 and 2015, where June had highest totals (110 and 113 mm, respectively; Figure 5-3). There was a marked decrease in daily fen ET rates, with mean daily rates in early years (2013-2015) ranging between 3.6 to 3.8 mm day^{-1}, in contrast to later years (2016 – 2019) with 2.5 – 2.9 mm day^{-1}. Diurnal trends in fen ET also shifted over time, with higher rates (>0.25 mm half $hour^{-1}$) of ET consistently throughout the

daylight window (8h – 20h) in early years (Figure 5-3). This temporal change is clear in early season ET trends (Figure 5-3). The effects of variable moisture supply (and atmospheric coupling) on ET were examined through the relationship between surface conductance (g_s) and VPD (Figure 5-4). The logarithmic relationship between g_s and VPD became more pronounced over time as the fen developed (Figure 5-4) and g_s decreased largely in response to increasing VPD. The slope (*m*, also referred to as the steepness or sensitivity parameter) was variable and ranged between 0.9 to 2.9 mm s^{-1}. Over time, *b* parameter decreased from 9 - 10.2 mm s^{-1} in early years (2013 - 2015) to 5.2 - 7.9 mm s^{-1} in later years (2017 onwards).

Seasonal upland ET remained relatively constant throughout the study period, with only a slight increase from 2013 to 2019 (Figure 5-2 and 5-3). However, although seasonal totals were similar across all years, intraseasonal/diurnal trends varied as the system developed (Figure 5-3). For example, early season (May) ET totals increased from an average of 25 mm (2013-2015) to 37 mm (2017-2019). Mean daily ET rates ranged from 1.2 mm day^{-1} (2016) to 2.2 mm day^{-1} (2018; Figure 5-3). In contrast to the fen, upland ET was consistently less than calculated PET (Figure 5-2) suggesting strong surface controls. Unlike the fen, total ET exceeded seasonal P only three out of seven years (2015, 2016 and 2017; Figure 5-2). Overall upland g_s was lower than in the fen and seasonal means ranged between 2.5 to 4.5 mm s^{-1}. g_s in relation to VPD followed a similar logarithmic pattern to the fen, with g_s decreasing rapidly between 0 to 1 kPa and then leveling out (Figure 5-4). The *m* parameter ranged between 1.1 and 2.2 and *b* increased slightly over time from 3.5 mm s^{-1} in 2014 to 5 mm s^{-1} in 2019.

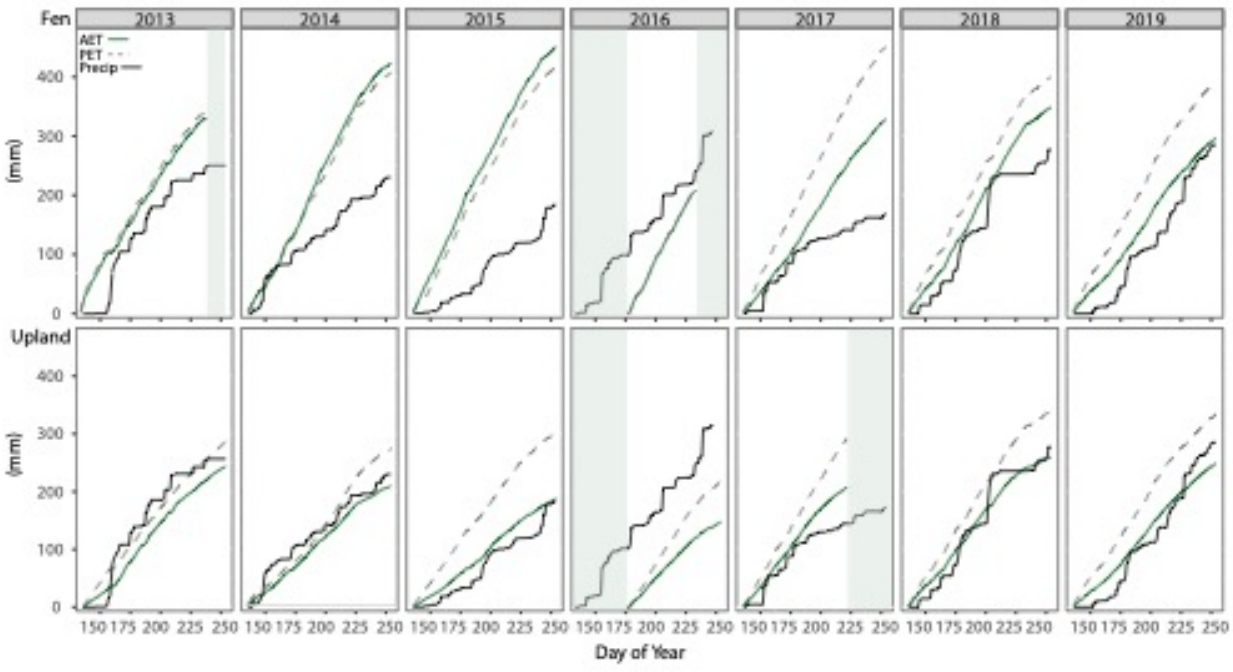


Figure 5-2: Cumulative seasonal AET (mm, green), PET (mm, dashed) and P (mm, black) for the fen (top) and upland (bottom) from 2013 to 2019. Nikanotee Fen Watershed, Fort McMurray, Alberta, Canada. Light green bands represent periods of missing data due to instrument malfunction.

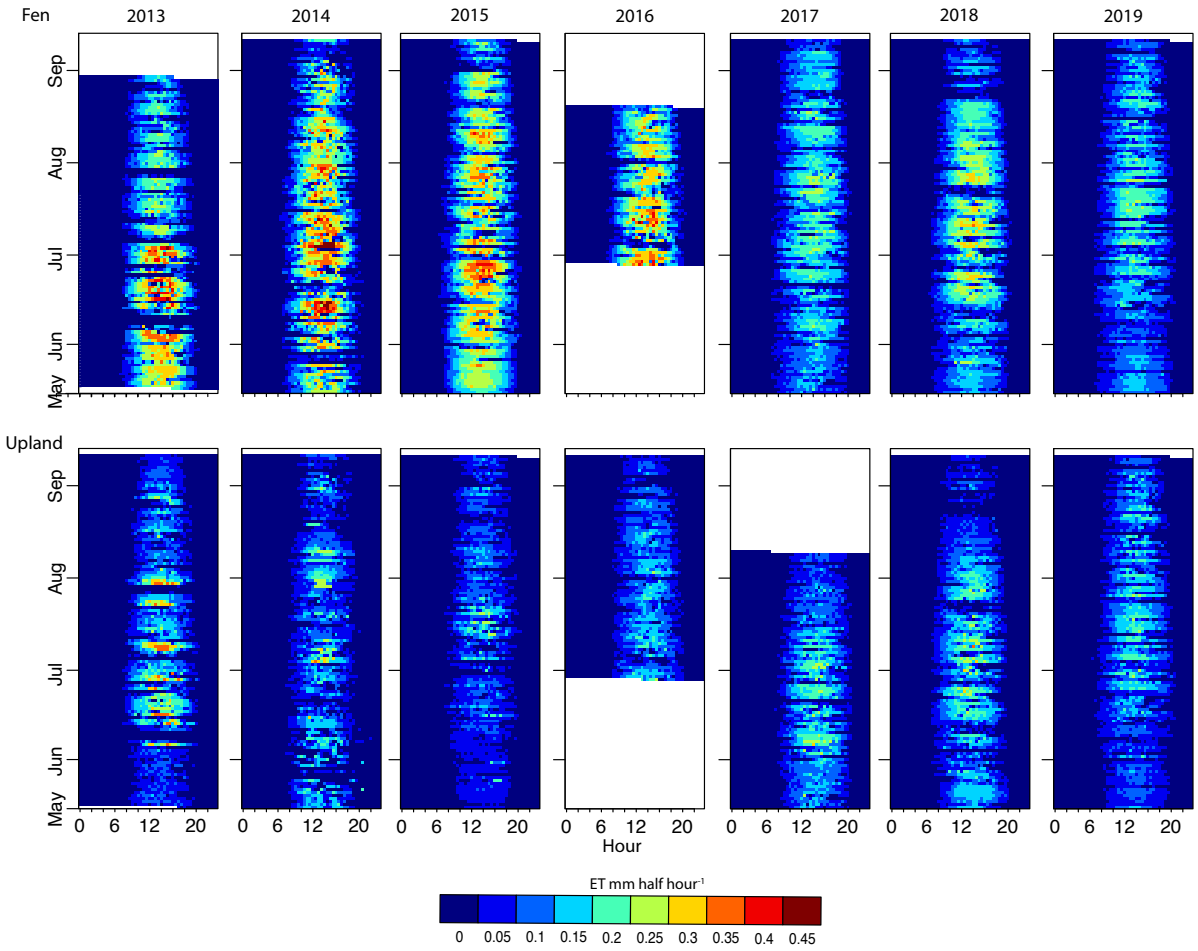


Figure 5-3: Fingerprint plot depicting gap-filled, half-hourly evapotranspiration (ET, mm) from 2013 – 2019 for the fen (top) and upland (bottom)at Nikanotee Fen Watershed, Fort McMurray, Alberta, Canada. Each square is a half-hourly measurement, and each row represents a full day. Plots show seasonal (May-Sept, y-axis) and diurnal (hourly, x axis) trends. 2016 missing data is due to Horse Creek Wildfire, other gaps are due to instrumentation malfunction.

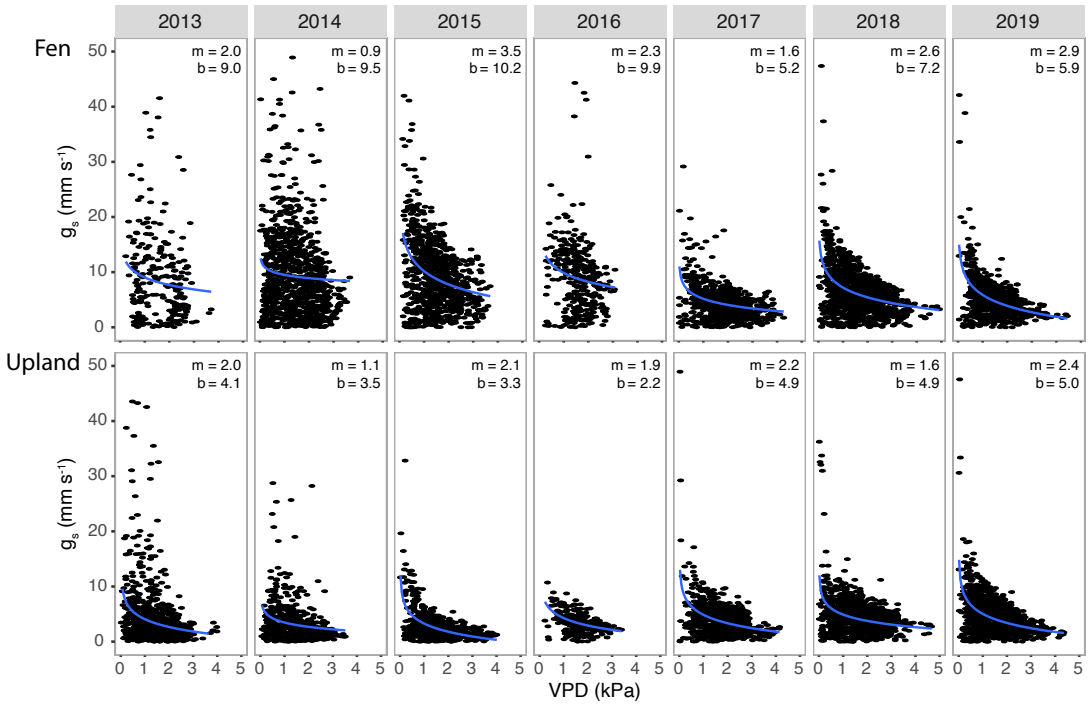


Figure 5-4: Sensitivity of gs to VPD from 2013 to 2019 in the fen (top) and upland (bottom).

5.3.3 Instantaneous Chamber Evapotranspiration

ET fluxes measured at vegetated plots from 2017 – 2019 varied between landscapes, species and years (Figure 5-5). Interseasonal mean ET for the fen was 2.6 mm day^{-1} while mean upland ET was slightly higher at 3.3 mm day^{-1} (Figure 5-5A). Moreover, surface evaporation (E_S) was generally higher in the upland than the fen (interseasonal mean of 1.8 and 0.9 mm day^{-1} respectively; Figure 5-5B), despite the upland being a drier landscape.

Mean seasonal fen ET rates were comparable in wetter years (3.3 and 2.8 mm day^{-1} in 2018 and 2019) and slightly lower in drier years (2.1 mm day^{-1} in 2017). Moreover, there was a slight increase in E_S in 2019 in *C. aquatilis*, *J. balticus* and mixed plots while *T. latifolia* saw a decrease compared to 2018. *T. latifolia* plots generally had higher rates of ET and E_S (interseasonal mean ET of 3.9 mm day^{-1} and E_S of 3.1 mm day^{-1}; Figure 5-5AB) with highest

rates observed in 2018 (Figure 5-5BC) with August mean ET reaching 4.8 mm day^{-1} . Similarly, ET was high across all plot types in July 2018 (Figure 5-5C). *C. aquatilis* plots typically had the lowest rates of E_S out of all fen species with seasonal means ranging between 0.4 to 1.0 mm day^{-1} (Figure 5-5B). *J. balticus* plots exhibited the largest seasonal variability across all years (Figure 5-5C) with monthly means fluctuating by up to 1.7 mm day^{-1}. Of note is the increase in *J. balticus* (and to lesser extent *C. aquatilis* and mixed plot) ET in August 2017 despite dry conditions.

In the upland, ET and E_S varied between years (Figure 5-5BC) with higher rates observed in 2018 (seasonal mean ET and $E_{S.}$ of 3.8 and 2.1 mm day^{-1}) than in 2019 (seasonal mean ET and E_S of 2.6 and 1.5 mm day^{-1}). In 2018 all treed plots exhibited similar rates of E_S (species specific seasonal mean E_S ranging between 1.8 to 2.3 mm day^{-1}; Figure 5-5B) while in 2019 E_S was lower in coniferous plots (*P. banksiana mean* of 1.4 mm day^{-1}, *P. mariana* mean of 1.3 mm day^{-1}) than broadleaf plots (*P. balsamifera* mean of 2.2 mm day-^{1}, *P. tremuloides* mean of 2.0 mm day^{-1}, Figure 5-5B). Understory plots had the lowest ET and E_S rates out of the upland species (Figure 5-5A-C) with an interseasonal mean of 1.8 and 1.0 mm day^{-1}. Broadleaf plots typically exhibited higher ET rates than coniferous and understory plots. *P. balsamifera* plots had the highest ET rates reaching monthly means of 4.6 and 4.3 mm day^{-1} in July 2018 and 2019 (Figure 5-5C).

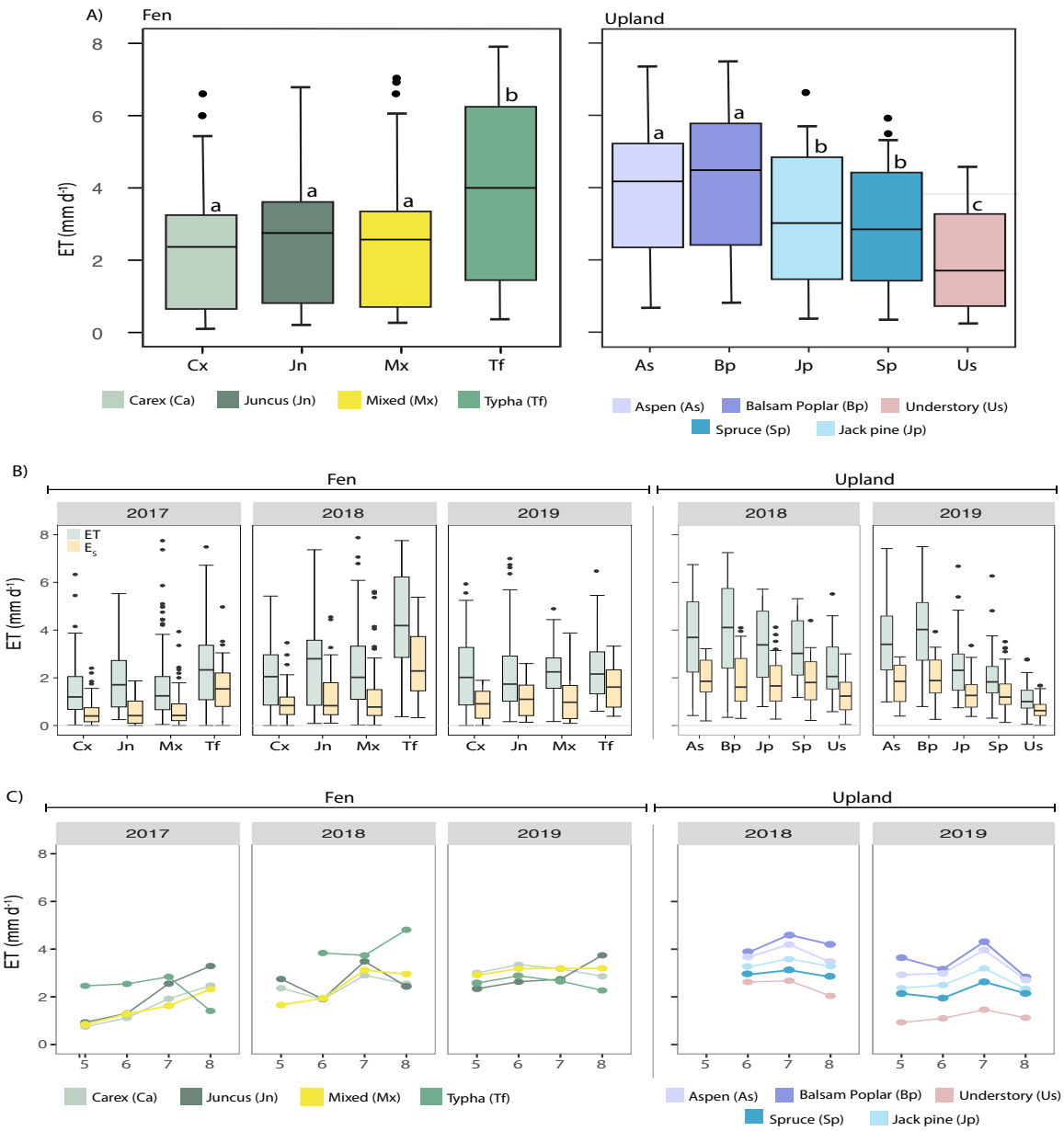


Figure 5-5: Results from chamber-based measurements, Nikanotee Fen Watershed, Fort McMurray, Alberta, Canada. A) ET fluxes by species in the fen (left, 2017 – 2019) and upland (right, 2018 – 2019). Compact letter display depicts results from post-hoc Dunn statistical analysis representing significant differences between species within each landscape. Black line indicates the median, the box represents the 25th to 75th quartile, the whiskers include 95% of the range, and the black circles are outliers. B) Partitioning of ET and E_S (surface evaporation) by species and year. C) Seasonal variability in chamber-based ET fluxes based on monthly means by species.

5.3.4 Environmental Controls

Figure 5-6 depicts landscape-scale Spearman rank coefficients (R_S) between environmental variables and ET for each year, providing insight into the strength of the relationship depending on the season (i.e., in a wet versus dry year). Figure 5-7 summarises the relationship between edaphic and atmospheric variables and ET for each species.

Results from the Spearman correlation depict a strong relationship between ET and atmospheric conditions across all years in both landscapes. WTD was largely insignificant in either landscape (with the exception of 2017 and 2018 in the fen (Figure 5-6)). Moreover, R_S results indicate that the strength of the relationship between environmental variables and fluxes varied depending on overall seasonal hydroclimatic conditions (i.e., wet versus dry years, frequency and intensity of events). Notably, edaphic controls on fen ET in 2017 (drier year) were opposite to that of wetter years (Figure 5-6) when ET and VWC were negatively, strongly and significantly correlated in 2017 (i.e., ET increased even as VWC decreased) indicating fen plant-water feedbacks are not solely linked to near surface (edaphic) properties. Moreover, there is increased correlation between WTD and fen ET in 2018. Generally, due to ample water availability, fen ET fluxes were more strongly correlated to atmospheric than edaphic controls. In the upland there was a temporal shift in edaphic controls as vegetation became more robust (2016 onwards, Figure 5-6). While atmospheric controls dominated, edaphic influence was stronger than observed in the fen, particularly the correlation with VWC and Tsoil.

At the landscape scale, results of LME model analysis reinforced Spearman results with significant atmospheric drivers in both landscapes (PAR, rH, Tair: upland: p=0.0004, 0.0007, 0.017; fen: p=0.0005, 0.0006, 0.025). WTD was not significant for upland fluxes and (weakly) significant for fen ET (p=0.0463). At the species level, fen species saw a greater variability in

controls between species due to the heterogeneity in surface conditions and plant physiology (Figure 5-7). In contrast to other fen species, as edaphic conditions in the fen were relatively stable and consistently wet (i.e., frequently ponded, high water availability) atmospheric controls were found to be the only significant factors driving ET at *T. latifolia* plots (Figure 5-7). Moreover, ET was significantly related to WTD only at *J. balticus* plots. Upland species largely exhibited similar environmental controls, although there was some variability between tree types (e.g., broadleaf versus coniferous). WTD was not significant for any ET-species relationships in the upland. ET was strongly driven by atmospheric controls across all species and to varying degrees by edaphic conditions (Figure 5-7). Notably, coniferous species showed a strong, significant relationship between VWC and ET but also a weaker (non-significant) relationship with Tsoil and ET ($p=0.0688$ and 0.0761 for *P. mariana* and *P. banksiana*, respectively), which was not observed at other plot types. Moreover, *P. balsamifera* plots did not exhibit edaphic controls on ET, whereas *P. tremuloides* did ($p=0.0391$). Understory plots differed from treed species with stronger edaphic than atmospheric controls on ET (Figure 5-7).

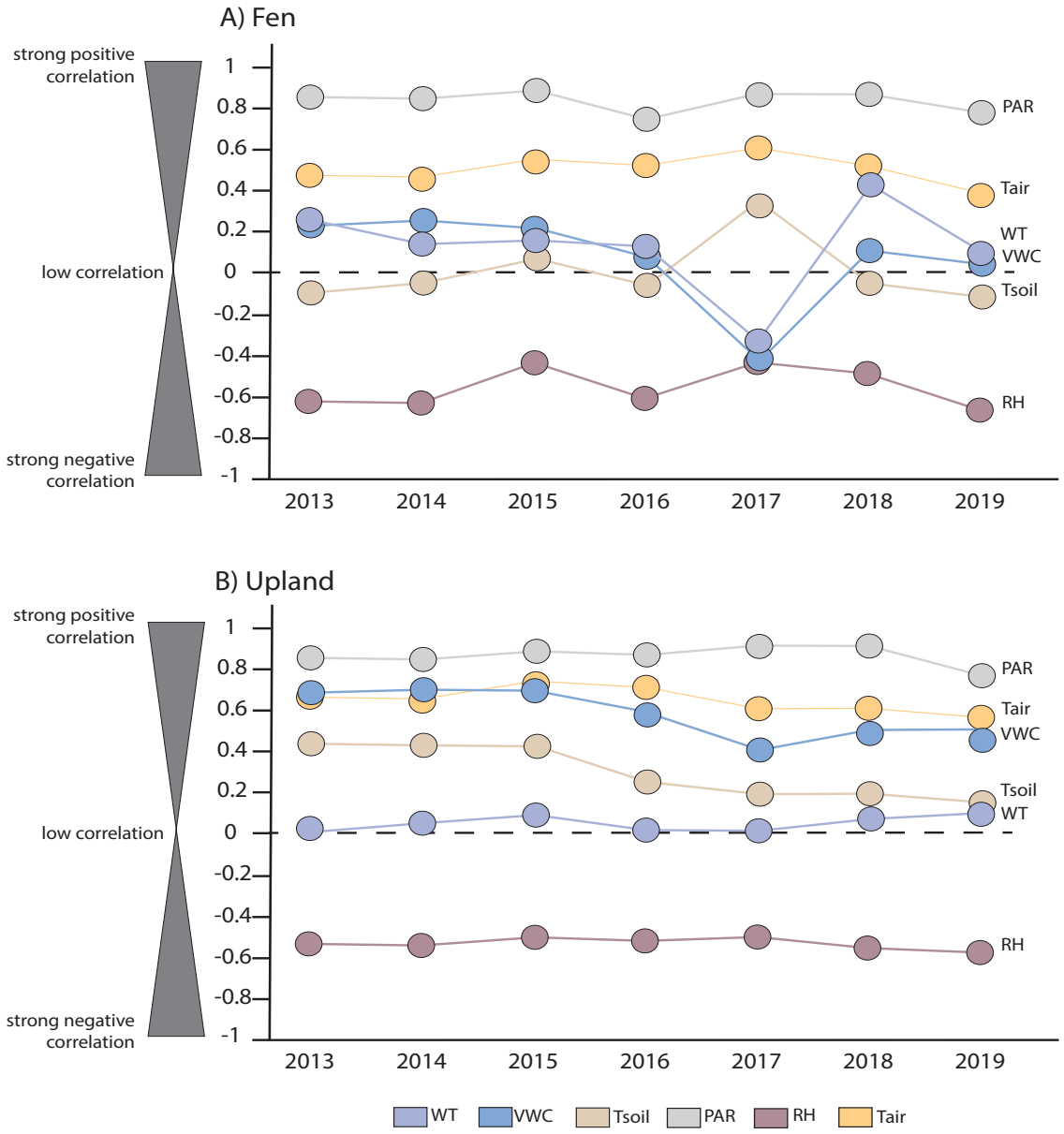


Figure 5-6: Temporal snapshot of Spearman rank coefficient (RS) depicting the relationship between environmental conditions and ET fluxes in the A) fen and B) upland from 2013 to 2019.

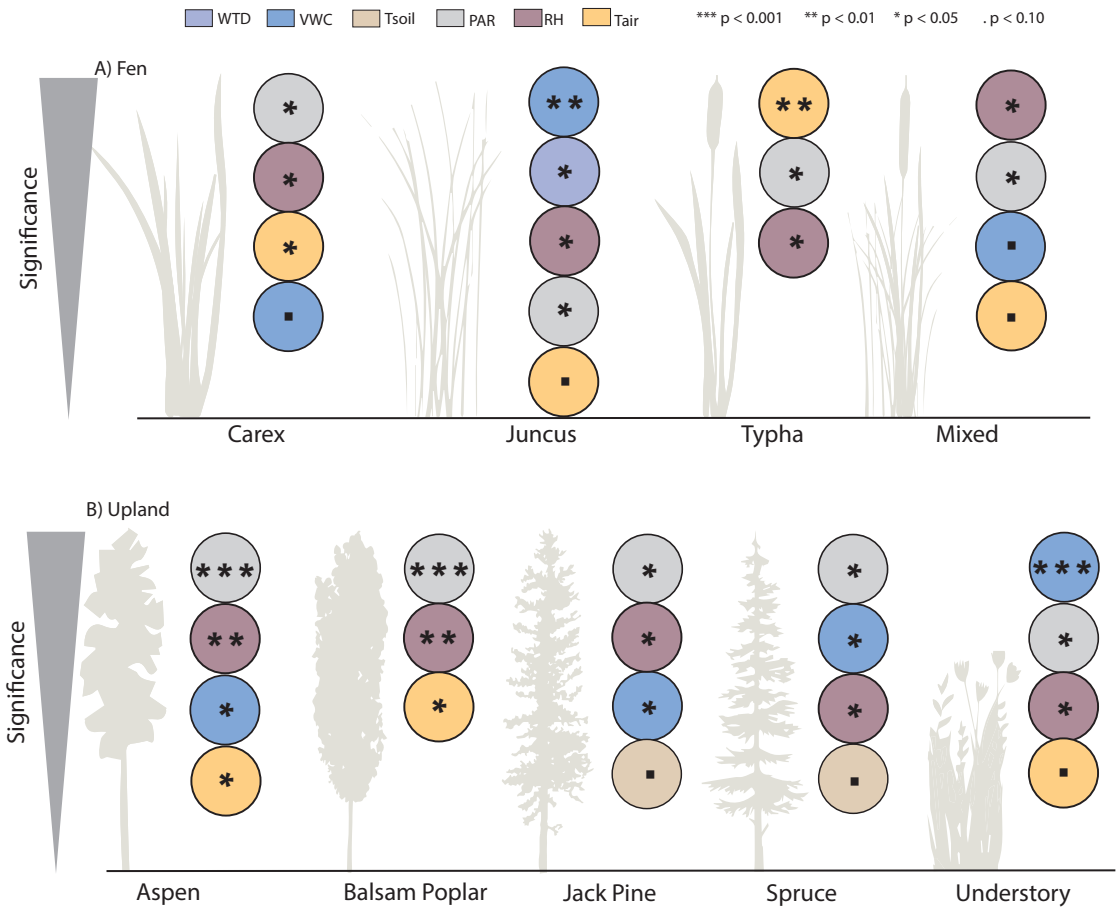


Figure 5-7: Graphical summary of results from the linear mixed effect model depicting the interaction between ET and environmental variables per each species in the A) fen and B) upland. Significance is denoted by * for $p < 0.05$, ** for $p < 0.01$, *** for $p < 0.001$. ■ $p < 0.10$ is not significant but exhibited some relationship and has been left in for discussion/context.

5.4 Discussion

5.4.1 Drivers and controls of surface-atmosphere moisture exchanges

While abiotic factors such as edaphic conditions, water availability and atmospheric forcing are central to surface-atmosphere moisture exchanges, a critical component driving temporal ET trends in both landscapes of this study (Figure 5-3) was the biophysical evolution of the system from bare ground to widespread plant coverage during the initial seven years post-construction (Figure 5-1C-E).

5.4.1.1 Fen

Initially following construction, fen ET was high with limited seasonal trends (Figure 5-3) and consisted largely of surface evaporative losses driven by atmospheric controls (Figure 5-6) as there was sufficient water available at the surface due to bare ground conditions and ponding (Figure 5-1 C-E). Other post-disturbance peatlands have exhibited similar high(er) rates of ET immediately following disturbance when vegetation is scarce and near-surface water is available (Thomspon et al., 2014, Petrone et al., 2004). Moreover, at this time, ET was close to PET (Figure 5-2), and g_s values were higher and less sensitive to VPD (Figure 5-4) further signifying ample water availability and limited surface (i.e., plant-mediated) controls. In natural peatland settings, ET approaching or being equal to PET occurs when water is not limited and there are large proportions of open water (Petrone et al., 2007; Price, 1994). Moreover, previous work has highlighted that surface evaporation can contribute to a high proportion of ET in peatland settings due to wet surface conditions (Warren et al., 2018; Raddatz et al., 2009; Humphreys et al., 2006; Comer et al., 2000). Consequently, fen g_s is less sensitive to VPD particularly during early years with sparse vegetation and ample surface water supply to satisfy atmospheric demands. As fen vegetation became more widespread and robust, the proportion of bare ground and ponded, open-water areas significantly decreased (Figure 5-1C-E) resulting in less surface evaporation and increased plant transpiration. This is observed in the shift in seasonal ET trends from 2017 onwards, which closely follow plant dynamics. During this time, fen ET rates were largely controlled by plant-mediated responses to atmospheric forcing and changing hydroclimatic conditions. Furthermore, once vegetated, the relationship between g_s and VPD followed similar logarithmic trend and was comparable to other studies (Helbig et al., 2020b; Alekseychik et al., 2018; Peichl et al., 2013; Humphreys et

al., 2006) with a higher degree of sensitivity when surface-atmosphere conditions are strongly coupled (Novick et al., 2016). Thus, higher sensitivity of g_s to VPD in the fen in later years was likely controlled by the dominant vascular plant community through transpiration, particularly in response to changing conditions. Previous work has stated that the behaviour of g_s is linked to the type and amount of vascular vegetation (Worral et al., 2021; Peichl et al., 2013; Lafleur, 2008; Humpherys et al., 2006; Oren et al., 1999).

The effects of vegetation on surface-atmosphere exchanges were observed when comparing two dry years with similar hydroclimatic conditions but varying stages of plant development (2015 versus 2017, Figure 5-3). 2015 was the first season with widespread plant growth, however plant density was thinner (than later years) and a litter layer had not yet developed allowing for higher rates of surface evaporation from the inundated peat surface. By 2017, plant density had reached its maximum (Figure 5-1E) and a thick litter layer had developed (Table 5-3) due to the high amount of seasonal biomass produced by *C. aquatilis* and *T. latifolia,* resulting in less exposed peat, ultimately supressing surface losses. As a result, we see varying ET signals between the two years (Figure 5-3) with very similar atmospheric forcing - the 2015 signal was dominated by atmospheric controls driving high rates of surface evaporation similar to earlier years with high water availability compared to 2017, when ET was largely driven by stomatal controls in response to atmospheric conditions with limited surface losses. The influence of plant development is also captured when plot-scale ET fluxes are compared to those measured at the same plots initially following construction. We observed decreased ET compared to control (unvegetated) and seedling plots in 2014, when seasonal mean ET was 3.2 and 3.7 mm day^{-1}, respectively (Scarlett et al., 2017) compared to an interseasonal mean of less than 2.7 mm day^{-1} in this study at non-*T. latifolia* plots. Initially,

open water regions exhibited high rates of evaporation (4.4 mm day^{-1}; Scarlett et al., 2017), but by the time of this study these ponded regions have been overtaken by *T. latifolia,* resulting in a slight decrease (interseasonal mean of 3.6 mm day^{-1}). The decrease in ET from initial years to this current study is attributed to altered surface conditions, where the widespread expansion of vegetation, coupled with the formation of litter layer, created a barrier between surface and atmosphere exchanges, suppressing surface losses. Petrone et al. (2004) similarly found the addition of mulch at a restored peatland resulted in an 8-13% decrease in evaporative surface losses.

Notably, in the fen edaphic controls were limited likely due to a combination of the following features: relatively persistent wet conditions, vascular vegetation being less sensitive to near-surface edaphic fluctuations (due to well established rooting architecture) and the presence of dense vegetation cover and litter resulting in surface sheltering. Similar strong atmospheric and vegetative controls have been reported in natural (Volik et al., 2021; Phillips et al., 2016; Humphreys et al., 2006; Lafleur, 1990) and post-disturbance peatlands (Scarlett et al., 2017; Nicholls et al., 2016; McCarter et al., 2013; Petrone et al., 2004). Moreover, previous studies have examined the influence of WT position on ET dynamics in peatlands (Volik et al., 2021; Brown et al., 2017; Moore et al., 2013; Wu et al., 2010; Humphreys et al., 2006; Lafleur et al., 2005) and found that like this study, small variation in WTD near the surface is negligible for ET, and often not significant. However, WT drawdown past a (site-specific) critical depth can in turn affect ET fluxes.

ET fluxes during the drier 2017 season were likely more strongly plant (transpiration) driven than by surface losses as the extensive, well-developed rooting system was able to access deeper stores of soil moisture during dry periods of water table drawdown. While the

drier year (2017) exhibited slightly lower ET (mean 2.1 mm day^{-1}) compared to wetter years (3.3 and 2.8 mm day^{-1} in 2018 and 2019) throughout the study period, they are within the range of natural fens dominated by vascular vegetation (1.5 to 4.5 mm day^{-1}; Volik et al., 2021; Phillips et al., 2016; Humphreys et al., 2006; Busch 2000; Bridgham et al., 1999). Moreover, evidence of plant mediated controls can be observed through the decrease in g_s in 2017 (Figure 5-4), signifying greater surface – atmosphere coupling. A decrease in g_s representing regulation of plant mediated moisture exchanges is well documented (Runkle et al., 2013; Oren et al., 1999; Schulze et al., 1995). The decrease in g_s observed during the 2017 season coincided with WT drawdown, a coupled relationship, which has been described in several peatland studies, particularly those with continuous vascular plant coverage (Alekseychik et al., 2018; Peichl et al., 2013; Raddatz et al., 2009; Acreman et al., 2003).

The complexity of ecohydrological feedbacks is highlighted when examining ET and environmental controls between two wet years (2018 and 2019). As a key input of water to ecosystems, precipitation trends influence many ecohydrological processes and feedbacks. Fluctuations in the timing and/or intensity of events elicits a biophysical response (e.g., changes in plant growth and function, changes to infiltration capacity, etc.) and can lead to altered ecohydrological feedbacks (Knapp et al., 2008; Rodriquez-Iturbe, 2000). While both years exhibited similar total seasonal precipitation, the timing, intensity and frequency of events varied significantly (Figure 5-2, Table 5-2) resulting in variable ET response across species (Figure 5-5) and variable drivers between years (Figure 5-6). 2018 was warm and punctuated by a few large, intense events including close to 90 mm over a four-day period in July. Intense rainfall over such a short time span led to reduced infiltration capacity (of the already wet peat) and resulted in ponded conditions that persisted well into August at some

plots. Moreover, VPD was notably higher in 2018 (reaching up to 4.8 kPa, Chapter 2) and August was warm with limited rainfall inputs (Figure 5-2, Table 5-2). As a result, in 2018 there was sufficient water and incoming radiation to satisfy high evaporative demand and ET rates were higher across all species (Figure 5-5C- July). Notably, E_S was also higher due to inundation (see E_S outliers in Figure 5-5B – 2018) particularly at *J. balticus* plots. The higher ET rates in 2018 are attributable to the rapid biophysical response (i.e., inundated conditions) to intense rainfall, followed by ideal evaporative conditions, likely explaining the increased correlation between WTD and ET in 2018 (Figure 5-6) compared to other years. Contrastingly, in 2019 while there was ample water available, more frequent rain events and overcast conditions limited the incoming energy available for latent heat of vaporization to occur. In an examination of the site's energy balance (Chapter 3) a corresponding decrease in latent heat flux (Q_E) in 2019 compared to other years. As a result of both wet conditions and limited incoming radiation, ET trends were lower and similar across all species throughout the season. The above conditions resulted in less drying, both of the peat and at the leaf/litter surface resulting in a slight increase in E_S compared to other years. Moreover, frequent rainfall resulted in more atmospheric moisture (higher rH, less of an atmospheric moisture deficit) and ET was driven more by surface losses than transpiration as higher atmospheric moisture (paired with lower PAR conditions) resulted in less of a physiological (i.e., stomatal) response (Helbig et al., 2020; Oren et al., 1999).

Differences in ET rates between species are driven partially by abiotic conditions as well as plant physiology. For example, *T. latifolia* plots were inundated, with high water availability across all years and as a result had the highest rates of E_S in the fen (Figure 5-5B). As such, due to ample water availability, fluctuations in *T. latifolia* ET are primarily driven by

atmospheric controls (Figure 5-7). Similarly, Price (1994) found evaporation rates of *T. latifolia* were high (4.8 mm day^{-1}) and close to the rate of open water evaporation. Contrastingly, Goulden et al. (2007) observed lower E_S rates in a *T. latifolia* dominated marsh due to the presence of a thick litter layer coupled with cool water temperatures in ponded regions.

However, similar to this study, both Price (1994) and Goulden et al. (2007) highlight the strong atmospheric controls on *T. latifolia* ET. Moreover, the role of the litter layer as a means to supress surface evaporative losses was observed with *C. aquatilis* plots exhibiting the lowest rates of E_S even though these plots exhibit relatively stable, wet, near-surface edaphic conditions (Table 5-2). This is further supported by the limited edaphic controls at *C. aquatilis* plots compared to *J. balticus* plots (Figure 5-7). Greater edaphic controls at *J. balticus* plots are attributed to stronger coupling between atmospheric and edaphic conditions as a result of less sheltering due to the thinner litter layer and thinner plot density (resulting in higher E_S and ET (compared to *C. aquatilis*). In a review of northern peatland feedbacks, Waddington et. al (2015) highlighted plant-mediated shading as a critical component of peatland function and means to limit water losses. Moreover, plant mediated sheltering has been extensively trialed in peatland restoration practices, where straw mulch is commonly added as an amendment to the surface to limit evaporative losses and create a suitable microclimate for moss initiation (Xu et al, 2021; Rowland et al., 2021; Chimner et al., 2017; Petrone et al., 2004; Rochefort 2000; Price et al., 1998).

A physiological plant response to changing environmental conditions can be observed. Remarkably, in 2017 during dry conditions (July and August; Table 5-2) there was a steady increase in ET in *J. balticus* and *C. aquatilis* dominated plots (Figure 5-5C). This is partially

attributed to plant-mediated water use and access to deeper water stores, resulting in a reduced dependency on near-surface edaphic conditions, allowing for transpiration to continue even during times of periodic stress. In a recent review of evaporative function at 35 boreal peatland sites, Helbig et al. (2020) found ET rates increased during warmer conditions, particularly when VPD > 2 kPa, due to greater water availability (than boreal forested sites). Wu et al. (2010) and Flanagan and Syed (2011) also observed higher ET rates during drier conditions and concluded ET was more strongly driven by atmospheric controls and mediated by plant physiology than edaphic controls (such as WTD). Moreover, the increase in ET during dry and warm conditions with limited rainfall may be a physiological response to mediate leaf temperature, reduce leaf scorching and ensure CO_2 and H_2O exchanges continue. Vascular plants have been shown to increase transpiration (when water is available) during warmer and drier periods to cool leaf surfaces and limit leaf damage (Sadok et al.,2020; Ruiz-Pérez et al., 2019; Crawford et al., 2012; Gates, 1968). Furthermore, at a nearby saline, sedge-dominated fen, Phillips et al. (2016) found more salt tolerant species maintained higher ET rates despite having lower leaf area and water table levels during times of periodic water stress. This may partially explain the higher ET rates of *J. balticus* plots (a more salt and drought tolerant species than *C. aquatilis*) in July and August of 2017. Physiological controls as a response to drier conditions are further supported by the (initially unexpected) results of a negative relationship between edaphic variables and ET in 2017 (i.e., decrease in VWC increase in ET; Figure 5-6). These results coincide with other boreal peatland studies (Moore et al., 2013; Brümmer et al., 2012; Sonnentag et al., 2010; Humphreys et al., 2006; Lafleur 2005) which found strong physiological and atmospheric controls as well as a limited relationship between ET and edaphic conditions, particularly WT at sites dominated by vascular vegetation unless a critical, site-specific threshold was surpassed. The decrease in *T. latifolia* ET during drier

conditions (Figure 5-5C - 2017, *Typha*) indicates the species may have reached some threshold of stress and mediated it through stomatal closure. Moreover, by August 2017 most *T. latifolia* plots were no longer inundated (although WT remained near or at the surface) resulting in less (open water) surface evaporation, likely further contributing to the decrease in ET.

5.4.1.2 Upland

As observed in natural (Brown et al., 2014; Zha et al., 2010) and recovering (Merlin and Landhäuser, 2019; Strilesky et al., 2017; Petrone et al., 2015) boreal forests, ET fluxes in this study were largely driven by atmospheric controls and soil moisture availability (Figure 5-6). Similar to the fen, temporal landscape-scale ET trends were strongly driven by plant development in the reclaimed upland. Initially, during bare ground conditions ET rates consisted of surface losses driven by edaphic and atmospheric controls, particularly following rain events (Figure 5-3, i.e., periods of high ET from wetted previously dry soils following precipitation; Small et al., 2001; Eltahir, 1998). However, once dry, surface evaporation at this site was likely controlled by the ability of water to move upwards through the soil column through either capillary rise or vapour diffusion, (Aluwihare and Watanabe 2003; van de Griend and Owe, 1994). Thus, in the upland at this time surface evaporation during dry periods is interpreted to be driven by (warmer) soil temperatures coupled with the strong capillary barrier between the capping layer and underlying tailing sand that retained soil moisture within the top 50 cm (Chapter 2; Sutton and Price 2020b). Once vegetation became established (2016 onwards) there is a clear shift in ET trends, where ET began to follow seasonal plant phenology (lower rates during leaf out and senescence, highest during peak leaf area), rather than solely meteorological inputs, likely due to an increase in plant transpiration (and decrease in surface evaporative losses). Moreover, the development of vegetation resulted an increase in ET from

1.5 mm day^{-1} (interseasonal mean ET 2013 – 2015) to 3.2 mm day^{-1} (2017 onwards). Notably, ET rates from sparse understory plots in this study are comparable to early bare ground rates (1.8 mm day^{-1} versus 1.5 mm day^{-1}, respectively). Upland ET had stronger edaphic controls than the fen (Figure 5-6, 5-7) due to drier edaphic conditions, open canopy and the discontinuous, and at times sparse nature of the understory (see Figure 5-1), resulting in greater coupling between the surface and atmosphere and often a rapid edaphic response to changing meteorological conditions. A similar sensitivity to drier (edaphic) conditions and subsequent decrease in ET has been observed in other juvenile post-disturbance forests. This differs from mature forests where the understory and/or canopy are better established, providing some degree of sheltering and shading of the surface, dampening moisture loss and limiting edaphic controls (Hart and Chen, 2006). Petrone et al. (2015) examined two regenerating boreal aspen stands within the first five years post-harvest and found ET decreased due to lower water availability following drier conditions. Carey (2008) observed a comparable response between wet and dry years during the initial three years of reclamation with the wetter year exhibiting greater ET. Moreover, Amiro et al. (2006) describe local moisture limitations as a key driver of annual ET variability in recovering uplands. A similar response to drier conditions is observed in this study with drier year (2015 and 2017) exhibiting decreased ET.

Higher ET and E_S rates at chamber plots in the upland compared to the fen (Figure 5-5) were initially surprising, as the fen has much more available water near and at the surface. However, examination of edaphic and physiological controls provides some insight. While the fen was a wetter landscape, it had a thick litter layer, which coupled with widespread plant coverage provided a barrier that supressed surface water losses by reducing the coupling between the surface and atmosphere. As a result, ET fluxes were largely driven by physiological and

atmospheric controls. In contrast, the thin and sparse litter coverage and discontinuous patches of bare ground and understory of the upland provided little to no barrier between the surface and atmosphere, and when coupled with the high evaporative demand of the region resulted in higher surface evaporative losses when adequate soil water was available. Similar large surface losses have been observed during the early stages of development or recovery in boreal forested ecosystems due to exposed surface conditions and low LAI and canopy coverage (Petrone et al., 2015; Ewers et al., 2005). Moreover, trees typically have higher transpiration rates than grasses or sedges, thus accounting for the higher species ET rates (compared to the fen). Variability between upland ecosystem scale and chamber scale ET rates is likely due to the proportion of trees to bare-ground/understory within the tower footprint.

ET differences between species are driven by plant structure, morphology and physiology and the availability and use of water. Broadleaf species exhibited higher rates of ET than coniferous species Figure 5-5a), driven by higher transpiration rates due to stomatal size and abundance, and greater water requirements for plant function (Brown et al., 2014, Blanken et al., 1997). In an analysis of vertical water fluxes in the NFW upland, Fettah et al. (2022) found transpiration accounted for 52% of water loss from the system, 71% of which was from broadleaf species. Coniferous species had less ET variability compared to broadleaf species (Figure 5-5A-C), particularly during changing environmental conditions throughout the growing season (Figure 5-5C). This is attributed to coniferous species requiring less water for plant function, being better adapted to variable soil moisture conditions, and having consistent LAI throughout the season (no budding/senescence) (Stephenson et al., 1990; Arnup et al., 1988). This coincides with results from Zha et al. (2010) who similarly observed significantly less seasonal variability in ET between coniferous (7-9%) and deciduous (33%) stands

throughout the course of a growing season. Differences in ET rates within tree types (i.e. between *P. banksiana* and *P. mariana*) are attributed to differences in tree size (Table 5-3) with the larger, more mature species exhibiting higher rates. Notably, we observe some variation in ET response to changing environmental conditions between *P. balsamifera* and *P. tremuloides*, particularly during drier conditions (e.g., August 2018, May 2019). Differences in ET trends between the two broadleaf species can be attributed to variability in tree size and root development. *P. balsamifera* was the larger of the two species and had likely developed a more robust (lateral and/or vertical) rooting system, providing greater access to soil water stores as well as greater interception of incoming radiation (due to larger LAI). Presence of a more robust rooting architecture is supported by the limited relationship between soil moisture and *P. balsamifera* ET (Figure 5-7) as well as ET rates remaining high during periods of drier surface conditions (Figure 5-5C, August 2018). A similar divergence in ET trends between the two broadleaf species can be observed in May 2019 (Figure 5-5C), a drier period with limited rainfall (Table 5-2, Figure 5-2). Here, lower *P. tremuloides* ET rates were likely driven by greater sensitivity to drier conditions, particularly in the early growing season when LAI was smaller. Clonal, adventitious, near-surface root development has been shown to play a significant role in continued plant function through soil moisture redistribution during drier periods in the region (Petrone et al., 2015; Brown et al., 2014). Thus, high *P. balsamifera* ET rates during drier periods were driven by ample water availability (mediated through root function) and incoming radiation. *P. tremuloides* likely mediated water loss during drier periods through physiological (stomatal) controls, which is supported by the steeper decrease in ET during drier periods (e.g., Figure 5-5C August 2018). Contrastingly, in 2019, near-surface water availability was higher (due to more consistent rainfall inputs June - August) and ET of both species was controlled by atmospheric processes (i.e., limited by decreased

incoming radiation and less VPD) resulting in a similar ET rate. Under conditions with sufficient soil moisture availability, broadleaf species had similar responses to changing atmospheric conditions but observed varying sensitivity to drier conditions. Higher rates of E_S at broadleaf plots (particularly in 2019; Figure 5-5B) is interpreted to be driven by variable partitioning of rainfall between tree types (i.e., interception versus throughfall and soil infiltration). Due to differences between leaf and needle morphology and orientation, coniferous species typically exhibit great rainfall interception than broadleaf species due to increased surface area from needle clumping, resulting in less throughfall of water to the soil surface (Fettah et al., 2022; Levia et al., 2011; Barbier et al.,2009). Higher rates of E_S at broadleaf plots in 2019 is likely the result of greater throughfall reaching the soil surface, thus increasing near-surface soil moisture available for E_S. Atmospheric controls on understory plots were lower due to shading and sheltering by surrounding treed vegetation and differences in plant (above and belowground) physiology (i.e., root architecture, leaf shape and orientation). Coniferous species experienced stronger edaphic controls as well as a (non-significant) degree of Tsoil influence (Figure 5-7) linked to the thickness and composition of the litter layer (thinner litter layer resulted in less surface sheltering and a more rapid warming response).

5.4.2 Implications for AOSR reclamation and future work

As reclamation is still a relatively new endeavour in the region, results from this study provide critical insight to system design, functionality and evolution. Once plant communities became established, ET rates and responses to changing environmental conditions were similar to those at nearby natural fens and juvenile post-disturbance uplands (Volik et al., 2021a,b; Clark et al., 2022; Straker et al., 2019; Strilesky et al., 2017; Petrone et al., 2015, Carey 2008) providing

perspective to the ecohydrological functionality of constructed systems. In particular, this study evaluated ET dynamics of native boreal species in constructed landscapes, which can be applied to future planting prescriptions. Results signify the benefit of a diversified planting campaign to ensure ecosystem function under varying environmental conditions. The sensitivity of juvenile broadleaf species to drier conditions, may limit their applicability as an early successional species in reclamation projects in the region, particularly as an increase in water-stress is predicted for the future (Ireson et al., 2015). The development of adventitious lateral rooting systems improves their ability to withstand periodic moisture stress, which is critical to plant function in a region like the AOSR. However, as broadleaf species mature, they require greater water use/uptake and typically exhibit more water loss (via increased transpiration), thus the mechanism that ensures constructed forest productivity during drier periods (soil water redistribution via rooting architecture) may subsequently limit the water available for the down-gradient fen. As tree species require more time to become robust (5-15 years; Amiro et al., 2010), establishing suitable edaphic conditions during the juvenile phase is critical to ensure long-term tree functionality, evolution and survival in reclaimed settings. An examination of ET dynamics at Nikanotee, now that the site is >10 years old, would provide useful insight to some of the aforementioned questions, particularly now that the upland is more robust with most trees greater than 3 m tall. Furthermore, an assessment of rooting architecture of AOSR upland species would help better quantify water use and movement. Moreover, results here suggest the important physical role plant cover has on ecohydrological feedbacks pertaining to water exchanges. Ensuring the rapid establishment of plant cover will help supress water losses and aide in continued ecosystem development and function. Plants in both fen and upland landscapes were able to mediate water losses under varying environmental conditions. However, during this study we only observed one dry year once

vegetation was robustly established in both landscapes. While the systems appear to be able to withstand periodic (seasonal) hydrologic stress, it is unclear how ecohydrological feedbacks and ET dynamics may shift under prolonged drought conditions. Other future work includes pairing results from this study with species-specific CO_2 fluxes to assess water use efficiency of native boreal species in reclaimed landscapes.

5.5 Conclusions

ET dynamics at a reclaimed upland-fen watershed were examined during the initial seven years post-construction through the eddy covariance method paired with instantaneous chamber measurements of dominant species. Results highlight the important role of plant development during early ecosystem evolution as a means to regulate water exchanges between the surface and atmosphere through both the suppression of surface evaporative losses and stomatal controls. Environmental drivers of ET varied temporally during ecosystem development. Initially following construction, ET was driven by abiotic controls (atmospheric and edaphic conditions) where soil water availability was the limiting factor, particularly in the upland. Once fully vegetated, near-surface edaphic controls decreased, and ET fluxes were largely controlled via plant responses to atmospheric conditions. This study provides insight to future reclamation design and the importance of initial, post-construction conditions to aide in the development of constructed systems. Moreover, variability in species responses to changing environmental conditions underlines the importance of biodiversity in planting campaigns.

Chapter 6: Summary of ecohydrological function during ecosystem development

Individually, the chapters of this thesis examined surface-atmosphere exchanges of energy, water and carbon during the initial seven years of ecosystem development. The aim of this chapter is to amalgamate the results of each chapter and provide a brief, ecosystem-scale, graphical summary of abiotic and biotic interactions.

Figure 6-1 depicts the temporal evolution of key ecohydrological indicators measured during development from bare ground conditions to a flourishing, vegetated ecosystem. A summary of key trends observed during ecosystem evolution are:

A) The fen rapidly evolved from a bare, dark, wet surface to widespread vegetation by year 3 (2015).
B) Treed upland species developed at a slower rate compared to the fen and understory development was gradual. The upland evolved from bare-ground conditions to robust vegetation by year 5 (2017)
C) Dark, wet peat and ponded regions resulted in a lower albedo and greater absorption of incoming radiation affecting energy partition. This is in contrast to the upland, where light-coloured, dry, sandy cover soil resulted in a higher albedo and greater reflection of incoming radiation.
D) Once vegetation became widespread, the two landscapes exhibited similar albedos, and were within the range of naturally vegetated landscapes.
E) Energy partitioning was driven by surface conditions and water availability, resulting in greater latent heat flux in the fen and more sensible heat flux in the upland. During

bare ground conditions edaphic and atmospheric controls drove energy fluxes. Plant development altered biophysical surface properties resulting in a shift to strong biotic controls.

F) During the drier season (2017) fen Bowen Ratio was >1 due to decreased near surface moisture availability.

G) Coinciding with plant growth, fen evolved from a CO_2 source to a sink by year 3 (2015)

H) Due to its size, drier edaphic conditions and the ratio of trees to understory, by year 7 the upland was still a minor CO_2 source, but on trajectory to becoming a sink in the near future as tree growth ensues.

I) Initially, ample water availability and ponded surface conditions resulted in high surface evaporation rates in the fen. Upland evaporation rates were lower and controlled by limited water availability.

J) Once a plant community was well established, fen plant and litter cover supressed surface evaporative losses, and ET was dominated by transpiration. Similarly, ET rates increased in the upland due to tree transpiration.

K) Fen WUE remained stable from 2015 onwards despite variable hydrometerological conditions (wetter versus drier years) indicating plant-mediated controls on water use, via rooting architecture and stomatal response.

L) Upland WUE steadily increased as treed species matured.

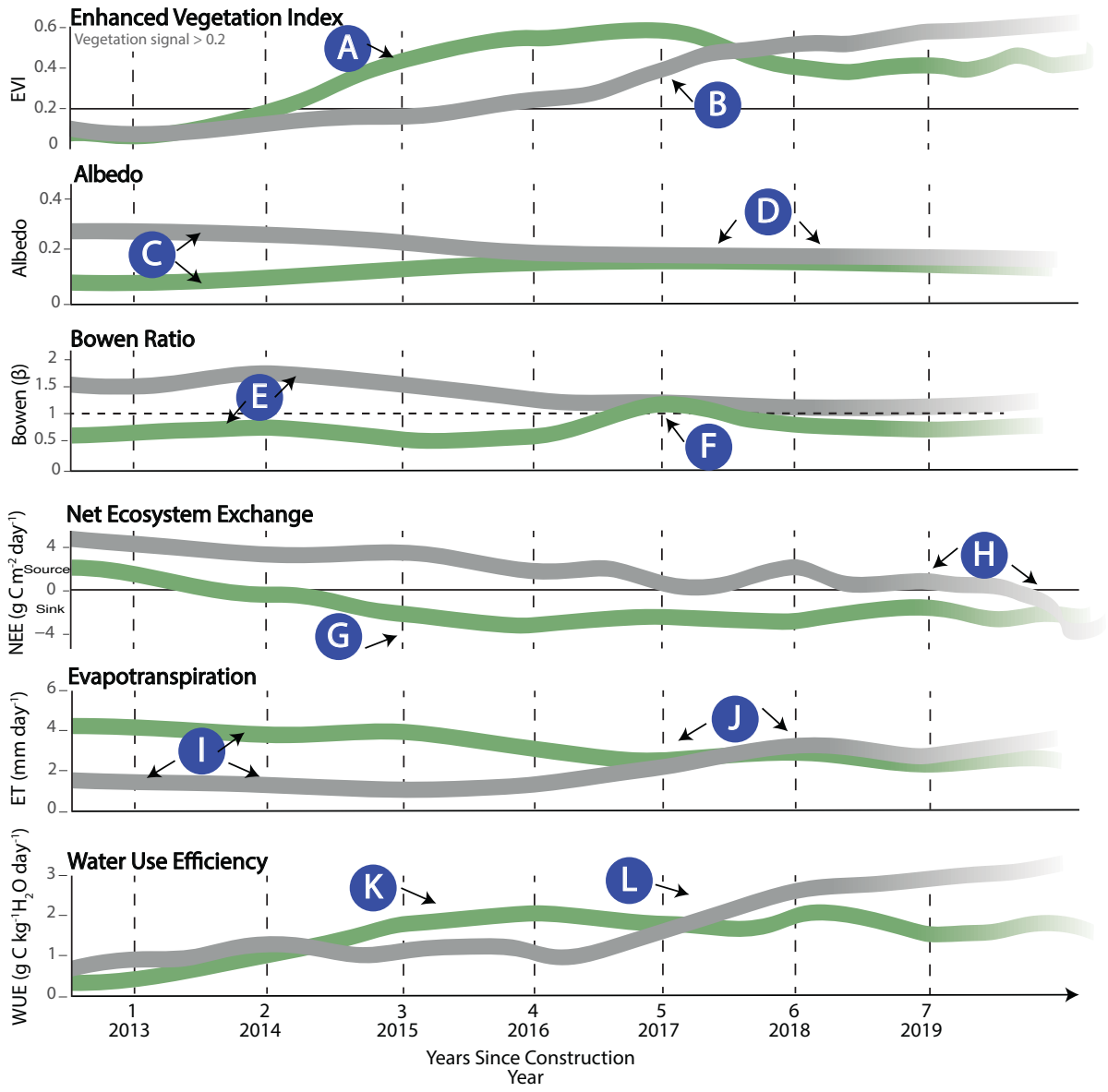


Figure 6-1: Graphical summary of temporal changes in key ecohydrological variables measured in this study in the fen (green) and upland (grey). Letters highlight key moments and are described in the text.

Figure 6-2 depicts both the intricacy of soil-plant-water-atmosphere interactions and the variability in these interactions between two contrasting phases of development (bare-ground

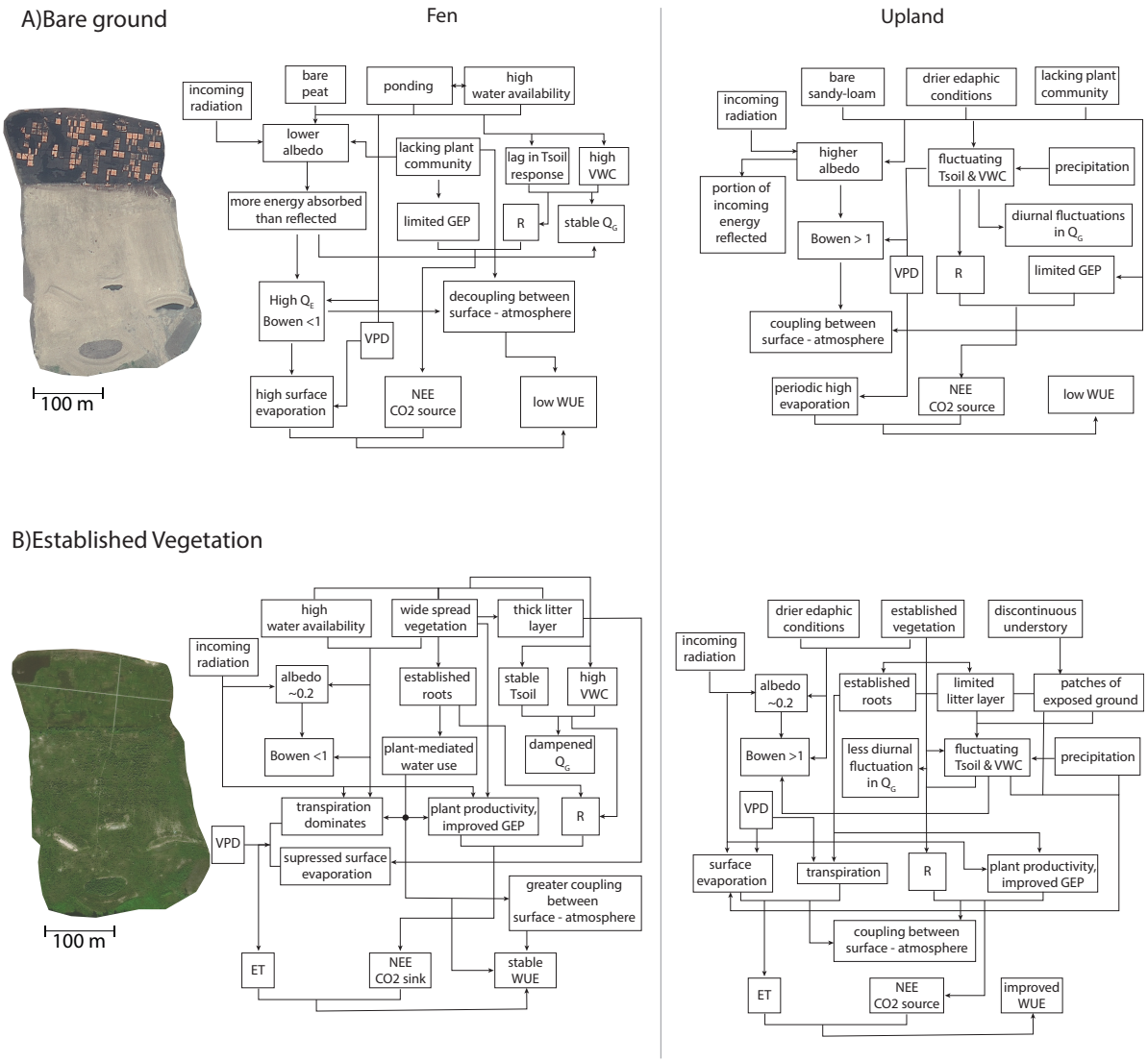


Figure 6-2: Conceptual diagram of ecohydrological interactions driving ET, CO_2 and WUE during two distinct phases of ecosystem development, A) bare ground and B) established vegetation.

and established vegetation) observed during this study. Initially, due to the lack of vegetation, abiotic factors controlled exchanges between the surface and atmosphere. Once vegetation became widespread, it became a key conduit for water and carbon exchanges but also modified biophysical surface characteristics, thus altering ecohydrological feedbacks. Many of the

feedbacks and processes discussed throughout this study are inherently controlled by the availability of water. Thus, establishing an adequate, self-sustaining hydrological regime is crucial to ensure ecosystem development and longevity. Figures 6-3 and 6-4 attempt to summarise the key drivers during ecosystem development and system trajectory. Ecosystem creation allows for some manual control of system trajectory as parent material, hydrology and planting campaigns are intentionally designed to mimic natural settings. However, climatic conditions during the initial few years can affect ecosystem development and potential trajectories. For example, how would fen development have differed if the intial three years were drier seasons? Would the rapid, widespread establishment of c. aquatilis still have occurred, or would an alternative plant community have emerged? How would this have affected the timing and rate of ecosystem processes (i.e., CO_2 sequstration). Thus, environmental conditions during system initiation ultimately dictate the early plant community and first phase of ecosystem development. The developing plant community and evolving soil conditions are interconnected to each other and are critical to both continued ecosystem evolution and current ecohydrological function. The trajectory and rate of evolution of these ecosystem components is driven by micrometerological influences. Moreover, the interaction and feedbacks between soil-plant-water processes coupled with the availability, use and movement of water between these three components is what drives ecosystem functionality. Changing environmental conditions (e.g., wet-dry years) results in interannual variability in CO_2 and H_2O dynamics. However, prolonged environmental forcings (e.g., multi-year drought) or a rapid change in conditions (changing hydrochemistry due to salinity influx from tailing sand) can result in a shift in the plant community and altered ecohydrological feedbacks. Understanding interactions and the variability in controls during different phases of ecosystem

evolution provides insight to ‘lessons learned’ during this pilot-scale endeavor and potential design aspects to consider in the future.

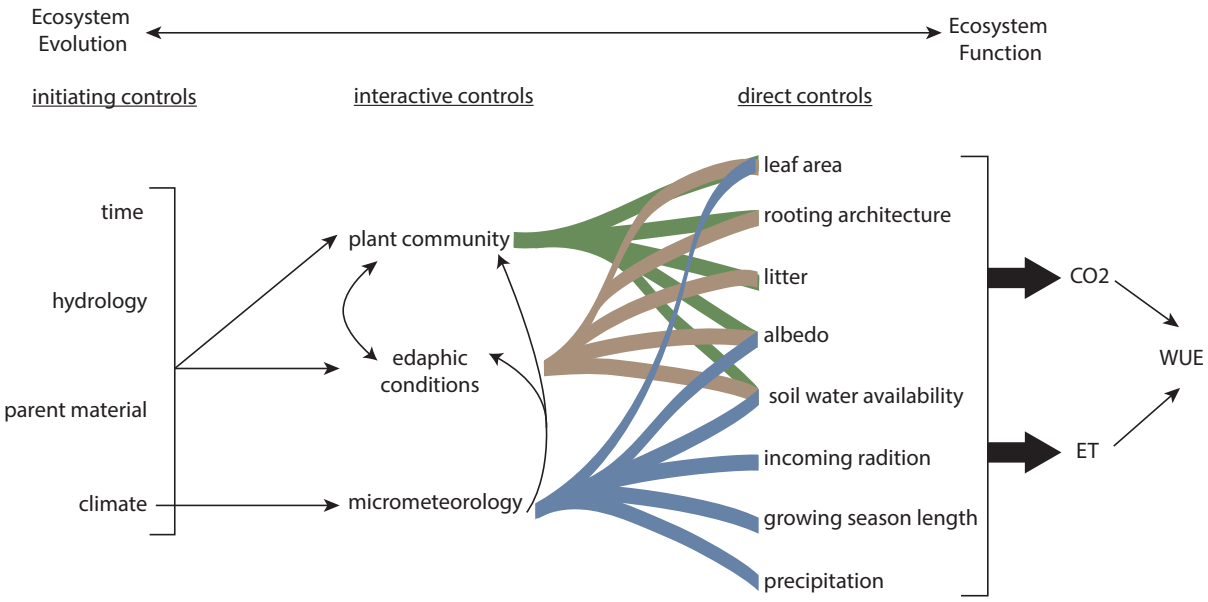


Figure 6-3: Conceptual diagram depicting the interaction of ecosystem components and key drivers of ecosystem evolution and function.

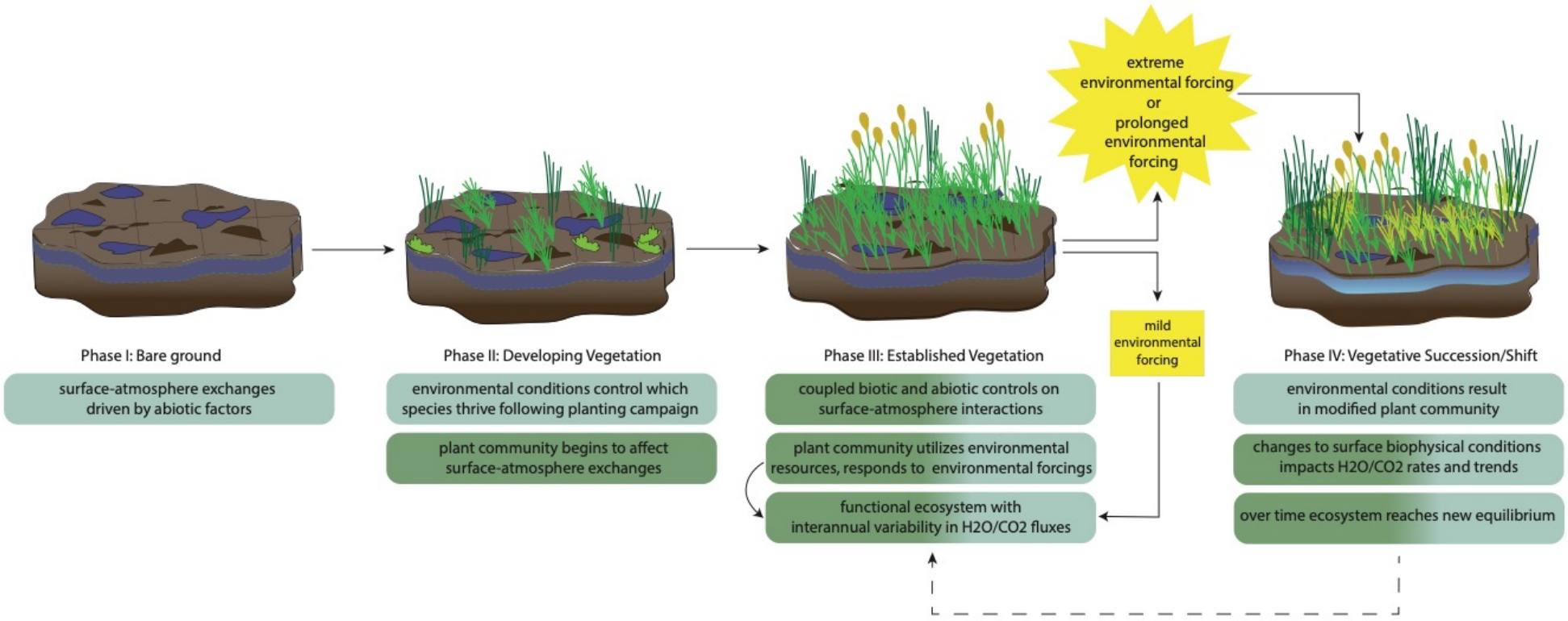


Figure 6-4: Summary of controls driving surface-atmosphere exchanges during the different phases of ecosystem evolution.

Chapter 7: Conclusions

The rationale for this work was driven by complementary motivations, both scientific curiosity (i.e., the functioning of novel, constructed ecosystems) and industry application (i.e., the pressing need for criteria to improve reclamation assessment and certification practices). To address these queries, this thesis set out to evaluate the performance of a novel, constructed watershed through a function-based, ecohydrological perspective. Here, key ecohydrological indicators, namely NEE, WUE and ET, were examined during the initial seven years post-construction. Given that fen reclamation is a relatively recent undertaking in the region, this study presents the longest record of surface-atmosphere exchanges at a reclaimed watershed consisting of multiple landscape units. Over the course of the study period, both the fen and upland exhibited significant biophysical evolution, from bare ground conditions to flourishing ecosystems. This transformation is reflected in surface-atmosphere exchanges of water, carbon and energy resources.

Remarkably, over the course of just seven years NFW appears to have achieved or be on trajectory to reaching many of the overarching targets set during conceptualization, namely the creation of functional, carbon-accumulating, self-sustaining ecosystems that are resilient to environmental stress. The fen quickly evolved from a growing-season carbon source to sink within the first 3 years following construction. The upland exhibited net carbon losses during the study period, however a marked improvement in sequestrations rates was observed with the growth and development of treed species, and the upland is expected to become a carbon sink in the near future. Once vegetation became robust, WUE remained relatively stable despite

hydroclimatic variability indicating a well-connected groundwater network between the two landscape units and the ability to self-regulate (and maintain plant function) during periods of moisture stress. Moreover, it is worth addressing the initial question posed at the outset of the NFW pilot project – whether fen reclamation in the AOSR is even possible? Results from this study echo that of the extensive research previously conducted at NFW, that yes, fen reclamation is indeed possible and can be successful.

While results from this study demonstrate that multi-landscape reclamation is possible, the examination and identification of key ecohydrological drivers and feedbacks during ecosystem development also highlighted potential considerations for future projects.

This research provides quantifiable evidence that supports the preliminary hypothesis assumed during NFW conceptualization, that establishing and maintaining a hydrologic regime in the moisture-limited setting of the AOSR would be the cornerstone of successful reclamation. In this study, we repeatedly observed the important role water availability played in ecohydrological dynamics and site performance. Thus, it is recommended that all future designs ensure hydrologic connectivity and ample water availability.

Throughout this study, we observed a significant shift in surface-atmosphere exchanges following plant establishment. In particular, upland performance (re: carbon and water dynamics) was impacted by the paucity of understory development. This contrasts with the fen where the rapid, widespread establishment of vegetation (and a thick litter layer) improved NEE (by limiting R) and supressed surface water losses. These results highlight the strong impact plant establishment has on ecohydrological function and feedbacks. Thus, amendments

to upland planting prescriptions, cover soil physical properties or the addition of woody debris is recommended to propagate positive feedbacks between plant-soil-atmospheric processes.

An assessment of community-scale carbon and water fluxes demonstrated the variability in species function under varying environmental conditions supporting the need for diverse planting campaigns. From a design perspective, limiting ponded regions immediately following construction is recommended to limit the invasion and expansion of invasive, unwanted species (e.g., *t. latifolia*). Moreover, due to the relatively stable, near surface water table position in the fen *c. aquatlis* has largely outcompeted other plant species and currently dominates the plant community. A homogenous plant community may hinder ecosystem resilience (and performance) during periods of environmental stress, especially if a species-specific threshold is reached. The addition of (micro)topography to fen design could help create more hydrologic variability, improving conditions for a wider range of species and producing a more diverse and ultimately resilient plant community.

Moreover, this study demonstrates the importance of measuring and monitoring ecohydrological indicators to assess reclamation success as relying solely on the presence of vegetation as a stand-alone metric of reclamation can overestimate system performance. This was observed in this study, where upland plants were at least partially established from years 3 to 7 yet the landscape exhibited limited CO_2 sequestration. Thus, it is recommended to assess ecosystem performance via ecohydrological indicators while using plant distribution and growth as ancillary, supporting evidence. This study also demonstrated the application of remote sensing techniques as a feasible, easily accessible method to capture spatial and temporal biophysical changes that should be incorporated into monitoring campaigns.

Given the decadal-nature of climate cycles of the region, at the time of this study NFW had yet to experience extended drought conditions. Thus, while the constructed system has shown resilience to periodic hydrologic stress it is currently unclear where its thresholds for continued functionality under prolonged moisture-limited conditions are. Understanding the tipping points of ecosystem function (and design) is pivotal to the long-term sustainability of these constructed systems, particularly as moisture deficits are anticipated to worsen under future climate scenarios. As such continued monitoring of ecohydrological indicators under variable hydroclimatic conditions is recommended.

This research is essentially a case-study of a singular constructed watershed. As such results reflect the bias of site-specific conditions such as distinct site location, consequences of construction and the specific hydroclimatological conditions during the study period. Thus, the timing of ecosystem evolution (re: plant growth), establishment and magnitude of key ecohydrological processes (e.g., CO_2 sequestration) and trajectory of future reclamation endeavours in the region may differ from those observed here, particularly if designs are adjusted or baseline environmental conditions differ. Despite limitations associated with the novel nature of this study, results presented here still provide valuable insights into surface-atmosphere interactions during ecosystem evolution that can help guide future reclamation efforts. Moreover, this research provides evidence of ecosystem performance comparable to that of surrounding natural, undisturbed landscapes further supporting the viability of successful, multi-landscape reclamation efforts in the region.

References

Abdul Halim, M., Chen, H. Y. H., & Thomas, S. C. (2019). Stand age and species composition effects on surface albedo in a mixedwood boreal forest. *Biogeosciences*, *16*(22), 4357–4375. https://doi.org/10.5194/BG-16-4357-2019

Acreman, M. C., Harding, R. J., Lloyd, C. R., & McNeil, D. D. (2003). Evaporation characteristics of wetlands: experience from a wetgrassland and a reedbed using eddy correlation measurements. *Hydrology and Earth System Sciences*, *7*(1), 11-21.

Admiral, S. W., & Lafleur, P. M. (2007). *Partitioning of latent heat flux at a northern peatland*. https://doi.org/10.1016/j.aquabot.2006.09.006

Adkinson, A. C., Syed, K. H., & Flanagan, L. B. (2011). Contrasting responses of growing season ecosystem CO2 exchange to variation in temperature and water table depth in two peatlands in northern Alberta, Canada. Journal of Geophysical Research: Biogeosciences, 116(1), 1004. https://doi.org/10.1029/2010JG001512

Adonsou, K. E., DesRochers, A., Tremblay, F., Thomas, B. R., & Isabel, N. (2016). The clonal root system of balsam poplar in upland sites of Quebec and Alberta. *Ecology and Evolution*, *6*(19). https://doi.org/10.1002/ece3.2441

Alberta Biodiversity Monitoring Institute (ABMI). 2017. Region overview. [Online.]Available fromhttp://abmi.ca/home/reports/2018/humanfootprint/details.html?id=16#urban_rural[accessed 21 June 2018]

Alberta Environment. 2008. Guideline for wetland establishment on reclaimed oil sands leases. 2nd ed. Prepared by M.L. Harris of Lorax Environmental for the Wetlands and Aquatics Subgroup of the Reclamation Working Group of the Cumulative Environmental Management Association, Fort McMurray, Alta.

Alberta Environment and Parks (AEP), and Environment and Climate Change Canada (ECCC). 2018. Oil Sands Monitoring Program. Annual Report for 2017–2018. [Online.]
Available from https://open.alberta.ca/dataset/dbe8811a-962e-4ce1-b2c2-ff40b8daad7a/resource/35be7d6d-083e-4d28-bf89-b92a7f3ab759/download/osm-annual-report-2017-2018-signed-by-aep-eccc.pdf [accessed 07 October 2019].

Alberta Environment and Parks (2020) Oil sands mine reclamation and disturbance tracking by year. In: osip.alberta.ca. http://osip.alberta.ca/library/Dataset/Details/27.

Alberta Environment and Parks (2020) Alberta Environment and Parks Oil Sands Mine Reclamation and Disturbance Tracking by Year http://osip.alberta.ca/library/Dataset/Details/27

Alberta Environment and Sustainable Resource Development, 2013. Criteria and Indicators Framework For Oil Sands Mine Reclamation Certification. Reclamation Working Group of the Cumulative Environmental Management Association. Alberta Environment and Sustainable Resource Development, Fort McMurray, AB. September 18, 2012

Alekseychik, P., Mammarella, I., Lindroth, A., Lohila, A., Aurela, M., Laurila, T., Kasurinen, V., Lund, M., Rinne, J., Nilsson, M. B., Peichl, M., Minkkinen, K., Shurpali, N. J., Tuittila, E. S., Martikainen, P. J., Tuovinen, J. P., & Vesala, T. (2018). Surface energy exchange in pristine and managed boreal peatlands. *Mires and Peat*, *21*, 1–26. https://doi.org/10.19189/MaP.2018.OMB.333

Allen, R. G., Pereira, L. S., Raes, D., & Smith, M. (1998). Crop evapotranspiration-Guidelines for computing crop water requirements-FAO Irrigation and drainage paper 56. *Fao, Rome*, *300*(9), D05109.

Allingham, S. M., Nwaishi, F. C., Andersen, R., Lamit, L. J., & Elliott, D. R. (2022). Microbial communities and biogeochemical functioning across peatlands in the Athabasca Oil Sands region of Canada: Implications for reclamation and management. *Land Degradation and Development*. https://doi.org/10.1002/ldr.4549

Allison, S. D., & Treseder, K. K. (2008). Warming and drying suppress microbial activity and carbon cycling in boreal forest soils. *Global Change Biology*, *14*(12). https://doi.org/10.1111/j.1365-2486.2008.01716.x

Aluwihare, S., & Watanabe, K. (2003). Measurement of evaporation on bare soil and estimating surface resistance. *Journal of Environmental Engineering*, *129*(12), 1157-1168.

Amiro, B. D., Barr, A. G., Barr, J. G., Black, T. A., Bracho, R., Brown, M., ... & Xiao, J. (2010). Ecosystem carbon dioxide fluxes after disturbance in forests of North America. Journal of Geophysical Research: Biogeosciences, 115(G4).

Amiro, B. D., Barr, A. G., Black, T. A., Iwashita, H., Kljun, N., McCaughey, J. H., … Saigusa, N. (2006a). Carbon, energy and water fluxes at mature and disturbed forest sites, Saskatchewan, Canada. Agricultural and Forest Meteorology, 136(3–4), 237–251. https://doi.org/10.1016/j.agrformet.2004.11.012

Amiro, B. D., Orchansky, A. L., Barr, A. G., Black, T. A., Chambers, S. D., Chapin, F. S., … Randerson, J. T. (2006b). The effect of post-fire stand age on the boreal forest energy balance. Agricultural and Forest Meteorology, 140(1–4), 41–50. https://doi.org/10.1016/j.agrformet.2006.02.014

Anderegg, W. R. L., Konings, A. G., Trugman, A. T., Yu, K., Bowling, D. R., Gabbitas, R., Karp, D. S., Pacala, S., Sperry, J. S., Sulman, B. N., & Zenes, N. (2018). Hydraulic diversity of forests regulates ecosystem resilience during drought. *Nature*, *561*(7724). https://doi.org/10.1038/s41586-018-0539-7

Arain, M. A., Black, T. A., Barr, A. G., Jarvis, P. G., Massheder, J. M., Verseghy, D. L., & Nesic, Z. (2002). Effects of seasonal and interannual climate variability on net ecosystem productivity of boreal deciduous and conifer forests. *Canadian Journal of Forest Research*, *32*(5). https://doi.org/10.1139/x01-228

Arias, P. A., Bellouin, N., Coppola, E., Jones, R. G., Krinner, G., Marotzke, J., ... & Zickfeld, K. (2021). Technical summary. *Climate change the physical science basis*, 33-144.

Arnup, R. W., Group, O. F. R, & Resources, O. M. of N. (1988). A silvicultural guide for the spruce working group in Ontario. Ontario Ministry of Natural Resources.

Asbjornsen, H., Goldsmith, G. R., Alvarado-Barrientos, M. S., Rebel, K., Van Osch, F. P., Rietkerk, M., Chen, J., Gotsch, S., Tobón, C., Geissert, D. R., Gómez-Tagle, A., Vache, K., & Dawson, T. E. (2011). Ecohydrological advances and applications in plant-water relations research: A review. In *Journal of Plant Ecology* (Vol. 4, Issues 1–2). https://doi.org/10.1093/jpe/rtr005

Aubinet, M., Vesala, T., & Papale, D. (2012). Eddy Covariance: A Practical Guide to Measurement and Data Analysis. Springer.

Aurela, M., Laurila, T., & Tuovinen, J. P. (2004). The timing of snow melt controls the annual CO2 balance in a subarctic fen. Geophysical Research Letters, 31(16). https://doi.org/10.1029/2004GL020315

Aurela, M., Lohila, A., Tuovinen, J. P., Hatakka, J., Riutta, T., & Laurila, T. (2009). Carbon dioxide exchange on a northern boreal fen. *Boreal Environment Research*, *14*(4).

Aurela, M., Riutta, T., Laurila, T., Tuovinen, J. P., Vesala, T., Tuittila, E. S., Rinne, J., Haapanala, S., & Laine, J. (2007). CO2 exchange of a sedge fen in southern Finland - The impact of a drought period. *Tellus, Series B: Chemical and Physical Meteorology*, *59*(5). https://doi.org/10.1111/j.1600-0889.2007.00309.x

Balandier, P., Gobin, R., Prévosto, B., & Korboulewsky, N. (2022). The contribution of understorey vegetation to ecosystem evapotranspiration in boreal and temperate forests: a literature review and analysis. In *European Journal of Forest Research* (Vol. 141, Issue 6). https://doi.org/10.1007/s10342-022-01505-0

Baldocchi, D. D., & Vogel, C. A. (1996). Energy and CO2 flux densities above and below a temperate broad-leaved forest and a boreal pine forest. *Tree Physiology*, *16*(1–2). https://doi.org/10.1093/treephys/16.1-2.5

Baldocchi, D. D., Vogel, C. A., & Hall, B. (1997). Seasonal variation of carbon dioxide exchange rates above and below a boreal jack pine forest. *Agricultural and Forest Meteorology*, *83*(1–2). https://doi.org/10.1016/S0168-1923(96)02335-0

Baldocchi, D., Chu, H., & Reichstein, M. (2018). Inter-annual variability of net and gross ecosystem carbon fluxes: A review. Agricultural and Forest Meteorology, 249, 520–533. https://doi.org/10.1016/j.agrformet.2017.05.015

Barbier, S., Balandier, P., & Gosselin, F. (2009). Influence of several tree traits on rainfall partitioning in temperate and boreal forests: A review. *Annals of Forest Science*, *66*(6). https://doi.org/10.1051/forest/2009041

Barr, A. G., Betts, A. K., Black, T. A., McCaughey, J. H., & Smith, C. D. (2001). Intercomparison of BOREAS northern and southern study area surface fluxes in 1994. In *Journal of Geophysical Research Atmospheres* (Vol. 106, Issue D24). https://doi.org/10.1029/2001JD900070

Barr, A. G., Black, T. A., Hogg, E. H., Kljun, N., Morgenstern, K., & Nesic, Z. (2004). Inter-annual variability in the leaf area index of a boreal aspen-hazelnut forest in relation to net ecosystem production. *Agricultural and Forest Meteorology*, *126*(3–4), 237–255. https://doi.org/10.1029/2002JD003011

Barr, A. G., Black, T. A., Hogg, E. H., Griffis, T. J., Morgenstern, K., Kljun, N., ... & Nesic, Z. (2007). Climatic controls on the carbon and water balances of a boreal aspen forest, 1994–2003. Global Change Biology, 13(3), 561-576.

Bazzaz, F. A. (1979). *THE PHYSIOLOGICAL ECOLOGY OF PLANT SUCCESSION*. www.annualreviews.org

Beamesderfer, E. R., Buechner, C., Faiola, C., Helbig, M., Sanchez-Mejia, Z. M., Yáñez-Serrano, A. M., Zhang, Y., & Richardson, A. D. (2022). Advancing Cross-Disciplinary Understanding of Land-Atmosphere Interactions. Journal of Geophysical Research: Biogeosciences, 127(2), e2021JG006707. https://doi.org/10.1029/2021JG006707

Beckingham, J. D., & Archibald, J. H. (1996). Field guide to ecosites of Northern Alberta (paperback, coil bound) (Vol. 5).

Ben-Ze'ev, E., Karnieli, A., Agam, N., Kaufman, Y., & Holben, B. (2006). Assessing vegetation condition in the presence of biomass burning smoke by applying the Aerosol-free Vegetation Index (AFRI) on MODIS images. International Journal of Remote Sensing, 27(15), 3203-3221.

Berry, J., & Bjorkman, O. (1980). Photosynthetic Response and Adaptation to Temperature in Higher Plants. *Annual Review of Plant Physiology*, *31*(1).

Betts, A. K., & Ball, J. H. (1997). Albedo over the boreal forest. Journal of Geophysical Research Atmospheres, 102(24), 28901–28909. https://doi.org/10.1029/96JD03876

Biagi, Kelly M., Clark, M. G., & Carey, S. K. (2021). Hydrological functioning of a constructed peatland watershed in the Athabasca oil sands region: Potential trajectories and lessons learned. Ecological Engineering, 166. https://doi.org/10.1016/j.ecoleng.2021.106236

Biagi, K. M., Oswald, C. J., Nicholls, E. M., & Carey, S. K. (2019). Increases in salinity following a shift in hydrologic regime in a constructed wetland watershed in a post-mining oil sands landscape. Science of the Total Environment, 653, 1445–1457. https://doi.org/10.1016/j.scitotenv.2018.10.341

Blanken, P. D., Black, T. A., Yang, • P C, Neumann, H. H., Nesic, Z., Staebler, • R, den Hartog, G., Novak, M. D., & Lee, X. (1997). Energy balance and canopy conductance of a boreal aspen forest: Partitioning overstory and understory components. JOURNAL OF GEOPHYSICAL RESEARCH, 102(D24), 915–943. https://doi.org/10.1029/97JD00193

Blodau, C. (2002). Carbon cycling in peatlands — A review of processes and controls. Environmental Reviews, 10(2), 111–134. https://doi.org/10.1139/a02-004

Bonan, G. B. (1993). Importance of leaf area index and forest type when estimating photosynthesis in boreal forests. Remote Sensing of Environment, 43(3). https://doi.org/10.1016/0034-4257(93)90072-6

Bonan, G. B. (2008). Forests and Climate Change: Forcings, Feedbacks, and the Climate Benefits of Forests. New Series, 320(5882), 1444–1449.

Bonan G.B. (2019). Ecological Climatology: Concepts and Applications. 3rd edition. Cambridge University Press

Borkenhagen, A. K., & Cooper, D. J. (2019). Establishing vegetation on a constructed fen in a post-mined landscape in Alberta's oil sands region: A four-year evaluation after species introduction. Ecological Engineering, 130, 11–22. https://doi.org/10.1016/J.ECOLENG.2019.01.023

Bothe RA, Abraham C. 1993. Evaporation and evapotranspiration in Alberta, 1986– 1992 Addendum. Water Resources Services, Alberta Environmental Protection: Edmonton, Canada.

Bridgham, S. D., Pastor, J., Updegraff, K., Malterer, T. J., Johnson, K., Harth, C., & Chen, J. (1999). Ecosystem control over temperature and energy flux in northern peatlands. *Ecological Applications*, *9*(4), 1345–1358. Britton, C. M., and J. D. Dodd. *Relationships of photosynthetically active radiation and shortwave irradiance.* Agricultural Meteorology 17, no. 1 (1976): 1-7.

Bronson, D. R., Gower, S. T., Tanner, Mm., Linder, S., & Van Herk, I. (2008). Response of soil surface CO2 flux in a boreal forest to ecosystem warming. *Global Change Biology*, *14*(4). https://doi.org/10.1111/j.1365-2486.2007.01508.x

Brown, R. L., & Naeth, M. A. (2014). Woody debris amendment enhances reclamation after oil sands mining in Alberta, Canada. *Restoration Ecology*, *22*(1). https://doi.org/10.1111/rec.12029

Brown, S. M., Petrone, R. M., Chasmer, L., Mendoza, C., Lazerjan, M. S., Landhäusser, S. M., … Devito, K. J. (2014). Atmospheric and soil moisture controls on evapotranspiration from above and within a Western Boreal Plain aspen forest. Hydrological Processes, 28(15), 4449–4462. https://doi.org/10.1002/hyp.9879

Brown, S. M., Petrone, R. M., Mendoza, C., & Devito, K. J. (2010). Surface vegetation controls on evapotranspiration from a sub-humid Western Boreal Plain wetland. Process, 24, 1072–1085. https://doi.org/10.1002/hyp.7569

Brümmer, C., Black, T. A., Jassal, R. S., Grant, N. J., Spittlehouse, D. L., Chen, B., … Wofsy, S. C. (2012). How climate and vegetation type influence evapotranspiration and water use efficiency in Canadian forest, peatland and grassland ecosystems. Agricultural and Forest Meteorology. https://doi.org/10.1016/j.agrformet.2011.04.008

Bubier, J. L., Bhatia, G., Moore, T. R., Roulet, N. T., & Lafleur, P. M. (2003). Spatial and Temporal Variability in Growing-Season Net Ecosystem Carbon Dioxide Exchange at a Large Peatland in Ontario, Canada. Ecosystems, 6(4), 353–367. https://doi.org/10.1007/s10021-003-0125-0

Bubier, J. L., Crill, P. M., Moore, T. R., Savage, K., & Varner, R. K. (1998). Seasonal patterns and controls on net ecosystem CO2 exchange in a boreal peatland complex. Global Biogeochemical Cycles, 12(4), 703–714. https://doi.org/10.1029/98GB02426

Burba, G., Schmidt, A., Scott, R.L., Nakai, T., Kathilankal, J., Fratini, G., Hanson, C., Law, B., McDermitt, D.K., Eckles, R., Furtaw, M., & Velgersdyk, M. (2012). Calculating CO2 and H2O eddy covariance fluxes from an enclosed gas analyzer using an instantaneous mixing ratio. Global Change Biology, 18, 385-399

Busch, J. (2000). Canopy transpiration rates in eutrophic wetlands dominated by sedges (Carex spp.) differ in a species specific way. *Physics and Chemistry of the Earth, Part B:*

Hydrology, Oceans and Atmosphere, *25*(7–8). https://doi.org/10.1016/s1464-1909(00)00072-1

Cai, T., Flanagan, L. B., & Syed, K. H. (2010). Warmer and drier conditions stimulate respiration more than photosynthesis in a boreal peatland ecosystem: Analysis of automatic chambers and eddy covariance measurementsp ce_2089 394..407. https://doi.org/10.1111/j.1365-3040.2009.02089.x

Cao, J.-S., Li, W., Deng, Z.-Y., & Hu, Y.-D. (n.d.). *Remote sensing inversion and spatial variation of land surface temperature over mining areas of Jixi, Heilongjiang, China*. https://doi.org/10.7717/peerj.10257

Carey, S. K. (2008). Growing season energy and water exchange from an oil sands overburden reclamation soil cover, Fort McMurray, Alberta, Canada. *Hydrological Processes*, *22*(15), 2847–2857. https://doi.org/10.1002/hyp.7026

Caylor, K. K., D'Odorico, P., & Rodriguez-Iturbe, I. (2006). On the ecohydrology of structurally heterogeneous semiarid landscapes. *Water Resources Research*, *42*(7), 1–13. https://doi.org/10.1029/2005WR004683

Cellier, P., Richard, G., & Robin, P. (1996). Partition of sensible heat fluxes into bare soil and the atmosphere. *Agricultural and forest meteorology*, *82*(1-4), 245-265.

Chambers, S. D., & Chapin III, F. S. (2002). Fire effects on surface-atmosphere energy exchange in Alaskan black spruce ecosystems: Implications for feedbacks to regional climate. Journal of Geophysical Research: Atmospheres, 107(D1), FFR-1.

Chambers, S. D., Beringer, J., Randerson, J. T., & Chapin III, F. S. (2005). Fire effects on net radiation and energy partitioning: Contrasting responses of tundra and boreal forest ecosystems. Journal of Geophysical Research: Atmospheres, 110(D9).

Charman, D. J., Beilman, D. W., Blaauw, M., Booth, R. K., Brewer, S., Chambers, F. M., … Earth, L.-D. (2013). Climate-related changes in peatland carbon accumulation during the last millennium. Biogeosciences, 10, 929–944. https://doi.org/10.5194/bg-10-929-2013

Chasmer, L., Mahoney, C., Millard, K., Nelson, K., Peters, D., Merchant, M., ... & Cobbaert, D. (2020). Remote sensing of boreal wetlands 2: methods for evaluating boreal wetland ecosystem state and drivers of change. Remote Sensing, 12(8), 1321.

Chasmer, L. E., Devito, K. J., Hopkinson, C. D., & Petrone, R. M. (2018). Remote sensing of ecosystem trajectories as a proxy indicator for watershed water balance. Ecohydrology, 11(7), 1–16. https://doi.org/10.1002/eco.1987

Chee, W.-L., & Vitt, D. H. (1989). The vegetation, surface water chemistry and peat chemistry of moderate-rich fens in central Alberta, Canada. Wetlands, 9(2), 227–261. https://doi.org/10.1007/BF03160747

Chen, J. M., & Cihlar, J. (1996). Retrieving leaf area index of boreal conifer forests using Landsat TM images. Remote sensing of Environment, 55(2), 153-162.

Chen, J.M., Rich, P.M., Gower, S.T., Norman, J.M., & Plummer, S. (1997). Leaf area index of boreal forest: Theory, techniques, and measurements. Journal of Geophysical Research. 102:24, P.29429-29443.

Chi, J., Zhao, P., Klosterhalfen, A., Jocher, G., Kljun, N., Nilsson, M. B., & Peichl, M. (2021). Forest floor fluxes drive differences in the carbon balance of contrasting boreal forest stands. *Agricultural and Forest Meteorology*, *306*. https://doi.org/10.1016/j.agrformet.2021.108454

Chimner, R. A., Cooper, D. J., Wurster, F. C., & Rochefort, L. (2017). An overview of peatland restoration in North America: where are we after 25 years?. Restoration Ecology, 25(2), 283-292.

Chimner, R. A., Pypker, T. G., Hribljan, J. A., Moore, P. A., & Waddington, J. M. (2017). Multi-decadal Changes in Water Table Levels Alter Peatland Carbon Cycling. *Ecosystems*, *20*(5). https://doi.org/10.1007/s10021-016-0092-x

Chivers, M. R., Turetsky, M. R., Waddington, J. M., Harden, J. W., & McGuire, A. D. (2009). Effects of experimental water table and temperature manipulations on ecosystem CO2 fluxes in an Alaskan rich fen. *Ecosystems*, *12*(8), 1329–1342.

Clark, M. G. (2018). The initial biometerology of the constructed Sandhill Fen Watershed in Alberta, Canada. Retrieved from https://curve.carleton.ca/system/files/etd/7f6817f3-18cb-4552-93d3-5e5c447495b3/etd_pdf/25807fea42ddb6705e977037a129f980/clark-theinitialbiometerologyoftheconstructedsandhill.pdf

Clark, M. G., Humphreys, E., & Carey, S. K. (2019). The initial three years of carbon dioxide exchange between the atmosphere and a reclaimed oil sand wetland. *Ecological Engineering*, *135*, 116–126. https://doi.org/10.1016/j.ecoleng.2019.05.016

Clark, M. G., Petrone, R. M., & Carey, S. K. (2022). Upland reclamation promotes forest evaporative losses in the Boreal Plains of Canada: A comparison of carbon and water fluxes. *Agricultural and Forest Meteorology*, *325*, 109127. https://doi.org/10.1016/J.AGRFORMET.2022.109127

Cooper, P. J. M., Gregory, P. J., Keatinge, J. D. H., & Brown, S. C. (1987). Effects of fertilizer, variety and location on barley production under rainfed conditions in Northern Syria 2. Soil water dynamics and crop water use. *Field Crops Research*, *16*(1). https://doi.org/10.1016/0378-4290(87)90054-2

Congedo, L. (2021). Semi-Automatic Classification Plugin: A Python tool for the download and processing of remote sensing images in QGIS. *Journal of Open Source Software*, *6*(64), 3172.

Coursolle, C., Margolis, H. A., Giasson, M. A., Bernier, P. Y., Amiro, B. D., Arain, M. A., Barr, A. G., Black, T. A., Goulden, M. L., McCaughey, J. H., Chen, J. M., Dunn, A. L., Grant, R. F., & Lafleur, P. M. (2012). Influence of stand age on the magnitude and seasonality of carbon fluxes in Canadian forests. *Agricultural and Forest Meteorology*, *165*.

Crawford, A. J., McLachlan, D. H., Hetherington, A. M., & Franklin, K. A. (2012). High temperature exposure increases plant cooling capacity. In *Current Biology* (Vol. 22, Issue 10). https://doi.org/10.1016/j.cub.2012.03.044

Czimczik, C. I., Trumbore, S. E., Carbone, M. S., & Winston, G. C. (2006). Changing sources of soil respiration with time since fire in a boreal forest. Global Change Biology, 12(6), 957–971. https://doi.org/10.1111/j.1365-2486.2006.01107.x

Daly, C., Price, J.S., Rezanezhad, F., Pouliot, R., Rochefort, L. & Graf, M. (2012) Initiatives in oil sand reclamation: considerations for building a fen peatland in a post-mined oil sands landscape. Restoration and Reclamation of Boreal Ecosystems: Attaining Sustainable Development (eds D.H. Vitt & J. Bhatti), pp. 179–201. Cambridge University Press, Cambridge

Dang, Q. L., Margolis, H. A., Sy, M., Coyea, M. R., Collatz, G. J., & Walthall, C. L. (1997). Profiles of photosynthetically active radiation, nitrogen and photosynthetic capacity in the boreal forest: Implications for scaling from leaf to canopy. *Journal of Geophysical Research Atmospheres*, *102*(24). https://doi.org/10.1029/97jd00194

Davidson, S. J., Goud, E. M., Malhotra, A., Estey, C. O., Korsah, P., & Strack, M. (2021). Linear disturbances shift boreal peatland plant communities toward earlier peak greenness. https://doi.org/10.1002/essoar.10506838.1

Davidson, S. J., Smith, M., Prystupa, E., Murray, K., Nwaishi, F. C., Petrone, R. M., & Strack, M. (2021). High sulfate concentrations maintain low methane emissions at a constructed fen over the first seven years of ecosystem development. Science of the Total Environment, 789, 148014. https://doi.org/10.1016/j.scitotenv.2021.148014

Devaraju, N., Bala, G., & Nemani, R. (2015). Modelling the influence of land-use changes on biophysical and biochemical interactions at regional and global scales. *Plant, Cell & Environment*, *38*(9), 1931–1946. https://doi.org/10.1111/PCE.12488

Devito, K. J., Creed, I. F., & Fraser, C. J. D. (2005). Controls on runoff from a partially harvested aspen-forested headwater catchment, Boreal Plain, Canada. *Hydrological Processes*, *19*(1). https://doi.org/10.1002/hyp.5776

Devito, K. J., Hokanson, K. J., Moore, P. A., Kettridge, N., Anderson, A. E., Chasmer, L., … Waddington, J. M. (2017). Landscape controls on long-term runoff in subhumid heterogeneous Boreal Plains catchments. Hydrological Processes, 31(15), 2737–2751. https://doi.org/10.1002/hyp.11213

Devito, K., Mendoza, C., & Qualizza, C. (2012). Conceptualizing water movement in the Boreal Plains. Implications for watershed reconstruction. Influence of Climate and geology on water and chemistry movement in the Boreal Plain View project. https://doi.org/10.7939/R32J4H

Dhar, A., Comeau, P. G., Karst, J., Pinno, B. D., Chang, S. X., Naeth, A. M., … Bampfylde, C. (2018). Plant community development following reclamation of oil sands mine sites in the boreal forest: A review. Environmental Reviews. https://doi.org/10.1139/er-2017-0091

Dhar, A., Forsch, K. B. C., & Naeth, M. A. (2022). Effects of Coarse Woody Debris on Soil Temperature and Water Content in Two Reconstructed Soils in Reclaimed Boreal Forest. *Soil Systems*, *6*(3). https://doi.org/10.3390/soilsystems6030062

Dieleman, C. M., Branfireun, B. A., Mclaughlin, J. W., & Lindo, Z. (2015). Climate change drives a shift in peatland ecosystem plant community: Implications for ecosystem function and stability. Global Change Biology, 21(1), 388–395. https://doi.org/10.1111/gcb.12643

Dietrich, S. T., & MacKenzie, M. D. (2018). Comparing spatial heterogeneity of bioavailable nutrients and soil respiration in boreal sites recovering from natural and anthropogenic disturbance. Frontiers in Environmental Science, 6, 126.

D'Odorico, P., Laio, F., Porporato, A., Ridolfi, L., Rinaldo, A., & Rodriguez-Iturbe, I. (2010). Ecohydrology of terrestrial ecosystems. *BioScience*, *60*(11). https://doi.org/10.1525/bio.2010.60.11.6

Elmes, M. C., & Price, J. S. (2019). Hydrologic function of a moderate-rich fen watershed in the Athabasca Oil Sands Region of the Western Boreal Plain, northern Alberta. Journal of Hydrology, 570, 692-704.

Elshorbagy, A., Jutla, A., Barbour, L., Kells, J., Elshorbagy, A., Jutla, A., … Kells, J. (2005). System dynamics approach to assess the sustainability of reclamation of disturbed watersheds 1, 32, 144–158. https://doi.org/10.1139/L04-112

Environment Canada. (2015). Canadian Climate Normals 1981-2010 Station Data

http://climate.weather.gc.ca/climate_normals/results_1981_2010_e.html?stnID=2519&autofwd=1 (accessed 2.10.19).

Eltahir, E. A. B. (1998). A Soil Moisture–Rainfall Feedback Mechanism: 1. Theory and observations. *WATER RESOURCES RESEARCH*, *34*(4), 765–776. https://doi.org/10.1029/97WR03499

Environment and Sustainable Resource Development (ESRD) (2015) Alberta Wetland classification system. Water Policy Branch, Policy and Planning Division, Edmonton, AB

Eppinga, M. B., Max, A. E., Ae, R., Ae, M. J. W., De Ruiter, P. C., Eppinga, M. B., … De Ruiter, P. C. (2009). Linking habitat modification to catastrophic shifts and vegetation patterns in bogs. Plant Ecol, 200, 53–68. https://doi.org/10.1007/s11258-007-9309-6

Eugster, W., Rouse, W. R., Pielke Sr, R. A., Mcfadden, J. P., Baldocchi, D. D., Kittel, T. G. F., ... & Chambers, S. (2000). Land–atmosphere energy exchange in Arctic tundra and boreal forest: available data and feedbacks to climate. *Global change biology*, *6*(S1), 84-115.

Ewers, B. E., Gower, S. T., Bond-Lamberty, B., & Wang, C. K. (2005). Effects of stand age and tree species on canopy transpiration and average stomatal conductance of boreal forests. *Plant, Cell and Environment*, *28*(5). https://doi.org/10.1111/j.1365-3040.2005.01312.x

Facelli, J. M., & Pickett, S. T. A. (1991a). Plant litter: Its dynamics and effects on plant community structure. *The Botanical Review*, *57*(1). https://doi.org/10.1007/BF02858763

Facelli, J. M., & Pickett, S. T. A. (1991b). Plant litter: light interception and effects on an old-field plant community. *Ecology*, *72*(3). https://doi.org/10.2307/1940602

Falge, E., Baldocchi, D., Tenhunen, J., Aubinet, M., Bakwin, P., Berbigier, P., … Wofsy, S. (2002). Seasonality of ecosystem respiration and gross primary production as derived from FLUXNET measurements. Agricultural and Forest Meteorology, 113(1–4), 53–74. https://doi.org/10.1016/S0168-1923(02)00102-8

Fettah, S. (2020). Quantifying water use and rainfall partitioning of dominant tree species in a post-mined landscape in the Athabasca Oil Sands Region, Alberta. UWSpace. http://hdl.handle.net/10012/16523

Fettah, S., Petrone, R. M., Elmes, M. C., & Price, J. S. (2022). Quantifying the vertical water exchange of dominant tree species in a reclaimed landscape in the Athabasca oil sands region, Alberta. *Ecohydrology*, e2476. https://doi.org/10.1002/ECO.2476

Ficken, C. D., Cobbaert, D., & Rooney, R. C. (2019). Low extent but high impact of human land use on wetland flora across the boreal oil sands region. *Science of the Total Environment*, *693*, 133647.

Firozjaei, M. K., Sedighi, A., Firozjaei, H. K., Kiavarz, M., Homaee, M., Arsanjani, J. J., Makki, M., Naimi, B., & Alavipanah, S. K. (2021). A historical and future impact assessment of mining activities on surface biophysical characteristics change: A remote sensing-based approach. *Ecological Indicators*, *122*. https://doi.org/10.1016/J.ECOLIND.2020.107264

Flanagan, L. B., & Syed, K. H. (2011). Stimulation of both photosynthesis and respiration in response to warmer and drier conditions in a boreal peatland ecosystem. *Global Change Biology*, *17*(7). https://doi.org/10.1111/j.1365-2486.2010.02378.x

Foken, T., & Leclerc, M. Y. (2004). Methods and limitations in validation of footprint models. Agricultural and Forest Meteorology, 127(3-4), 223-234.

Frolking, S. E., Bubier, J. L., Moore, T. R., Ball, T., Bellisario, L. M., Bhardwaj, A., Carroll, P., Crill, P. M., Lafleur, P. M., McCaughey, J. H., Roulet, N. T., Suyker, A. E., Verma, S. B., Waddington, J. M., & Whiting, G. J. (1998). Relationship between ecosystem productivity and photosynthetically active radiation for northern peatlands. *Global Biogeochemical Cycles*, *12*(1). https://doi.org/10.1029/97GB03367

Frolking, S., & Roulet, N. T. (2007). Holocene radiative forcing impact of northern peatland carbon accumulation and methane emissions. *Global Change Biology*, *13*(5), 1079-1088.

Fung, M. Y. P., & Macyk, T. M. (2015). Reclamation of oil sands mining areas. In Reclamation of Drastically Disturbed Lands (pp. 755–774). wiley. https://doi.org/10.2134/agronmonogr41.c30

Gates, D. M. (1968). Transpiration and Leaf Temperature. *Annual Review of Plant Physiology*, *19*(1). https://doi.org/10.1146/annurev.pp.19.060168.001235

Gaumont-Guay, D., Black, T. A., McCaughey, H., Barr, A. G., Krishnan, P., Jassal, R. S., & Nesic, Z. (2009). Soil CO2 efflux in contrasting boreal deciduous and coniferous stands and its contribution to the ecosystem carbon balance. *Global Change Biology*, *15*(5). https://doi.org/10.1111/j.1365-2486.2008.01830.x

Gažovič, M., Forbrich, I., Jager, D. F., Kutzbach, L., Wille, C., & Wilmking, M. (2013). Hydrology-driven ecosystem respiration determines the carbon balance of a boreal peatland ☆. Science of the Total Environment, The, 463–464, 675–682. https://doi.org/10.1016/j.scitotenv.2013.06.077

Gingras-Hill, T., Nwaishi, F. C., Macrae, M. L., Price, J. S., & Petrone, R. M. (2018). Ecohydrological functioning of an upland undergoing reclamation on post-mining landscape of the Athabasca oil sands region, Canada. Ecohydrology, 11(4), e1941. https://doi.org/10.1002/eco.1941

Glaeser, L. C., House, M., & Vitt, D. H. (2021). Reclaiming to brackish wetlands in the Alberta oil sands: Comparison of responses to sodium concentrations by carex atherodes and carex aquatilis. *Plants*, *10*(8). https://doi.org/10.3390/plants10081511

Gómez-Aparicio, L., Zamora, R., Gómez, J. M., Hódar, J. A., Castro, J., & Baraza, E. (2004). Applying plant facilitation to forest restoration: a meta-analysis of the use of shrubs as nurse plants. *Ecological applications*, *14*(4), 1128-1138.

Gorelick, N., Hancher, M., Dixon, M., Ilyushchenko, S., Thau, D., & Moore, R. (2017). Google Earth Engine: Planetary-scale geospatial analysis for everyone. Remote sensing of Environment, 202, 18-27

Gorham, E. (1991). Northern Peatlands : Role in the Carbon Cycle and Probable Responses to Climatic Warming. Ecological Applications, 1(2), 182–195. https://doi.org/doi.org/10.2307/1941811

Gorham, E., & Rochefort, L. (2003). Peatland restoration: A brief assessment with special reference to Sphagnum bogs. In *Wetlands Ecology and Management* (Vol. 11).

Goud, E. M., Moore, T. R., & Roulet, N. T. (2017). Predicting peatland carbon fluxes from non-destructive plant traits. *Functional Ecology*, *31*(9). https://doi.org/10.1111/1365-2435.12891

Goulden, M. L., Mcmillan, A. M. S., Winston, G. C., Rocha, A. V., Manies, K. L., Harden, J. W., & Bond-Lamberty, B. P. (2011). Patterns of NPP, GPP, respiration, and NEP during boreal forest succession. Global Change Biology, 17(2), 855–871. https://doi.org/10.1111/j.1365-2486.2010.02274.x

Goulden, M. L., Litvak, M., & Miller, S. D. (2007). Factors that control Typha marsh evapotranspiration. *Aquatic Botany*, *86*(2), 97–106. https://doi.org/10.1016/j.aquabot.2006.09.005

Government of Alberta. 2017b. Facts and statistics. [Online.] Available fromhttps://open.alberta.ca/dataset/b6f2d99e-30f8-4194-b7eb-76039e9be4d2/resource/063e27cc-b6d1-4dae-8356-44e27304ef78/download/fsoilsands.pdf[accessed 21 July 2018].

Graham, J., Hartsock, J., Vitt, D. H., Kelman Wieder, R., & Gibson, J. J. (2015). Linkages between spatio-temporal patterns of environemntal factors and distribution of plant assemblages across a boreal peatland complex. *Boreas*. https://doi.org/10.1111/bor.12151

Green, A., Bohrer, G., & Petrone, R. (2021). Microclimatic Effects of a Forest-to-Peatland Transition on Aerodynamic Resistance to Water Vapour Transfer in the Sub-humid Boreal Plains. *Boundary-Layer Meteorology*, *178*, 301–322. https://doi.org/10.1007/s10546-020-00572-3

Griffis, T. J., Black, T. A., Morgenstern, K., Barr, A. G., Nesic, Z., Drewitt, G. B., Gaumont-Guay, D., & McCaughey, J. H. (2003). Ecophysiological controls on the carbon balances of three southern boreal forests. *Agricultural and Forest Meteorology*, *117*(1–2). https://doi.org/10.1016/S0168-1923(03)00023-6

Griffis, T. J., & Rouse, W. R. (2001). Modelling the interannual variability of net ecosystem CO 2 exchange at a subarctic sedge fen . *Global Change Biology*, *7*(5). https://doi.org/10.1046/j.1354-1013.2001.00403.x

Gustafson, T. D. (1976). *Production, photosynthesis, and the storage and utilization of reserves in a natural stand of Typha latifolia L*. The University of Wisconsin-Madison.

Hamel, P., Mchugh, I., Coutts, A., Daly, ; Edoardo, Beringer, J., & Fletcher, T. D. (2014). Automated Chamber System to Measure Field Evapotranspiration Rates. *Journal of Hydrologic Engineering*, *20*(2), 04014037. https://doi.org/10.1061/(ASCE)HE.1943-5584.0001006

Harper, A. B., Powell, T., Cox, P. M., House, J., Huntingford, C., Lenton, T. M., ... & Shu, S. (2018). Land-use emissions play a critical role in land-based mitigation for Paris climate targets. *Nature communications*, *9*(1), 1-13.

Hart, S. A., & Chen, H. Y. H. (2006). Understory vegetation dynamics of North American boreal forests. In *Critical Reviews in Plant Sciences* (Vol. 25, Issue 4). https://doi.org/10.1080/07352680600819286

Hartsock, J. A., House, M., Clark, M. G., & Vitt, D. H. (2021). A comparison of plant communities and water chemistry at Sandhill Wetland to natural Albertan peatlands and marshes. Ecological Engineering, 169, 106313. https://doi.org/10.1016/j.ecoleng.2021.106313

Helbig, M., Humphreys, E. R., & Todd, A. (2019). Contrasting Temperature Sensitivity of CO2 Exchange in Peatlands of the Hudson Bay Lowlands, Canada. Journal of Geophysical Research: Biogeosciences, 124(7), 2126–2143. https://doi.org/10.1029/2019JG005090

Helbig, M., Waddington, J. M., Alekseychik, P., Amiro, B., Aurela, M., Barr, A. G., ... & Schulze, C. (2020a). The biophysical climate mitigation potential of boreal peatlands during the growing season. *Environmental Research Letters*, *15*(10), 104004.

Helbig, M., Waddington, J. M., Alekseychik, P., Amiro, B. D., Aurela, M., Barr, A. G., Black, T. A., Blanken, P. D., Carey, S. K., Chen, J., Chi, J., Desai, A. R., Dunn, A., Euskirchen, E. S., Flanagan, L. B., Forbrich, I., Friborg, T., Grelle, A., Harder, S., … Zyrianov, V. (2020b). Increasing contribution of peatlands to boreal evapotranspiration in a warming climate. *Nature Climate Change 2020 10:6*, *10*(6), 555–560. https://doi.org/10.1038/s41558-020-0763-7

Helbig, M., Živković, T., Alekseychik, P., Aurela, M., El-Madany, T. S., Euskirchen, E. S., Flanagan, L. B., Griffis, T. J., Hanson, P. J., Hattakka, J., Helfter, C., Hirano, T., Humphreys, E. R., Kiely, G., Kolka, R. K., Laurila, T., Leahy, P. G., Lohila, A., Mammarella, I., … Zaehle, S. (2020c). Warming response of peatland CO 2 sink is sensitive to seasonality in warming trends. *14 USDA Forest Service*. https://doi.org/10.1038/s41558-022-01428-z

Holdredge, C., & Bertness, M. D. (2011). Litter legacy increases the competitive advantage of invasive Phragmites australis in New England wetlands. *Biological Invasions*, *13*(2). https://doi.org/10.1007/s10530-010-9836-2

Howell, T. A., & Dusek, D. A. (1995). Comparison of vapor-pressure-deficit calculation methods-southern high plains.

Huete, A., Didan, K., Miura, T., Rodriguez, E. P., Gao, X., & Ferreira, L. G. (2002). Overview of the radiometric and biophysical performance of the MODIS vegetation indices. Remote Sensing of Environment, 83(1–2), 195–213. https://doi.org/10.1016/S0034-4257(02)00096-2

Huete, A., Justice, C., & Liu, H. (1994). Development of vegetation and soil indices for MODIS-EOS. Remote Sensing of environment, 49(3), 224-234.

Huete, A. R., Liu, H. Q., Batchily, K. V., & Van Leeuwen, W. J. D. A. (1997). A comparison of vegetation indices over a global set of TM images for EOS-MODIS. Remote sensing of environment, 59(3), 440-451.

Humphreys, E. R., Lafleur, P. M., Flanagan, L. B., Hedstrom, N., Syed, K. H., Glenn, A. J., & Granger, R. (2006). Summer carbon dioxide and water vapor fluxes across a range of northern peatlands. *J. Geophys. Res*, *111*, 4011. https://doi.org/10.1029/2005JG000111

IPCC, 2021: Summary for Policymakers. In: Climate Change 2021: The Physical Science Basis. Contribution of Working Group I to the Sixth Assessment Report of the Intergovernmental Panel on Climate Change [Masson-Delmotte, V., P. Zhai, A. Pirani, S.L. Connors, C. Péan, S. Berger, N. Caud, Y. Chen, L. Goldfarb, M.I. Gomis, M. Huang, K. Leitzell, E. Lonnoy, J.B.R. Matthews, T.K. Maycock, T. Waterfield, O. Yelekçi, R. Yu, and B. Zhou (eds.)]. In Press.

Ireson, A. M., Barr, A. G., Johnstone, J. F., Mamet, S. D., van der Kamp, G., Whitfield, C. J., … Sagin, J. (2015). The changing water cycle: the Boreal Plains ecozone of Western Canada. WIREs Water, 2(5), 505–521. https://doi.org/10.1002/wat2.1098

Irving, H. (2020). The Impact of LFH Mineral Mix on the Function of Reclaimed Landscapes in the Athabasca Oil Sands Region, Alberta, Canada (Master's thesis, University of Waterloo).

Jahan, N., & Gan, T. Y. (2011). Modelling the vegetation–climate relationship in a boreal mixedwood forest of Alberta using normalized difference and enhanced vegetation indices. International Journal of Remote Sensing, 32(2), 313-335.

Jarvis, P. G., & McNaughton, K. G. (1986). Stomatal control of transpiration: scaling up from leaf to region. In *Advances in ecological research* (Vol. 15, pp. 1-49). Academic Press

Jassey, V. E. J., Zielińska, M., Reczuga, M. K., & Słowińska, S. (2017). Tipping point effect in plant-fungal interactions under severe drought causes abrupt rise in peatland ecosystem respiration. *Global Change Biology*, *12*(10), 3218–3221. https://doi.org/10.1111/gcb.13928

Jia, G., E. Shevliakova, P. Artaxo, N. De Noblet-Ducoudré, R. Houghton, J. House, K. Kitajima, C. Lennard, A. Popp, A. Sirin, R. Sukumar, L. Verchot, 2019: Land–climate interactions. In: Climate Change and Land: an IPCC special report on climate change,

desertification, land degradation, sustainable land management, food security, and greenhouse gas fluxes in terrestrial ecosystems [P.R. Shukla, J. Skea, E. Calvo Buendia, V. Masson-Delmotte, H.-O. Pörtner, D.C. Roberts, P. Zhai, R. Slade, S. Connors, R. van Diemen, M. Ferrat, E. Haughey, S. Luz, S. Neogi, M. Pathak, J. Petzold, J. Portugal Pereira, P. Vyas, E. Huntley, K. Kissick, M, Belkacemi, J. Malley, (eds.)]. In press.

Jílková, V. (2020). Soil respiration in temperate forests is increased by a shift from coniferous to deciduous trees but not by an increase in temperature. *Applied Soil Ecology*, *154*. https://doi.org/10.1016/J.APSOIL.2020.103635

Jin, Y., Randerson, J. T., Goetz, S. J., Beck, P. S. A., Loranty, M. M., & Goulden, M. L. (2012). The influence of burn severity on postfire vegetation recovery and albedo change during early succession in North American boreal forests. *Journal of Geophysical Research: Biogeosciences*, *117*(G1), 1036. https://doi.org/10.1029/2011JG001886

Johnson, E. A., & Miyanishi, K. (2008). Creating new landscapes and ecosystems: the Alberta oil sands. *Annals of the New York Academy of Sciences*, *1134*(1), 120-145.

Kaimal, J., & Finnigan, J. (1994). Atmospheric boundary layer flows : their structure and measurement . New York: Oxford University Press

Kessel, E. D., Ketcheson, S. J., & Price, J. S. (2018). The distribution and migration of sodium from a reclaimed upland to a constructed fen peatland in a post-mined oil sands landscape. Science of the Total Environment, 630, 1553–1564. https://doi.org/10.1016/j.scitotenv.2018.02.253

Ketcheson, S. J. (2015). *Hydrology of a Constructed Fen Watershed in a Post-mined Landscape in the Athabasca Oil Sands Region , Alberta , Canada by*.

Ketcheson, S. J., Price, J. S., Sutton, O., Sutherland, G., Kessel, E., & Petrone, R. M. (2017). The hydrological functioning of a constructed fen wetland watershed. Science of the Total Environment. https://doi.org/10.1016/j.scitotenv.2017.06.101

Ketcheson, S. J., Price, J. S., Carey, S. K., Petrone, R. M., Mendoza, C. A., & Devito, K. J. (2016). Constructing fen peatlands in post-mining oil sands landscapes: Challenges and opportunities from a hydrological perspective. Earth-Science Reviews. https://doi.org/10.1016/j.earscirev.2016.08.007

Khomik, M., Arain, M. A., & McCaughey, J. H. (2006). Temporal and spatial variability of soil respiration in a boreal mixedwood forest. *Agricultural and Forest Meteorology*, *140*(1–4). https://doi.org/10.1016/j.agrformet.2006.08.006

Kljun, N., Calanca, P., Rotach, M.W., & Schmid, H.P. (2004). A Simple parameterisation for flux footprint predictions. Boundary-Layer Meteorology, 112, 503-523

Kljun, N., Black, T. A., Griffis, T. J., Barr, A. G., Gaumont-Guay, D., Morgenstern, K., McCaughey, J. H., & Nesic, Z. (2006). Response of net ecosystem productivity of three boreal forest stands to drought. *Ecosystems*, *9*(7). https://doi.org/10.1007/s10021-005-0082-x

Kokkonen, N. A., Laine, A. M., Laine, J., Vasander, H., Kurki, K., Gong, J., & Tuittila, E. S. (2019). Responses of peatland vegetation to 15- year water level drawdown as mediated

by fertility level. Journal of Vegetation Science, 30(6), 1206–1216. https://doi.org/10.1111/ jvs.12794

Koropchak S, Vitt DH, Bloise R, Wieder RK (2012) Fundamental paradigms, foundation species selection, and early plant responses to peatland initiation on mineral soils. In: Vitt DH, Bhatti J (eds) Restoration and reclamation of boreal ecosystems: attaining sustainable development. Cambridge University Press, Cambridge, pp 76–100

Koropchak, S., & Vitt, D. (2013). Survivorship and growth of Typha latifolia L. across a NaCl gradient: A greenhouse study. *International Journal of Mining, Reclamation and Environment*, *27*(2). https://doi.org/10.1080/17480930.2012.679860

Knapp, A. K., Beier, C., Briske, D. D., Classen, A. T., Yiqi, L., Reichstein, M., Smith, M. D., Smith, S. D., Bell, J. E., Fay, P. A., Heisler, J. L., Leavitt, S. W., Sherry, R., Smith, B., & Weng, E. (2008). Consequences of More Extreme Precipitation Regimes for Terrestrial Ecosystems. *BioScience*, *58*(9), 811–821. https://doi.org/10.1641/B580908

Knauer, J., El-Madany, T. S., Nke Zaehle, S., & Migliavacca, M. (2018). *Bigleaf-An R package for the calculation of physical and physiological ecosystem properties from eddy covariance data*. https://doi.org/10.1371/journal.pone.0201114

Krishnan, P., Black, T. A., Grant, N. J., Barr, A. G., Hogg, E. (Ted) H., Jassal, R. S., & Morgenstern, K. (2006). Impact of changing soil moisture distribution on net ecosystem productivity of a boreal aspen forest during and following drought. *Agricultural and Forest Meteorology*, *139*(3–4). https://doi.org/10.1016/j.agrformet.2006.07.002

Kurbatova, J., Arneth, A., Vygodskaya, N. N., Kolle, O., Varlargin, A. V., Milyukova, I. M., ... & Lloyd, J. (2002). Comparative ecosystem–atmosphere exchange of energy and mass in a European Russian and a central Siberian bog I. Interseasonal and interannual variability of energy and latent heat fluxes during the snowfree period. *Tellus B: Chemical and Physical Meteorology*, *54*(5), 497-513.

Kurz, W. A., Shaw, C. H., Boisvenue, C., Stinson, G., Metsaranta, J., Leckie, D., … Neilson, E. T. (2013). Carbon in Canada's boreal forest-A synthesis. Environmental Reviews. https://doi.org/10.1139/er-2013-0041

Lafleur, P. M. (1990). Evapotranspiration from sedge-dominated wetland surfaces. Aquatic Botany, 37(4), 341–353. https://doi.org/10.1016/0304-3770(90)90020-L

Lafleur, P. M. (2008). Connecting Atmosphere and Wetland: Energy and Water Vapour Exchange. *Geography Compass*, *2*(4), 1027–1057. https://doi.org/10.1111/J.1749-8198.2007.00132.X

Lafleur, P. M., Hember, R. A., Admiral, S. W., & Roulet, N. T. (2005). Annual and seasonal variability in evapotranspiration and water table at a shrub-covered bog in southern Ontario, Canada. *Hydrological Processes*, *19*(18). https://doi.org/10.1002/hyp.5842

Lafleur, P. M., & Rouse, W. R. (1988). The influence of surface cover and climate on energy partitioning and evaporation in a subarctic wetland. *Boundary-Layer Meteorology*, *44*(4). https://doi.org/10.1007/BF00123020

Laguë, M. M., Bonan, G. B., & Swann, A. L. S. (2019). Separating the impact of individual land surface properties on the terrestrial surface energy budget in both the coupled and

uncoupled land–atmosphere system. *Journal of Climate*, *32*(18), 5725–5744. https://doi.org/10.1175/JCLI-D-18-0812.1

Laine, A. M., Lindholm, T., Nilsson, M., Kutznetsov, O., Jassey, V. E., & Tuittila, E. S. (2021). Functional diversity and trait composition of vascular plant and Sphagnum moss communities during peatland succession across land uplift regions. *Journal of Ecology*, *109*(4), 1774-1789.

Lamothe, K. A., Dong, H., Senar, O. E., Teichert, S., Creed, I. F., Kreutzweiser, D. P., … Venier, L. (2018). Demand for nonprovisioning ecosystem services as a driver of change in the Canadian boreal zone 1. https://doi.org/10.1139/er-2018-0065

Lavigne, M. B., Ryan, M. G., Anderson, D. E., Baldocchi, D. D., Crill, P. M., Fitzjarrald, D. R., Goulden, M. L., Gower, S. T., Massheder, J. M., McCaughey, J. H., Rayment, M., & Striegl, R. G. (1997). Comparing nocturnal eddy covariance measurements to estimates of ecosystem respiration made by scaling chamber measurements at six coniferous boreal sites. In *Journal of Geophysical Research Atmospheres* (Vol. 102, Issue 24).

Lavoie, C., Saint-Louis, A., & Lachance, D. (2005). Vegetation dynamics on an abandoned vacuum-mined peatland: 5 Years of monitoring. Wetlands Ecology and Management, 13(6), 621–633. https://doi.org/10.1007/s11273-005-0126-1

Law, B., Falge, E., Gu, L., Baldocchi, D., Bakwin, P., Berbigier, P., Davis, K., Dolman, A., Falk, M., Fuentes, J. et al., (2002). Environmental controls over carbon dioxide and water vapor exchange of terrestrial vegetation. Agricultural and Forest Meteorology, 113, 97–120.

Lee, S. C., Black, T. A., Nyberg, M., Merkens, M., Nesic, Z., Ng, D., & Knox, S. H. (2021). Biophysical impacts of historical disturbances, restoration strategies, and vegetation types in a peatland ecosystem. *Journal of Geophysical Research: Biogeosciences*, *126*(10), e2021JG006532.

Lees, K. J., Quaife, T., Artz, R. R. E., Khomik, M., & Clark, J. M. (2018, February 15). Potential for using remote sensing to estimate carbon fluxes across northern peatlands – A review. Science of the Total Environment. Elsevier B.V. https://doi.org/10.1016/j.scitotenv.2017.09.103

Lemmer, M., Rochefort, L., & Strack, M. (2020). Greenhouse Gas Emissions Dynamics in Restored Fens After In-Situ Oil Sands Well Pad Disturbances of Canadian Boreal Peatlands. Frontiers in Earth Science, 8, 546.

Leuning, R., & Judd, M.J. (1996). The relative merits of open and closed path analysers for measurement of eddy fluxes. Global Change Biology, 2: 241-253.

Levia, D. F., Carlyle-Moses, D., & Tanaka, T. (2011). Forest Hydrology and Biogeochemistry: Synthesis of Past Research and Future Directions. *Analysis and Synthesis*, *216*.

Lewontin, R. C. (1969). The bases of conflict in biological explanation. *Journal of the History of Biology*, *2*(1). https://doi.org/10.1007/BF00137266

Li, G., Chen, T., Feng, B., Peng, S., Tao, L., & Fu, G. (2021). Respiration, Rather Than Photosynthesis, Determines Rice Yield Loss Under Moderate High-Temperature Conditions. *Frontiers in Plant Science*, *12*. https://doi.org/10.3389/fpls.2021.678653

Liu, P., Barr, A. G., Tianshan Zha, |, Black, | T Andrew, Rachhpal, |, Jassal, S., Nesic, Z., Helgason, W. D., Xin Jia, |, & Tian, Y. (2022). Re-assessment of the climatic controls on the carbon and water fluxes of a boreal aspen forest over 1996–2016: Changing sensitivity to long-term climatic conditions. *Global Change Biology*, *00*, 1. https://doi.org/10.1111/GCB.16218

Limpens, J., Berendse, F., Blodau, C., Canadell, J. G., Freeman, C., Holden, J., … Schaepman-Strub, G. (2008). Peatlands and the carbon cycle: from local processes to global implications – a synthesis. Biogeosciences, 5, 1475–1491. Retrieved from www.biogeosciences.net/5/1475/2008/

Litvak, M., Miller, S., Wofsy, S. C., & Goulden, M. (2003). Effect of stand age on whole ecosystem CO2 exchange in the Canadian boreal forest. Journal of Geophysical Research: Atmospheres, 108(3), 8225. https://doi.org/10.1029/2001jd000854

Liu, H., & Randerson, J. T. (2008). Interannual variability of surface energy exchange depends on stand age in a boreal forest fire chronosequence. *Journal of Geophysical Research: Biogeosciences*, *113*(G1), 1006. https://doi.org/10.1029/2007JG000483

Loisel, J., & Yu, Z. (2013). Surface vegetation patterning controls carbon accumulation in peatlands. Geophysical Research Letters, 40(20), 5508–5513. https://doi.org/10.1002/grl.50744

Lukeš, P., Stenberg, P., Rautiainen, M., Mõttus, M., & Vanhatalo, K. M. (2013). Optical properties of leaves and needles for boreal tree species in Europe. *Remote Sensing Letters*, *4*(7), 667–676. https://doi.org/10.1080/2150704X.2013.782112

Lund, M., Lafleur, P. M., Roulet, N. T., Lindroth, A., Christensen, T. R., Aurela, M., ... & Nilsson, M. B. (2010). Variability in exchange of CO2 across 12 northern peatland and tundra sites. Global Change Biology, 16(9), 2436-2448.

MacKenzie, M. D., & Quideau, S. A. (2010). Microbial community structure and nutrient availability in oil sands reclaimed boreal soils. Applied Soil Ecology, 44(1), 32–41. https://doi.org/10.1016/J.APSOIL.2009.09.002

Maestre, F. T., Bautista, S., Cortina, J., & Bellot, J. (2001). Potential for using facilitation by grasses to establish shrubs on a semiarid degraded steppe. Ecological Applications, 11(6), 1641-1655

Mahmood, R., Pielke, R. A., Hubbard, K. G., Niyogi, D., Dirmeyer, P. A., Mcalpine, C., Carleton, A. M., Hale, R., Gameda, S., Beltrán-Przekurat, A., Baker, B., Mcnider, R., Legates, D. R., Shepherd, M., Du, J., Blanken, P. D., Frauenfeld, O. W., Nair, U. S., & Fall, S. (2014). Land cover changes and their biogeophysical effects on climate. *International Journal of Climatology*, *34*(4), 929–953. https://doi.org/10.1002/JOC.3736

Marshall IB, Schut P, Ballard M (compilers). 1999. Canadian ecodistrict climate normals for Canada 1961–1990. A national ecological framework for Canada: Attribute Data.

Environmental Quality Branch, Ecosystems Science Directorate, Environment Canada and Research Branch, Agriculture and Agri-Food Canada, Ottawa/Hull.

McCarter, C. P. R., & Price, J. S. (2013). The hydrology of the Bois-des-Bel bog peatland restoration: 10 years post-restoration. *Ecological Engineering*, *55*. https://doi.org/10.1016/j.ecoleng.2013.02.003

Mcleod, M. K., Daniel, H., Faulkner, R., & Murison, R. (2004). Evaluation of an enclosed portable chamber to measure crop and pasture actual evapotranspiration at small scale. *Agricultural Water Management*, *67*, 15–34. https://doi.org/10.1016/j.agwat.2003.12.006

McNaughton, K. G., & Jarvis, P. G. (1991). Effects of spatial scale on stomatal control of transpiration. *Agricultural and Forest Meteorology*, *54*(2-4), 279-302.

Medhurst, J., Parsby, J., Linder, S., Wallin, G., Ceschia, E., & Slaney, M. (2006). A whole-tree chamber system for examining tree-level physiological responses of field-grown trees to environmental variation and climate change. *Plant, Cell and Environment*, *29*(9). https://doi.org/10.1111/j.1365-3040.2006.01553.x

Merlin, M., & Landhäusser, S. M. (2019). Seasonal patterns of water uptake in Populus tremuloides and Picea glauca on a boreal reclamation site is species specific and modulated by capping soil depth and slope position. *Plant and Soil*, *439*(1–2). https://doi.org/10.1007/s11104-019-04029-6

Messner, Lewis. (2019). Approaches for creating sustainable biomass production in a reclaimed. Thesis

Mkhabela, M. S., Amiro, B. D., Barr, A. G., Black, T. A., Hawthorne, I., Kidston, J., ... & Zha, T. (2009). Comparison of carbon dynamics and water use efficiency following fire and harvesting in Canadian boreal forests. Agricultural and forest meteorology, 149(5), 783-794.

Middleton, E. M., Sullivan, J. H., Bovard, B. D., Deluca, A. J., Chan, S. S., & Cannon, T. A. (1997). Seasonal variability in foliar characteristics and physiology for boreal forest species at the five Saskatchewan tower sites during the 1994 Boreal Ecosystem-Atmosphere Study. *Journal of Geophysical Research Atmospheres*, *102*(24). https://doi.org/10.1029/97jd02560

Minke, M., Augustin, J., Burlo, A., Yarmashuk, T., Chuvashova, H., Thiele, A., Freibauer, A., Tikhonov, V., & Hoffmann, M. (2016). Water level, vegetation composition, and plant productivity explain greenhouse gas fluxes in temperate cutover fens after inundation. *Biogeosciences*, *13*, 3945–3970. https://doi.org/10.5194/bg-13-3945-2016

Miura, T., Huete, A. R., Van Leeuwen, W. J. D., & Didan, K. (1998). Vegetation detection through smoke-filled AVIRIS images: An assessment using MODIS band passes. Journal of Geophysical Research: Atmospheres, 103(D24), 32001-32011.

Mölder, M., and E. Kellner (2002), Excess resistance of bog surfaces incentral Sweden,Agr. Forest. Meteorol.,112(1), 23–30, doi:10.1016/S0168-1923(02)00043-6

Monteith, J. (1965) Evaporation and environment.In:Fogg GE,editor.Symp.Soc.Exp.Biol.vol.19. Cambridge University Press;1965.p. 205–234.

Monteith, J. L. (1995). A reinterpretation of stomatal responses to humidity. *Plant, Cell & Environment*, *18*(4). https://doi.org/10.1111/j.1365-3040.1995.tb00371.x

Monteith, J., & Unsworth, M. (2008). *Principles of environmental physics: plants, animals, and the atmosphere*. Academic Press.

Montemayor, M. B., Price, J. S., Rochefort, L., & Boudreau, S. (2008). Temporal variations and spatial patterns in saline and waterlogged peat fields. 1. Survival and growth of salt marsh graminoids. *Environmental and Experimental Botany*, *62*(3), 333–342. https://doi.org/10.1016/j.envexpbot.2007.10.004

Moore, P. A., Pypker, T. G., & Waddington, J. M. (2013). Effect of long-term water table manipulation on peatland evapotranspiration. *Agricultural and Forest Meteorology*, *178–179*, 106–119. https://doi.org/10.1016/J.AGRFORMET.2013.04.013

Morison, M. Q., Petrone, R. M., Wilkinson, S. L., Green, A., & Waddington, J. M. (2020). Ecosystem scale evapotranspiration and CO2 exchange in burned and unburned peatlands: Implications for the ecohydrological resilience of carbon stocks to wildfire. Ecohydrology, 13(2), e2189

Morris, P. J., Belyea, L. R., & Baird, A. J. (2011). Ecohydrological feedbacks in peatland development: a theoretical modelling study. *Journal of Ecology*, *99*, 1190–1201. https://doi.org/10.1111/j.1365-2745.2011.01842.x

Munir, T. M., Xu, B., Perkins, M., & Strack, M. (2014). Responses of carbon dioxide flux and plant biomass to water table drawdown in a treed peatland in Northern Alberta: A climate change perspective. *Biogeosciences*, *11*(3), 807–820. https://doi.org/10.5194/bg-11-807-2014

Murray, K. R., Barlow, N., & Strack, M. (2017). Methane emissions dynamics from a constructed fen and reference sites in the Athabasca Oil Sands Region, Alberta. *Science of the Total Environment*, *583*. https://doi.org/10.1016/j.scitotenv.2017.01.076

Naeth, M. A., Wilkinson, S. R., Mackenzie, D. D., Archibald, H. A., & Powter, C. B. (2013). Potential of LFH Mineral Soil Mixes for Reclamation of Forested Lands in Alberta. Retrieved from http://hdl.handle.net/10402/era.17507.

Nelson, K., Thompson, D., Hopkinson, C., Petrone, R., & Chasmer, L. (2021). Peatland-fire interactions: A review of wildland fire feedbacks and interactions in Canadian boreal peatlands. *Science of The Total Environment*, *769*, 145212.

Nicholls, E. M., Carey, S. K., Humphreys, E. R., Clark, M. G., & Drewitt, G. B. (2016). Multi-year water balance assessment of a newly constructed wetland, Fort McMurray, Alberta. Hydrological Processes, 30(16), 2739-2753.

Nijp, J. J., Limpens, J., Metselaar, K., Peichl, M., Nilsson, M. B., van der Zee, S. E., & Berendse, F. (2015). Rain events decrease boreal peatland net CO 2 uptake through reduced light availability. Global Change Biology, 21(6), 2309-2320

Nilsson, M., Sagerfors, J., Buffam, I., Laudon, H., Eriksson, T., Grelle, A., … Lindroth, A. (2008). Contemporary carbon accumulation in a boreal oligotrophic minerogenic mire - A significant sink after accounting for all C-fluxes. Global Change Biology, 14(10), 2317–2332. https://doi.org/10.1111/j.1365-2486.2008.01654.x

Ni-Meister, W., & Gao, H. (2011). Assessing the impacts of vegetation heterogeneity on energy fluxes and snowmelt in boreal forests. *Journal of Plant Ecology*, *4*(1-2), 37-47.

Novick, K. A., Ficklin, D. L., Stoy, P. C., Williams, C. A., Bohrer, G., Oishi, A. C., Papuga, S. A., Blanken, P. D., Noormets, A., Sulman, B. N., Scott, R. L., Wang, L., & Phillips, R. P. (2016). *The increasing importance of atmospheric demand for ecosystem water and carbon fluxes*. https://doi.org/10.1038/NCLIMATE3114

Nugent, K. A., Strachan, I. B., Roulet, N. T., Strack, M., Frolking, S., & Helbig, M. (2019). Prompt active restoration of peatlands substantially reduces climate impact. *Environmental Research Letters*, *14*(12), 124030.

Nugent, K. A., Strachan, I. B., Strack, M., Roulet, N. T., & Rochefort, L. (2018). Multi-year net ecosystem carbon balance of a restored peatland reveals a return to carbon sink. Global Change Biology, 24(12), 5751–5768. https://doi.org/10.1111/gcb.14449

Nwaishi, F., Petrone, R. M., Macrae, M. L., Price, J. S., Strack, M., & Andersen, R. (2016). Preliminary assessment of greenhouse gas emissions from a constructed fen on post-mining landscape in the Athabasca oil sands region, Alberta, Canada. Ecological Engineering, 95, 119–128. https://doi.org/10.1016/j.ecoleng.2016.06.061

Nwaishi, F., Petrone, R. M., Price, J. S., & Andersen, R. (2015a). Towards Developing a Functional-Based Approach for Constructed Peatlands Evaluation in the Alberta Oil Sands Region, Canada. Wetlands, 35(2), 211–225. https://doi.org/10.1007/s13157-014-0623-1

Nwaishi, F., Petrone, R. M., Price, J. S., Ketcheson, S. J., Slawson, R., & Andersen, R. (2015b). Impacts of donor-peat management practices on the functional characteristics of a constructed fen. Ecological Engineering. https://doi.org/10.1016/j.ecoleng.2015.04.038

Oechel, W. C., Vourlitis, G. L., Hastings, S. J., Ault, R. P., & Bryant, P. (1998). The effects of water table manipulation and elevated temperature on the net CO2 flux of wet sedge tundra ecosystems. *Global Change Biology*, *4*(1), 77–90. https://doi.org/10.1046/J.1365-2486.1998.00110.X

Oren, R., Sperry, J. S., Katul, G. G., Pataki, D. E., Ewers, B. E., Phillips, N., & Schäfer, K. V. R. (1999). Survey and synthesis of intra- and interspecific variation in stomatal sensitivity to vapour pressure deficit. *Plant, Cell & Environment*, *22*(12), 1515–1526. https://doi.org/10.1046/J.1365-3040.1999.00513.X

Otieno, D., Kreyling, J., Purcell, A., Herold, N., Grant, K., Tenhunen, J., Beierkuhnlein, C., & Jentsch, A. (2012). Drought responses of Arrhenatherum elatius grown in plant assemblages of varying species richness. *Acta Oecologica*, *39*. https://doi.org/10.1016/j.actao.2011.10.002

Padilla, F. M., Ortega, R., Sánchez, J., & Pugnaire, F. I. (2009). Rethinking species selection for restoration of arid shrublands. Basic and Applied Ecology, 10(7), 640-647.

Pearson, M., Penttila, T., Harjunpaa, L., Laiho, R., Laine, J., Sarjala, T., Silvan, K., & Silvan, N. (2015). Effects of temperature rise and water-table level drawdown on greenhouse gas fluxes of boreal sedge fens. *Boreal Environmental Research*, *20*, 489–505.

Peichl, M., Gažovič, M., Vermeij, I., De Goede, E., Sonnentag, O., Limpens, J., & Nilsson, M. B. (2018). Peatland vegetation composition and phenology drive the seasonal trajectory of maximum gross primary production. Scientific reports, 8(1), 1-11.

Peichl, M., Sagerfors, J., Lindroth, A., Buffam, I., Grelle, A., Klemedtsson, L., Laudon, H., & Nilsson, M. B. (2013). Energy exchange and water budget partitioning in a boreal minerogenic mire. *Journal of Geophysical Research: Biogeosciences*, *118*(1), 1–13. https://doi.org/10.1029/2012JG002073

Penman. (1948). Natural Evaporation from Open Water, Bare Soil and Grass. *Proceedings of the Royal Society of London. Series A, Mathematical and Physical Sciences*, *193*(1032).

Peterson, B. G., Carl, P., Boudt, K., Bennett, R., Ulrich, J., Zivot, E., Cornilly, D., Hung, E., Lestel, M., & Balkissoon, K. (2018). Package 'performanceanalytics.' *R Team Cooperation*, *3*.

Petrone, R., Chasmer, L., Hopkinson, C., Silins, U., Landhäusser, S., Kljun, N., & Devito, K. (2015). Effects of harvesting and drought on CO 2 and H 2 O fluxes in an aspen-dominated western boreal plain forest: early chronosequence recovery. Can. J. For. Res. Can. J. For. Res, 4519. https://doi.org/10.1139/cjfr-2014-0253

Petrone, R. M., Silins, U., & Devito, K. J. (2007). Dynamics of evapotranspiration from a riparian pond complex in the Western Boreal forest, Alberta, Canada. Hydrological Processes, 21(11), 1391–1401. https://doi.org/10.1002/hyp.6298

Petrone, Richard M, Price, J. S., Waddington, J. M., & Von Waldow, H. (2004). Surface moisture and energy exchange from a restored peatland, Québec, Canada. Journal of Hydrology, 295(1–4), 198–210. https://doi.org/10.1016/j.jhydrol.2004.03.009

Petrone, Richard M, Waddington, J. M., & Price, J. S. (2003). Ecosystem-scale flux of CO 2 from a restored vacuum harvested peatland. Wetlands Ecology and Management (Vol. 11).

Petrone, Richard M, Waddington, J. M., & Price, J. S. (2001). Ecosystem scale evapotranspiration and net CO2 exchange from a restored peatland. Hydrological Processes, 15(14), 2839–2845. https://doi.org/10.1002/hyp.475

Phillips, T., Petrone, R. M., Wells, C. M., & Price, J. S. (2016). *Characterizing dominant controls governing evapotranspiration within a natural saline fen in the Athabasca Oil Sands of Alberta , Canada*. *829*(September 2015), 817–829. https://doi.org/10.1002/eco.1685

Pinheiro, J., Bates, D., DebRoy, S., & Sarkar, D. (2014). R Core Team (2014). nlme: linear and nonlinear mixed effects models. R package version 3.1–117. *URL: Http://Cran. r-Project. Org/Web/Packages/Nlme/Index. Html*.

Pinno, B. D., & Hawkes, V. C. (2015). Temporal trends of ecosystem development on different site types in reclaimed boreal forests. Forests, 6(6), 2109-2124.

Popović, N., Petrone, R. M., Green, A., Khomik, M., & Price, J. S. (2022). A temporal snapshot of ecosystem functionality during the initial stages of reclamation of an upland-fen complex. *Journal of Hydrology: Regional Studies*, *41*, 101078. https://doi.org/10.1016/j.ejrh.2022.101078

Popović, N., Petrone, R. M., Green, A., Khomik, M., & Price, J. S. (2023). Evolution of ecosystem-scale surface energy fluxes of a newly constructed boreal upland-fen watershed. *Ecological Engineering*, *194*. https://doi.org/10.1016/j.ecoleng.2023.107059

Poscente, M., & Charette, T. (2011). Criteria and indicator framework for oil sands mine reclamation. In Proceedings of the Sixth International Conference on Mine Closure (pp. 455–462). Australian Centre for Geomechanics, Perth.

Poulin, M., Andersen, R., & Rochefort, L. (2013). A new approach for tracking vegetation change after restoration: A case study with peatlands. Restoration Ecology, 21(3), 363–371. https://doi.org/10.1111/j.1526-100X.2012.00889.x

Pouliot, R., Rochefort, L., & Graf, M. D. (2012). Impacts of oil sands process water on fen plants: Implications for plant selection in required reclamation projects. Environmental Pollution. https://doi.org/10.1016/j.envpol.2012.03.050

Preston, C. M., & Trofymow, J. A. (2000). Variability in litter quality and its relationship to litter decay in Canadian forests. *Canadian Journal of Botany*, *78*(10). https://doi.org/10.1139/cjb-78-10-1269

Price, J. S. (1994a). Evapotranspiration from a lakeshore Typha marsh on Lake Ontario. *Aquatic Botany*, *48*(3–4). https://doi.org/10.1016/0304-3770(94)90019-1

Price, J. S. (1994b). Water exchanges in a shoreline Typha marsh on Lake Ontario. *Journal of Hydrology*, *161*(1–4). https://doi.org/10.1016/0022-1694(94)90128-7

Price, J. S., McLaren, R. G., & Rudolph, D. L. (2010). Landscape restoration after oil sands mining: Conceptual design and hydrological modelling for fen reconstruction. International Journal of Mining, Reclamation and Environment, 24(2), 109–123. https://doi.org/10.1080/17480930902955724

Price, J., Rochefort, L., & Quinty, F. (1998). Energy and moisture considerations on cutover peatlands: surface microtopography, mulch cover and Sphagnum regeneration. Ecological engineering, 10(4), 293-312.

Prentice, T. M. (2020). Quantifying the Influence of Soil Prescriptions on Ecosystem Processes in Reclaimed Forests of Varying Age in a Post-Oil Sands Landscape in the Athabasca Oil Sands Region, Alberta, Canada (Master's thesis, University of Waterloo).

Province of Alberta (2020) Environmental Protection and Enhancement Act - Chapter/Regulation: E-12 RSA 2000. Alberta Queen's Printer from https://www.qp.alberta.ca/1266.cfm?page=E12.cfm&leg_type=Acts&isbncln=9780779822706

Province of Alberta (2021) Environmental Protection and Enhancement Act, Revised Statues of Alberta 2000, Chapter E-12. Published by Alberta King's Printer. Accessed: February 3, 2021. https://www.kings-printer.alberta.ca/1266.cfm?page=E12.cfm&leg_type=Acts&isbncln=9780779801657

Pugh, C. A., Reed, D. E., Desai, A. R., & Sulman, B. N. (2018). Wetland flux controls: how does interacting water table levels and temperature influence carbon dioxide and

methane fluxes in northern Wisconsin? *Biogeochemistry*, *137*(1–2), 15–25. https://doi.org/10.1007/s10533-017-0414-x

Pulliainen, J., Aurela, M., Laurila, T., Aalto, T., Takala, M., Salminen, M., … Vesala, T. (2017). Early snowmelt significantly enhances boreal springtime carbon uptake. ATMOSPHERIC, AND PLANETARY SCIENCES, 17. https://doi.org/10.1073/pnas.1707889114

Purdy, B. G., Macdonald, S. E., & Lieffers, V. J. (2005). Naturally saline boreal communities as models for reclamation of saline oil sand tailings. Restoration Ecology, 13(4), 667–677. https://doi.org/10.1111/j.1526-100X.2005.00085.x

QGIS, 2021. QGIS Geographic Information System. QGIS Association. http://www.qgis.org

Quideau, S. A., Swallow, M. J. B., Prescott, C. E., Grayston, S. J., & Oh, S. W. (2013). Comparing soil biogeochemical processes in novel and natural boreal forest ecosystems. *Biogeosciences*, *10*(8), 5651-5661.

R Core Team (2021). R: A language and environment for statistical computing. R Foundation for Statistical Computing, Vienna, Austria. https://www.R-project.org/.

Raddatz, R. L., Papakyriakou, T. N., Swystun, K. A., & Tenuta, M. (2009). Evapotranspiration from a wetland tundra sedge fen: Surface resistance of peat for land-surface schemes. *Agricultural and Forest Meteorology*, *149*(5), 851-861.

Radu, D. D., & Duval, T. P. (2018). Response of hydrology and CO2 flux to experimentally altered rainfall frequency in a temperate poor fen, southern Ontario, Canada. *Biogeosciences*, *15*(13). https://doi.org/10.5194/bg-15-3937-2018

Randerson, J. T., Liu, H., Flanner, M. G., Chambers, S. D., Jin, Y., Hess, P. G., ... & Zender, C. S. (2006). The impact of boreal forest fire on climate warming. *science*, *314*(5802), 1130-1132.

Raupach, M. R. (1998). Influences of local feedbacks on land–air exchanges of energy and carbon. *Global Change Biology*, *4*(5), 477–494. https://doi.org/10.1046/J.1365-2486.1998.T01-1-00155.X

Rankin, T., Strachan, I. B., & Strack, M. (2018). Carbon dioxide and methane exchange at a post-extraction, unrestored peatland. Ecological Engineering, 122, 241–251. https://doi.org/10.1016/j.ecoleng.2018.06.021

Reich, P. B., Sendall, K. M., Stefanski, A., Rich, R. L., Hobbie, S. E., & Montgomery, R. A. (2018). Effects of climate warming on photosynthesis in boreal tree species depend on soil moisture. *Nature*, *562*(7726). https://doi.org/10.1038/s41586-018-0582-4

Reichstein, M., Falge, E., Baldocchi, D., Papale, D., Aubinet, M., Berbigier, P.,….Valentini, R.(2005). On the separation of net ecosystem exchange into assimilation and ecosystem respiration: review and improved algorithm. Global Change Biology, 11(9), 1424-1439.

Rezanezhad, F, Andersen, R., Pouliot, R., & Price, J. S. (2012). How Fen Vegetation Structure Affects the Transport of Oil Sands Process-affected Waters, 557–570. https://doi.org/10.1007/s13157-012-0290-z

Rigden, A. J., & Li, D. (2017). Attribution of surface temperature anomalies induced by land use and land cover changes. *Geophysical Research Letters*, *44*(13), 6814-6822.

Riutta, T., Laine, J., & Tuittila, E. S. (2007). Sensitivity of CO2 exchange of fen ecosystem components to water level variation. *Ecosystems*, *10*(5), 718–733. https://doi.org/10.1007/s10021-007-9046-7

Rochefort, L., Quinty, F., Campeau, S., Johnson, K., & Malterer, T. (2003). North American approach to the restoration of Sphagnum dominated peatlands. Wetlands Ecology and Management, 11(1), 3-20.

Rochefort, L. (2000). Sphagnum: a keystone genus in habitat restoration. The Bryologist, 103(3), 503-508.

Rodriguez-Iturbe, I. (2000). Ecohydrology: A hydrologic perspective of climate-soil-vegetation dynamics. *WATER RESOURCES RESEARCH*, *36*(1), 3–9.

Rodriguez-Iturbe, I., & Porporato, A. (2004). Ecohydrology of Water-Controlled Ecosystems: soil moisture and plant dynamics.

Rooney, R. C., Bayley, S. E., & Schindler, D. W. (2012). Oil sands mining and reclamation cause massive loss of peatland and stored carbon. Proceedings of the National Academy of Sciences of the United States of America, 109(13), 4933–4937. https://doi.org/10.1073/pnas.1117693108

Roulet NT, Lafleur PM, Richard PJH, Moore TR, Humphreys ER, Bubier J (2007) Contemporary carbon balance and late Holocene carbon accumulation in a northern peatland. Global Change Biology, 13, 397–411.

Rowland, J. A., Bracey, C., Moore, J. L., Cook, C. N., Bragge, P., & Walsh, J. C. (2021). Effectiveness of conservation interventions globally for degraded peatlands in cool-climate regions. *Biological Conservation*, *263*, 109327.

Rowland, S. M., Prescott, C. E., Grayston, S. J., Quideau, S. A., & Bradfield, G. E. (2009). Recreating a Functioning Forest Soil in Reclaimed Oil Sands in Northern Alberta: An Approach for Measuring Success in Ecological Restoration. Journal of Environmental Quality, 38(4), 1580–1590. https://doi.org/10.2134/jeq2008.0317

Ruckstuhl, K. E., Johnson, E. A., & Miyanishi, K. (2008). Introduction. The boreal forest and global change. *Philosophical Transactions of the Royal Society B: Biological Sciences*, *363*(1501), 2243-2247.

Rudolph T.D. and P.R. Laidley. 1990. Pinus banksiana Lamb. In R.M. Burns and B.H. Honkala (eds.). Silvics of North America: Volume 1, Conifers. pp. 280–293. USDA For. Serv. Agricultural Handbook 654. Washington, DC

Ruiz-Pérez, G., Launiainen, S., & Vico, G. (2019). Role of plant traits in photosynthesis and thermal damage avoidance under warmer and drier climates in boreal forests. *Forests*, *10*(5). https://doi.org/10.3390/f10050398

Runkle, B. R. K., Wille, C., Gažovič, M., Wilmking, M., & Kutzbach, L. (2014). The surface energy balance and its drivers in a boreal peatland fen of northwestern Russia. *Journal of Hydrology*, *511*, 359–373. https://doi.org/10.1016/j.jhydrol.2014.01.056

Sadok, W., Lopez, J. R., & Smith, K. P. (2021). Transpiration increases under high-temperature stress: Potential mechanisms, trade-offs and prospects for crop resilience in a warming world. In *Plant Cell and Environment* (Vol. 44, Issue 7). https://doi.org/10.1111/pce.13970

Samaritani, E., Siegenthaler, A., Yli-Petäys, M., Buttler, A., Christin, P. A., & Mitchell, E. A. (2011). Seasonal net ecosystem carbon exchange of a regenerating cutaway bog: How long does it take to restore the C-sequestration function?. Restoration Ecology, 19(4), 480-489.

Schulze, E. D., Leuning, R., & Kelliher, F. M. (1995). Environmental regulation of surface conductance for evaporation from vegetation. In *Global change and terrestrial ecosystems in monsoon Asia* (pp. 79-87). Springer, Dordrecht.

Semeraro, V., Vacchiano, G., Aretano, R., & Ascoli, D. (2019). Application of vegetation index time series to value fire effect on primary produc- tion in a southern European rare wetland. Ecological Engineering, 134, 9–17. https://doi.org/10.1016/j.ecoleng.2019.04.004

Scarlett, S. J., Petrone, R. M., & Price, J. S. (2017). Controls on plot-scale evapotranspiration from a constructed fen in the Athabasca Oil Sands Region, Alberta. Ecological Engineering, 100, 199–210. https://doi.org/10.1016/j.ecoleng.2016.12.020

Scarlett, S. J., & Price, J. S. (2019). The influences of vegetation and peat properties on the hydrodynamic variability of a constructed fen, Fort McMurray, Alberta. Ecological Engineering, 139, 105575. https://doi.org/10.1016/j.ecoleng.2019.08.005

Schloerke, B., Cook, D., Larmarange, J., Briatte, F., Marbach, M., Thoen, E., Elberg, A., Toomet, O., Crowley, J., Hofmann, H., & Wickham, H. (2020). *Ggally: Extension to ggplot2*. R Package Version 0.5.0.

Schmidt, M., Davidson, S. J., & Strack, M. (2022). CO2 uptake decreased and CH4 emissions increased in first two years of peatland seismic line restoration. *Wetlands Ecology and Management*, *30*(2). https://doi.org/10.1007/s11273-022-09858-4

Schubert, P., Eklundh, L., Lund, M., & Nilsson, M. (2010). Estimating northern peatland CO2 exchange from MODIS time series data. Remote Sensing of Environment, 114(6), 1178–1189. https://doi.org/10.1016/j.rse.2010.01.005

Scheffer, M. (2010). Foreseeing tipping points. Nature, 467(7314), 411-412.

Sendall, K. M., Reich, P. B., Zhao, C., Jihua, H., Wei, X., Stefanski, A., Rice, K., Rich, R. L., & Montgomery, R. A. (2015). Acclimation of photosynthetic temperature optima of temperate and boreal tree species in response to experimental forest warming. *Global Change Biology*, *21*(3). https://doi.org/10.1111/gcb.12781

Seyfried, M. S., Grant, L. E., Du, E., & Humes, K. (2005). Dielectric loss and calibration of the Hydra Probe soil water sensor. Vadose Zone Journal, 4(4), 1070-1079.

Shih, J. G., & Finkelstein, S. A. (2008). Range dynamics and invasive tendencies in Typha latifolia and Typha angustifolia in eastern North America derived from herbarium and pollen records. Wetlands, 28(1), 1-16.

Simhayov, R. B., Price, J. S., Smeaton, C. M., Parsons, C., Rezanezhad, F., & Van Cappellen, P. (2017). Solute pools in Nikanotee Fen watershed in the Athabasca oil sands region. Environmental Pollution, 225, 150–162. https://doi.org/10.1016/j.envpol.2017.03.038

Small, E. E., Tech, N. M., Kurc, S., & Assistant, R. (2001). *The Influence of Soil Moisture on the Surface Energy Balance in Semiarid Environments*.

Slack, N. G., Vitt, D. H., & Horton, D. G. (1980). Vegetation gradients of minerotrophically rich fens in western Alberta. *Canadian Journal of Botany*, *58*(3), 330–350. https://doi.org/10.1139/b80-034

Smerdon, B.D., Mendoza, C.A., Devito, K.J., 2008. Influence of subhumid climate and water table depth on groundwater recharge in shallow outwash aquifers. Water Resour. Res. 44 (8), W08427.

Sonnentag, O., van der Kamp, G., Barr, A. G., & Chen, J. M. (2010). On the relationship between water table depth and water vapor and carbon dioxide fluxes in a minerotrophic fen. *Global Change Biology*, *16*(6). https://doi.org/10.1111/j.1365-2486.2009.02032.x

Spennato, H. M., Ketcheson, S. J., Mendoza, C. A., & Carey, S. K. (2018). Water table dynamics in a constructed wetland, Fort McMurray, Alberta. Hydrological Processes, 32(26), 3824-3836.

Stamatinos, M. (2019). *Varying Root Distributions Between Jack Pine, Aspen, and Mixed-Wood Stands in Sandy Boreal Soils* (Doctoral dissertation, Thesis Submitted to the Department of Geography, Environmental Earth Sciences, University of Saskatchewan, Saskatoon, Saskatchewan).

Stannard, D. I. (1988). Use of a Hemispherical Chamber for Measurement of Evapotranspiration. *U.S. Geol. Surv. Open File Rep., 88-452.*

Strack, M., Davidson, S. J., Hirano, T., & Dunn, C. (2022). The Potential of Peatlands as Nature-Based Climate Solutions. *Current Climate Change Reports*. https://doi.org/10.1007/s40641-022-00183-9

Strack, Maria, Keith, A. M., & Xu, B. (2014). Growing season carbon dioxide and methane exchange at a restored peatland on the Western Boreal Plain. Ecological Engineering, 64, 231–239. https://doi.org/10.1016/j.ecoleng.2013.12.013

Strack, M., & Zuback, Y. C. A. (2013). Annual carbon balance of a peatland 10 yr following restoration. Biogeosciences, 10(5), 2885-2896.

Strack, M., Waddington, J. M., Rochefort, L., & Tuittila, E. S. (2006). Response of vegetation and net ecosystem carbon dioxide exchange at different peatland microforms following water table drawdown. Journal of Geophysical Research: Biogeosciences, 111(2), n/a-n/a. https://doi.org/10.1029/2005JG000145

Stephenson, N. L. (1990). Climatic control of vegetation distribution: the role of the water balance. *American Naturalist*, *135*(5). https://doi.org/10.1086/285067

Straker, J. R., Carey, S. K., Petrone, R. M., Baker, T. D., & Strilesky, S. L. (2019). Developing a Functional Approach to Assesment of Landscape Capability: Utilizing Ecosystem

Water and Carbon Nutrient Fluxes as Integrated Measures of Reclamation Performance.

Striegl, R. G., & Wickland, K. P. (1998). Effects of a clear-cut harvest on soil respiration in a jack pine - Lichen woodland. *Canadian Journal of Forest Research*, *28*(4). https://doi.org/10.1139/x98-023

Strilesky, S. L., Humphreys, E. R., & Carey, S. K. (2017). Forest water use in the initial stages of reclamation in the Athabasca Oil Sands Region. Hydrological Processes, 31(15), 2781–2792. https://doi.org/10.1002/hyp.11220

Strilesky, S. L. (2019). Functioning of reclaimed oil sands ecosystems and the implications for reclamation certification. Thesis

Ström, L., Mastepanov, M., & Christensen, T. R. (2005). Species-specific effects of vascular plants on carbon turnover and methane emissions from wetlands. *Biogeochemistry*, *75*(1). https://doi.org/10.1007/s10533-004-6124-1

Strong, W. L., & La Roi, G. H. (1983). Root-system morphology of common boreal forest trees in Alberta, Canada. *Canadian Journal of Forest Research*, *13*(6). https://doi.org/10.1139/x83-155

Sulman, B. N., Desai, A. R., Saliendra, N. Z., Lafleur, P. M., Flanagan, L. B., Sonnentag, O., MacKay, D. S., Barr, A. G., & Van Der Kamp, G. (2010). CO2 fluxes at northern fens and bogs have opposite responses to inter-annual fluctuations in water table. *Geophysical Research Letters*, *37*(19). https://doi.org/10.1029/2010GL044018

Sutton, O.F. (2021). Projecting the Hydrological and Geochemical Evolution of a Constructed Fen Watershed in the Athabasca Oil Sands Region, Alberta, Canada. UWSpace. http://hdl.handle.net/10012/16965

Sutton, O. F., & Price, J. S. (2020a). Modelling the hydrologic effects of vegetation growth on the long-term trajectory of a reclamation watershed. https://doi.org/10.1016/j.scitotenv.2020.139323

Sutton, O. F., & Price, J. S. (2020b). Soil moisture dynamics modelling of a reclaimed upland in the early post-construction period. Science of the Total Environment, 718, 134628. https://doi.org/10.1016/j.scitotenv.2019.134628

Tariq, S., Nawaz, H., Ul-Haq, Z., & Mehmood, U. (2021). Investigating the relationship of aerosols with enhanced vegetation index and meteorological parameters over Pakistan. Atmospheric Pollution Research, 12(6), 101080.

Tuittila, E. S., Komulainen, V. M., Vasander, H., & Laine, J. (1999). Restored cut-away peatland as a sink for atmospheric CO 2. Oecologia, 120(4), 563-574.

Thom, A. 1. (1972). Momentum, mass and heat exchange of vegetation. *Quarterly Journal of the Royal Meteorological Society*, *98*(415), 124-134.

Thom, D., & Seidl, R. (2016). Natural disturbance impacts on ecosystem services and biodiversity in temperate and boreal forests. *Biological Reviews*, *91*(3), 760-781.

Thompson, C., Beringer, J., Chapin, F. S., & Mcguire, A. D. (2004). Structural Complexity and Land-Surface Energy Exchange along a Gradient from Arctic Tundra to Boreal Forest. *Source: Journal of Vegetation Science*, *15*(3), 397–406.

Thompson, C., Mendoza, C. A., & Devito, K. J. (2017). Potential influence of climate change on ecosystems within the Boreal Plains of Alberta. Hydrological Processes, 31(11), 2110–2124. https://doi.org/10.1002/hyp.11183

Thompson, D. K., Baisley, A. S., & Waddington, J. M. (2015). Seasonal variation in albedo and radiation exchange between a burned and unburned forested peatland: implications for peatland evaporation. *Hydrological Processes*, *29*(14), 3227–3235. https://doi.org/10.1002/HYP.10436

Thompson, D. K., Benscoter, B. W., & Waddington, J. M. (2014). Water balance of a burned and unburned forested boreal peatland. *Hydrological Processes*, *28*(24), 5954–5964. https://doi.org/10.1002/HYP.10074

Tilman, D. (1988). Plant Strategies and the Dynamics and Structure of Plant Communities. *Monographs in Popoulation Biology*, *26*. https://doi.org/10.1046/j.1420-9101.1989.2050388.x

Tinoco Ojanguren, C., & Goulden, M. L. (2013). Photosynthetic acclimation within individual Typha latifolia leaf segments. *Aquatic Botany*, *111*, 54–61. https://doi.org/10.1016/j.aquabot.2013.08.007

Tjoelker, M. G., Oleksyn, J. K., Reich, P. B., & Zytkowiak, R. (2008). Coupling of respiration, nitrogen, and sugars underlies convergent temperature acclimation in Pinus banksiana across wide-ranging sites and populations. *Global Change Biology*, *14*(4). https://doi.org/10.1111/j.1365-2486.2008.01548.x

Trites, M., & Bayley, S. E. (2009). Vegetation communities in continental boreal wetlands along a salinity gradient: Implications for oil sands mining reclamation. Aquatic Botany, 91(1), 27–39. https://doi.org/10.1016/j.aquabot.2009.01.003

van de Griend, A. A., & Owe, M. (1994). Bare soil surface resistance to evaporation by vapor diffusion under semiarid conditions. *Water Resources Research*, *30*(2). https://doi.org/10.1029/93WR02747

Vasander, H., & Kettunen, A. (2006). Carbon in boreal peatlands. In Boreal peatland ecosystems (pp. 165-194). Springer, Berlin, Heidelberg.

Verma, S. B. (1989). Aerodynamic resistances to transfers of heat, mass and momentum.

Vermote, E., Justice, C., Claverie, M., & Franch, B. (2016). Preliminary analysis of the performance of the Landsat 8/OLI land surface reflectance product. Remote Sensing of Environment, 185, 46-56.

Vestin, P., Mölder, M., Kljun, N., Cai, Z., Hasan, A., Holst, J., Klemedtsson, L., & Lindroth, A. (2020). Impacts of clear-cutting of a boreal forest on carbon dioxide, methane and nitrous oxide fluxes. *Forests*, *11*(9). https://doi.org/10.3390/f11090961

Vitt, DH, Halsey, L, Thormann, M and Martin, T (1996) Peatland inventory of Alberta: Phase 1: Overview of Peatland Resources in the Natural Regions and Subregions of the Province. University of Alberta.

Vitt, D. H., Glaeser, L. C., House, M., & Kitchen, S. P. (2020). Structural and functional responses of Carex aquatilis to increasing sodium concentrations. Wetlands Ecology and Management, 28(5), 753–763. https://doi.org/10.1007/s11273-020-09746-9

Vitt, D. H., House, M., & Hartsock, J. A. (2016). Sandhill fen, an initial trial for wetland species assembly on in-pit substrates: Lessons after three years. Botany, 94(11), 1015–1025. https://doi.org/10.1139/cjb-2015-0262

Vitt, D. H., House, M., & Glaeser, L. (2022). The response of vegetation to chemical and hydrological gradients at a patterned rich fen in northern Alberta, Canada. *Journal of Hydrology: Regional Studies*, *40*. https://doi.org/10.1016/j.ejrh.2022.101038

Volik, O., Petrone, R. M., & Price, J. S. (2021). Soil respiration and litter decomposition along a salinity gradient in a saline boreal fen in the Athabasca Oil Sands Region. *Geoderma*, *395*, 115070. https://doi.org/10.1016/j.geoderma.2021.115070

Volik, O., Petrone, R., Kessel, E., Green, A., Price, J. (2021a) Understanding the peak growing season ecosystem water-use efficiency at four boreal fens in the Athabasca Oil Sands Region. Hydrological Processes. DOI: 10.1002/hyp.14323

Volik, O., Kessel, E., Green, A., Petrone, R., & Price, J. (2021b). Growing season evapotranspiration in boreal fens in the Athabasca Oil Sands Region: Variability and environmental controls. *Hydrological Processes*, *35*(2). https://doi.org/10.1002/HYP.14020

Volik, O., Elmes, M., Petrone, R., Kessel, E., Green, A., Cobbaert, D., & Price, J. (2020a). Wetlands in the athabasca oil sands region: The nexus between wetland hydrological function and resource extraction. Environmental Reviews, 28(3), 246–261. https://doi.org/10.1139/er-2019-0040

Volik, O., Petrone, R. M., Quanz, M., Macrae, M. L., Rooney, R., & Price, J. S. (2019). Environmental Controls on CO 2 Exchange along a Salinity Gradient in a Saline Boreal Fen in the Athabasca Oil Sands Region. Wetlands, 1-14.

Volik, O., Petrone, R.M., Wells, C.M. (2018) Impact of Salinity, Hydrology and Vegetation on Long-Term Carbon Accumulation in a Saline Boreal Peatland and its Implication for Peatland Reclamation in the Athabasca Oil Sands Region. Wetlands 38, 373–382 (2018). https://doi.org/10.1007/s13157-017-0974-5

Waddington, J. M., Strack, M., & Greenwood, M. J. (2010). Toward restoring the net carbon sink function of degraded peatlands: Short-term response in CO 2 exchange to ecosystem-scale restoration . Journal of Geophysical Research, 115(G1), 1008. https://doi.org/10.1029/2009jg001090

Waddington, J. M., Morris, P. J., Kettridge, N., Granath, G., Thompson, D. K., & Moore, P. A. (2015). Hydrological feedbacks in northern peatlands. *Ecohydrology*, *8*(1), 113–127. https://doi.org/10.1002/eco.1493

Waddington, J. M., & Price, J. S. (2000). Effect of peatland drainage, harvesting, and restoration on atmospheric water and carbon exchange. *Physical Geography*, *21*(5), 433–451. https://doi.org/10.1080/02723646.2000.10642719

Wang, T. (2022). *The combined impact of salinity and water table on Juncus balticus growth: Implications for fen construction in the Athabasca Oil Sands Region* (Master's thesis, University of Waterloo).

Warren, R. K., Pappas, C., Helbig, M., Chasmer, L. E., Berg, A. A., Baltzer, J. L., Quinton, W. L., & Sonnentag, O. (2018). Minor contribution of overstorey transpiration to landscape evapotranspiration in boreal permafrost peatlands. *Ecohydrology*, *11*(5). https://doi.org/10.1002/eco.1975

Watts, J. D., Natali, S. M., Minions, C., Risk, D., Arndt, K., Zona, D., Euskirchen, E. S., Rocha, A. V., Sonnentag, O., Helbig, M., Kalhori, A., Oechel, W., Ikawa, H., Ueyama, M., Suzuki, R., Kobayashi, H., Celis, G., Schuur, E. A. G., Humphreys, E., … Edgar, C. (2021). Soil respiration strongly offsets carbon uptake in Alaska and Northwest Canada. *Environmental Research Letters*, *16*(8). https://doi.org/10.1088/1748-9326/ac1222

Webb, E.K., Pearman, G., & Leuning, R. (1980). Correction of flux measurements for density effects due to heat and water vapour transfer. Quarterly Journal of the Royal Meteorology Society, 106, 85–100.

Wells, C., Ketcheson, S., & Price, J. (2017). Hydrology of a wetland-dominated headwater basin in the Boreal Plain, Alberta, Canada. Journal of Hydrology, 547, 168-183.

Weltzin, J. F., Keller, J. K., Bridgham, S. D., Pastor, J., Allen, P. B., & Chen, J. (2005). Litter controls plant community composition in a northern fen. *Oikos*, *110*(3), 537–546. https://doi.org/10.1111/j.0030-1299.2005.13718.x

Wilson, D. G., Tuittila, E. S., Alm, J., Laine, J., Farrell, E. P., & Byrne, K. A. (2007). Carbon dioxide dynamics of a restored maritime peatland. *Ecoscience*, *14*(1). https://doi.org/10.2980/1195-6860(2007)14[71:CDDOAR]2.0.CO;2

Wilson, K. B., Baldocchi, D. D., Aubinet, M., Berbigier, P., Bernhofer, C., Dolman, H., Falge, E., Field, C., Goldstein, A., Granier, A., Grelle, A., Halldor, T., Hollinger, D., Katul, G., Law, B. E., Lindroth, A., Meyers, T., Moncrieff, J., Monson, R., … Wofsy, S. (2002). Energy partitioning between latent and sensible heat flux during the warm season at FLUXNET sites. *WATER RESOURCES RESEARCH*, *38*(12), 30–31

Winckler, J., Reick, C. H., & Pongratz, J. (2017). Robust identification of local biogeophysical effects of land-cover change in a global climate model. *Journal of Climate*, *30*(3), 1159-1176.

Winslow, LA, JA Zwart, RD Batt, HA Dugan, RI Woolway, JR Corman, JS Read (2016). LakeMetabolizer: An R package for estimating lake metabolism from free- water oxygen using diverse statistical models. Inland Waters, In Press.

Worrall, F., Boothroyd, I. M., Gardner, R. L., Howden, N. J. K., Burt, T. P., Smith, R., Mitchell, L., Kohler, T., & Gregg, R. (2019). The Impact of Peatland Restoration on Local Climate: Restoration of a Cool Humid Island. *Journal of Geophysical Research: Biogeosciences*, *124*(6), 1696–1713. https://doi.org/10.1029/2019JG005156

Worrall, F., Burt, T. P., Clay, G. D., & Moody, C. S. (2015). A 19-year long energy budget of an upland peat bog, northern England. *Journal of Hydrology*, *520*, 17-29.

Wutzler, T., Lucas-Moffat, A., Migliavacca, M., Knauer, J., Sickel, K., & Šigut, L. et al., (2018). Basic and extensible post-processing of eddy covariance flux data with R EddyProc. Biogeosciences, 15(16), 5015-5030. doi: 10.5194/bg-15-5015-2018

Wu, J., Kutzbach, L., Jager, D., Wille, C., & Wilmking, M. (2010). Evapotranspiration dynamics in a boreal peatland and its impact on the water and energy balance. *Journal of Geophysical Research: Biogeosciences*, *115*(4), 1–18. https://doi.org/10.1029/2009JG001075

Wu, Y., Xi, Y., Feng, M., & Peng, S. (2021). *remote sensing Wetlands Cool Land Surface Temperature in Tropical Regions but Warm in Boreal Regions*.

Xia, J., Niu, S., Ciais, P., Janssens, I. A., Chen, J., Ammann, C., Arain, A., Blanken, P. D., Cescatti, A., Bonal, D., Buchmann, N., Curtis, P. S., Chen, S., Dong, J., Flanagan, L. B., Frankenberg, C., Georgiadis, T., Gough, C. M., Hui, D., … Luo, Y. (2015). Joint control of terrestrial gross primary productivity by plant phenology and physiology. *Proceedings of the National Academy of Sciences of the United States of America*, *112*(9). https://doi.org/10.1073/pnas.1413090112

Xu, B., Rochefort, L., Bird, M., Khadka, B., & Strack, M. (2021). Restoration of boreal peatland impacted by an in-situ oil sands well-pad 1: Vegetation response. *Restoration Ecology*, e13514. https://doi.org/10.1111/REC.13514

Yang, S., Sutton, O. F., Kessel, E. D., & Price, J. S. (2022). Spatial patterns and mass balance of sodium in near-surface peat of a constructed fen. *Journal of Hydrology: Regional Studies*, *41*. https://doi.org/10.1016/j.ejrh.2022.101073

Yu, Z. C. (2012). Northern peatland carbon stocks and dynamics: a review. Biogeosciences, 9, 4071–4085. https://doi.org/10.5194/bg-9-4071-2012

Zha, T., Barr, A. G., van der Kamp, G., Black, T. A., McCaughey, J. H., & Flanagan, L. B. (2010). Interannual variation of evapotranspiration from forest and grassland ecosystems in western canada in relation to drought. *Agricultural and Forest Meteorology*, *150*(11). https://doi.org/10.1016/j.agrformet.2010.08.003

Zhang, T., Gong, W., Wang, W., Ji, Y., Zhu, Z., & Huang, Y. (2016). Ground level PM2.5 estimates over China using satellite-based geographicallyweighted regression (GWR) models are improved by including NO2 and enhanced vegetation index (EVI). International Journal of Environmental Research and Public Health, 13(12), 1215. https://doi.org/10.3390/ijerph13121215

Zoltai, S. C., & Vitt, D. H. (1995). *Canadian wetlands: Environmental gradients and classification* (Vol. 118). http://nofc.cfs.nrcan.gc.ca/bookstore_pdfs/19047.pdf

Appendices

Appendix A: Utilizing vegetation indices to capture ecosystem recovery

In order to determine which plant index to apply at NFW, two commonly used indices (Normalized Difference Vegetation Index (NDVI) and Enhanced Vegetation Index (EVI)) were run and examined. The main difference between the two indicies is NDVI uses just the red and infared bands, while EVI uses the red, infared and addiationally the blue band, as well as a few additional parameters for background soil and atmospheric interfernces. The aerosol interference aspect is quiet important for a study site like NFW as its frequently affected by mine dust as well as forest fire haze. Results from multispectral analysis show NDVI overestimated dark, wet bare ground as vegetation, and under estimated the emergence of understory vegetation in the upland making it less favorable for studies capturing early, post-disturbance development. However, once fully vegetated, the two indices performed similarly. To further validate these results, NDVI and EVI values were compared to tower GEP to confirm the presence or absence of vegetation (i.e., no/low GEP when plant community is limited). This analysis confirmed the above results, as such EVI was deemed the better fit for this study.

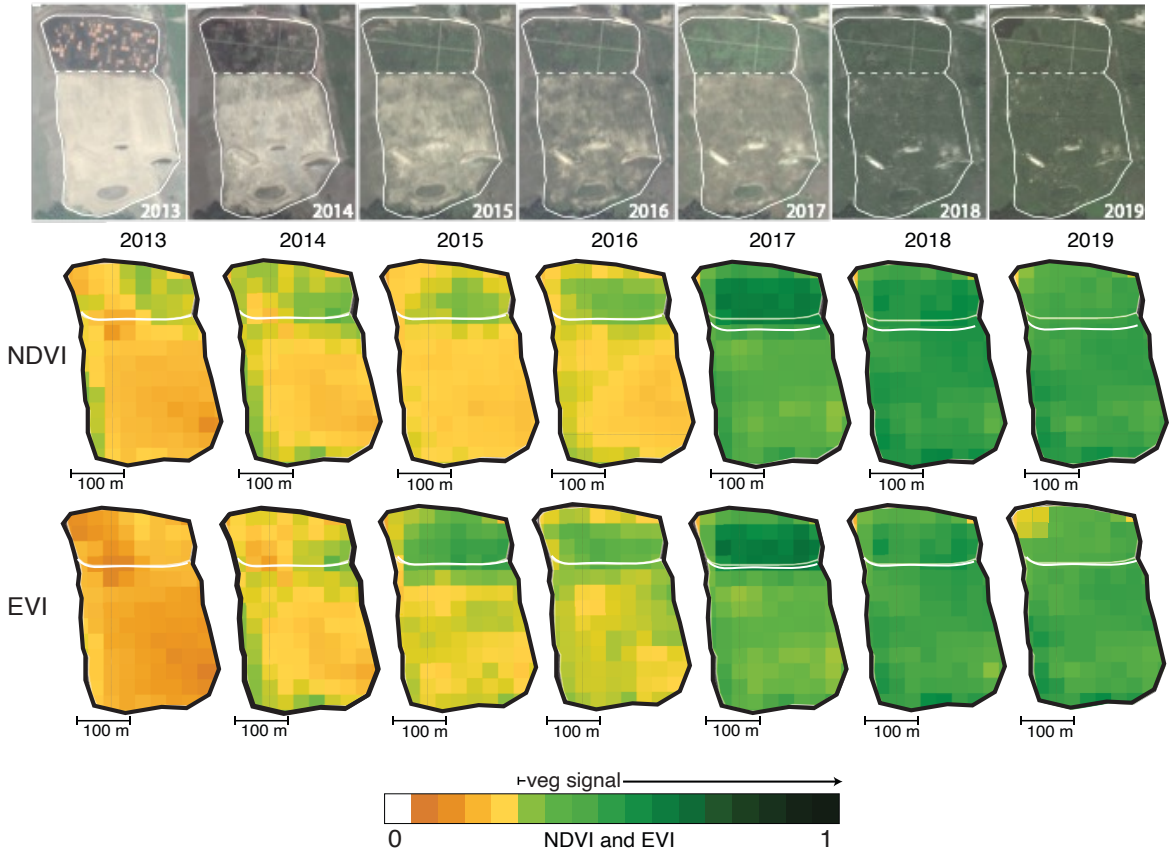


Figure A-1: Temporal snapshot of plant development in the fen and upland from 2013-2019. Ecosystem scale mean peak season (DoY 170-220) satellite imagery (top), Normalized Difference Vegetation Index (NDVI; middle) and Enhanced Vegetation Index (EVI; bottom).

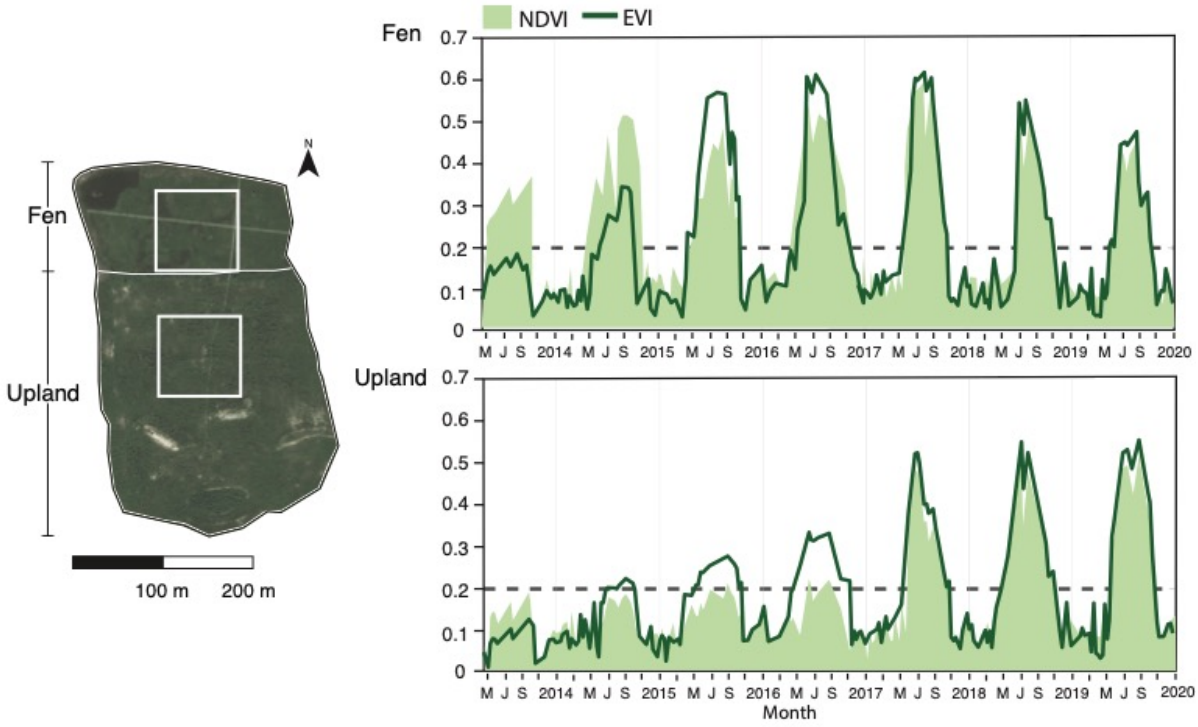


Figure A-2: Timeseries of NDVI and EVI values from the mean of a pixel grid (60 x 60 m) located at the epicenter of flux tower footprints (white square). Note the overestimation of NDVI in the fen and underestimation in the upland during early development. Values greater than 0.2 represent a plant signal.

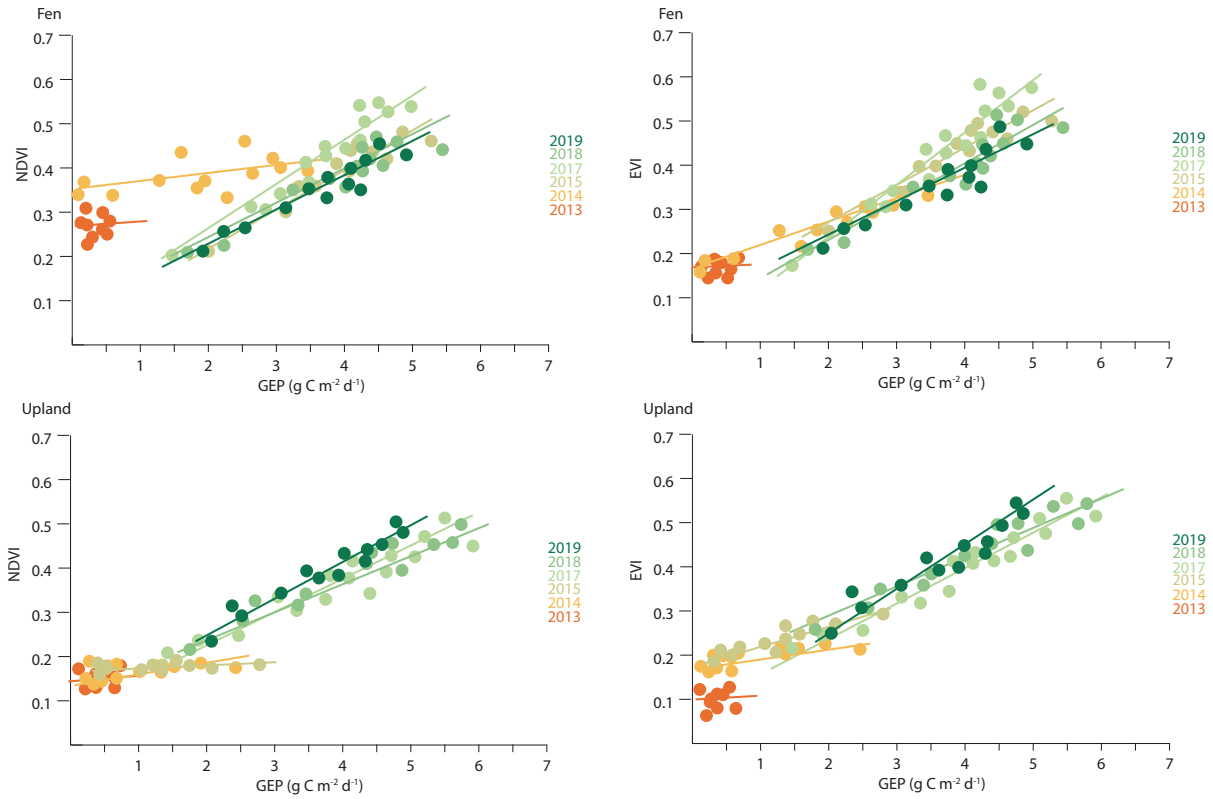
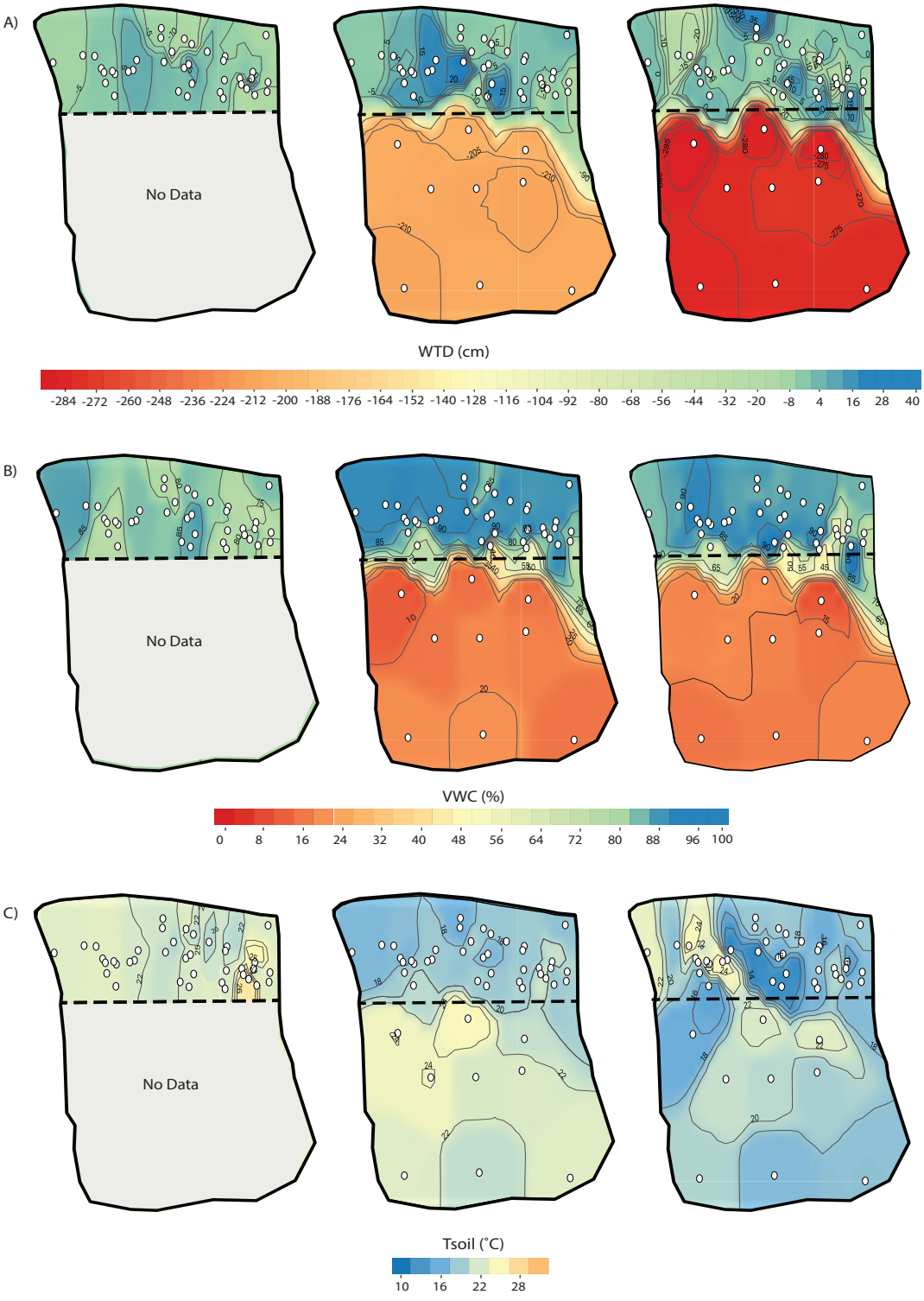


Figure A-3: Relationship between NDVI and GEP (left), and EVI and GEP (right) from 2013 to 2019. Based on mean daily GEP for weeks when spectral imagery is collected (every 8-16 days). Values greater than 0.2 represent a plant signal. Note that NDVI indicates a plant signal when there is limited to no GEP (2013,2014, red orange) confirming the overestimation of wet dark peat as plant matter.

Appendix B: Spatial variability in environmental conditions and fluxes from 2017 to 2019

Due to spatial heterogeneity and variability in environmental conditions between years (i.e., dry versus wet, timing and frequency of precipitation) an inverse distance weighted (IDW) interpolation was derived using QGIS to provide a spatial overview of environmental and flux trends relative to chamber plot location. Here, a mean of all peak season values for each plot was used from 2017-2019. In the upland, due to the proximity of flux plots (and species), a mean was calculated for each upland quadrant rather than each individual plot.


A)
No Data
WTD (cm)
-284 -272 -260 -248 -236 -224 -212 -200 -188 -176 -164 -152 -140 -128 -116 -104 -92 -80 -68 -56 -44 -32 -20 -8 4 16 28 40
B)
No Data
VWC (%)
0 8 16 24 32 40 48 56 64 72 80 88 96 100
C)
No Data
Tsoil (°C)
10 16 22 28

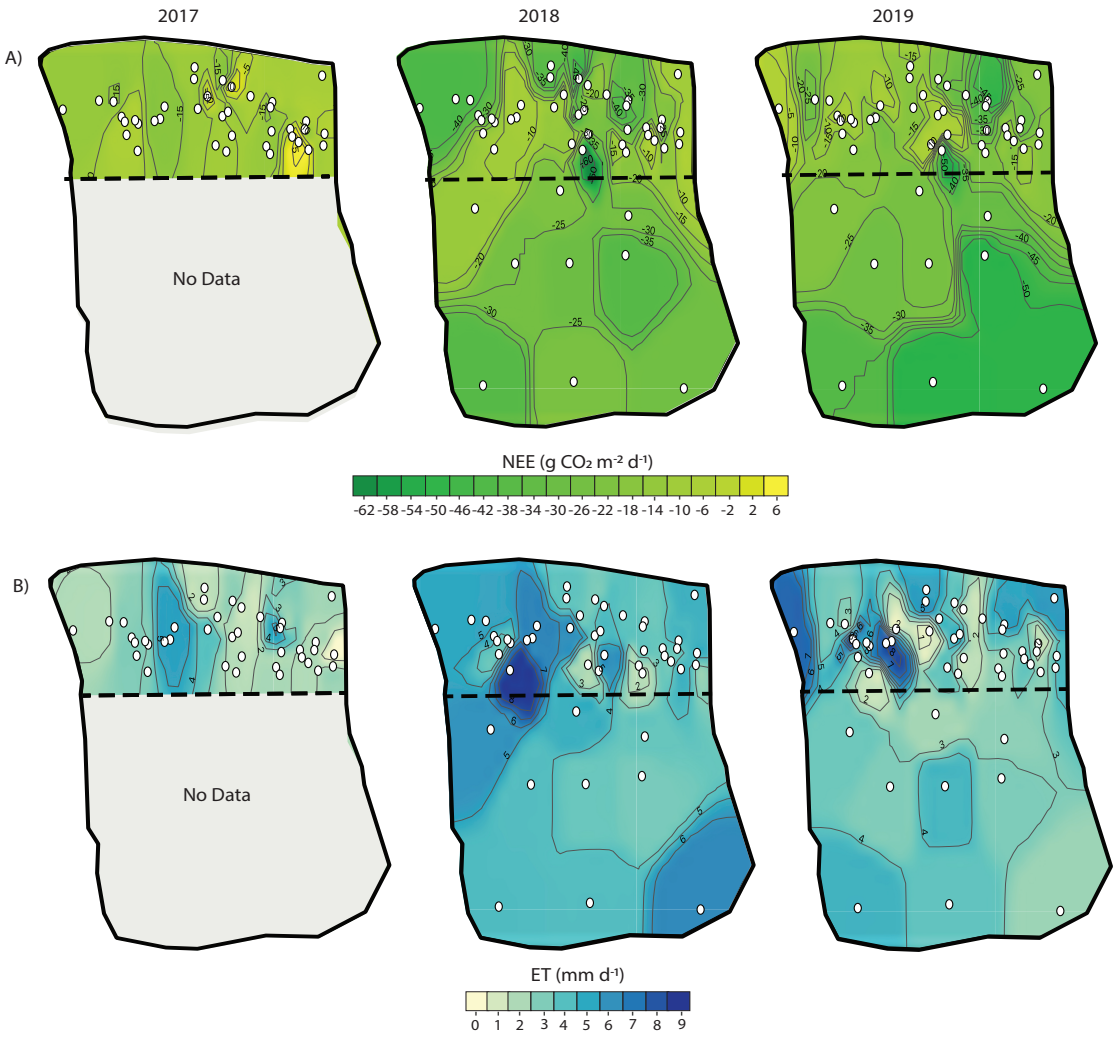


Figure A-4: Spatial interpolation of mean peak season edaphic conditions and CO_2 and ET fluxes from 2017 to 2019. A) water table depth (cm) where a negative value indicates below ground, B) soil moisture (%), C) soil temperature (°C), D) net ecosustem exchange (g CO_2 m^{-2} d^{-1}), E) evapotranspiration (ET, mm/day). White circles represent flux plot measurement locations. In the upland, the mean of each quadrant (rather than plot) was used No measurements were taken in the upland in 2017.